Synthesis of two-photon sensitive pro-fluorescent photoremovable protecting groups

Elie Abou Nakad

UNIVERSITÉ DE STRASBOURG

ÉCOLE DOCTORALE DES SCIENCES CHIMIQUES

Laboratoire de Conception et Application de Molécules Bioactives (CAMB)

UMR7199

THÈSE présentée par :

Elie ABOU NAKAD

Soutenue le : **16 Novembre 2018**

pour obtenir le grade de : **Docteur de l'Université de Strasbourg**

Discipline/ Spécialité : Chimie Organique

Synthèse de groupements protecteurs photolabiles pro-fluorescents sensibles à l'excitation bi-photonique

THÈSE dirigée par :

M SPECHT Alexandre	Directeur de recherche au CNRS, Université de Strasbourg

RAPPORTEURS :

Mme JOSEPH Delphine	Professeur, Université de Paris-Sud
Mme MAHUTEAU-BETZER Florence	Directeur de recherche au CNRS, Institut Curie-Orsay

---

AUTRES MEMBRES DU JURY :

M BLANC Aurélien	Chargé de recherche au CNRS, Université de Strasbourg

UNIVERSITÉ DE STRASBOURG

ÉCOLE DOCTORALE DES SCIENCES CHIMIQUES

Laboratoire de Conception et Application de Molécules Bioactives (CAMB)

UMR7199

THÈSE présentée par :

Elie ABOU NAKAD

Soutenue le : **16 Novembre 2018**

pour obtenir le grade de : **Docteur de l'Université de Strasbourg**

Discipline/ Spécialité : Chimie Organique

Synthèse de groupements protecteurs photolabiles pro-fluorescents sensibles à l'excitation bi-photonique

THÈSE dirigée par :

M SPECHT Alexandre	Directeur de recherche au CNRS, Université de Strasbourg

RAPPORTEURS :

Mme JOSEPH Delphine	Professeur, Université de Paris-Sud
Mme MAHUTEAU-BETZER Florence	Directeur de recherche au CNRS, Institut Curie-Orsay

---

AUTRES MEMBRES DU JURY :

M BLANC Aurélien	Chargé de recherche au CNRS, Université de Strasbourg

"Teach me knowledge and good judgment,
for I trust your commands."
Psalms 119:66

To my lovely late Aunt Salwa,

You've always believed in me

This is my gift to you...

ACKNOWLEDGEMENTS

All the thesis work presented in this manuscript was done in the lab of “Conception et Applications des Molécules Bioactives” in the Chimie et Neurobiologie Moléculaire” group at the Faculty of Pharmacy of Strasbourg under the direction of Dr Alexandre SPECHT.

First of all, I would like to express my sincere gratitude to the jury members: Prof Delphine JOSEPH, Dr Florence MAHUTEAU-BETZER and Dr Aurélien BLANC, for accepting to evaluate this thesis work and also for spending important time in reading this manuscript.

Alexandre, or as you like us to call you, **Alex**, I have a lot to thank you for. I want to thank you for accepting me to be a PhD student in your lab and putting your trust in me that I can do the best for this project. A big thank you for all the help you gave me since the day of my arrival, with all the paper work and the administrative stuff. I am so grateful to have had a director like you; thank you for all the time you spend with me on “chemical discussions” as well as “polymer chain mass calculations” … Thanks to you, my knowledge on chemistry has grown day after day and my skills have evolved a lot. I am so glad that we were able to get the most out of this project. You will always be the “big brother who’s watching me”. Endless thanks for you!

Fred, I would like to thank you for all the time you put in doing the photophysical analysis and thank you for the 20 fluorophores you gave me to decorate my bench. Thank you for all the help in understanding the wide world of photophysics and for giving me a lot of your expertise in the domain. It was always a pleasure working with you with all your English-French-Italian sense of humor and even though you are a busy man thank you for making everything “EASY!”.

Thomas, thanks a lot for your wisdom and for sharing with us your highly-respected knowledge. Thank you for always being there when I had hesitations in biology and thank you for all the advice and because of you I know a lot on the historical part of Strasbourg.

Thierry, Le Jeune, thank you for making every single lab meeting a stress-less time, thank you for always giving us the push to continue and thank you for all the rich discussions we had.

Juline, my labmate, you were always saying time is going by slowly, now we’ve reached the end of this 3-year journey, we started together, and we are graduating together…Thank you for being the funniest labmate, thank you for reminding me when it is time to eat. Thank you for being beside me in all the hard times and thanks for helping me organize all the lab activities (including the unforgettable Pancakes Party). I wish you, from the bottom of my heart, all the best in your endeavors.

I would like to thank as well, **Bastien** and **Laurie** for making the lab a great working atmosphere and thank you for all the help and fruitful discussion we had. You stood beside me since my arrival to the lab, you will always be the best labmates and the dearest friends. I wish you all the best in your future jobs.

Kate, I wish you also all the best in your PhD, you still have time to change your mind…I guess… I will miss you correcting my American English with your British one. Thank you for making me memorize all your iTunes library. Wish you all the success and perseverance.

I would like to thank all the lab members who worked with me during these 3 years: Florian, Lucas, Clément and Benoit. A sincere thank you for **Philippe** and **Elodie** who worked with me as master students, the project gave amazing results during your presence and with your help. Best of luck in your PhDs.

Issam and **Lodi** (Les Issas) thank you for being my family in France and thank you for all the help and care and for making me discover lots of places in Alsace. You made this period the best time of my life, with you I have never felt far away from home. And to my 3 little siblings: **Timothé**, **Pauline** and **Elena**, I love you!

I would like to thank as well: Dr **Halim**, Dr **Ghina**, Dr **Eliane**, and the future Drs **Fatima**, **Elias**, **Naimah**, and my friends: **Carole**, **Alexa**, **Dima**, **Fadi**, **Mireille** and the long list of friends who stayed beside me and supported me especially during the writing period. You guys are the best!

To my everlasting support my aunt **Hayat** and the 2 best cousins: **Tony** and **Rawad**, thank you for always believing that I can do the best and for supporting me throughout the 8 years of chemistry. You are the greatest gift in my life!

To my biggest support rock, my brother, **Georges**, thank you for being there for me all these times, and thank you for making me laugh when I was in need. To my childhood friend, **Miray**, you are the sister that I never had, you are the one of the most amazing souls I know, thank you for standing by my side at all times. To my nephew, **Charbel**, thank you for bringing joy to my life and thank you for making me the luckiest uncle in the world. You are my second family, I love you all.

To my parents, **Roukos** and **Hiam**, you have waited a lot for this moment, I am sure that as much as I say, it will not be enough. Thank you for the full support, thank you for staying beside me all this time, thank you for believing in me and having faith in my skills. It is because of you that I had this chance and because of your endless prayers I reached this moment. Thank you for standing by my side in the hard times and the good times. It is to you that I owe my success. You've sacrificed a lot in order to make my dream a reality and today my dream, and your dream, is coming true. I respectfully love you!

My first, last and forever thanks are to you, my biggest teacher. You gave me a lot since day 1 and now, I am giving you this work to bless it as you blessed my entire life… None of this would have been possible without you…I am grateful for you endlessly…**GOD**!

Table of Contents

List of Abbreviations and Symbols

α : Alpha

ε : Molar extinction coefficient

ϕ : Quantum yield

λ : Wavelength

ν : Frequency

h : Planck's constant 6.62607004 × 10^{-34} m^2. kg/s

π : Pie

UV : Ultraviolet

Vis : Visible

o-NB : *ortho*-nitrobenzyl

o-NPP : *ortho*-nitrophenethyl

TLC : Thin Layer Chromatography

CC : Column Chromatography

THF : Tetrahydrofuran

DCM : Dichloromethane

IR : Infra-red

GM : Göppert-Mayer

PEG : Polyethylene glycol

DNA : Deoxyribonucleic acid

RNA : Ribonucleic acid

cAMP : cyclic Adenosine Monophosphate

ATP : Adenosine triphosphate

DIBAL-H : Di-isobutyl Aluminum Hydride

DIC : N,N'-Diisopropylcarbodiimide

DMF : N,N'-Dimethylformamide

DMSO : Dimethyl sulfoxide

AcOEt : Ethyl Acetate

p-TsOH : *para*-toluenesulfonic acid

p-TsCl : *para*-toluenesulfonyl chloride

HCl : Hydrochloric acid

PyBoP : Benzotriazol-1-yl-oxytripyrrolidinophosphonium hexafluorophosphate

D^iPEA : N,N-Diisopropylethylamine

GABA : γ-aminobutyric acid

Glu : Glutamic acid

HPLC : High Performance Liquid Chromatography

LC-MS : Liquid Chromatography – Mass Spectrometry

MCM : 7-methoxycoumarinyl-4-methyl

MCM-OH : hydroxy-7-methoxycoumarinyl-4-methyl

PBS : Phosphate Buffer Saline

NMR : Nuclear Magnetic Resonance

t_R : Retention time

mL : Milliliter

min : Minutes

R_f : Frontal ratio

°C : Degrees Celsius

h : hours

mmol : millimole

mM : millimolar

mg : milligram

g : gram

Zn : Zinc

CDNI : 4-carboxymethoxy-5,7-dinitroindolinyl

MNI : 4-methoxy-7-nitroindolinyl

μs : micro-seconds

AMPA : α-amino-3-hydroxy-5-methyl-4-isoxazolepropionic acid

PMNB : p-methoxynitrobiphenyl

BNSMB : 4,4'-bis-{8-[4-nitro-3-(2-propyl)- styryl]}-3,3'-di-methoxybiphenyl,

BNSF : 2,7-bis- {4-nitro-8-[3-(2-propyl)-styryl]}-9,9-bis-[1-(3,6-dioxaheptyl)]- fluorene

nm : nanometer

μL : micro-liters

μM : micro-molar

M : Molar

RESUME DES TRAVAUX DE THÈSE

Les groupements protecteurs photolabiles (GPP) sont des composés chimiques photoactivables, qui lorsqu'ils sont attachés à une biomolécule (comme un neurotransmetteur ou une molécule de signalisation cellulaire) permettent de restaurer la fonctionnalité de la biomolécule sous l'action de la lumière. Ce processus dénommé « uncaging » génère également un sous-produit de photolyse.

Si ce dernier est un rapporteur capable de générer un signal spécifique (par exemple un signal fluorescent), le processus de photolibération pourrait être analyser et ainsi nous devrions pouvoir quantifier le saut de concentration de l'effecteur biologique en particulier lors d'études sur des milieux complexes comme les organes ou les tissus. (Schéma 1). Le développement de rapporteur optiques de la photolibération n'a attiré que très peu d'attention et ce, principalement en raison de la faible différence de fluorescence observée entre le précurseur photolabile de biomolécule (« caged-compound ») et le sous-produit de photolyse.

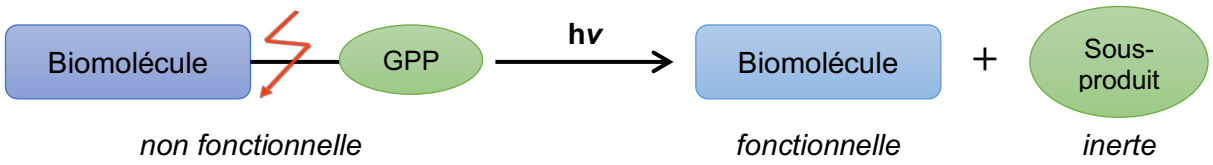

Schéma 1: Représentation du processus de libération par photoclivage.

Le premier exemple de libération d'un effecteur biologique avec une augmentation de la fluorescence associée à la libération de ce dernier été rapporté avec des nucléotides cycliques photoactivables qui utilisent un GPP de type coumarinique (Schéma 2). Cependant, l'absence d'émission de fluorescence des précurseurs photolabiles de nucléotides a été réalisée par une extinction de la fluorescence (« quenching ») de la coumarine par le substrat nucléotidique.

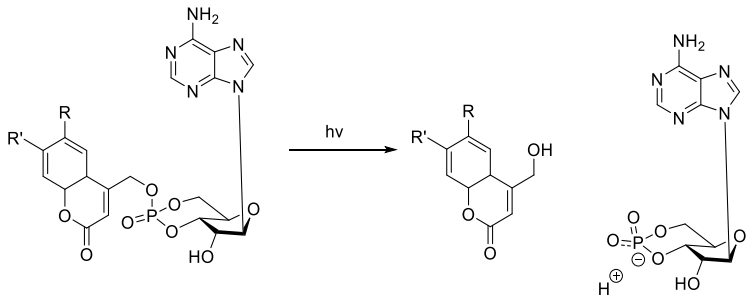

Schéma 2: Photoclivage de coumarin Adenosine monophosphate cagé.

Une stratégie plus intéressante et indépendante du substrat a été développée plus récemment par le groupe de L. Jullien, en utilisant des groupes photolabiles de type *o*-hydroxycinnamate conçus pour libérer un sous-produit présentant une bonne fluorescence. Dans cette série, le groupement photolabile non fluorescent est en mesure de libérer efficacement une biomolécule, masquée via une fonction alcool, avec libération concomitante d'un sous-produit de type coumarinique.

Toutefois, cette plate-forme très efficace du point de vue du relargage d'un rapporteur optique de la photolyse est restée limitée à quelques substrats bien spécifiques.

Dans le laboratoire, des nouveaux groupements photolabiles ont été développé récemment: les composés *ortho*-Nitro biphényle divisés en 2 familles majeures : les *ortho*-nitrophenéthyles ([I], o-NPE) et les *ortho*-nitrobenzyles ([II], o-NB) (Schéma 3).

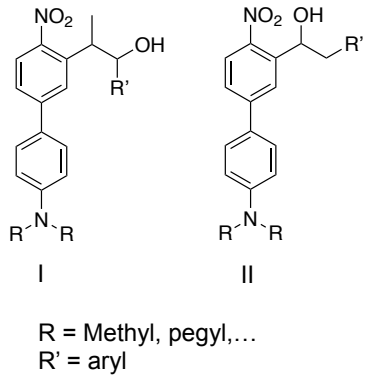

Schéma 3: Les 2 familles de GPP de type *ortho*-Nitro biphényle.

Ces composés présentent une efficacité élevée pour l'absorption à 2 photons en raison d'une structure biphenylique donneur-accepteur (schéma 4-5). Le phénomène d'absorption bi-photonique repose sur la capacité d'un chromophore à absorber simultanément deux photons afin d'accéder à des états excités de haute énergie. Lorsque cette propriété d'optique non-linéaire est appliquée aux groupements protecteurs photolabiles cela permet d'envisager une photoactivation localisée dans la fenêtre de transparence optique des tissus (comprise le plus souvent entre 600 et 1200 nm).

Pour suivre avec précision la photo-libération, par exemple sur des cellules, nous souhaitons développer des nouveaux groupes photolabiles basés sur le noyau o-nitrobiphenyl en implémentant une propriété de rapporteur de fluorescence au sous-produit de photolyse.

Sur la base des mécanismes photolytiques de nos groupements photolabiles sensibles à deux photons, nous souhaitions concevoir des nouveaux groupements photolabiles peu fluorescents qui libèrent un sous-produit fortement fluorescent (A et B) induit par la conjugaison crée par les doubles liaisons (respectivement alcène et énol) lors de la formation des sous-produits de photolyse (Schémas 4 et 5).

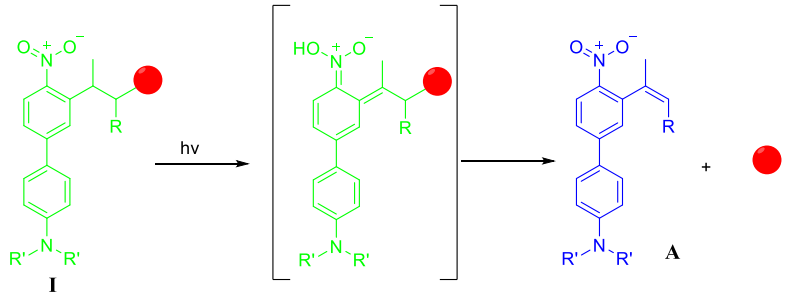

Schéme 4: Mécanisme de photoclivage de I.

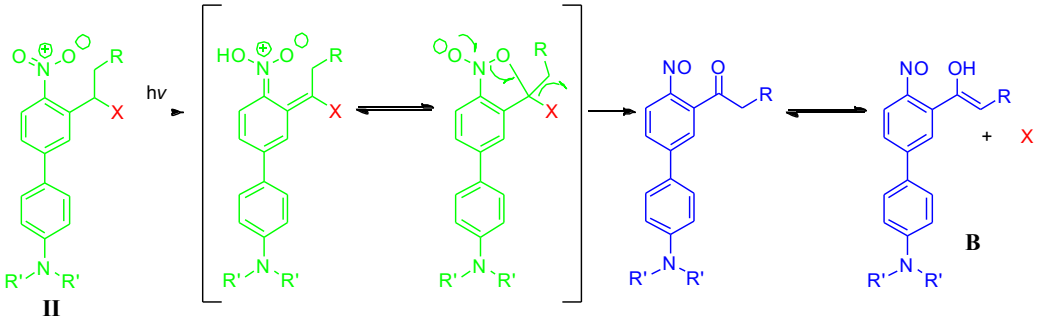

Schéma 5: Mécanisme de photoclivage de II.

Afin de développer ces nouveaux GPP, un schéma rétrosynthétique (Schéma 6) a été imaginé afin d'accéder aux deux familles de GPP via l'époxyde **3**.

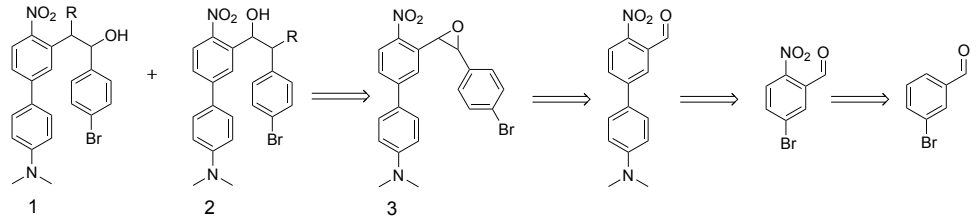

Schéma 6: Une stratégie rétrosynthétique pour le développement de ce groupe de cage.

Après avoir obtenu l'époxyde **3** en 5 étapes. Plusieurs essais d'ouverture de l'époxyde ont été réalisés à l'aide d'agents de méthylation dérivés de composés organométalliques commerciaux tels que: MeLi, MeMgBr, Me_3Al et d'autres agents de méthylation qui ont été générés *in situ* tels que Me_2CuLi et Me_3ZnLi avec ou sans activateurs ($AlCl_3$, $BF_3.EtO_2$, CuI). Tous les essais mentionnés ci-dessus n'ont pas permis d'ouvrir efficacement l'époxyde en raison d'une réaction acido-basique survenante plus rapide que l'ouverture de l'époxyde.

Une nouvelle stratégie a été explorée, cette dernière repose sur l'utilisation de **4** pour effectuer une réaction de Barbier en utilisant un composé organozincique. Cette stratégie fonctionne très bien avec une conversion très élevée et donne exclusivement un accès direct à la famille des GPP de type *o*-nitrobenzyle **II**. Nous avons réussi à synthétiser quatre composés tout en variant les substituants entre les groupements électro-donneur (NMe_2 et OCH_3) et les groupements électro-attracteur (NO_2) (schéma 7) visant à observer une longueur d'onde décalée vers le rouge du signal fluorescent photoinduit via le mécanisme présenté dans le schéma 5.

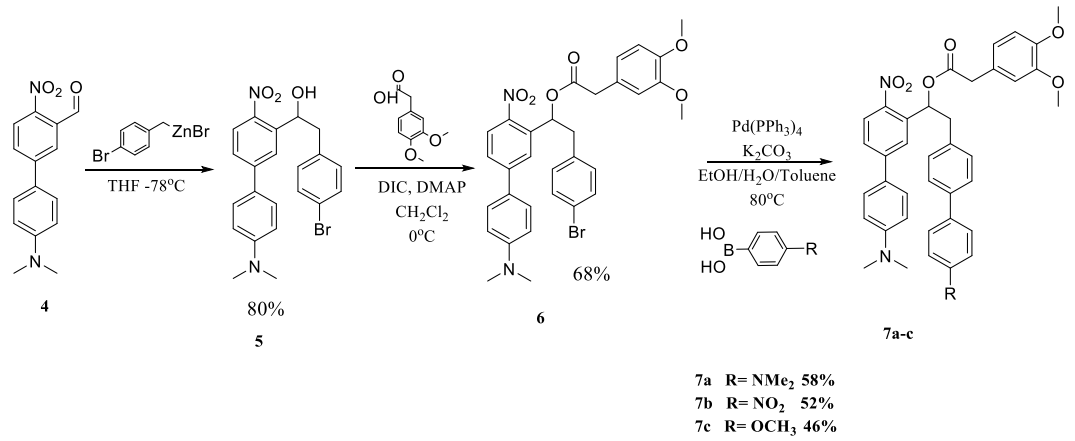

Schéma 7: Synthèse de groupement o-nitrobenzyl 7a-c cagés.

Ces GPP présentent des propriétés photophysiques, photochimiques et optiques très intéressantes lorsqu'elle est couplée à un chromophore. Lors de l'irradiation (libération monophotonique à 405 nm), nous avons observé une diminution de l'absorbance UV (Schéma 8A) et une augmentation considérable de la fluorescence (Schéma 8B) due à la formation du nitroso-énol conjugué (B, schéma 5) après libération du chromophore (utilisé ici pour quantifier, par CLHP, le taux de conversion de la photolyse en fonction du temps d'irradiation).

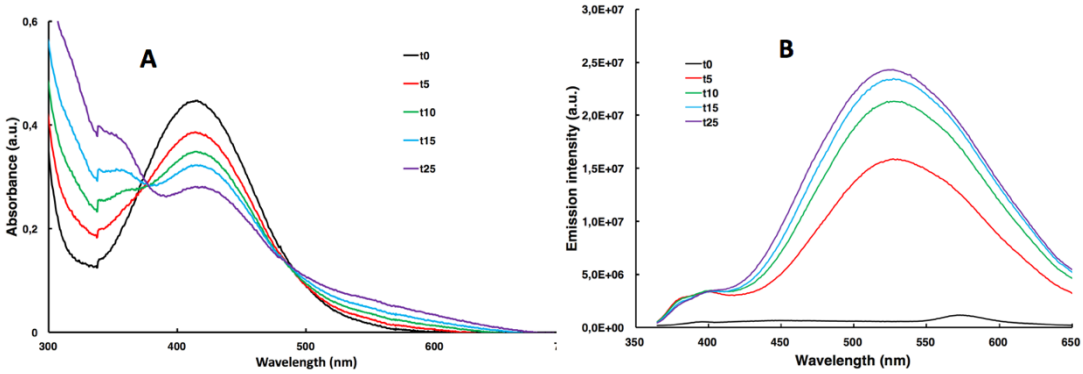

Schéma 8: (A) Variation de l'absorbance UV pendant l'irradiation et (B) Variation de l'intensité de fluorescence entre le produit de départ et le produit de photolibération de composé **7c**.

En comparant les propriétés photochimiques et photophysiques de ces composés **7a-c**, on a observé une augmentation importante de l'intensité de fluorescence après photolyse complète des composées (100% de libération (I_{full})) comparé à l'intensité avant irradiation I_0. De façon remarquable, l'ajout d'un groupement électro-donneur (OCH_3) engendre un décalage vers le rouge de la longueur d'onde d'émission λ_{emm} du fluorophore photolibéré et avec une augmentation de fluorescence de 200x (Tableau 1).

Composé	λ_{em}(nm)	$I_0 \times 10^8$	% de libération moyenne*	$I_{full} \times 10^8$ moyenne*	I_{full} / I_0
6	504	0.5254	95	21.006	40
7a	489	4.4211	93	143.233	32
7b	480	0.3409	83	-**	-**
7c	526	1.0296	97	214.721	208

* Moyenne de trois manipes différentes

** le sous-produit subit beaucoup de bleaching, on n'a pas pu calculer les intensités de fluorescence correspondantes.

La formation d'un sous-produit en équilibre céto-enolique a été confirmée à l'aide d'analyses RMN-^{1}H, cela a permis de vérifier la formation du produit énol (**B**, Schéma 5), en équilibre avec un apha-hydroxystibene fortement conjugué responsable du signal fluorescent du sous-produit de photolyse.

Les excellentes propriétés du composé **7c,** qui présente la plus forte augmentation linéaire de fluorescence photo-induite et une émission de fluorescence la plus déplacée vers le rouge, nous a permis d'utiliser ce GPP pour évaluer la possibilité de suivre la photolibération par microscopie de fluorescence sur des cellules en culture. Pour ce faire, nous avons synthétisé le composé **11**, une version soluble dans l'eau du dérivé méthoxy-o-nitrobiphenyl **7c** (Schéma 9).

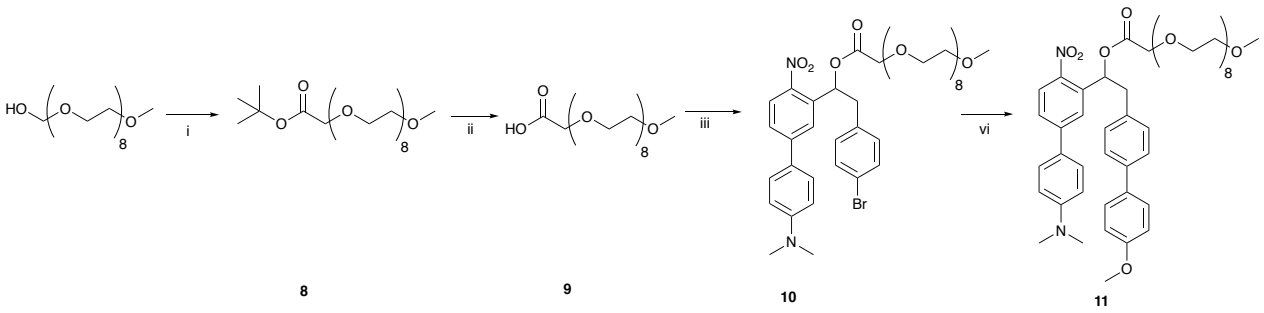

Schéma 9: Synthèse de **11**: une version soluble du composé méthoxy-o-nitrobiphenyl **7c**.

i) NaH, bromoacetate d'éthyl, THF, 0°C, 2h, 87 %; ii) CF_3COOH/ dichlorométhane, 3h, température ambiante, 100 %; iii) **5**, DMAP, diisopropylcarbodiimide, dichlorométhane, 0°C, 48 %; vi) 4-méthoxyphényl acide boronique, K_2CO_3, Ethanol/Toluène/eau, $Pd(PPh_3)_4$, 80°C, 45 min, 30 %.

Des cellules HeLa ont été incubées avec une solution de **11**. Les cellules ont été incubées pendant 5 minutes puis irradiées (365 nm) pendant 15 min en continue. Une nette augmentation de l'intensité de fluorescence a été observée lors de l'irradiation. Par contre, les cellules incubées pendant 35 min avec une solution de **11** montraient une très faible intensité de fluorescence qui montre que la fluorescence observée dans les cellules est dû de l'accumulation de sous-produit de photolyse du composé **11**. Par conséquent, nous pouvons suivre l'événement de libération de ce nouveau type de GPP par l'augmentation d'un signal de fluorescence dans les cellules.

Après avoir testé la photolyse de GPP de série *o*-nitrobenzyle **7a-c** et **11**, et ses propriétés de fluorescence très avantageuses, nous avons décidé d'adapter la même stratégie de synthèse sur un GPP récemment développer au sein du laboratoire. Ce composé présente un cœur hétéroaromatique de type thiophène[7] plus sensible à la lumière et permet d'envisager des temps d'irradiation plus court afin de pouvoir envisager des applications biologiques du GPP (Schéma 10). Nous avons utilisé la même stratégie de synthèse afin d'accéder au GPP capable de former un sous-produit fluorescent après photolyse.

La molécule **13** a été synthétisée en 8 étapes et a montré après photolyse un sous-produit avec des propriétés de fluorescence très intéressantes. Un dérivé soluble de **13** est actuellement utilisé au sein du laboratoire afin de développer des précurseurs photolabiles du Glutamate (le principal neurotransmetteur excitateur des cellules neuronales).

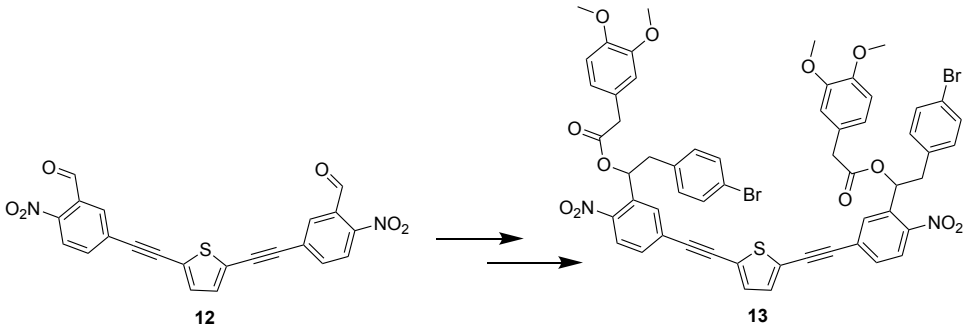

Schéma 10: Synthèse de groupement o-nitrobenzyl à cœur hétéroaromatique cagé **13**.

Il existe un besoin important de GPP capables de générer un sous-produit de photolyse facilement quantifiable, en particulier pour être en mesure d'évaluer le saut de concentration photo-induit d'un effecteur biologique donné couplé. Cela nous a amené à synthétiser une nouvelle classe de groupements photolabiles de la famille des o-nitrobenzyles capables de générer un sous-produit de photolyse fluorescent. Ces derniers composés ont été conçus afin de produire après photoréaction un sous-produit de type nitrosocétone capable de réaliser une tautomérie céto-énolique conduisant à un produit conjugué de type α-hydroxystilbene. Chaque GGP synthétisé a montré un signal de fluorescence très faible avant irradiation. À l'exception du dérivé **7b**, une libération presque quantitative (≥93%) a été observée après la photolyse complète de chaque précurseur **7a-c**. Tous ces composés ont montré une augmentation intéressante du signal fluorescent induite par la réaction photolytique.

En particulier, le dérivé **7c** a montré une augmentation de l'intensité de fluorescence de plus de 200x avec un décalage de la longueur d'onde d'émission vers le rouge (526 nm) après photoclivage complet. Par conséquent, une version soluble dans l'eau de ce composé a été utilisée avec succès dans des expériences d'imagerie sur des cellules et a permis de suivre en temps réel le signal fluorescent induit par la formation du sous-produit de photolyse sur des cellules en culture.

Nos futures études vont se concentrer sur l'utilisation de cette stratégie pour le développement de groupes photolabiles sensibles à la lumière visible plus efficaces dans la serie *o*-NB afin de pouvoir corréler la libération d'un effecteur biologique, comme un neurotransmetteur, à la formation d'un signal fluorescence induit par la libération du sous-produit de photolyse.

CHAPTER I

Introduction to Photoremovable Protecting Groups: A Breakthrough in Synthesis and Biology

1. Photoremovable Protecting Groups (PPGs)

1.1. Definition:

Photoremovable or so-called photo-cleavable, photo-activatable, photo-releasable **P**rotecting **G**roups (**PPG**s) are photolabile chemical compounds that when attached to a biomolecule (for example neurotransmitters or cell signaling molecules) form a stable inactive "**caged compound**"; this designates that the biomolecule is protected by the PPG. Upon photo-irradiation of the resulting compound, the biomolecule is released and restores its active functionality along with the by-product of the PPG; this process is called uncaging (Klàn *et al.,* 2013) (Scheme I.1).

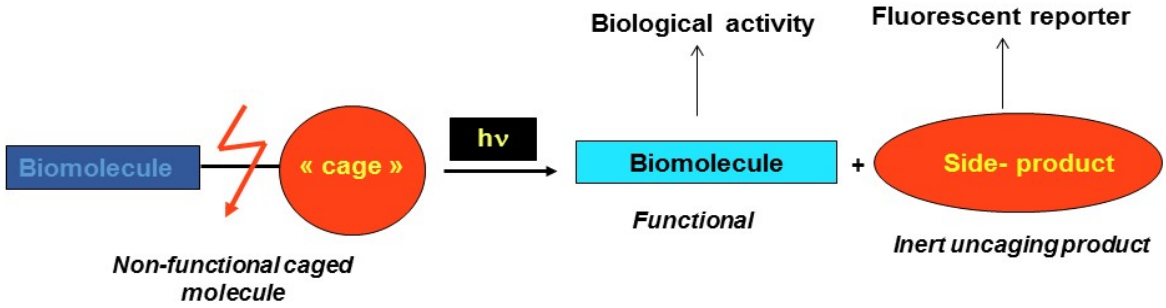

Scheme I.1: Description of the uncaging process and the release of the biomolecule.

Photoremovable protecting groups provide spatial and temporal control over the release of diverse compounds such as biomolecules (neurotransmitters), organic acids and bases or ions (Ca^{2+}) [Baltrop *et al.,* 1962, Barton *et al.,* 1962; 1965, Ellis-Davies., 2007]

1.2. Requirements:

Several requirements need to be fulfilled by the PPG depending on its application, not all the protecting groups follow the same requirements because they vary depending on the application needed or expected for the system. Many of these properties were originally introduced by Sheehan and Umezawa (Sheehan *et al.,* 1973) and were used to evaluate the potential of a PPG:

i- The PPG should show an absorption wavelength above 300 nm, because irradiations below this wavelength tend to be absorbed by biological entities like proteins and nucleic acids and thus leading to photo-damage resulting in the formation of initiators for mutations.

ii- The PPG should be stable, clean and pure prior to use because any trace of impurities could affect the irradiation and the cleavage process. The chosen PPG should show stability during the irradiation process as well.

iii- The photocleavage reaction should be clean and occur with a remarkable quantum yield of release ϕ_{rel}. This quantum yield is described as:

$\phi_{rel} = n_{rel} / n_p$ where n_{rel} is the amount of substrate released and n_p is the number of photons absorbed by the caged compound upon irradiation

iv- The PPG should be stable and soluble in the media of examination and if possible should present an affinity toward the target molecules (binding site on cancer cells, active sites on enzymes…).

v- The by-product released after the release of the bioactive molecule should show no competitive absorbance with the starting material i.e be transparent to the wavelength of irradiation.

vi- The released by-product should be inert and biocompatible i.e does not react with the system investigated.

These are the important guidelines and properties for an ideal PPG, but still, a caged compound is considered useful even if it lacks one or two of these properties. The absence of several requirements may be a huge limitation of the PPG in several applications.

1.3. Types of PPGs

Several examples of PPG that fulfill the requirements mentioned above, have been reported and found to have interesting chemical, photophysical and optical properties.

1.3.1. Benzoin PPGs

Sheehan and Wilson (Sheehan *et al.,* 1964, 1971) were the first to explore the photochemical rearrangements of certain benzoin derivatives yielding a 2-phenylbenzofuran by-product. These rearrangements occur by the release of the group attached in position α to the carbonyl function. It was found that 3',5'-dimethoxybenzoin (DMB) could serve as a PPG for carboxylic acids releasing 2-phenyl-5, 7-dimethoxybenzofuran (DMBF) as a side product, after irradiation in quantitative yields and with a quantum yield of 0.64 ± 0.03 (Scheme I.2).

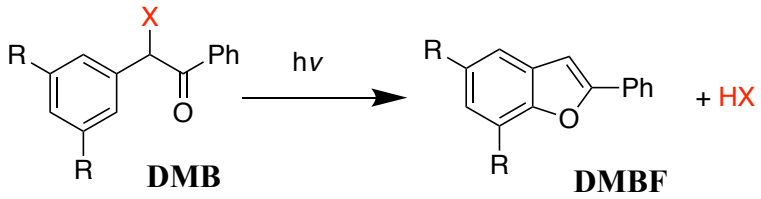

X= acetate
R= OMe

Scheme I.2: Photocyclization of DMB acetate.

DMB phototriggers have been used for several applications for example in the drug delivery field, in order to study protein folding and muscle relaxation (Rock *et al.,* 1996, Rock *et al.,* 2004).

Another benzoin derivative (R=H) was reported by Givens *et al.,* 2012 this latter showed a quantitative release of phosphates. This study was extended for the release of neucleotides through the synthesis and photolysis of benzoin-cAMP. The same derivative was found to likely protect and release GABA and glutamates (α- or N- protected Glu).

1.3.2. Arylcarbonylmethyl or Phenacyls (Pac)

Arylcarbonylmethyl groups are aromatic ketones that are thermally stable and easy to access by synthesis. These groups undergo a mechanism of photocleavage that involves hydrogen abstraction from an H-donor by an excited state of the carbonyl function of the phenacyl leading to a ketyl ester intermediate (scheme I.3).

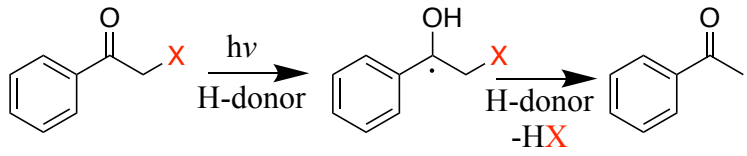

Scheme I.3: H-abstraction mechanism of photocleavage of phenacyls.

A very recent application of phenacyls was reported by Speckmeier and his co-workers (Speckmeier *et al.,* 2018) where in this study, this PPG was used to protect amine function by the formation of Phenacyl (Pac) Urethanes (the amines were linked to Pac by the formation of carbamate linkage). The latter "caged amine" undergoes a photocatalytical cleavage using blue LEDs (λ =455 nm) in the presence of a Ruthenium photocatalyst in order to release the amine function along with acetophenone (Scheme I.4). This method avoids the drawbacks of using UV irradiation and is carried out in a mixture of acetonitrile and water (4:1), in addition to its applicability to a diverse family of amines, amino acids and anilines.

The presence of the [Ru (bipy)$_3$](PF$_6$)$_2$ is significant to avoid the oxidation of the released amine in combination with ascorbic acid as a reductive quencher in water acetonitrile mixture.

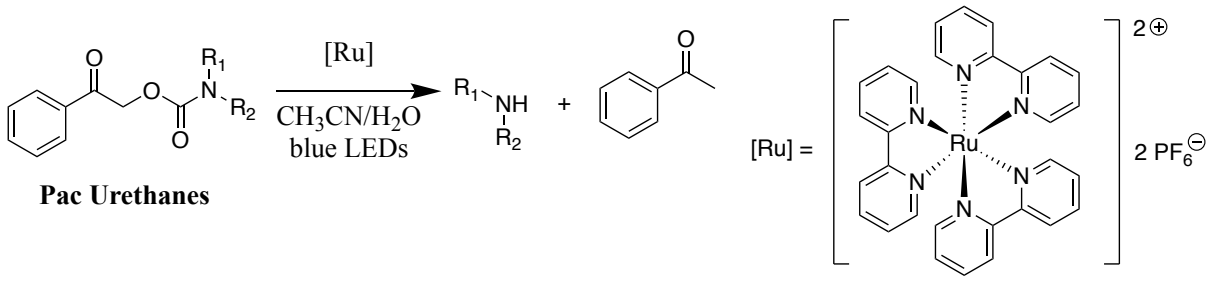

Scheme I.4: Photocatalytical cleavage of phenacyl protected amines.

1.3.3. Coumarin-4-ylmethyl

The photolysis of 7-methoxycoumarinyl-4-methyl (MCM) derivatives was first introduced by Givens and collaborators (Givens *et al.,* 1984) that demonstrated the use of coumarins as photoactivatable phosphate-releasing groups (Entry1, Scheme I.5).

The use of these derivatives was limited until the introduction of coumarin protecting carboxylic acids by Schade and his colleagues (Schade *et al.,* 1999) that shows upon the irradiation of MCM-ester, the release of the free carboxylic acid along with MCM-OH in water (Entry 2, Scheme I.5).

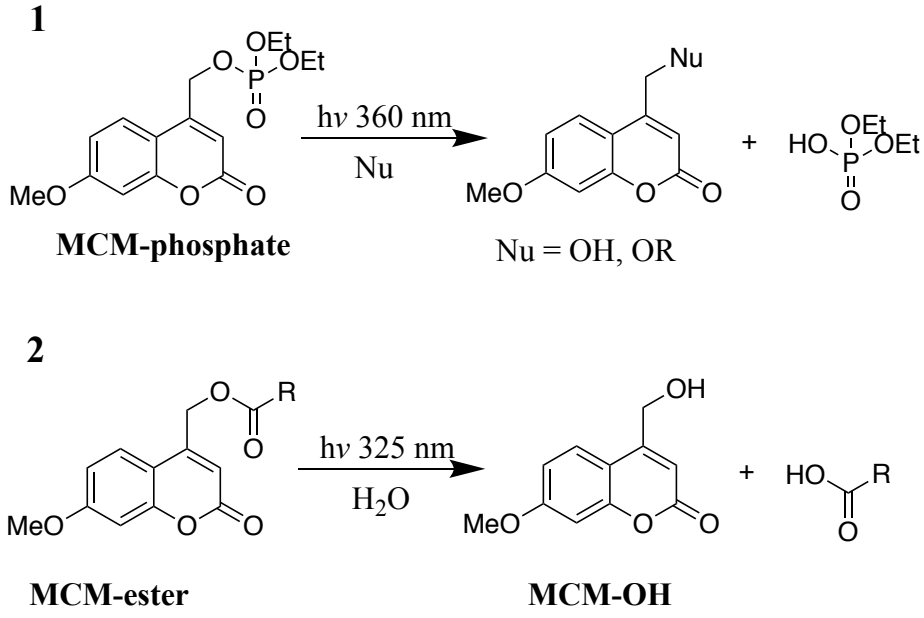

Scheme I.5: **1**-Photocleavage of MCM phosphate derivative liberating free phosphate.
2-Photocleavage of MCM-ester derivative liberating free carboxylic acid.

Compared to other PPGs the coumarin derivatives doesn't possess a very high quantum yield (ϕ = 0.25 for the best derivative), but they possess a remarkable molar extinction coefficient along with their rapid photolysis that makes these coumarin derivatives great candidates for the photo-liberation of biomolecules.

That's why these derivatives where applied in several research works for the liberation of carboxylic acids (Schade *et al.,* 1999), phosphates (Givens and Matuszewski, 1984), cyclic nucleotides (Furuta and Iwamura, 1998) and glutamates (Furuta *et al.,* 1999). A selection of coumarin caged compounds with their relative quantum yield of disappearance ϕ_{dis} and their molar extinction coefficient ε is presented in Table 1.

Caged compounds	Substrate	ϕ_{dis}	ε (325nm)
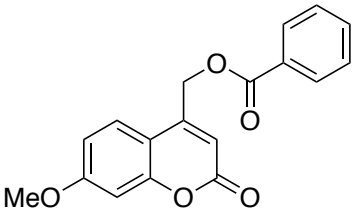	Benzoic acid	0.005	13000
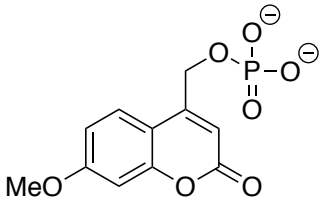	Phosphate	0.05	14000
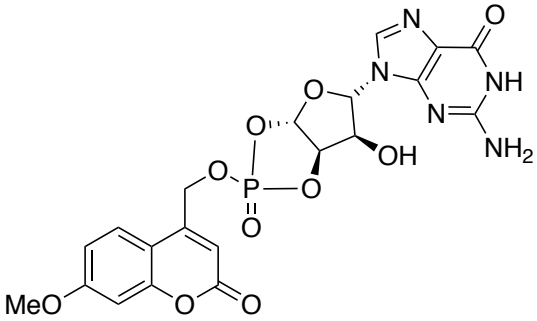	cGMP	0.21	13300
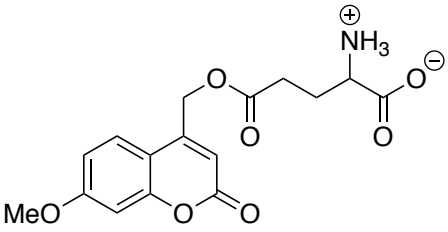	Glutamate	0.02	15000

Table 1: Liberation quantum yield of different caged compounds of the 7-methoxycoumarinyl-4-methyl family in 1:1 methanol/HEPES buffer

Over the time, several structural modifications were studies in order to modify the photochemical and optical properties of coumarin derivatives.

Certain modifications succeeded in presenting the first coumarin Photoremovable Protecting Group model sensitive to two-photon excitation based on 6-bromo-7-hydroxycoumarin-4-ylmethyl (Bhc) which presents an interesting two-photon efficiency cross section δ_u of 1 GM (Goeppert-Mayer) at 740 nm for the release of glutamates as described by Furuta and co-workers (Furuta *et al.,* 1999), but this series suffers from low water-solubility. Another interesting and more soluble generation of coumarin was presented by introducing an electron donating amino group in position 7 for example, 7-N,N-diethylamino-coumarin-4-yl (DEACM). This structural modification permitted to observe an important red-shift in the absorbance maximum from 325 nm to around 400 nm which makes these derivatives more adapted for in vivo applications (Shembekar *et al.,* 2005). The performance in two-photon excitation of the DEACM PPG in water was studied by Lin and collaborators (Lin *et al.,* 2012) and showed an efficiency cross section δ_u = 0.12 GM at 800 nm. These values of cross section are relatively important and permits the uses of these derivatives for the photo-regulation of various biological events (plasma membrane-specific photoactivation, modulation of calcium ion oscillations).

Recently the group of Ellis-Davies used the DEACM platform to synthesize a new PPG, the DEAC450. This latter presents an extended π-conjugated system that induces a red-shifted absorbance leading to an absorption maximum λ_{max} at 450 nm. Also, the DEAC450 Photoremovable Protecting Group shows an interesting activity for two-photon excitation with an uncaging cross section δ_u = 0.5 GM at 900 nm for the liberation of glutamates (Olson *et al.,* 2013). These interesting results make this coumarin derivative an intriguing tool for biological experimentation. The structure of the 3 PPG mentioned above are presented in Scheme I.6.

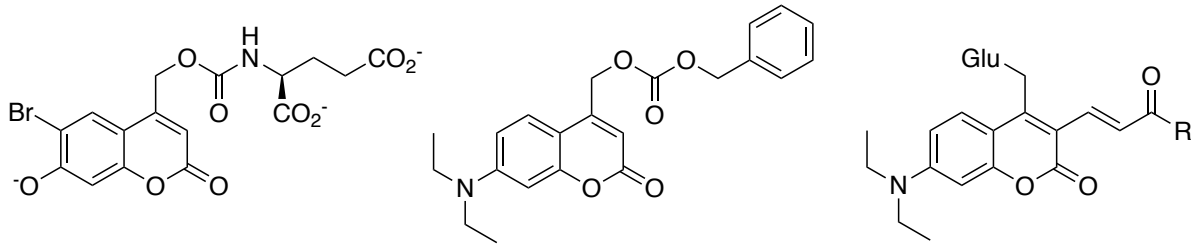

Bhc-Glu
λ_{abs} = 365 nm
δ_u = 1 GM at 740 nm

DEACM-OPMB
λ_{abs} = 395 nm
δ_u = 0.12 GM at 800 nm

DEAC450
λabs = 450 nm
δu = 0.5 GM at 900 nm

Scheme I.6: Structures of the coumarin derivatives efficient in two-photon excitation.

1.3.3.1. Thio-carbonyl Coumarin PPGs

Most of the presently reported photoremovable protecting groups show strong absorbance below 450 nm, a region where riboflavin and carotenoids absorb light. Research groups are working on adjusting the chemical structure of these groups in order to overcome this limitation of absorbance. One of the explored strategies is to increase the conjugation of the absorbing chromophore and/or to insert heteroatoms in the backbone of the chromophore.

An interesting study on the photophysics and the photochemistry of thiocarbonyls (thiones) was established by Maciejewski and his co-workers (Maciejewski *et al.,* 1993) and emphasizing on the fact that the energy of the C=S bond is weaker than a C=O bond therefore the excited electronic states are found at lower energies in the sulfur-containing species leading to the fact that C=S species absorb light at higher wavelengths compared to that of C=O.

A more recent work on thiones and their use in the field of PPG photoactivation focuses on the use of thiocoumarin (tc) backbone which possesses a red-shifted absorption compared to the carbonyl analogue (Fournier *et al.,* 2013). This derivative was used to cage cyclofen-OH (Ind) in order to photocontrol the activity of a transcription factor (En2) fused into modified estrogen receptors. The tcInd system shows a maximum of absorbance at 469 nm with ε_{tcInd} = 270000 M^{-1} cm^{-1} and upon irradiation tcInd is converted into tcOH and Ind (Scheme I.7).

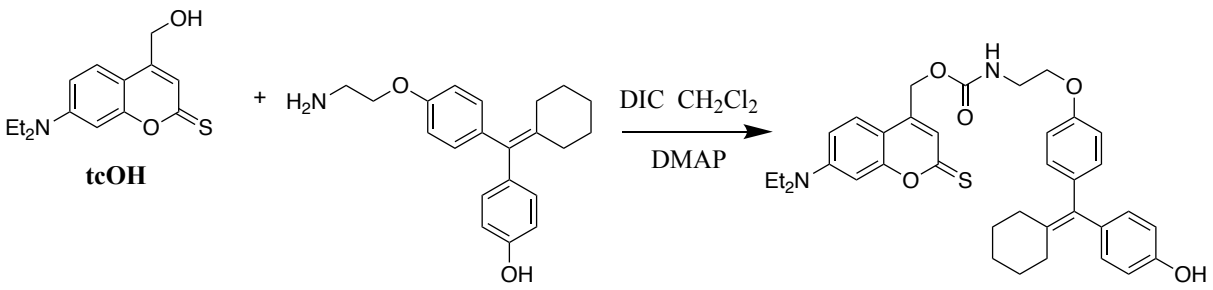

Scheme I.7: Synthesis of a caged thicoumarin-cyclofen system.

Another research work on coumarin groups was established recently aiming to increase the absorption wavelength of these derivatives (Lin *et al.,* 2018). This work focused on the development of new coumarin based PPGs by modifying position 3 by adding an electron rich (donor) styryl moieties which give access to red-shifted absorption wavelengths. Several donor groups were used like 4'-N,N-dimethylaminostyryl (**1a**, Scheme I.8) and julolidinestyryl (**1b**, Scheme I.8), and these groups were also incorporated in the thiocoumarin platforms (**2a** and **2b** Scheme I.8).

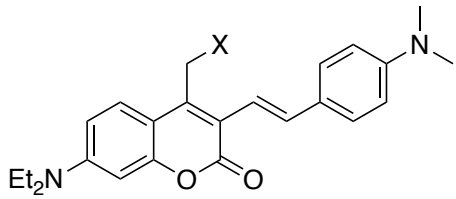

1a
λ_{max} = 446 nm

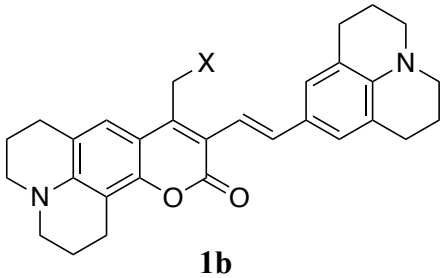

1b
λ_{max} = 467 nm

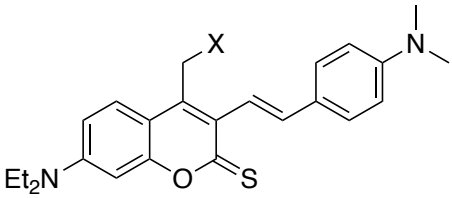

2a
λ_{max} = 490 nm

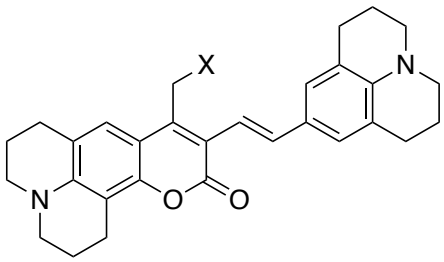

2b
λ_{max} = 515 nm

Scheme I.8: Different structural modifications of coumarin and their effect on the absorption wavelength.

In this study, the incorporation of julolidine rings contributes to a 10 nm shift due to the better conjugation of the amino group with the aromatic core and the incorporation of the sulfur atom induces a 40-50 nm shift due to an intramolecular charge transfer to the empty 3d orbitals of the sulfur atom.

1.3.3.2. Coumarin-Caged Adenosine Cyclic 3',5'-Monophosphates

Fluorescence is very important for following the liberation of the attached biomolecules after irradiation of the caged compounds and can be used to monitor the "uncaging" event. Coumarin derivatives like MCM and DEAC possess a fluorescence emission between 397 and 491 nm in methanol/HEPES buffer depending on the substitution on the coumarinyl moiety.

One drawback of coumarins is that the starting PPG possesses the same fluorescence as the released by-product (MCM-OH) and in this manner the follow up of the uncaging becomes impossible.

Only one example of the uncaging event quantification by fluorescence using a coumarin PPG was reported by Bendig and co-workers (Bendig *et al.,* 1999) in the case of coumarin-caged Adenosine Cyclic 3',5'-Monophosphates (MCM-caged cAMP).

This work focuses on the fact that CM-caged nucleotides are weakly fluorescent whereas their by-product MCM-OH presents strong fluorescence which facilitates monitoring the release process (Scheme I.9).

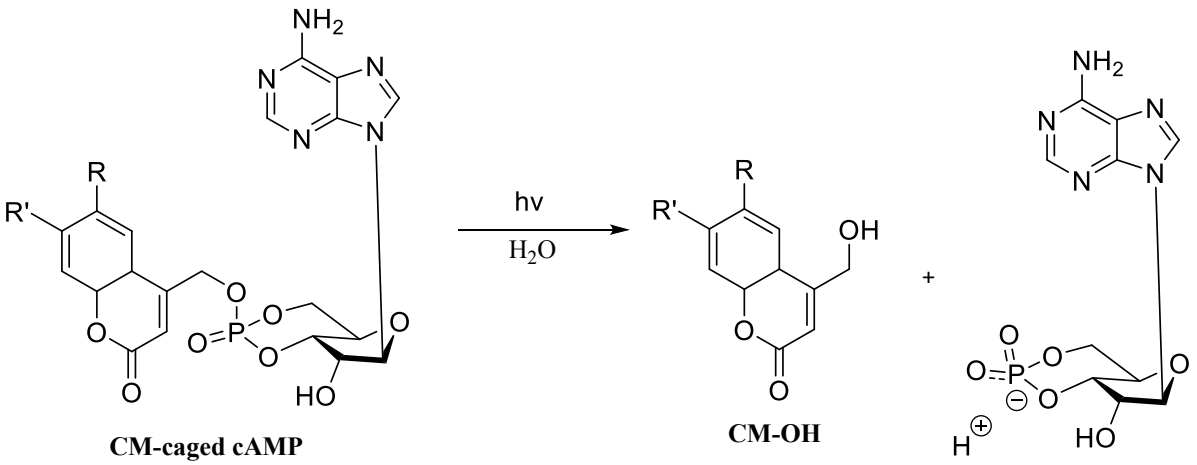

Scheme I.9: Photocleavage of coumarin-caged cAMP

This system is characterized by the difference in fluorescence between the starting caged compound and the uncaging by-product. Normally coumarin-based caged compounds are fluorescent before photocleavage but when attached to adenosine nucleotides they show a very weak fluorescence due to an accelerated internal conversion from the excited state caused by mixing the $\pi\pi^*$ and the $n\pi^*$ states. This energy transfer between the coumarin moiety and the adenosine moiety leads to a drop in the fluorescence or so-called fluorescence quenching. This quenching is advantageous in this case because it helps in quantifying the release of cAMP from the fluorescence observed after photocleavage due to the liberation of the coumarin by-product.

As much as this example is interesting it still has an important limitation were this fluorescence quenching is exclusive for coumarin-caged adenosine and is not valid for other biomolecules attached to coumarins.

1.3.3.3. Coumarins for signaling lipids uncaging at the plasma membrane

Another interesting use of coumarin PPGs was demonstrated by Schultz and co-workers (Nadler *et al.,* 2015) in the end of 2015, this study focused on the use of the fluorescence characteristic of coumarin for plasma membrane-specific photoactivation.

The principle of this study was to synthesize hydrophilic sulfonated coumarin caged fatty acids that shows before uncaging a fluorescent signal on the cellular membrane, followed by a lipid flip-flop. Upon photocleavage by UV light the fatty acid remains in the plasma membrane whereas the coumarin-OH by-product is released inside the cellular space and a fluorescence is observed at the vesicles level due to the entrance of the highly hydrophilic coumarin-OH to these vesicles by endocytosis. With further irradiations the fluorescence signal starts to decrease due to photobleaching (Scheme I.10, Nadler *et al.,* 2015).

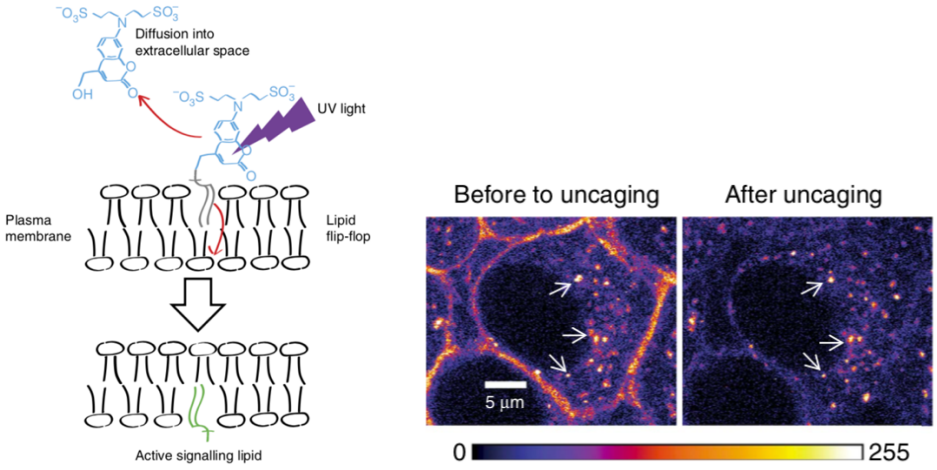

Scheme I.10: The mechanism of plasma membrane photoactivation using sulfonated coumarin caged fatty acid.

This method, that was recently developed using coumarin derivatives, acts as a tool in plasma membrane marking. But yet this method has its limitations since it doesn't provide any information about the concentration jump of the biological effector and it remains a qualitative method (fluorescence) more than quantitative (concentration).

1.3.4.*O*-hydroxycinnamates PPGs

In 2007, inspired by the work of Porter's group in the late 1980s (Turner *et al.,* 1988), Ludovic Jullien and his coworkers (Gagey *et al.,* 2007) investigated the use of hydroxycinnamates for alcohols uncaging. This work focuses on the release of a coumarin by-product and taking advantage of the fluorescence signal induced by this uncaging by-product after photo-cleavage to quantify the release and report the uncaging event. These cinnamates occur in two stereoisomers, the Z and E isomers, induced by light irradiation.

The transformation of the E isomer to the Z isomer under the action of light leads to the liberation of an alcohol along with a coumarin by-product (Scheme I.11).

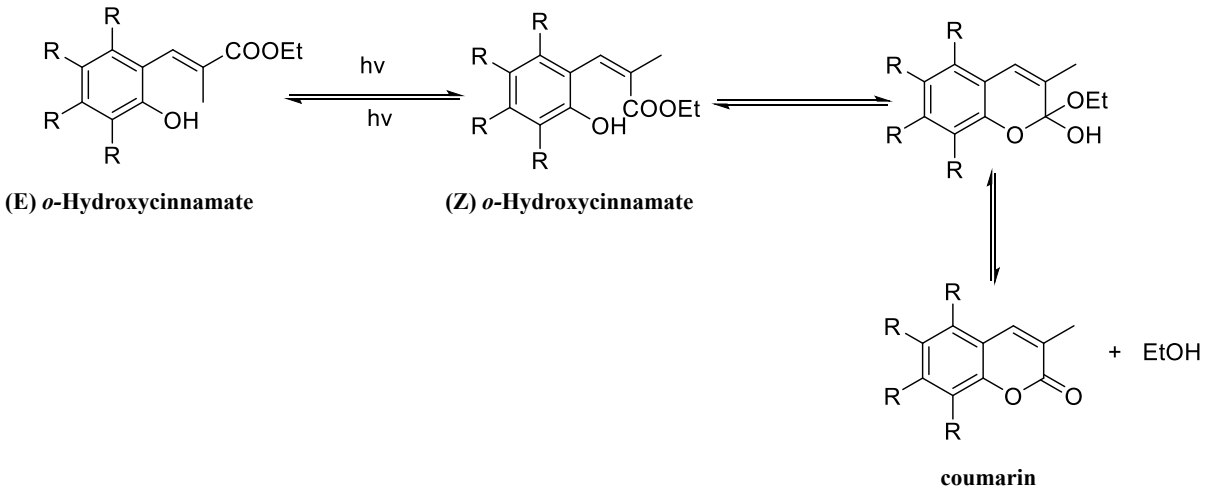

(E) *o*-Hydroxycinnamate **(Z) *o*-Hydroxycinnamate** **coumarin**

Scheme I.11: Mechanism of photo-release of alcohols and coumarin after irradiation of hydroxycinnamates.

Both isomers show weak fluorescence as long as the alcohol is attached, and whenever the alcohol is released under the action of light, strong fluorescent coumarin by-product is released. This signal is helpful to quantify the release of alcohols from these caged-systems.

Another very recent interesting example for the use of *o*-hydroxycinnamates is that illustrated by Paul and his collaborators (Paul *et al.*; 2017). This example introduces excited-state intramolecular proton transfer (ESIPT) induced fluorescent *o*-hydroxycinnamates. ESIPT is an ultrafast enol-keto phototautomerization exhibited by a proton transfer intramolecularly in the excited state.

In this study, ESIPT induces a fluorescence that help monitoring the uncaging in real time by the release of the benzothiazole-coumarin by-product and this study can extend to diverse bioactive molecules containing a terminal hydroxyl function. The ESIPT has two advantageous effects on these hydroxycinnamates; (1) a huge stokes' fluorescence shift (orange color) and (2) a distinct fluorescence color change upon photorelease. In other words, the uncaging is monitored by the drastic change in fluorescence color from orange (hydroxycinnamates) to blue (benzothiazole-coumarin) after photocleavage (Scheme I.12).

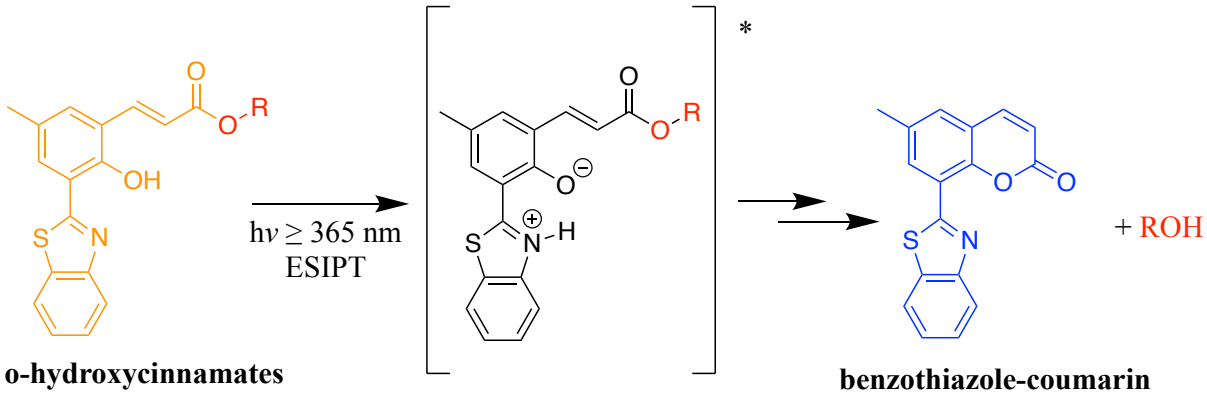

Scheme I.12: Photoinduced uncaging of alcohols from the ESIPT induced fluorescent *o*-hydroxycinnamates.

But still this system has its limitations and drawbacks since these cinnamates tend to auto-isomerize even in absence of light leading to a leak in the biomolecule since the transformation of the E isomer to Z isomer leads to the release of the alcohol attached. Another drawback is that this system is only adapted for the release of alcohols and thus it is not valid for a diversity of biomolecules.

1.3.5. Nitroindoline groups

The 7-nitroindoline (NI) derivatives were first introduced as photo-labile protecting groups in organic synthesis for the protection of carboxylic acids in aprotic medium (Amit *et al.,* 1976). After that, the group of Papageorgiou (Papageorgiou *et al.,* 1999) adapted these derivatives in order to adjust their photochemical properties and to render them useful as photoremovable protecting groups that are stable (in aqueous media) and efficient caged compounds for the photo-release of L-glutamates (Scheme I.13).

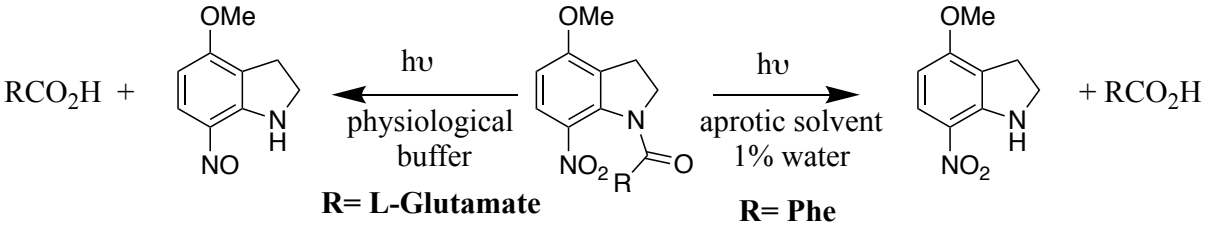

Scheme I.13: Different photolysis pathways for the nitroindoline derivatives with respect to the medium used. In aprotic medium, the irradiation releases a nitroindoline by-product along with the carboxylic acid attached (right pathway). In physiological buffer, the irradiation releases a nitrosoindoline by-product of photolysis along with the release of L-Glutamate (left pathway).

These nitroindoline derivative present a negligible hydrolysis percentage in physiological conditions in contrary to coumarins, and in addition to that, Kerry and his group (Kerry *et al.,* 1988) has demonstrated that the photochemical reaction leads to the liberation of glutamate from nitroindoline is faster (order of nanoseconds) compared to the kinetics of activation of glutamate receptors.

Inspite of their low quantum yields ($\phi = 0.085$), these groups have a very weak basal activity due to the hydrolytical stability (Canepari *et al.,* 2001) making them a good candidate in investigating the central nervous system using caged neurotransmitters.

1.3.6. *O*-nitroaryls

1.3.6.1. *O*-nitrobenzyl groups

The *o*-nitrobenzyl (*o*-NB) groups have been introduced by in 1970 and they have been reported as the most used protecting groups due their efficiency in protecting different functional groups: carboxylic acids, imidazoles, phosphates for the synthesis of nucleosides, alcohols and amines (Patchornik *et al.,* 1970). These groups undergo the following mechanism upon irradiation (Scheme I.14): (a) photoactivation of the nitro function leading to the formation of an *aci-nitro* intermediate (**I_1**), followed by a (b) cyclization to form a 1,3-dihydrobenz-isoxazol-1-ol intermediate (**I_2**), that upon (c) ring opening releases the attached biomolecule (X) along with the nitrosocarbonyl by-product (R=H nitrosoaldehyde, R=Ar, Ph, CH_3,… nitrosoketone).

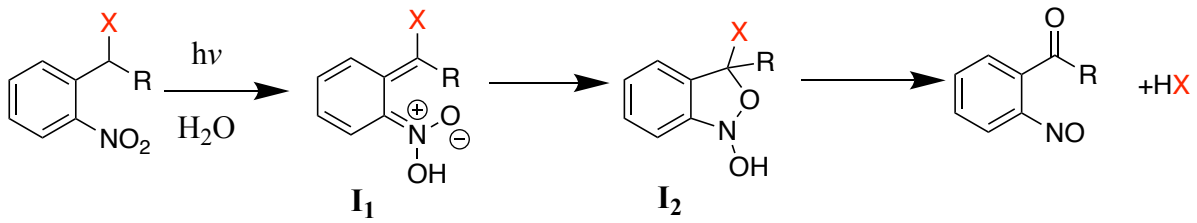

Scheme I.14: Mechanism of photocleavage of *o*-NB protecting groups.

O-nitrobenzylic protecting groups have been the most used PPGs for synthetic and biological applications. One example is the use of *o*-NB under mild conditions for automated RNA and DNA synthesis developed by Stutz and Pitsch (Stutz *et al.,* 1999) by protecting the oxygen atom of the four nucleic bases (Adenine, Cytosine, Guanine, and Uracil) for the synthesis of oligoribonucleotides (Scheme I.15).

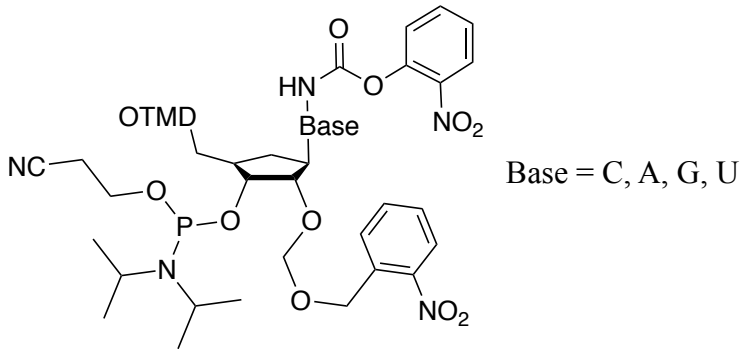

Scheme I.15: *O*-NB caged nucleotides as building blocks for the automated RNA synthesis.

Also, *o*-nitrobenzyl PPGs were used in natural product synthesis like the one reported by Wong in 1993 in the total synthesis of Leukotriene (LTC4). During the final steps of the synthetic route, a deprotection is done by irradiating the *o*-NB-caged system at 350 nm to afford the final compound (Scheme I.16).

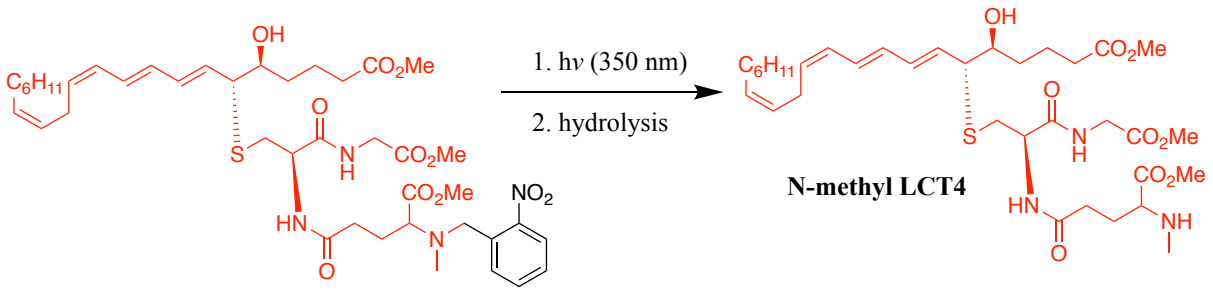

Scheme I.16: Final steps in the total synthesis of N-methyl LTC4.

Over the years, several modifications were applied to this type of PPGs in order to render them more stable, more efficient, and also to increase the quantum yield and/or the wavelength of absorbance (for efficiency in biological applications) together with the rate of release. In order to do that two important modifications were done: (1) substitution in the benzylic position and (2) substitution of the aromatic ring of the *o*-NB group.

1.3.6.1.1. Substitution in the benzylic position

In the 1970s, Woodward has proposed such modification by adding a substituent in the benzylic position. These substituents provide an electronic effect at the benzylic site and also adds a second hydrogen-abstracting unit that helps in increasing the efficiency of the group.

One synthetic drawback could be faced when having a chiral benzylic center (due to a substituent different from the *o*-NB core) because it will be more difficult to protect chiral molecules especially in the synthesis of amino acids and oligonucleotides.

When using substituted *o*-NB core at the benzylic position, a significant increase in the quantum yield of release was observed. This increase could be explained through the mechanism of photocleavage of this family of PPG after the formation of the *aci*-nitro intermediate, leading to the release of nitrosocarbonyl. In the case of substituted *o*-NB, the molecule released is a nitrosoketone which shows a higher quantum yield of release compared to that observed for nitrosoaldehyde (originating from no benzylic position substitution) after photocleavage.

It is also known that water-solubility is really an important criterion for the use of PPGs in biological applications, this property can be achieved by adding substituents that render the molecule more soluble such as COOH functions. Forming more water-soluble groups tend to increase the yield of release compared to that of the non-soluble analog. This was confirmed by an example illustrated by Bassani and his group (Bassani *et al.,* 2010), where α-carboxy-6-nitroveratryl (αCNV) tend to release carboxylic acids with $\phi = 0.17$ and a yield of release 3 times more than the parent compound α-carboxynitrobenzyl (αCNB). This proves that adding a water-solubilizing substituent to the molecule increase the yield of release of the protected compound (Scheme I.17).

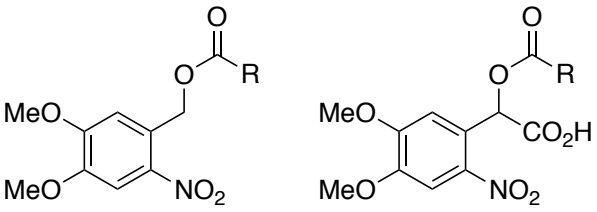

Scheme I.17: Structures of αCNB and αCNV.

1.3.6.1.2. Substitution of the aromatic ring of the *o*-NB group

Due to the drawback of chirality that could be induced by the substitution on the benzylic position and their negligible effect on the absorbance wavelength, numerous modifications have been applied on the aromatic ring of the *o*-NB chromophore.

These modifications could induce 3 important effects: (1) tuning the absorbance wavelength and/or having a better quantum yield, (2) possibility of attaching the compound to a solid support or on a linker and (3) possibility to modify the solubility properties of the molecule. For example, addition of another electron-withdrawing nitro substituent leads to an increase of the quantum yield from 0.13 for **1** to 0.62 for **2** for the release of amines from carbamates.

Another example of modification is the addition of a carboxylic acid with one carbon spacer to form compound **3** making it more soluble than the parent compound **1**. Also, the addition of 2 methoxy group substituents to **1** makes compound **4** absorb at longer wavelength (>350 nm). These examples are illustrated in Scheme I.18.

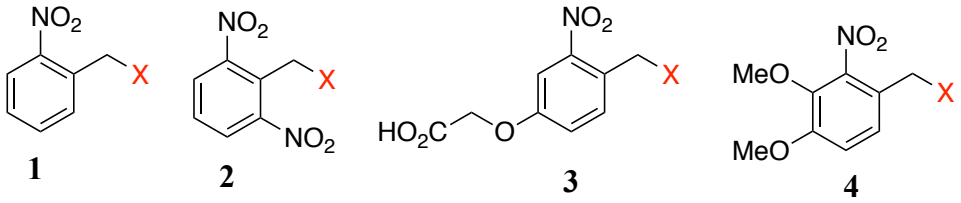

Scheme I.18: Different modification on the aromatic ring of *o*-NB.

As a conclusion, the substitution at the benzylic position and the substitution on the aromatic ring of *o*-NB protecting groups has a significant effect on the photochemical and photophysical properties. Substituent effects are not only of crucial importance for the absorption spectrum of the chromophore but are also prominent for the stability of the C–R bond (where R is the caged function).

By only making minor changes in the substitution pattern of structural derivatives of the *ortho*-nitrobenzyl protecting group it is possible to create PPGs that can be photocleaved with different wavelengths of light ($\lambda_{deprotect}$: 345–420 nm). The most useful way to obtain a bathochromic (red) shift of the absorption band is the addition of an electron-withdrawing group (EWG) at the *para*-position. Additionally, substituting the *ortho*-nitrobenzyl core with a moderately electron-donating group (EDG) like alkoxy (–OR) in the *meta*-position permits cleavage with longer wavelength of light. A significant hypsochromic shift can be obtained by changing the α-substituent with respect to the R-group. Furthermore, extending the linker between the chromophore and the cleavable C–R bond gives similar results. Scheme I.19 shows the shift in wavelength of absorbance depending on the different substitutions and modifications on the molecules.

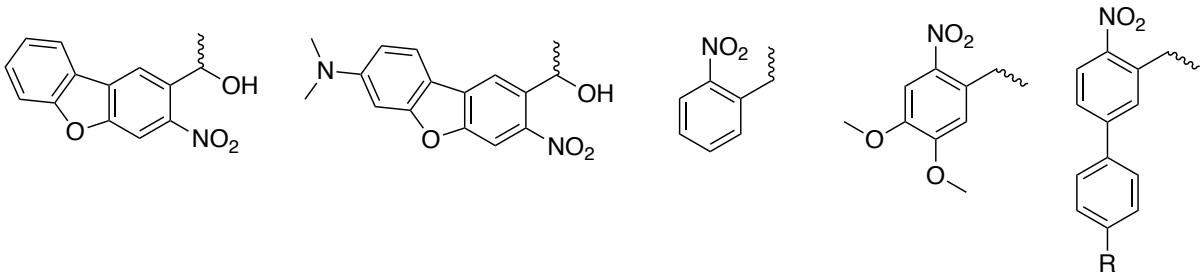

NDBF-OH λ_{abs}=312 nm | **DMA-NDBF-OH** λ_{abs}=424 nm | **NB** λ_{abs}=260 nm | **DMNB** λ_{abs}=355 nm | **NBP** λ_{abs}=405 nm

Scheme I.19: Effect of modification on the aromatic ring and the benzylic position of *o*-NB on the wavelength of absorption.

Alexander Heckel group has demonstrated very recently (Becker *et al.,* 2018) that the addition of a dimethyl amino (DMA) group to the nitro dibenzofuran (NDBF) shifts the wavelength of absorbance from 312 nm to 424 nm. Another system was developed by Specht and his co-workers in 2012 based on a nitro biphenyl core (NBP) with different R groups, this system shows a maximum of absorbance at 405 nm which is due to the conjugation of the nitrobenzene with the second phenyl ring (Donato *et al.,* 2012).

1.3.6.2. *o*-Nitrophenethyl groups

Another interesting series of *o*-nitroaryls is the *o*-nitrophenethyl (*o*-NPP), where the biomolecule is attached on carbon 2 of the ethyl substituent at the *ortho* position to the nitroaryl moiety. These PPGs have been synthesized and tested for their efficiency in photocleavage mainly by Specht's group (Donato *et al.,* 2012 and Herbivo *et al.,* 2013) for the release of GABA and inorganic phosphate. These groups undergo a complex mechanism that was described in 2001 (Walbert *et al.,* 2001). In fact, two mechanistic photochemical pathways for these *o*-NPP groups exist. One of these pathways is a *β*-elimination based pathway (Pathway A) which is commonly known as the major pathway leading to the photo-liberation of the biomolecule in aqueous medium. But there exists a second pathway considered as the minor one which leads to the formation of the nitroso-derivative (Pathway B). This latter mechanism doesn't induce any photolysis leading to photo-liberate biomolecule attached. Upon irradiating the *o*-NPP PPG, it absorbs an amount of energy that permits the system to pass from a fundamental state to an excited state, in this state an *α-exo*-cyclic hydrogen transfer towards the nitro group occurs, that leads to the formation of the *aci*-nitro intermediate which is kinetically favored (Scheme I.20).

The acid-base equilibrium of the *aci*-nitro intermediate is the determining step of which photochemical pathway is adopted. The weak basic character of water is sufficient for the deprotonation of the aci-nitro intermediate to form a new anionic form which undergoes further a *β*-elimination liberating the biomolecule along with *o*-nitrostyrene (Pathway **A**, Scheme I.20). In the presence of an acidic medium (millimolar order of hydrochloric acid) the acid base equilibrium is shifted toward the formation of the neutral *aci*-nitro intermediate which then favors the formation of a cyclic intermediate followed by the formation of the *o*-nitroso derivative (Pathway **B**, Scheme I.20).

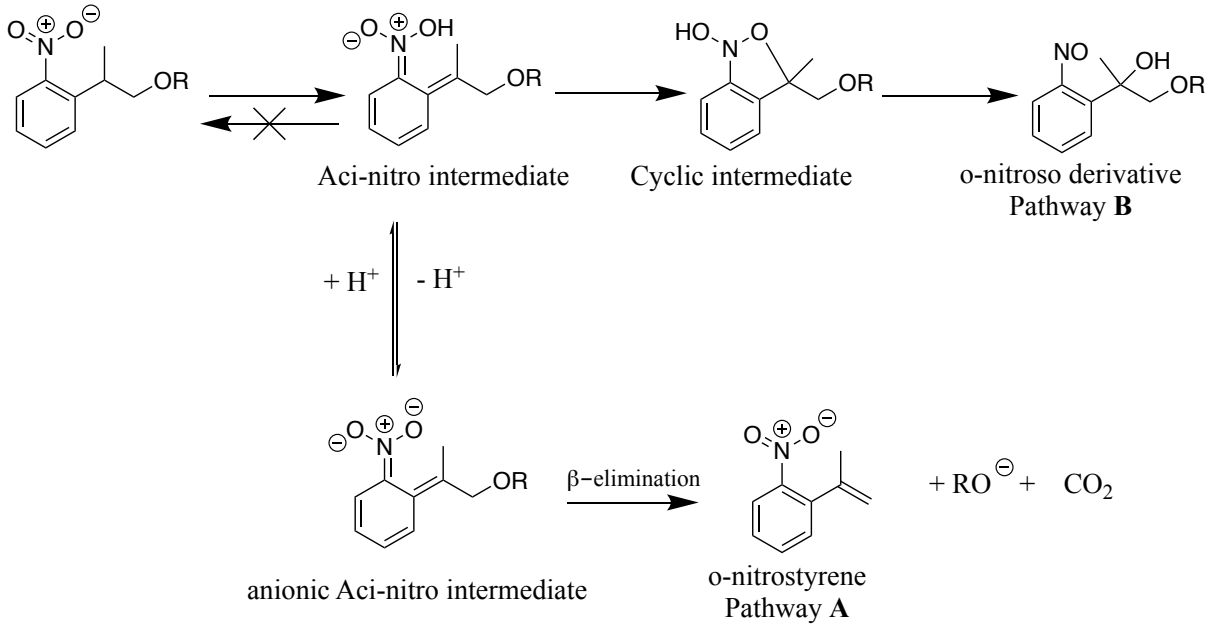

Scheme I.20: Mechanism of photo-liberation of a biomolecule from the *o*-NPP series following 2 pathways: (**A**) which is the favored mechanism in basic medium releasing *o*-nitrostyrene along with the liberation of the biomolecule and (**B**) which is favored in "acidic" medium and forms *o*-nitroso derivative and doesn't permit the liberation of the biomolecule.

The removal of the organic molecule attached to the protecting groups mentioned previously (among many others) necessitates the use of UV-near visible irradiations. It is well known that these irradiation wavelengths are not biocompatible since these lights are absorbed by tissues mainly oxyhemoglobin which absorbs every light below 650 nm. On the other hand, water molecules become absorbent at wavelengths >950 nm. Depending on this information a "phototherapeutic window" could be defined for the tissue transparency above 650 nm and below 950 nm (Scheme I.21, Juzenas *et al.,* 2002).

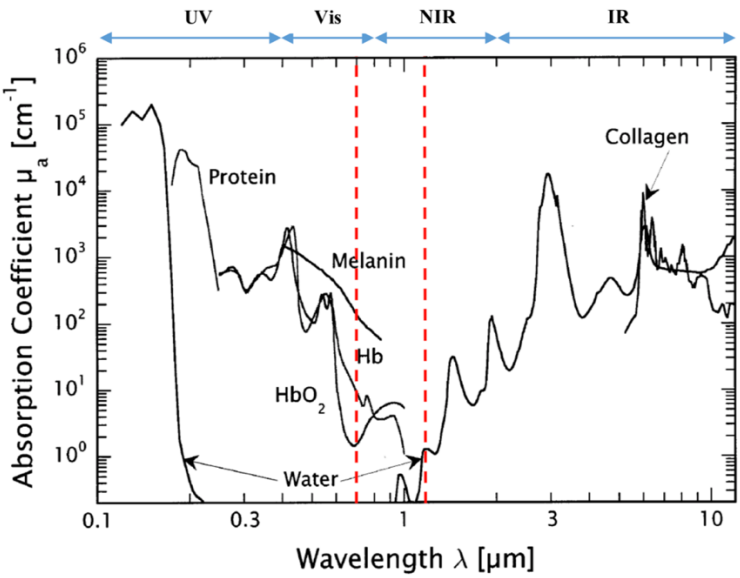

Scheme I.21: Transparency window for living tissue absorbance showing the absorption spectra of various endogenous relevant molecules.

The majority of chromophores absorb light in the regions below 400 nm and some caged compounds absorb visible light which makes them very complicated to handle. In addition to that, the use of wavelengths between 650-950 helps in reducing photodamage and phototoxicity as well as increasing the depth of tissue penetration. In order to overcome these problems and to use a diversity of PPG in biological applications an important approach is the use of two-photon excitation (2-PE).

2. Two-Photon Excitation

2.1. Overview

The use of mono-photonic excitation in the field of *in vivo* applications of Photoremovable Protecting Groups has been problematic until the introduction of two-photon excitation was proposed. This technique uses types of irradiations different from those used for the classical mono-photon excitation. The two-photon excitation functions in a non-linear optic process defined by the following equation (1):

$$P \propto \frac{1}{2}\delta_a I^2 \qquad (1)$$

Where P is the molecule excitation probability, δ_a is two-photon absorption cross section. The efficiency of a molecule to absorb two photons is expressed in GM (1 GM = 10^{-50} cm^4. s. $photon^{-1}$) in the honor of Maria Goeppert-Mayer that was the first to introduce the theoretical phenomenon of non-linear optics in 1930 (Goeppert-Mayer *et al.,* 1931). Finally, I is the light intensity of the excitation source. P is directly proportional to the square of the light intensity I, this shows that the possibility to excite a molecule will be higher in the zone where the light intensity is at its maximum. In other words, the focal point of the optical system used for irradiation in 2-PE presents the highest light intensity for excitation whereas in the classical confocal microscopy the excitation takes place over the full optical length (Scheme I.22).

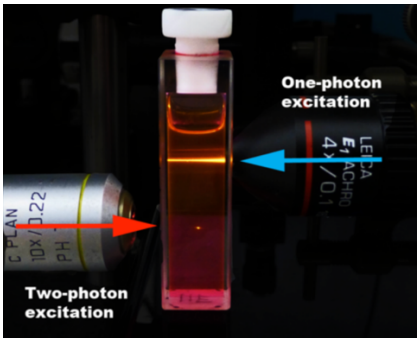

Scheme I.22: Difference in fluorescence emission between mono and bi-photonic excitation.

This phenomenon was used in the development of 3D imaging, photonics, photodynamic therapy… The two-photon excitation technique requires light irradiations with very high intensities which can only be achieved by using ultrafast pulsed laser like the titanium:sapphire laser that provides 3 mm bean at 100 fs pulse duration with a frequency of 90 MHz. This laser type provides optimum radiations at 800 nm which is compatible with biological applications and corresponds to minimum mammalian tissue absorbance.

The excitation of a molecule is observed when the molecule absorbs one or more photons with a certain energy in order to pass from the fundamental ground state to the excited state. In order for this to happen, the molecule absorbs either one photon with E = hν (mono-photonic absorption) or two photons with E = hν/2 (bi-photonic absorption). Using lower energy for 2-PE reduces photodamage and cytotoxicity and using higher excitation wavelengths reduces the risk of tissue proteins absorbance and mutations (Scheme I.23, Benninger and Piston, 2013).

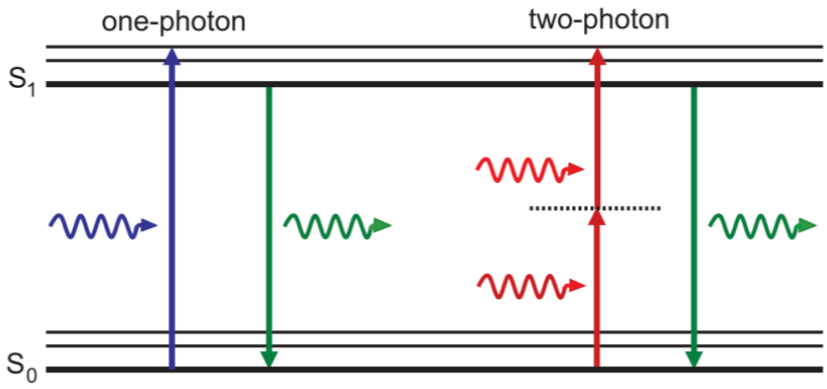

Scheme I.23: Simplified Jablonski (energy-level) diagram of conventional one-photon excitation (left) and nonlinear two-photon excitation (right). In each case, the absorption of photon(s) populates an excited state from which the molecule can relax by emitting a photon.

2.2. Design

In order to increase the efficiency of compounds to increase their two-photon excitation sensitivity, several approaches have been developed on fluorophores and chromophores. Numerous chromophore geometries have been investigated; linear (1D), planar (2D) and tetrahedral (3D) structures, and these investigations led to the construction of the optimal and typical chromophore architecture.

The smallest system to be useful in biology is composed of a donor (D)-acceptor (A) system with π-system cores incorporated in the system as well. The extension of the π-system (increase in conjugation) improves the 2-PE properties of the molecule (Scheme I.24).

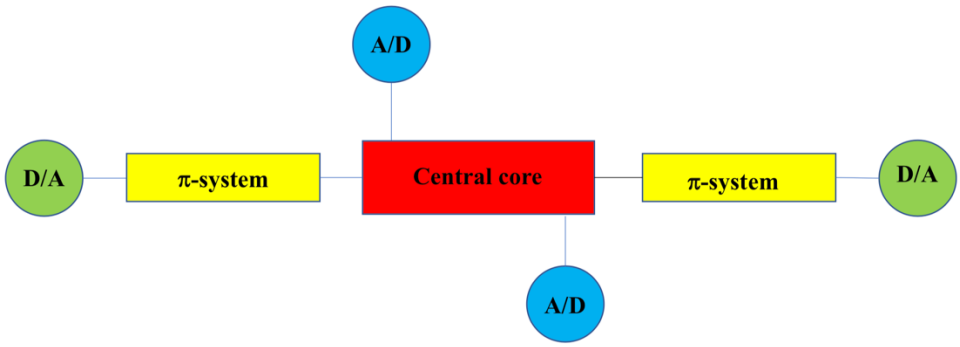

Scheme I.24: Typical structure of 1D two photon absorption chromophore

A wide range of electron-donating and electron-accepting terminal groups have been investigated including many π-deficient heterocycles (Albota *et al.,* 1998, Mongin *et al.,* 2007 and Terenziani *et al.,* 2008) and it was found that D-π-D and D-π-A-π-D structures are more efficient than A-π-A and A-π-D-π-A systems (Pawlicki *et al.,* 2009) as shown in Scheme I.25.

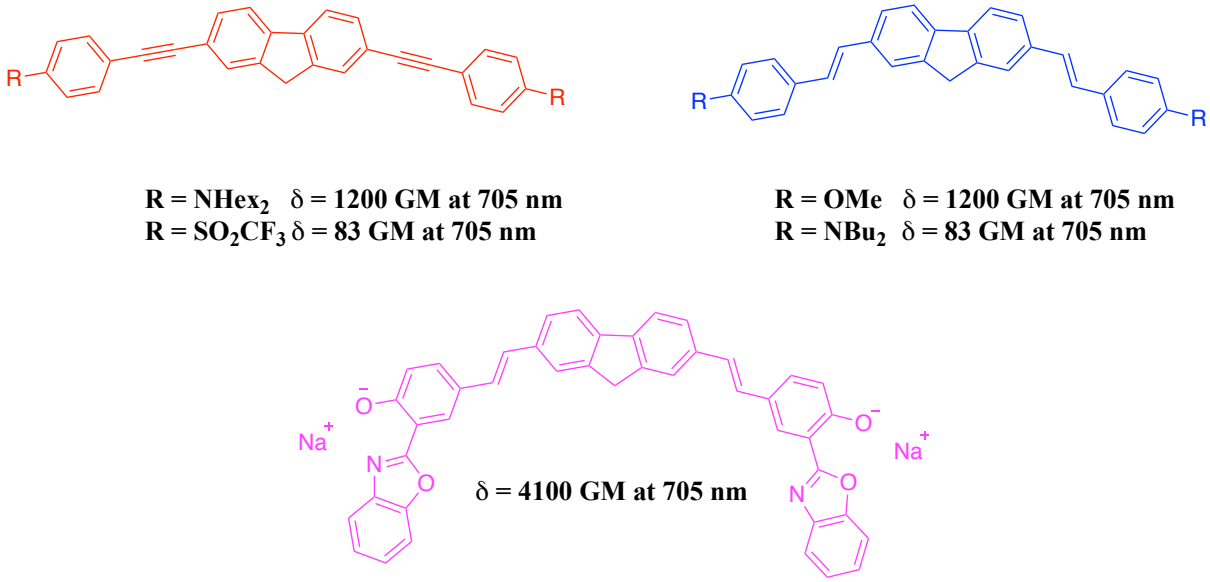

R = $NHex_2$ δ = **1200 GM at 705 nm**
R = SO_2CF_3 δ = **83 GM at 705 nm**

R = OMe δ = **1200 GM at 705 nm**
R = NBu_2 δ = **83 GM at 705 nm**

δ = **4100 GM at 705 nm**

Scheme I.25: Variation of two-photon action cross section by structural modifications.

It is known that the use of electron donating groups (EDG) like alkylamino increases the two-photon efficiency more than electron accepting groups (EAG) like SO_2CF_3. And also, the use of alkylamino as EDG is more efficient than using alkoxy or other oxygen-based donors. And it is remarkably interesting to use phenoxides which are very strong donors and give very high 2-PE cross sections as in the case of the pink molecule in Scheme I.25 (Pawlicki *et al.,* 2009). Similarly to mono-photon absorption, it is possible to determine the two-photon uncaging action cross section (δ_u) of a molecule by multiplying the two-photon absorption cross section (δ_a expressed in GM) by the two-photon quantum yield of uncaging (ϕ_u):

$$\delta u = \delta a \,.\, \phi u \qquad (2)$$

Not all PPGs present a structure that shows efficiency in two-photon excitation since few PPGs have the donor-acceptor core with an extended π-system. It has been demonstrated that a photoremovable protecting group with $\delta_a < 0.1$ GM and $\phi_u < 10\%$ is considered as non-efficient for biological applications (Corrie *et al.,* 2005).

In order to develop new molecules with good performance in 2-PE, there are several factors that influence the values of the two-photon absorption cross section (δ_a) (He *et al.,* 2008; Pawlicki *et al.,* 2009).

The main parameters that affect these values of δ_a are mainly the (a) presence of a coplanar conjugated system in the main structure and its length, (b) the presence of electron donating and/or electron accepting groups, (c) the rigidity or flexibility of the likers between the donor-acceptor moiety and (d) the nature of the linker (alkene or alkyne). (Scheme 26).

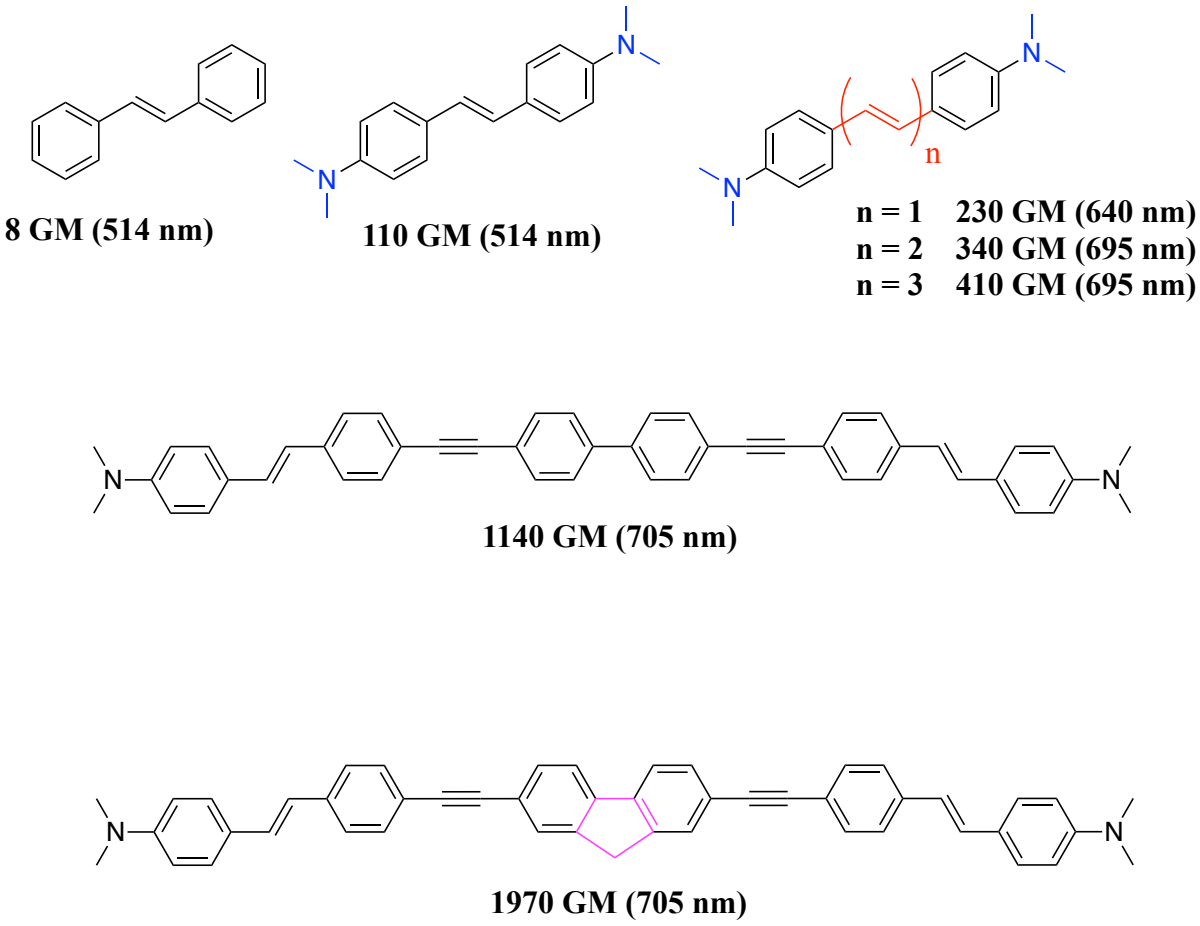

Scheme I.26: Structural modifications of different systems with efficiency in two-photon excitation.

As shown in the scheme above, 3 important factors or structural modifications have a huge influence on the values of δ_a: (1) the addition of electron donating groups (blue) like dimethylamino, (2) the extension of the conjugation inside the molecule (red) that favors the electrons delocalization and (3) blocking the free rotation of the molecule by making the structure more rigid (pink).

These important factors that show an effect on the values of δ_a have led to identify a series of photoremovable protecting groups sensitive to bi-photonic excitation.

With several modification in the structures of these groups initially used in mono-photon excitation, these groups became active in two-photon excitation, like the example of the *ortho*-nitrophenethyl series *o*-NPP (Scheme I.27).

The addition of electron donating/accepting groups or the extension of the conjugation inside the molecule as well as rendering the structure more rigid led to the transformation of these *o*-NPP from mono-photon sensitive groups to two-photon active molecules for the liberation of *γ*-amino butyric acid (GABA) and Glutamates (Glu).

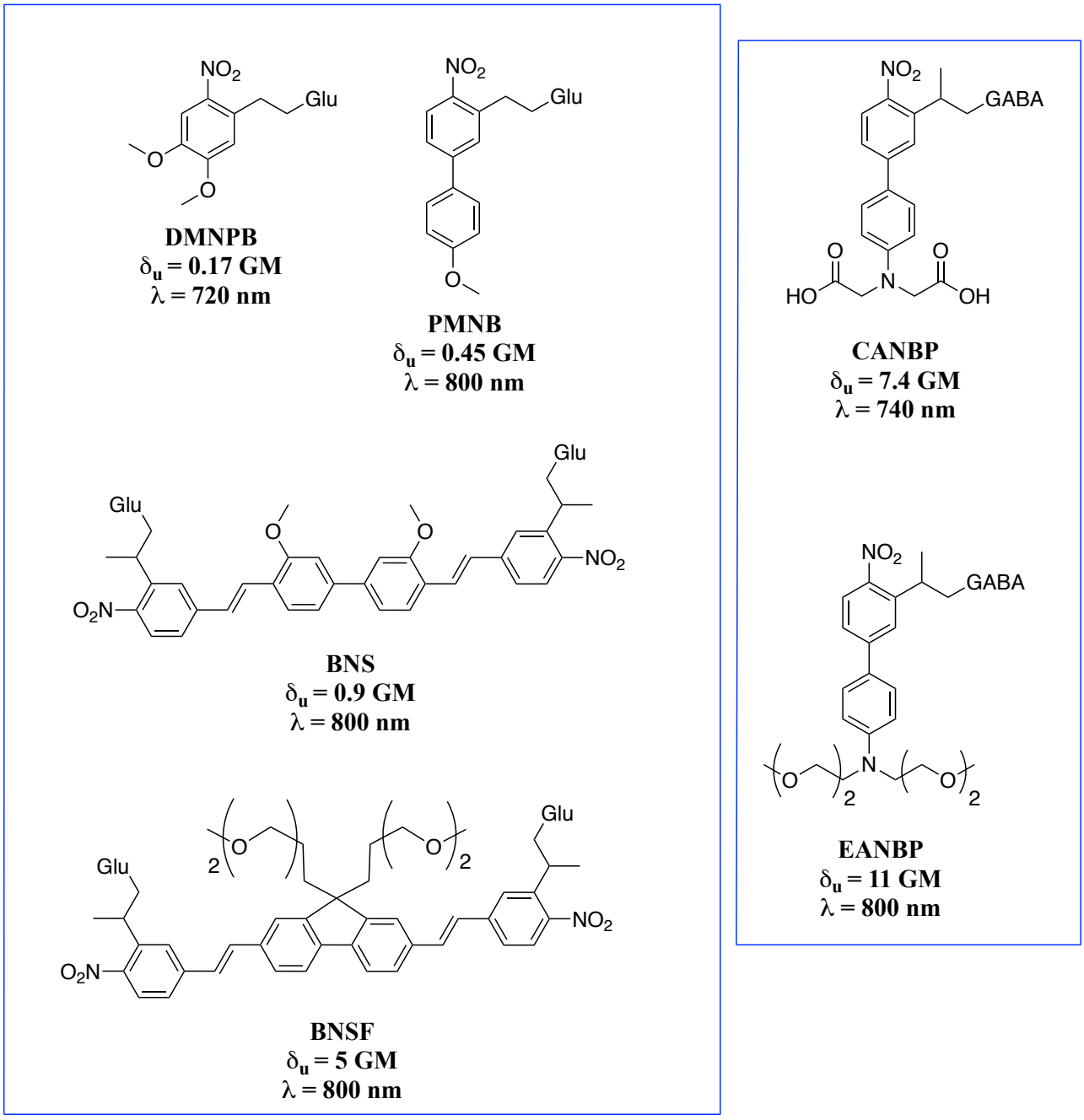

Scheme I.27: Effect in the structural modification on the value of δ_a for the *o*-NPP series used for two-photon liberation of Glutamates (left) and *γ*-amino butyric acid (right).

3. Applications of two-photon sensitive PPGs in biology

Photoremovable protecting groups have made a breakthrough in the domains of synthesis, inorganic chemistry, biochemistry and biology. The development of these groups has attracted the researchers' attention for several years now and their use is biological applications is providing access to novel methods to control the functions of the cells such as cellular regulations that can be temporally and spatially defined.

Photomanipulation of cellular chemistry using caged compounds especially those sensitive to two-photon excitation can allow light to pass through the cellular membrane allowing the release of a biomolecule into the cytoplasm and also irradiation at the extracellular region allows to observe changes like the case mentioned in section 1.3.3.3 for the coumarins used in cell signaling lipids. Also, in the domain of caged biomolecules, *o*-nitroaryls have also made a breakthrough in numerous domains of biology and the results obtained were interesting and promising in the field. The control of biological systems dose-dependently in time and space is a key requirement for studying dynamic cellular processes in tissues or organisms in *vivo*. The use of photolabile groups attached to a biomolecule can render biologically active compounds inactive. This approach typically leads to excellent ON/OFF behavior and has formed the basis of very interesting studies in chemical biology and material sciences. Two-photon excitation can achieve tissue penetration using near-IR light reaching up to 1 cm depth. Several interesting applications will be discussed in the coming section.

3.1. Light control release of neurotransmitters

Caged neurotransmitters are useful photochemical tools for selective stimulation of synapses. Before illumination, the caged compound is biologically inert. Photolysis breaks a covalent bond, liberating the neurotransmitter. Release can be rapid, so the resultant synaptic stimulation can mimic a natural one (Matsuzaki *et al.,* 2001). Uncaging does not replace traditional electrode stimulation commonly used to study the neurotransmission; rather, it is a useful complementary method to it for several reasons: (1) a single neurotransmitter is normally photoreleased, (2) stimulation of voltage-gated ion channels is not required for neurotransmitter release, (3) receptors at many synapses can be activated simultaneously according to the area (or volume) of illumination and (4) subquantal or supraquantal neurotransmitter release is feasible. Photochemical uncaging of neurotransmitters is especially useful when studying neurons in acutely isolated brain slices (Callaway *et al.,* 2002).

3.1.1. Two-Photon Uncaging of GABA (the principal inhibitory neurotransmitter)

GABA is one of the major inhibitory neurotransmitters in the adult brain, but the description of caged GABA has been limited to few examples. One example is the use of two-photon uncaging of GABA from CDNI (4-carboxymethoxy-5,7- dinitroindolinyl) in brain tissues but this cage shows low two-photon uncaging cross section (δ_u = 0.3 GM at 720 nm).

Another example for two-photon uncaging of GABA is N-DCAC- GABA (N-DCAC = 7-(dicarboxymethyl)-aminocoumarin) at 800 nm on hippocampal neurons in brain slices.

This system has two limitations: (1) the low two-photon excitation efficiency of 0.37 GM at 800 nm and also (2) the long half time of GABA release (4 ms). The release of GABA is an important field of study and it is yet challenging in the neuroscience domain to develop a two-photon efficient caged-GABA. In 2012, Donato and co-workers have described the release of the GABA neurotransmitter at 800 nm using a two-photon sensitive photoremovable protecting group based on a *o*-nitrobiphenyl core (Donato *et al.,* 2012). The same group have been developing two-photon efficient groups in the 2-(*o*-nitrophenyl)-propyl series with donor-acceptor chromophores with high two-photon absorption cross sections like the PMNB cage mentioned above for the release of glutamates with a two-photon uncaging efficiency of 3.1 GM at 740 nm. Replacing the alkoxy donor group with a functionalized di-alkylamino leads to the formation of a new PPG with improved solubility and an increased two-photon uncaging cross section up to 11 GM at 800 nm. The new groups: 2-(4'-(bis(carboxymethyl)amino)-4-nitro-[1,1'- biphenyl]-3-yl) propan-1-ol (CANBP) and 2-(4'-(bis((2-methoxyethoxy)ethyl)amino)-4-nitro-[1,1'-biphenyl]-3-yl) propan-1-ol (EANBP) were used for the rapid and spatially controlled GABA release in intact brain slices. EANBP-GABA samples were irradiated at 405 nm in a phosphate buffer (pH = 7.4) and it was obvious the caged compound's concentration started to decrease as the irradiation times increase and a new absorption band related to the uncaging by-product starts to appear with time (Scheme I.28).

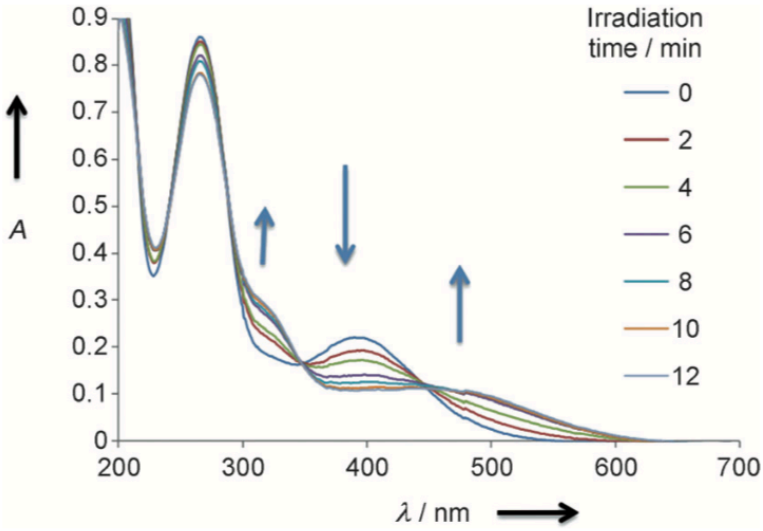

Scheme I.28: UV/Visible spectrum changes of EANBP-GABA during photolysis at 405 nm in phosphate buffer (50 mM pH 7.4).

The caged CANBP-GABA system was tested *ex vivo* to evaluate the release of GABA at the neuronal level of intact brain tissue. A voltage clamp recording was performed in rat cortical brain slices to record the outward GABAergic currents.

An 800 nm laser light was scanned over the aptical dendrite (Scheme I.29, A) and results in an outward current (Scheme I.29, B-CTR) that validates the fact that GABA was released from the cage molecule during the light scanning. Another experiment was done by blocking the GABA channel receptors using picrotoxin (PTX) which led to a complete destruction of the current confirming that the current previously obtained was completely originated from the GABA receptors activated by the GABA released after photocleavage (Scheme I.29, B-PTX).

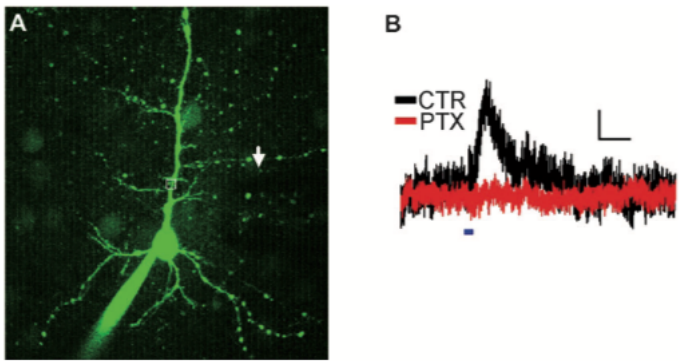

Scheme I.29: Laser light scanning (λ = 800 nm) of aptical dendrite of rat cortical brain slices (A) and the resulting current recording upon GABA release (B - black) and its destruction upon the use of GABA channel blockers (B - red).

This research work has validated that changing the alkoxy group into a PEG or bis (carboxymethyl) amino group increases the solubility of the molecule in water and also enhances the efficiency of uncaging of GABA.
The two studied molecules of the 2-(*o*-nitrophenyl)-propyl series has proven to have interesting activity in two-photon excitation (up to 11 GM) at wavelengths compatible with biological experiments (800 nm).

3.1.2. Two-Photon Uncaging of Glutamates (the principal excitatory neurotransmitter)

Glutamate is generally acknowledged to be the most important transmitter for normal brain function. Nearly all excitatory neurons in the central nervous system are glutamatergic, and it is estimated that over half of all brain synapses release this agent. Glutamate plays an especially important role in clinical neurology because elevated concentrations of extracellular glutamate, released as a result of neural injury, are toxic to neurons.
Ellis-Davies and his group have synthesized a caged glutamate (4-carboxymethoxy-5,7-dinitroindolinylglutamate or **CDNI-Glu**) that releases glutamate with an uncaging quantum yield of 0.5 GM (Ellis-Davies *et al.,* 2007).

A small comparison between this new cage and the 4-methoxy-7-nitroindolinylglutamate or **MNI-Glu** (developed by Corrie *et al.,* 1999 and Matsuzaki *et al.,* 2001) showed that the CDNI cage is 6 times more efficient (quantum yield is 6 times higher) than the MNI cage in monophoton irradiations (350 nm) and two-photon excitation at 720 nm. The structures of MNI-Glu and CDNI-Glu are represented in the Scheme I.30.

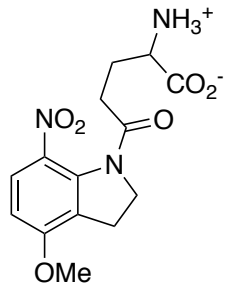

MNI-Glu

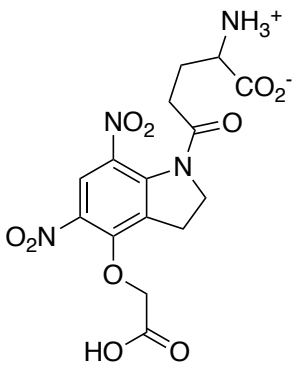

CDNI-Glu

Scheme I.30: Structures of MNI-Glu and CDNI-Glu.

AMPA-type glutamate receptors open with rise-times of approximately 100 –500 μs, so, ideally, the rate of glutamate uncaging should be 100,000/s.

Irradiations were done on neurons in isolated cortical brain slices and it was evident that the response of glutamate receptors was higher when using CDNI-Glu and the AMPA-receptor induced current was four to five times larger than that of MNI-Glu (Scheme I.31).

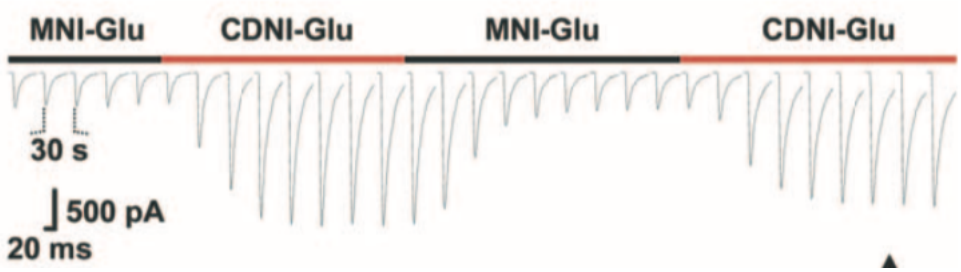

Scheme I.31: AMPA-receptor current induced upon the release of glutamate after uncaging from MNI (black) and CDNI (red).

Another example of the design of caged glutamates was the one by Specht's group (Gug *et al.,* 2008), where they designed a series of two-photon sensitive caged glutamates with efficiencies that were never reported for caged glutamates. The design focused on several chemical modifications that help in red-shifting the wavelength of absorbance and also the two-photon efficiency of uncaging. The main modifications were adding electron-donating groups or by extending the conjugation by adding π systems (Scheme I.32).

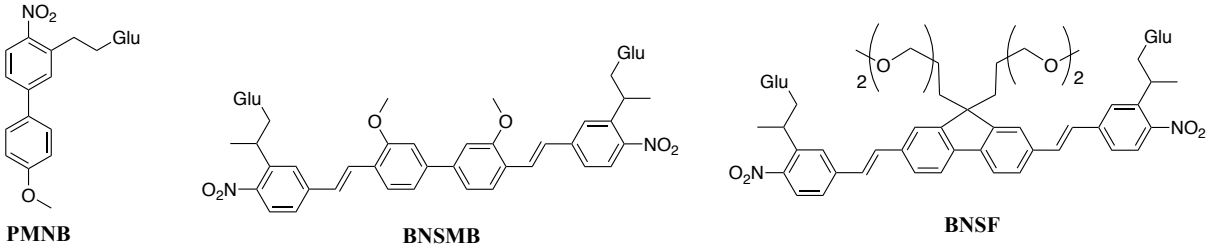

Scheme I.32: Structure of the new caged glutamate with high two-photon efficiency.

These newly developed groups show interesting advantages on previously designed caged-glutamates like CDNI-Glu and MNI-Glu. Caged glutamates **BNSMB-Glu** and **BNSF-Glu** afforded 60 % and 65 % yields of glutamate release per glutamate unit, respectively. As each caging system incorporates two caged glutamates, the overall yield of glutamate release reaches 120% per molecule. A significant red-shift is evident for these two new cages, as well as a strong increase in molar extinction coefficient (Table 2).

Caged Glutamate	λ_{max} (nm)	ε (λ_{max}) [M^{-1} cm^{-1}]	$\delta_u\phi_u$ (GM)
BNSMB-Glu	400	39340	0.9
BNSF-Glu	415	63960	5.0
MNI-Glu	350	4300	0.06
CDNI-Glu	350	4500	0.5
PMNB-Glu	317	9900	0.45

Table 2: One- and two-photon photophysical properties of caged glutamates.

These examples of caged-GABA and caged-Glutamates have demonstrated the importance of the use of two-photon sensitive photoremovable protecting groups in neuroscience.

The design of several PPGs has led to a breakthrough for the use of caged neurotransmitters, and it has led to the introduction of new families of two-photon sensitive caged neurotransmitters that recently showed interesting photophysical properties in terms of absorption wavelength, molar extinction coefficient, yield of neurotransmitter release and two-photon uncaging cross section.

3.2. Calcium as second messenger in physiological and biochemical processes.

Photomanipulation of cellular chemistry using caged compounds provides a uniquely powerful means to interact with such cellular dynamics, as it can touch upon any one of the above dimensions. Thus, since light passes through cell membranes, uncaging can rapidly release a biomolecule in an intracellular compartment. This space is not readily accessible to many second messengers (inositol-1,4,5-trisphosphate (IP_3), ATP, Ca^{2+}, cAMP, cGMP) when they are applied to cells externally, as their charge makes them impermeable to the plasma membrane. Furthermore, uniform illumination results in release throughout the cytosol, or the release can be localized by focusing the uncaging beam on one part of a cell.

Calcium is an important second messenger for wide variety of physiological and biochemical processes such as muscle contraction, neurotransmitter release, ion-channel gating, exocytosis, etc… One approach for the use of calcium developed by Tsien and co-workers (Tsien *et al.,* 1988) that involves reducing the Ca^{2+}-buffering capacity of a 1,2-**b**is(*o*-**a**mino**p**henoxy)-ethane-N, N, N', N'-**t**etraacetic **a**cid derivative (BAPTA).

Another approach was that described by Ellis-Davies and his group (Ellis-Davies *et al.,* 1994), that consists on synthesizing photosensitive derivatives (NP-EGTA) that have high affinity for Ca^{2+} that upon irradiation produces two moieties that are known to have very low affinity to Ca^{2+} and thus the bound calcium ions are released (Scheme I.33). Upon irradiation, the coordination sphere of calcium with the chelator is broken into diacetic acid by-products that show very low affinity towards calcium ions that are freely released inside the medium.

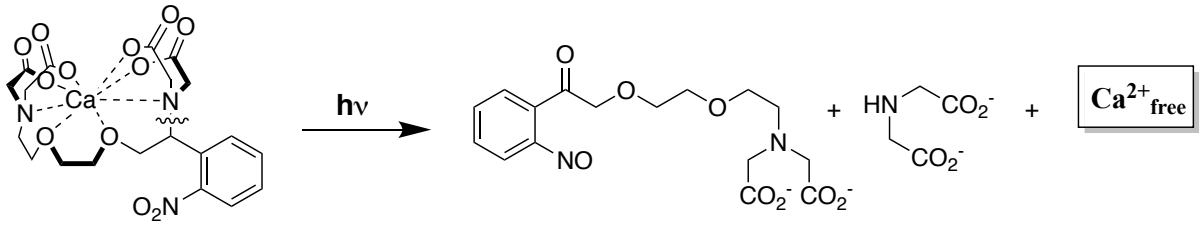

NP-EGTA

Scheme I.33: Photorelease of Ca^{2+} from NPEGTA. Ca^{2+} is liberated from the chelator cation complex by lysis of the chelator backbone. The two imino di-acetic acid photoproducts have a lower affinity for Ca^{2+}.

Normally, PPGs are linked by covalent bonds to the biomolecule, but in the case of calcium ions uncaging, new strategy has been developed focusing on the synthesis of photolabile groups with known high affinity calcium chelators (BAPTA, EDTA, and EGTA) releasing by-product with much lower affinity to calcium and thus releasing free Ca^{2+} in the system.

Another interesting and more recent example for photo-releasable caged calcium was the one described in 2016 (Agarwal *et al.,* 2016). Uncaging remains a uniquely powerful way to control the concentration of intracellular calcium ions. An *o*-nitrobenzyl based cage was developed by Ellis-Davies and co-workers with a new chromophore; **biss**tyryl**t**hiophene (BIST, blue core Scheme I.34). This PPG has a one-photon absorption maximum at 440 nm and also shows a large two-photon absorption cross-section of at least 250 GM in the range of 720-830 nm. A photosensitive PPG was developed using ethylene glycoltetra-acetic acid (EGTA) as a Calcium chelator that upon photoirradiation releases the nitroso derivative of BIST along with the amino diacetic acid and the free calcium ions (Scheme I.34).

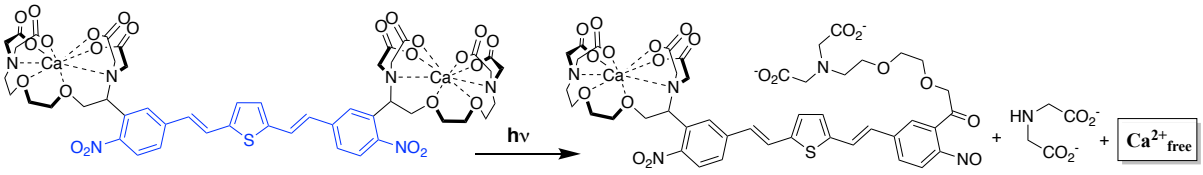

Scheme I.34: Photo-liberation of calcium ions from *o*-NB-BIST-EGTA caged chelator.

Since this calcium caged BIST shows high efficiency in two-photon, it was used for the photocontrol of local Ca^{2+} signaling. In cardiac myocyte cells a small amount of Ca^{2+} enters the cytoplasm upon depolarization and initiates Ca^{2+}- induced Ca^{2+} release from the sarcoplasmic reticulum (SR) store. Such release events can remain highly localized or initiate "Ca^{2+} waves" that propagate through the cell.

Some of the cells were treated with caffeine, this latter completely offloads calcium ions from SR and allows the pure photolytic calcium to be detected. Examined myocytes were loaded with BIST-2EGTA and rhodamine (rhod-2) as a fluorescent dye, followed by a two-photon irradiation at 810 nm releasing calcium ions in a larger manner than that observed with BIST-2EGTA in caffeine-treated cells (Scheme I.35).

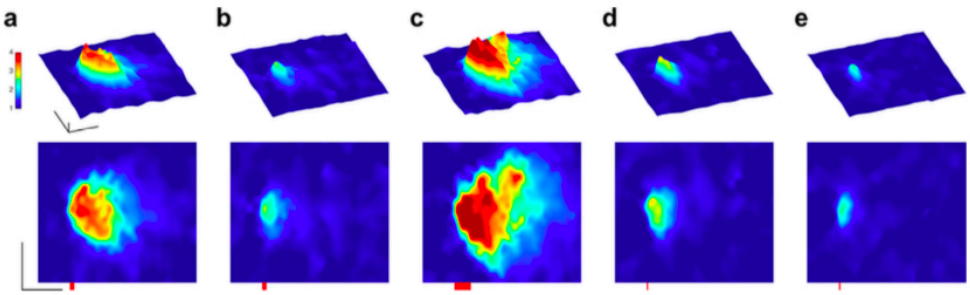

Scheme I.35: Localized control of Ca^{2+}-induced Ca^{2+} release in cardiac myocytes using 2P photolysis. Single cardiac myocytes were loaded with BIST-2EGTA and rhod-2. Changes in $[Ca^{2+}]_{free}$ were monitored in line scan mode using laser-scanning confocal microscopy at 561 nm after 2P uncaging at the center of the line with a mode-locked Ti:sapphire laser tuned to 810 nm. (a) Point 2P irradiation with 5 ms pulse (red bar) triggered local Ca^{2+}-induced Ca^{2+} release from the SR. (b) Photolysis of BIST-2EGTA produced highly spatially confined Ca^{2+} release. The cell was treated with caffeine (20 mM) to unload the Ca^{2+} from the SR. (c) Increasing pulse duration to 20 ms initiated a Ca^{2+} "mini" wave, with discrete Ca^{2+} release events apparent beyond the initial uncaging location. (d) Reducing pulse duration to 1 ms produced rapid, efficient, and highly localized Ca^{2+}-induced Ca^{2+} release. (e) Pure photolytic release of Ca^{2+} from BIST-2EGTA during irradiation for 1 ms (cell treated with caffeine as in b).

The newly developed BIST protecting group showed to be an exceptional photosensitive caged Ca^{2+} probe that presents interesting activity in one-photon and two-photon excitation. This cage molecule was used to quantify the release of calcium ions inside cells and to photocontrol calcium ion signaling as well.

3.3. Light control of Protein Expression

Generally, RNA is known as an essential molecule involved in various biological roles, particularly, in regulating gene expression: messenger RNA (mRNA) and interfering RNA (iRNA). These two types of RNA have become the most used tools to study gene expression. However, it is very difficult to regulate such molecules through a strictly optogenetic-based approach. In order to overcome this difficulty, making these mRNA/iRNA spatially and temporally controllable, by the use of light as an activator, would broaden their range of use. Therefore, the use of a chemical approach, using photoremovable protecting groups, helps in strictly applying an optogenetic approach; light-controlled of protein expression.

3.3.1. DNA Hybridization by Two-Color Two-Photon Uncaging

In a recent study by Heckel group in collaboration with our group (Fichte *et al.,* 2016) aimed to introduce two-photon sensitive caged phosphoramidites into DNA and to prove that DNA hybridization could be controlled with 3D resolution. This study developed and "orthogonal" two-color two-photon uncaging that is defined as the selective addressing to one group among a set of coexisting photolabile groups while leaving the others untouched.

Two uncaging chromophores were used for this study, [7-(diethylamino) coumarin-4-yl]methyl (DEACM) used to nucleobase-protect a dT residue (Scheme I.36, blue) and p-dialkylaminonitrobiphenyl (ANBP) for a dG residue (Scheme I.36, red), with two-photon action cross-sections of 0.12 and 11 GM, respectively at 800 nm.

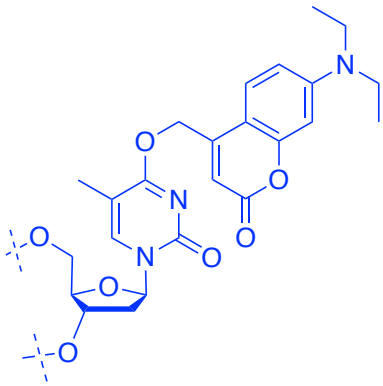

X = dT^{DEACM}

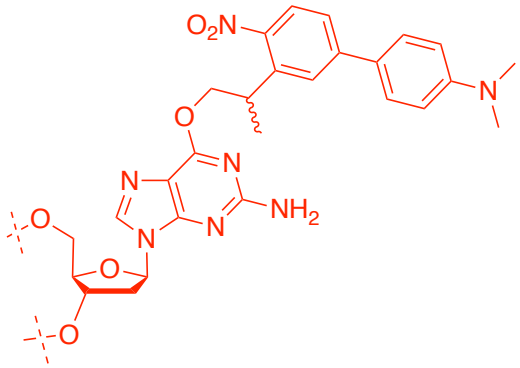

Y = dG^{ANBP}

DNA 1: HS-$(CH_2)_6$-GCA **X**AA A**X**A AAG G**X**G
DNA 2: HS-$(CH_2)_6$-A**Y**A TAC A**Y**A TAC **Y**CA

Scheme I.36: Two different caged thiol-modified DNA sequences: DNA 1 and DNA 2. X and Y represent the caged nucleotides dT^{DEACM} and dG^{ANBP} respectively.

Since the uncaging process in DNA cannot be followed by spectroscopic methods, a **strand-displacement** assay where to each strand **DNA1** and **DNA2** a DNA duplex probe consisting of a **fluophore** and a **quencher** (shorter-sense strand).

Upon uncaging, the shorter sense strand (quencher) is displaced marking the uncaging at a specific site with the characteristic emission of the fluophore (Scheme I.37, top); the uncaging process was studied on hippocampal neurons with specific site irradiations (Scheme I.37, bottom).

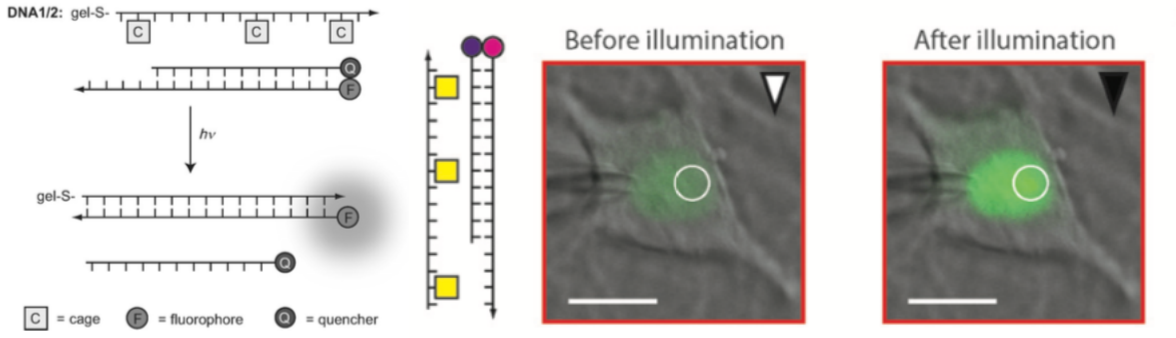

Scheme I.37: (Left) Schematic representation of the strand-displacement strategy used for the visualization of one-photon and two-photon uncaging, (Right) the duplex probe together with **DNA1** were holographically illuminated at 780 nm for two-photon excitation (white circle indicates the location of the illumination spot).

3.3.2. Light Induced Gene Expression

Alternatively to the regulation of RNAs, the light control of gene expression can also be performed at the post-transcriptional level using small caged trans-activator together with ligand-induced gene expression systems.

The Tet system is the most commonly used ligand-inducible gene expression systems that takes advantage of an Escherichia coli antibiotic resistance mechanism. This tetracycline-responsive gene regulation system is highly specific and efficient and is thus used widely for transgene expression. Its main element is the homodimeric Tet repressor (TetR) (Gossen *et al.,* 1992 and Gossen *et al.,* 1995).

TetR tightly binds its effector tetracycline, or the more potent derivative doxycycline, as a magnesium (II) chelate to a regulatory core domain. This leads to an allosteric conformational change in TetR that results in its dissociation from the operator DNA sequence (TetOff system). Expansion of the biological space for TetR-based expression systems has led to novel eukaryotic transcriptional activators.

Random mutagenesis coupled with phenotypic screening has given rise to variants termed rtTA (reverse tetracycline-controlled trans-activator), which exhibit a reversed allosteric response and require the tetracycline agonists anhydrotetracycline or doxycycline for DNA binding (TetOn system) (Das *et al.,* 2016, Urlinger *et al.,* 2000).

In a very recent work, Specht's group have described two caged Doxycycline systems: EANBP-9-aminodoxycyline and PEG_7-DEACM-9-aminodoxycycline (Goegan *et al.,* 2018 Scheme I.38).

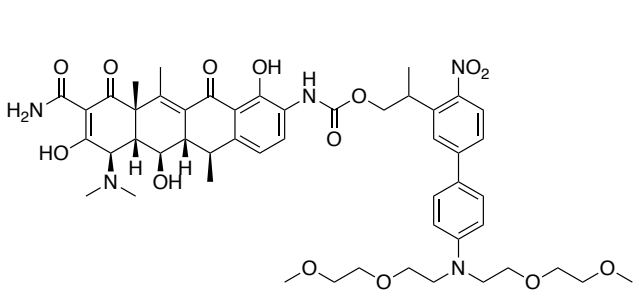

EANBP-9-aminodoxycyline

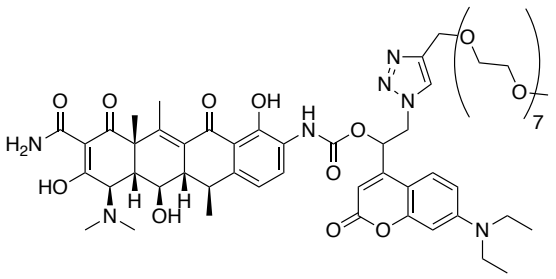

PEG_7-DEACM-9-aminodoxycycline

Scheme I.38: Structures of the two caged-doxycycline systems used for light induced gene expression.

Adding PEG_7-DEACM-9-aminodoxycycline to Tet system competent neuronal cultures did not produce any appreciable levels of background fluorescence. In turn, quantitative photoactivation of PEG7-DEACM-9- aminodoxycycline before adding it to the cultures yielded levels of GFP fluorescence that were very similar to those induced by unmodified PEG_7-DEACM-9-aminodoxycycline. This strongly suggested that the side product of the photolytic reaction (PEG_7-DEACM-OH) did not exhibit any significant toxicity as the sensitive gene expression as well as neuronal morphology were not impaired (Scheme I.39).

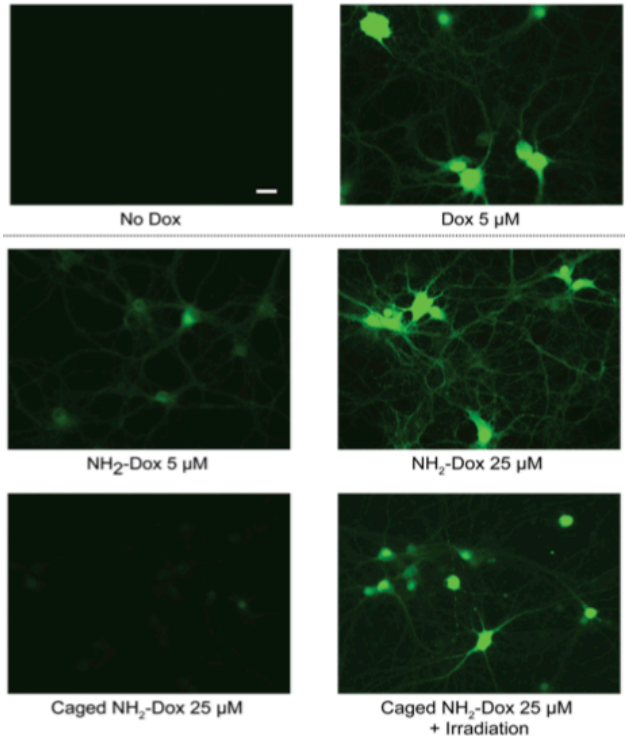

Scheme I.39: Photoactivated transgene induction with doxycycline (Dox) derivatives. Representative images of GFP expression (24 h after induction) with different doxycycline derivatives. One-photon irradiation (430 nm) was performed prior to administration to cells. (caged NH_2-Dox = PEG7-DEACM-9-aminodoxycycline).

There is a sizeable need for two-photon sensitive caged doxycycline derivatives which can be used to induce transgene expression in dense three-dimensional tissue with two-photon irradiation. The use of 9-aminodoxycycline allows easy and efficient grafting of visible-light and two-photon sensitive photoremovable chromophores onto it (i.e. EANBP and PEG7-DEACM). The 9- aminodoxycyline derivative induces similar transgene expression levels as the 'gold standard' doxycycline, albeit at higher concentrations. In summary, a new caged doxycycline derivative can be used in combination with the TetOn system for photoactivated gene expression.

3.4. Photo-triggering of Cell Adhesion

One of the fundamental biological processes are cell migration and cell adhesion which are implicated in several biological phenomena like cellular development or the metastasis propagation (Ridley *et al.,* 2004). The study of the selectivity and the mechanism that drives the cells to adhere to a certain surface has been an interesting subject to study.

Different methods to control the adhesion were studied: thermal control (Okano *et al.,* 1995), electrochemical control (Yeo *et al.,* 2001) and even photochemical control (Nakanishi *et al.,* 2007), all these served in establishing an artificial control for the triggering of cell adhesion (Scheme I.40).

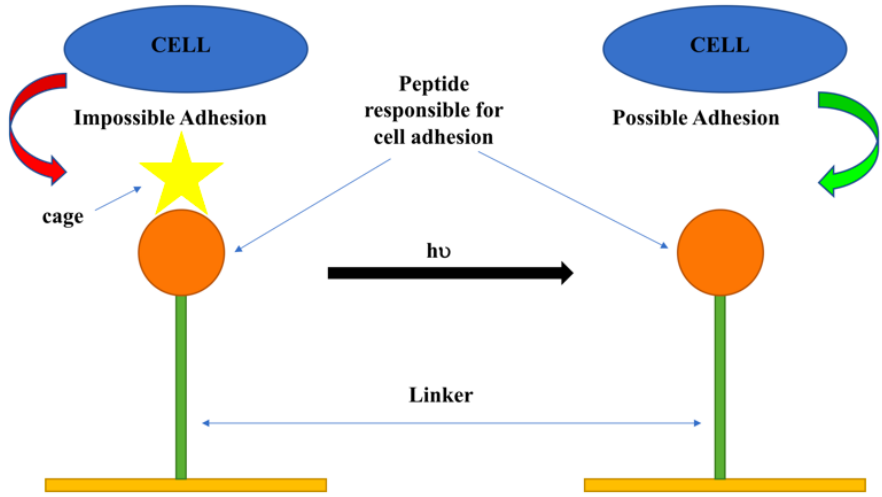

Scheme I.40: The functioning principal of photo-triggered cell adhesion.

Since photo-labile protecting groups have the capacity to liberate a biological effector that retains it reactive functionality after irradiation, in the case of cellular adhesion the peptide responsible for adhesion is liberated. The use of two-photon excitation is not only advantageous because it used near IR wavelengths that fall in the transparency window for biology, but also because it allows an important spatial control.

An important example of Photo-triggering cell adhesion was described using cyclopeptide RGD that was caged with a 3-(4,5-Dimethoxy-2-nitrophenyl)-2-butyl ester (DMNPB) photoremovable group (Petersen *et al.,* 2008). The presence of the cage compounds with the peptide blocks the integrin receptors on the surface of the cells from recognizing the peptide, but after irradiation and the departure of the PPG, the RGD is released and the integrin receptors could recognize this peptide and thus permits the cells to adhere (Scheme I.41).

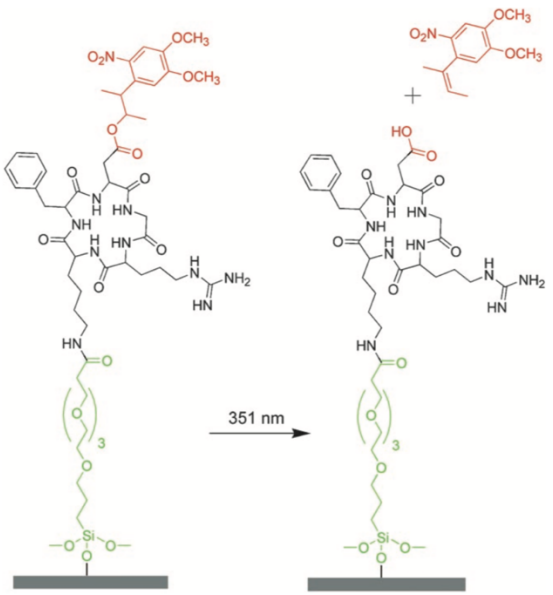

Scheme I.41: Chemical structure of cyclo[RGD(DMNPB)fK] (pentapeptide: cyclo (-Arg-Gly-Asp-D-Phe-Val-), DMNPB (red) attached to the surface through the TEG linker (green). The caging group is released upon irradiation at 351 nm.

These results show that cell attachment to surfaces can be inhibited efficiently by blocking the carboxylic acid side chain of the aspartic acid residue in the RGD motif by connecting a PPG. In conclusion, the cells attached to RGD-containing surfaces already show a high degree of spreading, whereas cells attached to caged-RGD-containing surfaces show much slower spreading. The use of the photosensitive DMNBP cage as a trigger for light-modulated cell adhesion provides much better results in terms of efficiency and selectivity than other reported photoactivation strategies based on the azobenzene unit (Schutt *et al.,* 2003, Milbardt *et al.,* 2005, Auernheimer *et al.,* 2005).

4. Recently Developed Photoremovable Protecting Groups with New Properties

The importance of photolabile protecting groups has been evident in several domains and their usage has increased in the last decade and their activity has attracted researchers' attention. Several modifications in the chemical structure of these groups has led to significant modifications in their respective photochemical and photophysical properties. A major limitation of these popular photocages is that their chromophores absorb mostly in the ultraviolet region of the optical spectrum. Ultraviolet light has limited tissue penetration, restricting photo-caging studies to cells and tissue slices. In addition, exposure of cells or tissues to intense UV light results in phototoxic cell damage or death. The ideal wavelength range to be used in animal tissues, known as the biological window, is ~600- 1000 nm, where tissues have maximal light transmittance. At these far red/near-IR wavelengths, light achieves maximal tissue penetration while minimizing phototoxicity.

This part will be dedicated to research works on photoremovable protecting groups recently published. These research works still present limitations like (1) the sensitivity of the PPG to light presenting **long irradiation times** or (2) the release of **non-fluorescent by-product** which is a major drawback for the usage in biological systems that makes it impossible to follow the uncaging events in cellular media or (3) **solvent-dependent photolysis**; photochemical reaction that work in specific solvents that are not biocompatible like DMSO.

4.1. BODIPY Photocages

One recent work by Petersen and co-workers (Petersen *et al.,* 2018) describes a family of BODIPY photocages using Visible/Near IR light. The photocleavage of these BODIPY photocages is realized in alcohols under light irradiation in order to break the carbamate or carbonate linkage and release the attached molecule (Scheme I.42).

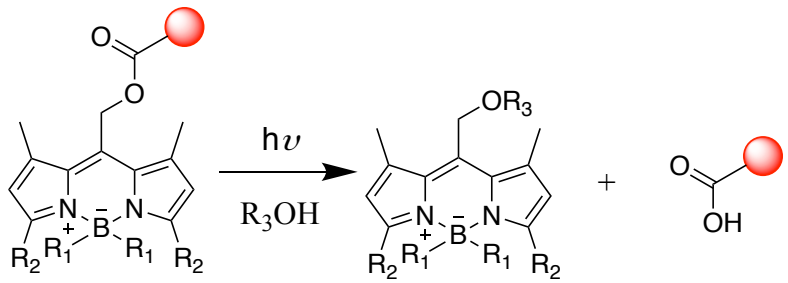

Scheme I.42: Mechanism of photocleavage of BODIBY-photocages in alcohols.

Following the structure-activity relationship, this group described the synthesis of a set of BODIPY photocages by chemically modifying several positions aiming to tune the photophysical and photochemical properties (Scheme I.43).

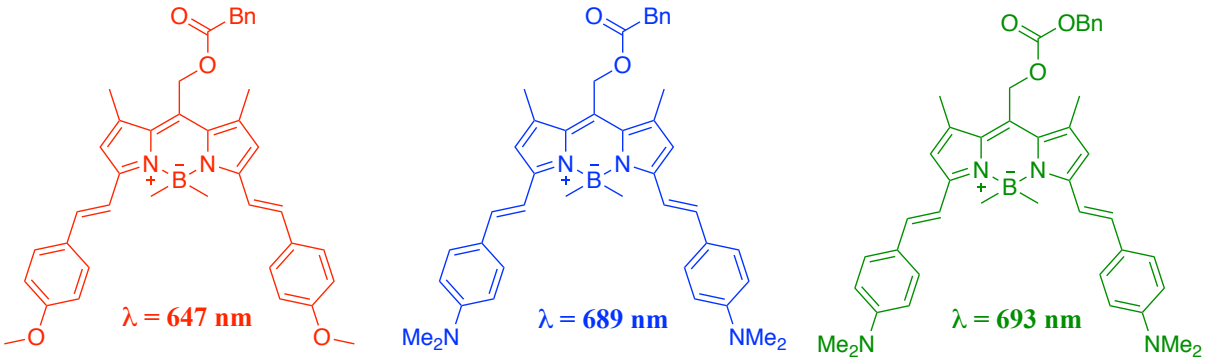

Scheme I.43: Structures of different BODIPY photocages with their respective wavelength of absorption.

However, boron-alkylation leads to a large increase in the quantum yield of release, while not significantly perturbing the λ_{max} of the chromophore. For example, the boron-alkylated derivative (Scheme I.43, red) shows a quantum yield ~20 times larger than its boron- fluorinated analog. Whereas, adding strong electron-donating groups (bismethyl amino) to the bis(styryl) linker leads to a red-shifted absorption maximum up to 50 nm (Scheme I.43, red and green).
One of these derivatives was chemically modified in the aim for testing the usefulness of these photocages in live cell imaging. 4-nitrobenzoic acid was used as the leaving group, since nitrobenzoic acids are known fluorescence quenchers of BODIPY dyes. A short ethylene glycol chain was added to the bis(styryl) groups to aid with water solubility. The synthesized compound (Scheme I.44) does not exhibit detectable fluorescence when kept in the dark at room temperature. Upon irradiation, the nitrobenzoic acid is released and thus the photocage retains its fluorescence signal and thus shows an increase in fluorescence in cells at 610 nm after 6 minutes of irradiation. Also, the incubation of the compound with the cells doesn't show any fluorescence without irradiation even after 6 minutes, this implies that the fluorescence obtained is due to the release of the quencher and not due to the interaction of the photocage with cellular proteins (Scheme I.44).

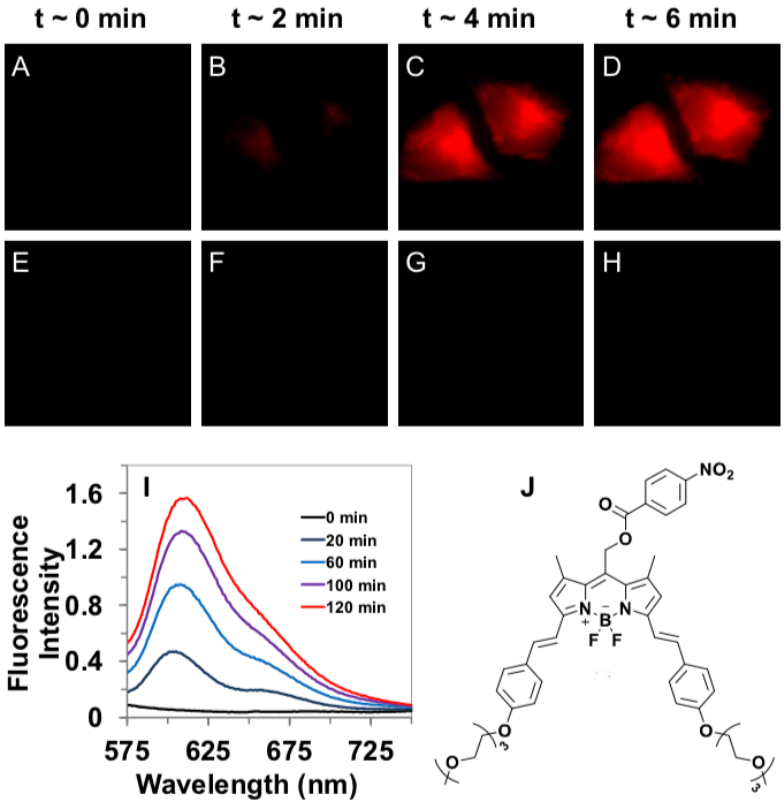

Scheme I.44: Fluorescence images of HeLa cells incubated with 20 µM of the compound: (A-D) irradiated with 635 nm light and (E-H) cells incubated with the compound with no irradiation as a function of time. (I) Increase in the fluorescence intensity upon irradiation of compound (red, Scheme I.44) in a cuve for up to 120 minutes in H_2O with 5% BSA (J) structure of the compound incubated with the cells.

This example shows that BODIPY can be useful photocages that help to follow the uncaging event by fluorescence in cells. These photocages exhibit interesting absorbance wavelength that fall in the transparency window for biological experiments. But these photocages present two major limitations:

A) These cages are already fluorescent without photocleavage except when attached to fluorescence quenchers (nitrobenzoic acid for example) making them not interesting for attaching a diversity of biological effectors that don't act as quenchers for such photoremovable protecting groups.

B) These cages show low sensitivity towards light and this demonstrated by the low values of the one-photon quantum yield (0.0041% - 0.14%) and by the long irradiation times that go up to 2 hours in order to observe a strong fluorescence which is contradictory to what is awaited from an efficient PPG in biology; a rapid cleavage resulting in a rapid jump in the concentration of the biological effector.

4.2. Thiochromone-Type Groups

Another research work on photoremovable protecting groups that release a fluorescent by-product has been recently described for the quantification of the photo-deprotection of caged resveratrol by fluorescence (Hikage *et al.,* 2017). In this study the authors have used thiochromone (TCM)-type PPG for the release of resveratrol by light irradiation following the release mechanism that releases a highly fluorescent by-product (Scheme I.45).

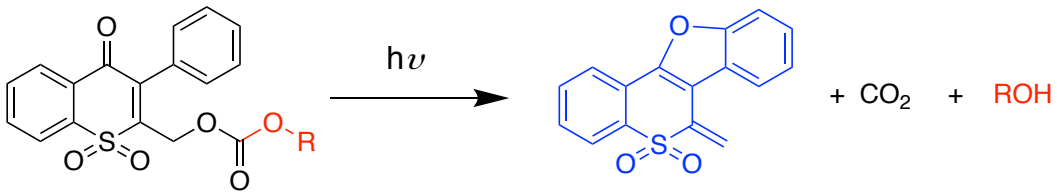

Thiochromone-type PPG

Scheme I.45: Mechanism of photocleavage of thiochromone-type PPG.

A reaction called luciferin−luciferase reaction generates the chemiluminescent (CL) product oxyluciferin, and resveratrol is known to be an antioxidant or an inhibitor of luciferase. Thus, when resveratrol is present in the luciferin− luciferase reaction, it has been reported to insert preferentially into the active site of luciferase thus blocking the luciferin− luciferase reaction and inhibiting the formation of oxyluciferin and diminishing its generation. III-caged resveratrol (III corresponds to the attachment of 3 thiochromone units on resveratrol) was used in order to block the formation of oxyluciferin and the uncaging process was followed by fluorescence induced from the released by-product. Upon irradiation at 360 nm, the photo-deprotection of III-caged resveratrol in DMSO induces a fluorescent signal where its intensity increases with the increase in irradiation time where more resveratrol is released and more by-product of photocleavage is accumulated (Scheme I.46).

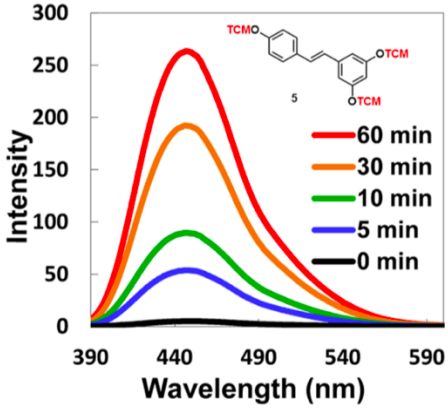

Scheme I.46: Fluorescence spectra of the photo-deprotection process of III-caged resveratrol (irradiated at 360 nm in DMSO).

As the time of irradiation increases, more resveratrol is released in the medium and thus more luciferase reactions are blocked and thus less oxyluciferin is generated. Using these caged-resveratrol, the inhibitory ability of resveratrol was evaluated; as the irradiation time increase the relative luminescence unit (RLU); which defines the amount of oxyluciferin present in the medium; decreases as more resveratrol is released in the medium (Scheme I.47).

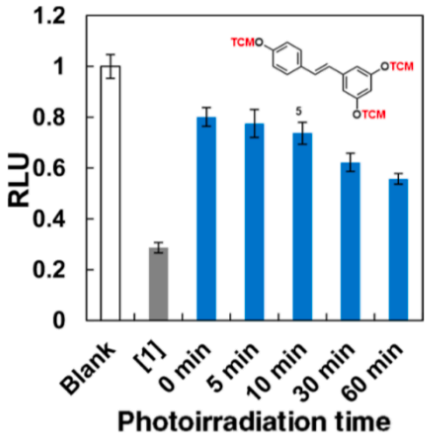

Scheme I.47: RLU of oxyluciferin in each photo-deprotection process of III-caged resveratrol.

This is one example of how to monitor the uncaging process via fluorescence measurements through a newly developed thiochromone-type caged resveratrol. The caged resveratrol with thiochromone-type PPGs succeeded in increasing the oxyluciferin generation through the inhibitory ability of resveratrol.

After photoirradiation of the caged resveratrol in DMSO, the CL intensity of oxyluciferin, derived from the luciferin−luciferase reaction, diminished. Therefore, the original inhibitory ability of resveratrol was regenerated.

Additionally, the fluorescence intensity of the highly fluorescent by-product which is released from the thiochromone- type PPG during photoirradiation, increased. Furthermore, a good linear correlation was observed between the increasing rate of FL intensity and diminishing rate of CL intensity. This example shows that one way to quantitatively monitor the uncaging of caged resveratrol is by measuring fluorescence, but this work has a major limitation: the photocleavage could only be done in DMSO due to the poor solubility of the caged compound in other solvents and the by-product shows interesting fluorescence but only when released in DMSO which is known to be a toxic solvent for biological experiments and toxic for cellular media.

4.3. Bimane-Based Photolabile Groups

An example of a recently developed Photoremovable Protecting Group is the one described by Chaudhuri and his colleagues (Chaudhuri *et al.,* 2017). In this work, the authors have reported the synthesis of bimane-based PPG that induce fluorescent signal after the single or dual release of respectively carboxylic acids and amino acids. The bimane moiety present several interesting properties like a strong fluorescent nature, significant absorbance in the visible region and good water solubility and in addition to those, such groups have been used for biological purposes like labeling of human red cells (Kosower *et al.,* 1979) and thiol sensing (Montoya *et al.,* 2015). This work describes the photolysis of these bimane-based PPGs for the release of one or two (similar or different) carboxylic acids or amino acids according to the mechanism presented in Scheme I.48.

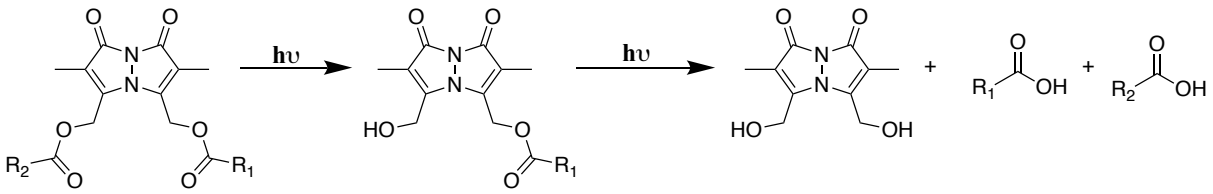

Scheme I.48: Mechanism of photocleavage of bimane-based PPG and the dual release of carboxylic or amino acids.

Upon irradiation the bimane-type caged acids undergo photolysis releasing the attached acids in a mixture of acetonitrile/water at 365 nm and the reaction was monitored by HPLC in order to quantify the release of the acid and the by-product. It is evident that the caged compound starts to disappear and thus liberating the free acid previously attached to it (Scheme I.49).

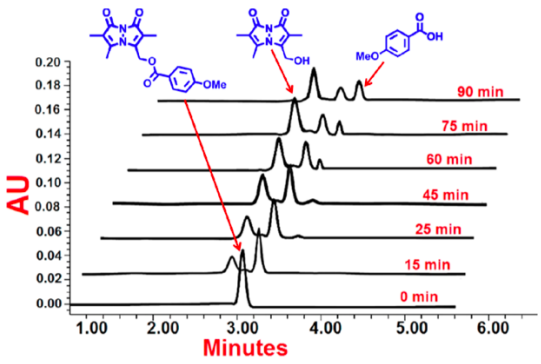

Scheme I.49: HPLC follow-up of the photolysis of a mono-acid bimane caged compound with irradiation time in acetonitrile/water (7/3).

These systems could be used as well with a range of biological effectors since they can attach to molecules with acid functionality thus to a diversity of bio-efficient molecules (eg: amino acids). But this PPG has a major limitation; the irradiation times are too long, and this makes the system less efficient to light (after 90 minutes of irradiation, 20% of starting material is still present), this makes the bimane-type cage less efficient for certain biological experiments because in such cases a rapid release followed by a rapid increase in the biological effector's concentration is required.

In conclusion, these groups present interesting photochemical and photophysical properties and they show promising results in biological tests. Despite the limitation of usage (solvent, irradiation time, absorption wavelength…) they present a fluorescence signal that permits to follow the uncaging event and to monitor the release of the biomolecule into the biological medium.

5. Fluorescence as an Important Method to Monitor Uncaging

Throughout the several parts discussed above it was evident that photoremovable protecting groups act as an important method for controlling biological processes as well as synthetic chemical steps. These groups present interesting photochemical properties that makes them sensitive to light and undergo photochemical reactions in their excited state and also interesting photophysical properties shown by their ability to absorb light at wavelengths that fall in the transparency window for tissues that makes them efficient utilities in biological experiments.
However, it's difficult to calibrate the light intensity to efficiently induce the uncaging events, and any biological application requires a time-consuming study to find the right light intensity on a given biological system. Therefore, it might be advantageous if the uncaging event could be monitored by the emergence of fluorescence (e.g. Optical reporting). Except for cinnamate type and thiochromone-type photoremovable groups, the development of optical reporters of uncaging has only attracted little attention. Interestingly, these two last PPGs have been designed to release a fluorophore as a side product.
As fluorophores play the central role in fluorescence spectroscopy and imaging we will start with an investigation of their manifold interactions with light. A fluorophore is a component that causes a molecule to absorb energy of a specific wavelength and then re-remit energy at a different but equally specific wavelength. The amount and wavelength of the emitted energy depend on both the fluorophore and the chemical environment of the fluorophore. Fluorophores are specific chromophores, that are not only able to absorb light through their chromophoric unit, but also to emit light after excitation. Fluorescence denotes allowed transitions with a lifetime in the nanosecond range from higher to lower excited singlet states of molecules.
Several factors affect the intensity of fluorescence and the fluorescence emission efficiency: the nature of the chromophoric unit (presence or absence of a heteroatom), the nature of the bonds linking the several units (single, double or triple), the chemical environment surrounding the molecule (coordination bonds with metals as an example) and the length of the conjugation inside the system that determines the extension of the electron delocalization throughout the system.

6. Project

The first project was financed by an IdEx Grant “Linus Pauling 2015” and the work was done in the “Laboratoire de Conception et d’Application de Molècules Bioactives” (CAMB) at the University of Strasbourg - Faculty of Pharmacy.

This project aimed for the design of two-photon sensitive photoremovable protecting groups of the *o*-nitroaryl series releasing a fluorescent by-product for the monitoring of uncaging in biological media. These compounds have been widely used in synthesis and biological applications, but no example of fluorescent by-products release was reported. We wish to optimize a synthetic route for the development of photoremovable protecting groups from the *o*-nitroaryl family. We also aim to synthesize groups with high efficiency in two-photon excitation making them useful candidates for biological applications. Also, photoremovable groups with a conjugated system would increase the fluorescence of the by-product and also would modulate the photophysical and photochemical properties. The obtained compounds will be used for testing the uncaging of neurotransmitters and their release in neurons while taking advantage of the fluorescence of the by-product that will act as an optical reporter for the uncaging event.

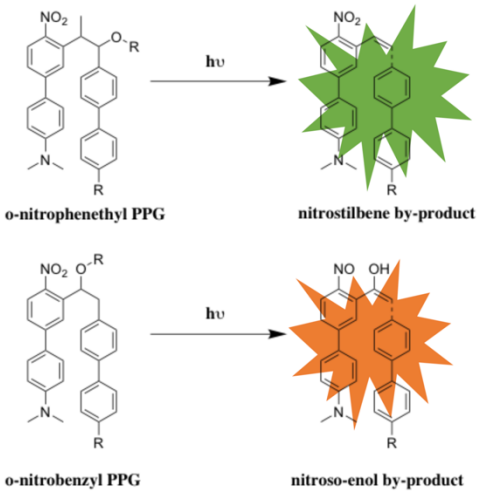

Scheme I.50: Design of *o*-nitroaryl PPG releasing a fluorescent by-product.

The second project was done in collaboration between the "Laboratoire de Conception et d'Application de Molècules Bioactives" (CAMB) at the Faculty of Pharmacy of Strasbourg and "Laboratoire de Chimie Biophysique" (UMR 8640) at the École Normale Supérieure-Département de Chimie in Paris-France.

This project aimed for the design of new photoremovable protecting groups for light-controlled cell adhesion. The architecture of the used system includes the photoremovable protecting group with long polyethylene glycol (PEG) chains. This system is further coupled to Poly-L-Lysine (PLL) chains. We wish to use compounds previously developed in the lab to optimize the synthesis of new analogs that are further coupled to long polymeric chain of Poly-L-Lysine. These caged-polymers will be used in the photoregulation of adhering cells using fluorophores or long chains with reactive terminals for further surface modifications.

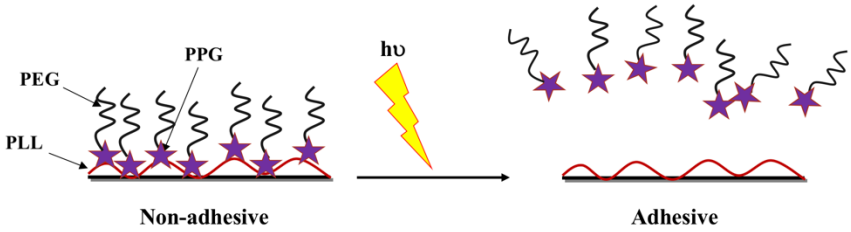

Scheme I.51: Use of Photoremovable Protecting Group for the light control of cell adhesion.

CHAPTER II

Towards the Synthesis of Two-Photon Efficient Photoremovable Protecting *O*-Nitroaryls Groups

1. Strategy

The design of the pro-fluorescent photoremovable protecting group to be synthesized was inspired by the previous work done in the lab. EANBP (**5**, R = bis (2-methoxyethoxy)ethyl, Scheme II.1) was the *o*-nitrophenethyl (*o*-NPP) protecting group previously used for caged glutamates and caged doxycycline. It showed important two-photon efficiency due to the conjugated biphenyl core and the donor-acceptor nitro and bis-alkylamino groups (Donato *et al.,* 2012 and Goegan *et al.,* 2018). The photochemical properties were promising, and this was evident from the irradiation times that translated the sensitivity of this group to light and the efficient photo-release of the biomolecule after irradiation. We took these advantages into account and decided to synthesize a structural analog with an extended conjugation.

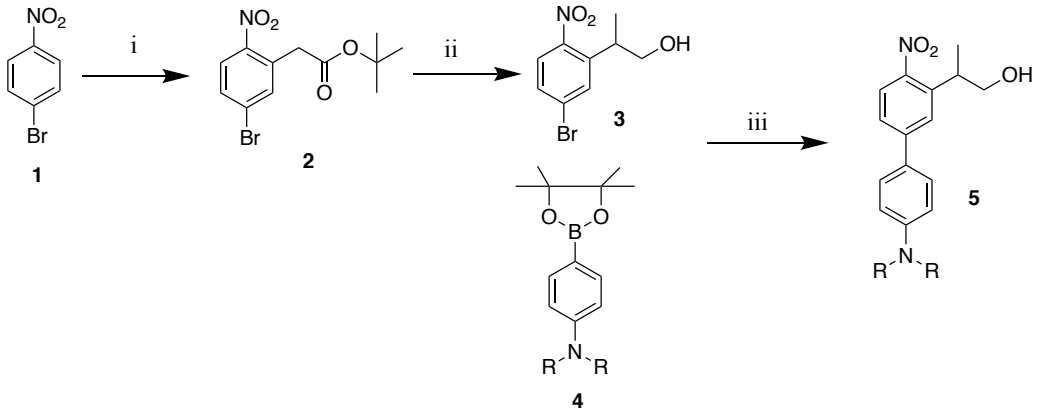

Scheme II.1: Synthesis of two-photon efficient photremovable protecting group – EANBP (**5**).

(i) ^{t}BuOK, *tert*-butylchloroacetate, DMF, room temp., 2 h, 96 % (ii) a) NaH, CH_3I, THF, room temp., 5 h, b) DIBAL-H, THF, room temp., 3 h, 83 %, (iii) K_2CO_3, Bu_4NBr, $Pd(OAc)_2$, EtOH/H_2O (2:1), microwave, 160 °C, 10 min, 70 %.

In order to have access to EANBP analogs with an extended conjugation of the uncaging by product (Scheme I.50, Top), we proposed to adapt two synthetical strategies for the construction of this PPG family already reported in the literature.

The first strategy is using a vicarious nucleophilic substitution (VNS) of the nitrobenzene derivative **1**. This substitution was described by Makosza and co-workers (Makosza *et al.,* 1987 and Makosza *et al.,* 2010); substitution of aromatic H-adducts by an α-halocarbanions to nitroarenes undergo fast base induced β-elimination giving nitrobenzylic carbanions that affords products of replacement of the ring hydrogen with the carbanion moiety (Scheme II.2). It includes the substitution of an aromatic proton in *ortho* or *para* position to nitro group with the carbanion of an α-halo carbonyl, sulfonyl, esters and malonate derivatives.

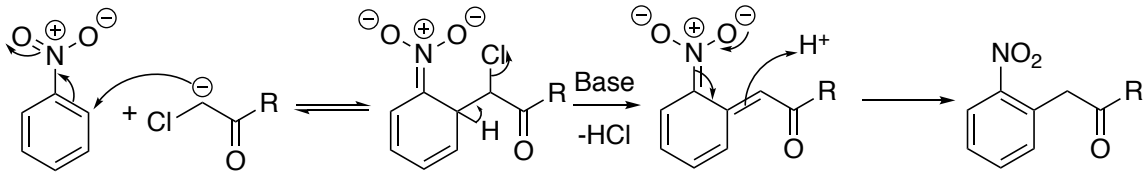

Scheme II.2: Mechanism of the vicarious nucleophilic substitution of aromatic protons with carbonyl compounds

In the synthesis of EANBP, derivative **2** was obtained by the VNS of the enolate of tert-butylchloroacetate on the nitrobenzene derivative **1**.

The second reported strategy for the construction of *o*-nitrophenethyl derivatives is based on the coupling of nitro ethylbenzene **6** and paraformaldehyde (Bühler *et al.,* 2004 and Smirnova *et al.,* 2005). The strategy implements the deprotonation of the CH_2 of the ethyl chain with ^{t}BuOK in ^{t}BuOH followed by the nucleophilic attack of the anion on the carbonyl function in order to form the alcohol **7**. This strategy was tested by Bühler and co-workers (Bühler *et al.,* 2004) on several nitro ethylbenzene derivatives (R_1, R_2, R_3, R_4 = H, NH_2, NO_2, Cl, Br, I) but only on paraformaldehyde as electrophile. (Scheme II.3).

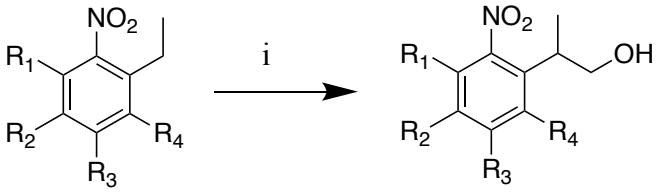

6 **7**

Scheme II.3: Synthesis of *o*-nitrophenethyl **7** via carbanion of **6** and paraformaldehyde.

(i) Paraformaldehyde, ^{t}BuOK, ^{t}BuOH, DMSO, room temp, 1h, 100%.

Another recent work by Silvestri and his group (Silvestri *et al.,* 2015) uses a similar strategy based on the deprotonation of substituted nitrotoluene derivatives **8** by sodium ethoxide in DMSO in order to form the alcohol **9** by a nucleophile addition of the formed carbanion with benzaldehyde. By using aromatic aldehydes, it is possible to access more conjugated *o*-nitrophenethyl groups (Scheme II.4)

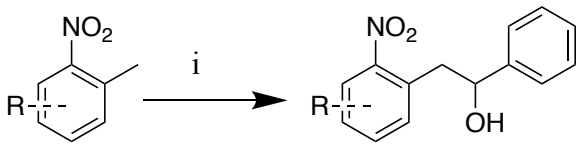

8 **9**

Scheme II.4: Synthesis of *o*-nitrophenethyl **9** via carbanion of **8** and benzaldehyde.

(i) Benzaldehyde, EtONa, anhydrous DMSO, room temp, 12h, 44%.

2. Design

These two strategies are promising for the synthesis of *o*-nitrophenthyl derivatives and our aim is to adapt those strategies for the synthesis of EANBP analogs with the possibility to extend the conjugation. This conjugation would give rise to a fluorescent by-product after photocleavage according to the mechanism of photocleavage of the *o*-nitrophenethyl series presented in section 1.3.6.2. This mechanism is illustrated in Scheme II.5 (where the red circle represents the biomolecule, R = Ar-X and R' = CH_3).

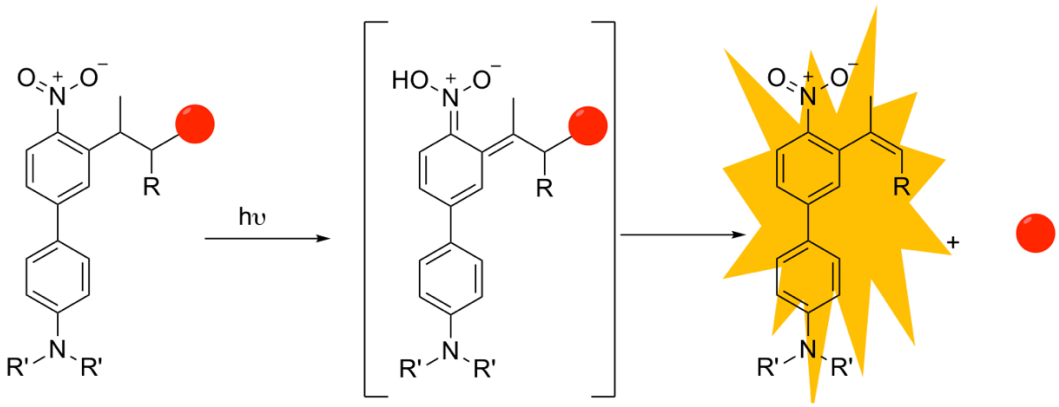

Scheme II.5: Mechanism of photoactivation of *o*-nitrophenethyl PPG with an extended conjugation for the release of a fluorescent by-product.

So, we suggested two different retrosynthetic strategies (Scheme II.6) for the construction of a conjugated analog of EANBP using modified procedures of the strategies discussed above.

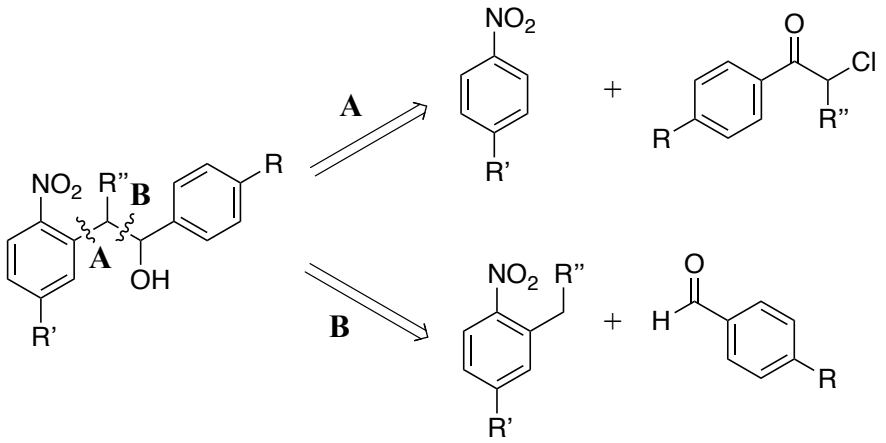

Scheme II.6: Retrosynthetic analysis for the synthesis of *o*-nitrophenethyl derivative: conjugated analog of EANBP.
Retrosynthesis pathway **A**: Vicarious Nucleophilic Substitution using para substituted nitrobenzene derivatives with para substituted α-chlorocarbonyl derivatives.
Retrosynthesis pathway **B**: Nucleophilic attack of carbanion derived from methyl or ethyl nitrobenzene on para substituted benzaldehyde derivatives.

2.1. Exploration of Pro-Fluorescent EANBP Analog Synthesis Via Vicarious Nucleophilic Substitution

The key step for the synthesis of EANBP analog was via vicarious nucleophilic substitution. Various *para*-substituted aromatic α-chlorocarbonyl derivatives **11** were used in order to be able to extend the conjugation on the target product (Compound **14** Scheme II.7).

We suggested a retrosynthetic pathway in order to synthesize the conjugated analog of EANBP **15** starting from the nitrobenzene derivative **1**.

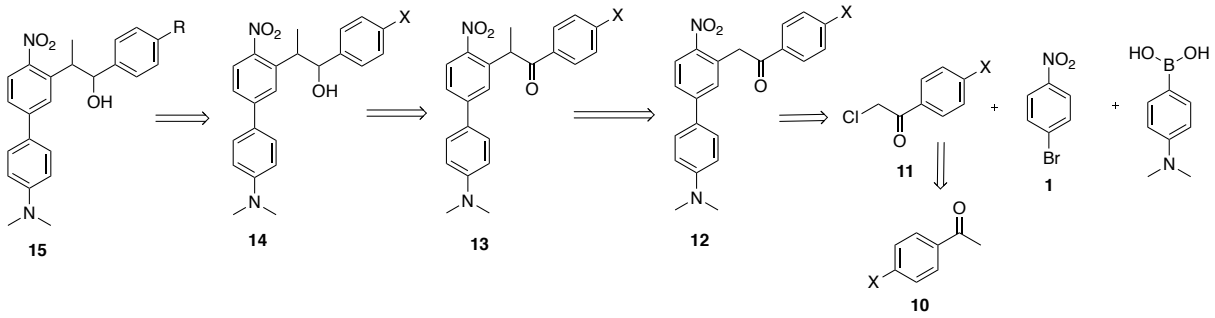

Scheme II.7: Retrosynthetic strategy for the synthesis of the conjugated analog **15** of EANBP.

The first aim was to synthesize the α-chlorocarbonyl derivatives **11** starting from the commercially available *para*-substituted acetophenones **10** described by Lee and collaborators (Lee *et al.,* 2003, Scheme II.8).

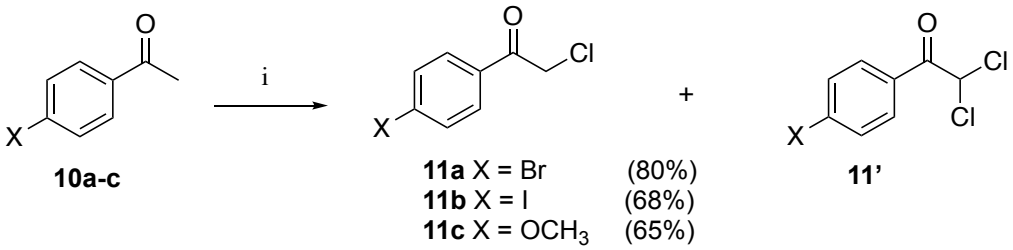

Scheme II.8: Synthesis of α-chlorocarbonyl derivatives **11a-c**.

(i) N-chlorosuccinimide, *p*-TsOH, acetonitrile, 85°C.

The reaction was carried out in acetonitrile at reflux with NCS as chlorinating agent overnight, and the reaction was tested on 3 different derivatives of **10**: *p*-bromo acetophenone **10a**, *p*-iodo acetophenone **10b** and *p*-methoxy acetophenone **10c**.

The target compounds were obtained in good yields and we noticed an 8-12% of dichlorinated compound **11'** which was characterized by the chemical shift of the proton on the carbon holding the 2 chloro groups that appears at 6.58 ppm in $CDCl_3$ whereas the characteristic peak of the target compound appears at 4.65 ppm.

The following step of the synthesis is the vicarious nucleophilic substitution of **11a-c** with 4-nitro bromobenzene **1**. This step had previously been optimized in the lab with aliphatic α-halo esters like *tert*-butylchloroacetate and the same conditions were used for our synthesized aromatic α-halo ketones **11a-c**.

Using $^{t}BuO^{-}K^{+}$ as base, the reaction of the 3 chlorinated derivatives **11a-c** with **1** was tried out but unfortunately, we succeeded to isolate only the product **16c** from **11c**, but **16a** and **16b** were not obtained (Scheme II.9).

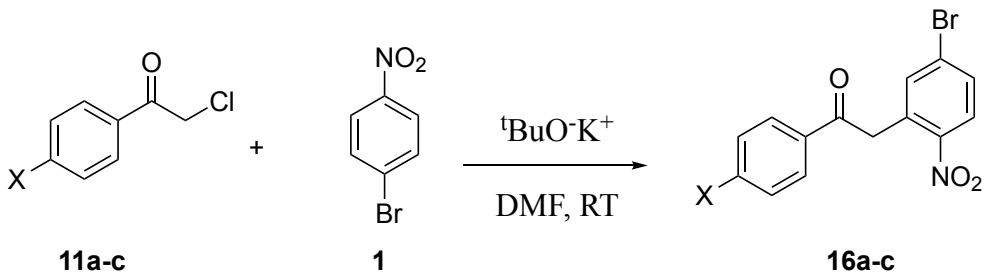

Scheme II.9: Synthesis of derivative **16a-c** through a vicarious nucleophilic substitution.

Trying to solve the problem of the substrate dependency of this reaction, we tried to modify several parameters:

i- We tried to add the ^{t}BuOKbase on our solution in DMF either at 0°C or at room temperature (20-25°C) and also, we tried to carry out the reaction at 25°C-50°C-80°C and 100°C but all what we obtained after quenching the reaction was the 2 non-reacted starting compounds

ii- We tried to modify the order of addition of the reagents; (1) adding the suspension of ^{t}BuOK in DMF over the 2 compounds **1** and **11** and the reverse, and also (2) we tried to prepare the enolate before adding the nitrobenzene **1** derivative by reacting the ^{t}BuOK base with the chlorinated derivative **11** and (3) adding the mixture of **1** and **11** onto a freshly prepared suspension of ^{t}BuOK in DMF and this trial was the only one that worked and only for **11c**. We succeeded to isolate the target product **16c** with yields varying from 39-68% but the reaction was not reproducible using **11a** and **11b**.

iii- As an alternative, we tried to change the base; instead of using ^{t}BuOK we used sodium hydride (NaH) and 1,8-Diazabicyclo [5.4.0] undec-7-ene (DBU) and varying the conditions previously discussed (temperature and order of reagent addition) the reaction only yielded starting material for **11a** and **11b**. However, by changing these 3 parameters, compounds **16a** and **16b** were never obtained.

An alternative has been put for trial; constructing the bis (methylamino) nitro-biphenyl **17** at first and then trying the vicarious using the previously synthesized derivatives **11a-c** in order to obtain the target compound **12a-c** (Scheme II.10).

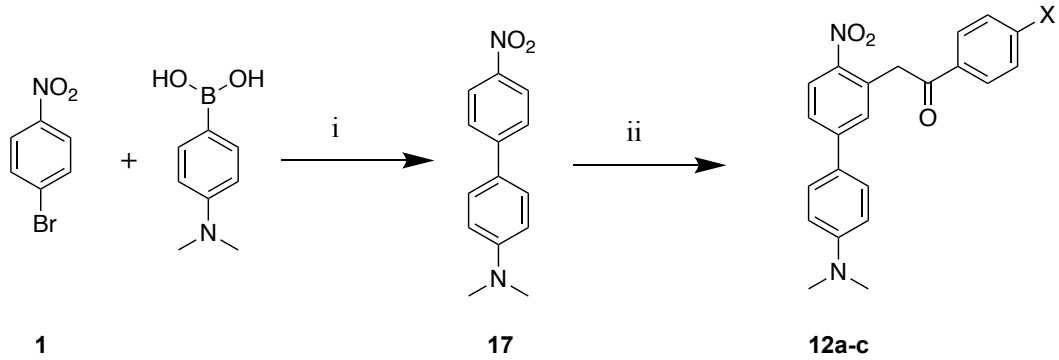

1 **17** **12a-c**

Scheme II.10: Synthesis of compound **12** through a VNS on the nitrobiphenyl **17**

(i) K_2CO_3, Bu_4NBr, $Pd(OAc)_2$, EtOH/H_2O (2:1), microwave, 160 °C, 15 min, 100 % (ii) ^{t}BuOK, **11a-c**, DMF, room temp, 2h, Yields **12a** (24-52%) and **12c** (30-35%).

The synthesis of **17** was done following the classical Suzuki-Miyaura conditions (Suzuki, Miyaura, 1995) using dimethylamino phenylboronic acid along with **1** in a mixture of ethanol and water (2:1) with potassium carbonate as base and tetrabutylammonium bromide. The mixture is degassed 3 times before adding palladium (II) acetate [$Pd(OAc)_2$] in order to remove any traces of air and the reaction was performed under microwave heating at 160 °C and in only 15 minutes the reaction was done and the target product **17** was obtained quantitatively. The following step is the vicarious nucleophilic substitution under the same conditions used for the derivative **1** and using the reaction conditions that gave the best results for **16c** we succeeded to obtain the target compounds **12a** in 24-52% yield and **12c** in 30-35% yield.

The next step, to get access to EANBP analogs, is the methylation in α-to ketone using methyl iodide (MeI) as methylation agent while testing the strength of several bases in order to obtain compounds **19a** and **19c** respectively. The same procedure was followed for the methylation of compound **16c** obtained previously to obtain the methylated compound **18c** (Scheme II.11).

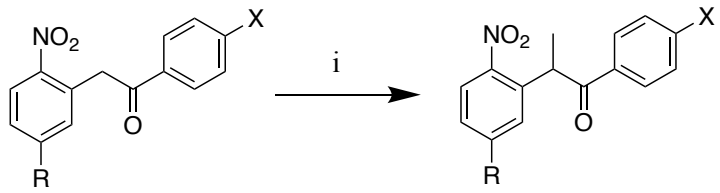

16c **R = Br**
X = OCH_3
12a **R = Ph-$N(CH_3)_2$**
X = Br
12c **R = Ph-$N(CH_3)_2$**
X = OCH_3

18c **R = Br**
X = OCH_3
19a **R = Ph-$N(CH_3)_2$**
X = Br
19c **R = Ph-$N(CH_3)_2$**
X = OCH_3

Scheme II.11: Methylation of compounds **16c** and **12a**,**c** in the presence of MeI and a base.

(i) MeI, Base, Solvent, T°C, overnight.

Several reaction conditions were tested for this methylation reaction varying the base used, the solvent of the reaction and the reaction temperature. The results are described in the following table.

Entry	Compound	Base	Solvent	Temperature (° C)	Time (h)	Yield (%)
1	16c	NaH	THF	0→ room temp	14	20
2	16c	NaH	THF	0→ room temp	24	18
3	16c	NaH	THF	50	14	23
4	16c	DBU	CH_3CN	0→ room temp	14	64
5	12a	NaH	THF	0→ room temp	14	-
6	12a	NaH	THF	50	14	-
7	12a	DBU	CH_3CN	0→ room temp	14	-
8	12c	DBU	CH_3CN	0→ room temp	14	36
9	12c	DBU	CH_3CN	0→ room temp	24	35

Table 3: Results for the methylation of **16c** and **12a,c** varying several reaction conditions.

We tried to optimize the methylation reaction by varying the reaction conditions, it was found that the bromo derivative **12a** shows no conversion with either bases used. It could be explained that the anion, if formed, tends to be weakly nucleophilic and doesn't trap the methyl cation.

The two versions of the methoxy derivative (**16c** and **12c**) tend to weakly react with the NaH base and showed partial conversion but by using a more hindered base like DBU we were able to overcome this problem and obtain higher yields (Entries 1 and 4). The addition of the base was done at 0°C in all reactions, and the mixtures were left to warm up to room temperature, in some cases we tired heating to 50°C in order to push the reaction of the anion formed with the methylation agent but unfortunately it didn't have a significant influence on the yield of the reaction (Entries 1 and 3) and sometimes it had no influence at all (Entries 5 and 6).

The step following the methylation is the reduction of the ketone into a secondary alcohol, this step should be less problematic since selective reducing agents are accessible. There are two functions that can undergo reduction; the nitro group and the ketone group. To our knowledge, the best reducing agent that can reduce selectively the ketone group is the diisobutyl aluminum hydride (DIBAL-H). The reduction of the two methoxy derivatives **18c** and **19c** was successful and the reduced compounds **20c** and **21c** were obtained in 85% and 78% yield respectively (Scheme II.12).

The construction of the biphenyl core from derivative **20c** was done using the same conditions for the synthesis of **17**. By the help of microwave heating the target compound **21c** was obtained from **20c** in 100% yield after 45 minutes.

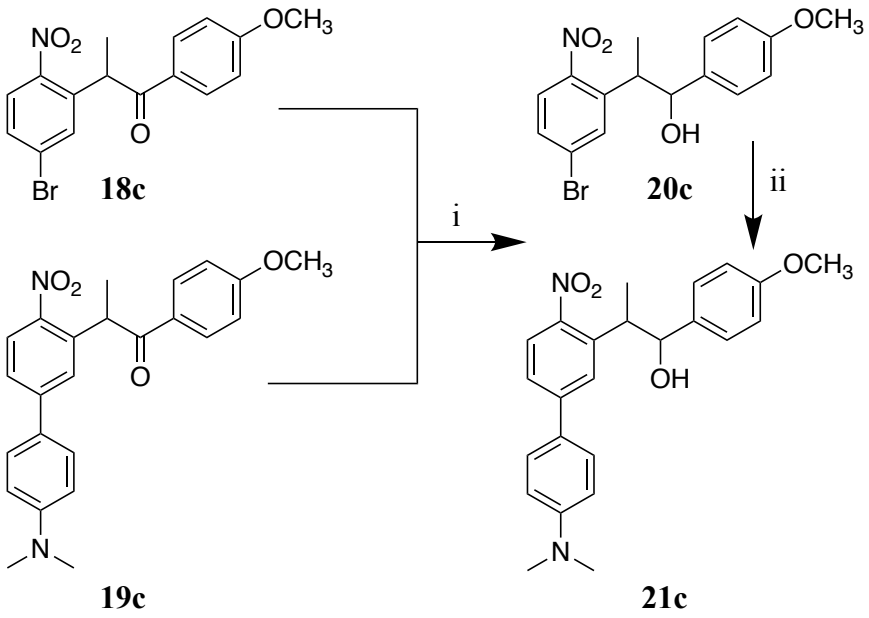

Scheme II.12: Reduction of the methoxy derivatives **18c** and **19c** into their respective secondary alcohols **20c** and **21c** followed by the Suzuki coupling on derivative **20c** to obtain the photoremovable group **22c**.

(i) DIBAL-H, THF, room temp, overnight (ii) K_2CO_3, Bu_4NBr, $Pd(OAc)_2$, $EtOH/H_2O$ (2:1), microwave, 160 °C, 15 min, 100%

As an overall view, the vicarious nucleophilic substitution strategy was not the right way to synthesize EANBP analogs with an extended conjugation of the uncaging sub-product. The strategy worked in the case of the bromoaryl derivative, but it was not reproducible and even the yields were too low. In the case of the iodo aryl derivatives, we never succeeded to obtain the target compound. The only case where the VNS strategy could be used to synthesis pro-fluorescent EANBP analogs efficiently, is related to the methoxy-aryl derivative **21c**. But unfortunately, this EANBP derivative could not be further functionalized in order to extend its conjugation and the structure as it is, doesn't promise to give a huge fluorescence increase after irradiation.

This molecule **21c** has been previously tested by Dr Bastien GOEGAN for the release of organic acids and the fluorescence increase was also evaluated.

It was found that the molecule was able to release 95% of the acid and it appeared to be sensitive to light (very short irradiation times) releasing the by-product **21'c** (Scheme II.13).

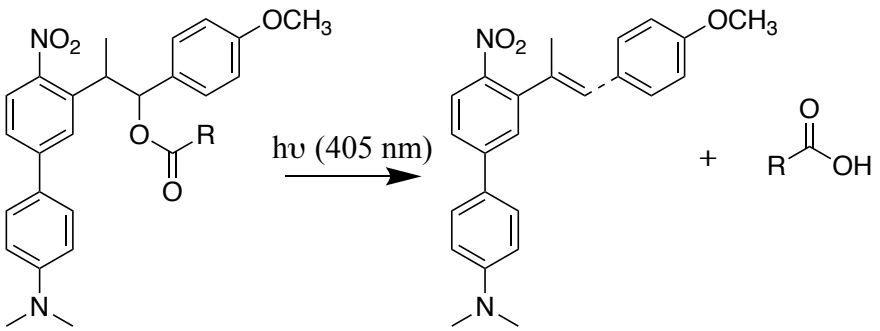

21c **21'c**

Scheme II.13: Photolysis of **21c** under irradiation at 405 nm and the release of the acid along with the by-product **21'c.**

The fluorescence study of this photolysis reaction showed that **21c** presents a weak fluorescence before irradiation (Scheme II.14, blue) and upon irradiation and the release of the organic acid, the by-product of uncaging, **21'c** shows a significant increase in the fluorescence intensity (Scheme II.14, green).

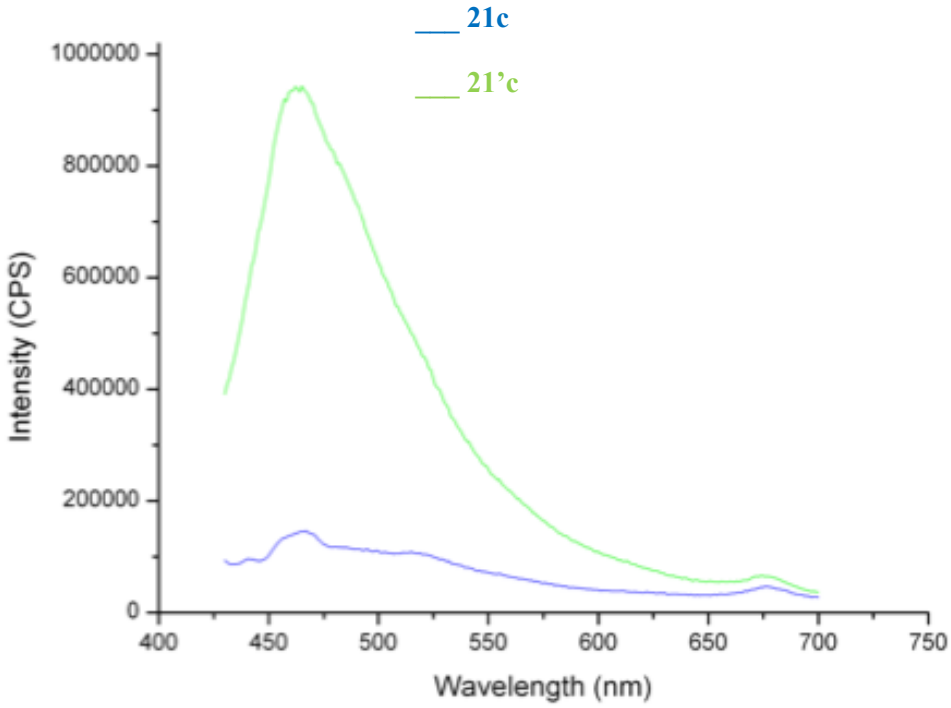

Scheme II.14: Fluorescence increase before and after irradiation of **21c** and the release of the acid along with by-product **21'c**.

Even though this molecule shows the liberation of a by-product with fluorescent properties, this fluorescence increase is still not quite eligible for application in biology in particular since the fluorescent increase is only around 10 times and the emission wavelength is in the blue region; that's why our aim was to synthesize an EANBP derivative that could be modified in order to extend the conjugation and increase the electronic delocalization over the system giving rise to a more intense red shifted fluorescent signal. Unfortunately, the vicarious nucleophilic substitution step was problematic and cannot really be reproducible when we change from α-chloro-aliphatic esters (*tert*-butyl chloroacetate) to α-chloro-aromatic ketones (compounds **11a-c**).

The alternative strategy to synthesize these pro-fluorescent EANBP analogs **15** is based on the deprotonation of alkyl benzene and the reaction with various benzaldehydes (Retrosynthetic pathway B, Scheme II.6).

2.2. Exploration of Pro-Fluorescent EANBP Analog Synthesis Via Deprotonation of Methyl/Ethyl Nitrobenzene

This strategy that have been developed by Pfleiderer and his co-workers (Bühler *et al.,* 2004 and Smirnova *et al.,* 2005) describes the synthesis of 2-(2-nitrophenyl propan-1-ol) derivatives **7** through the deprotonation of 1-ethyl-2-nitrobenzene derivatives in the presence of ^{t}BuOK as a base and reacting the formed carbanion with paraformaldehyde.
We decided to use this strategy in order to construct our conjugated *o*-nitrophenethyl derivatives of EANBP **15** following the retrosynthetic pathway presented in Scheme II.15.

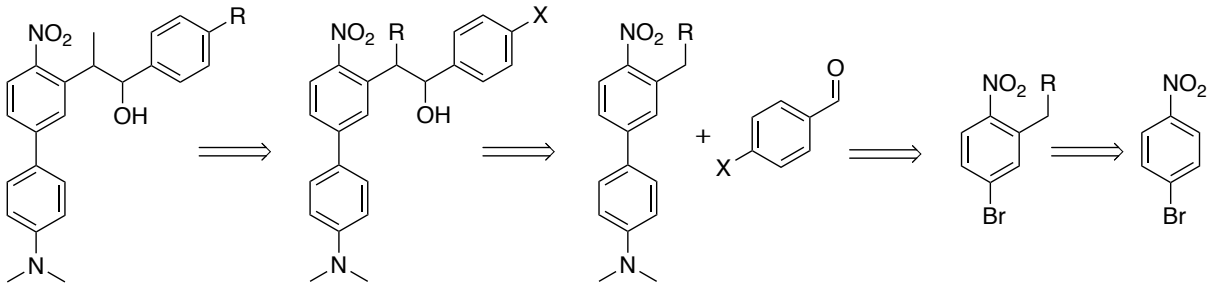

15 **14** **22** **23** **24** **1**

Scheme II.15: Retrosynthetic analysis for the construction of **15** via deprotonation of ethyl nitrobenzene derivative **24**.

The first step is the synthesis of **24** through the methylation (**24a**, R = H) or the ethylation (**24b**, R = CH_3) of **1** using organometallic reagents like RMgX (Bartoli *et al.,* 1985) or RLi (Kienzle, 1978) in the presence of oxidants like potassium permanganate ($KMnO_4$) or 2,3-Dichloro-5,6-dicyano-1,4-benzoquinone (DDQ).

The purpose behind the synthesis of the ethylated compound **24b** is to have readily the methyl group at the benzylic position after the reaction with aldehyde. Of note, and as mentioned in the introduction, the presence of an alkyl function at the benzylic position of *o*-nitrophenethyl PPGs dramatically increases the quantum yield of uncaging. The synthesis of compounds **24a,b** is presented in Scheme II.16.

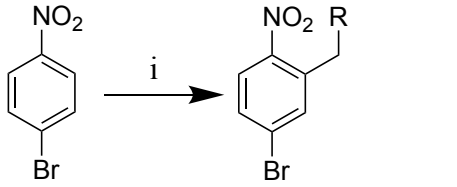

1 **24a** (R = H)
24b (R = CH_3)

Scheme II.16: Synthesis of methylated (**24a**) and ethylated (**24b**) compounds using organometallic reagents.

(i) RMgX or RLi, DDQ or $KMnO_4$, THF, -30°C, room temperature, overnight.

For the synthesis of compound **24a,** we first used MeMgBr as a Grignard reagent and DDQ as oxidant at -30°C. This reaction showed 60% conversion and the increase of the time of reaction (overnight to 24h) did not increase the yield of conversion.
After purification the product **24a** was obtained in 46% yield. Changing the oxidant to $KMnO_4$ (using the same MeMgBr Grignard reagent) yielded the same results almost with the same conversion.
Interestingly, the replacement of MeMgBr with MeLi showed a complete conversion of the starting 4-nitro bromobenzene **1** in the presence of DDQ and the target product **24a** was obtained in 88% yield. On the contrary, the use of EtMgBr along with DDQ yielded 81% of the ethylated compound **24b** with a 100% conversion of the starting material.
Following the alkylation step is the deprotonation step followed by the reaction with the aldehyde using the conditions adapted from La Regina's work (La Regina *et al.,* 2015).

We chose to use the 4-bromo benzaldehyde which is commercially available and the bromoaryl function should grant an access for further conjugation of the system using palladium catalyzed cross-coupling reactions.

The deprotonation of **24a** was done using sodium alkoxide in anhydrous DMSO and the resulting carbanion was reacted with 4-bromo benzaldehyde to obtain compound **25** (Scheme II.17).

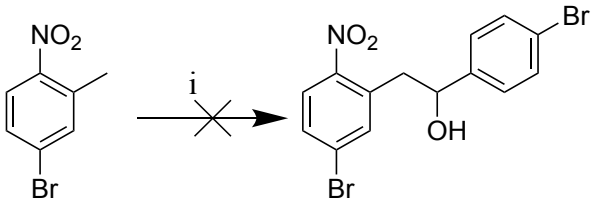

24a **25**

Scheme II.17: Synthesis of derivative **25** via deprotonation of **24a** in presence of 4-bromo benzaldehyde.

(i) Sodium ethoxide, anhydrous DMSO, 4-bromo benzaldehyde, 25°C < T < 80°C, 14h-24h.

The reaction was tried in the presence of sodium ethoxide (NaOEt) as a base in anhydrous DMSO at -30°C, in order to prepare the carbanion before adding the aldehyde. The reaction was done afterwards at room temperature, unfortunately it only resulted in starting material **24a**. Using the same base and solvent, the reaction was repeated by heating the reaction media at 80°C. We aimed, by heating, to kinetically drive the nucleophilic attach of the carbanion on the aldehyde, but again the reaction yielded only starting compound.

Finally, the reaction was repeated using the condition described by Bühler's group (Bühler *et al.,* 2004 and Smirnova *et al.,* 2005). Therefore, using potassium *tert*-butoxide (^{t}BuOK) as base in a mixture of anhydrous *tert*-butanol (^{t}BuOH) and DMSO.
Varying the temperature reaction from 25°C up to 80°C didn't change the reactivity of the either reagents and yielded only starting material too.
We switched to 4-bromo-2-ethyl-1-nitrobenzene **24b** where we used the same reaction conditions as for **24a**; varying the base either ^{t}BuOK or NaOEt and the temperature between 25°C and 80°C; unfortunately, we never succeeded to obtain the target product **26** (Scheme II.18).

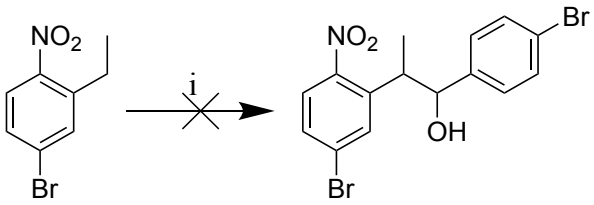

24b **26**

Scheme II.18: Synthesis of derivative **26** via deprotonation of **24b** in presence of 4-bromo benzaldehyde.

(i) NaOEt or ^{t}BuOK, anhydrous DMSO, 4-bromo benzaldehyde, 25°C < T < 80°C, 14h-24h.

Seeing that these 2 reaction conditions yielded only starting material, we suggested an alternative method; using *n*-BuLi as base, but in this case, we have to construct the biphenyl unit before going through the deprotonation in order to avoid the lithium halogen exchange.
The synthesis of the methylated/ethylated biphenyl compound **27a,b** could be done either by a Suzuki cross-coupling reaction starting from **24a,b** and dimethylamino phenylboronic acid, or by alkylating the previously synthesized compound **17**. The methylation of the nitro dimethylamino biphenyl **17** using MeLi yielded 82% of compound **27a** and the ethylation using EtMgBr gave **27b** in 78% yield (Scheme II.19).

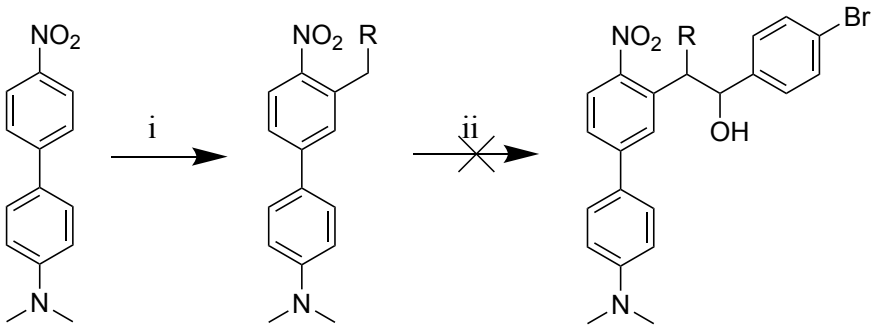

17 **27a** R = H (82%) **14a** R = H
27b R = CH_3 (78%) **14b** R = CH_3

Scheme II.19: Synthesis of **14a,b** via deprotonation of alkyl biphenyl **27a,b** synthesized by alkylation of **17**.

(i) MeLi / DDQ for **27a** and EtMgBr / DDQ for **27b**, THF, -30°C, room temperature, overnight (ii) *n*-BuLi, anhydrous THF, -80°C, 4-bromo benzaldehyde, room temperature, overnight.

When *n*-BuLi was added to compound **27a,b** at -80°C for couple tenth of minutes we observed an extreme change in the color of the solution from brownish-red to bright purple. This latter change in the color of the solution is in agreement with the formation of the carbanion of **27a,b** (a highly delocalized species).

After adding the 4-bromo benzaldehyde to the carbanion formed *in situ*, and after leaving the reaction warm up to room temperature overnight we observed only starting material after 14h of reaction. This latter result could be explained by the weak reactivity of the aldehyde used, so in order to increase the reactivity of the latter we decided to use an electron deficient aldehyde like 5-bromo-2-nitrobenzaldehyde. The reaction of **27a,b** with the chosen aldehyde didn't show any progress and didn't provide except starting material.

Seeing that this strategy had lots of problems and yielded no target compound **14a,b**, we decided to completely change the strategy. Therefore, an original strategy using the umpolung effect was explored in order to synthesize the conjugated EANBP analogs.

2.3. Exploration of Pro-Fluorescent EANBP Analog Synthesis Via Umpolung Effect

The methodology of synthetic organic chemistry has been greatly enriched by the development of functional group equivalents which provide an umpolung of the normal pattern of reactivity. In this concept, acyl anions and enolate cations are particularly valuable reactive functions.

The term umpolung was coined by Corey and Seebach to describe this temporary reversal of the characteristic pattern of reactivity of a functional group (Corey *et al.,* 1965 and Seebach and Corey., 1975). They suggested that certain sulfur stabilized anions could be suitable for use as masked nucleophilic acylating agents. The most successful sulfur stabilized acyl anion equivalents that have been studied to date, in terms of availability, ease of preparation and stability, are the cyclic 1,3-dithiane derivatives II (Scheme II.20).

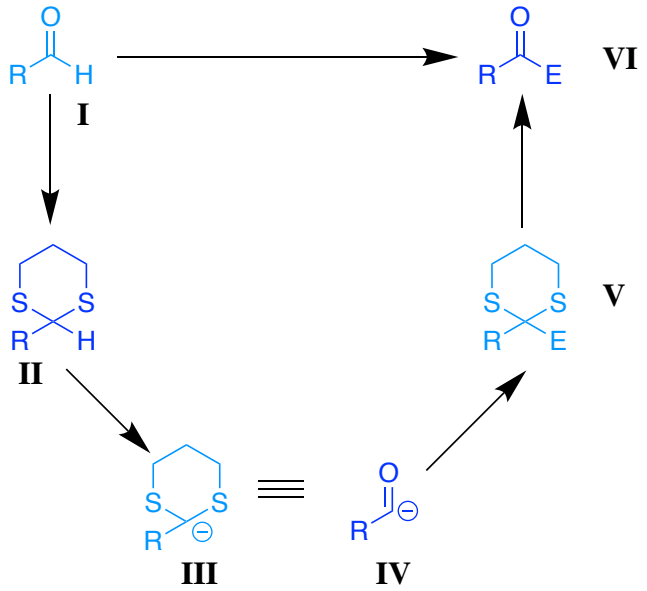

Scheme II.20: The mechanism of umpolung effect; reverse reactivity of carbonyl groups.

As indicated in Scheme II.19, the sulfur stabilized anion **III** directly reverses the normal pattern of reactivity of the carbonyl group and is thus an equivalent of an acyl anion **IV**. After reaction with an electrophile "E" the formed dithioacetal compound **V** may be hydrolyzed to provide the corresponding ketone **VI**.

In order to adapt this strategy to our target molecules, we suggested the following retrosynthetic analysis to access compound **14** via an umpolung effect of a carbonyl function (Scheme II.21).

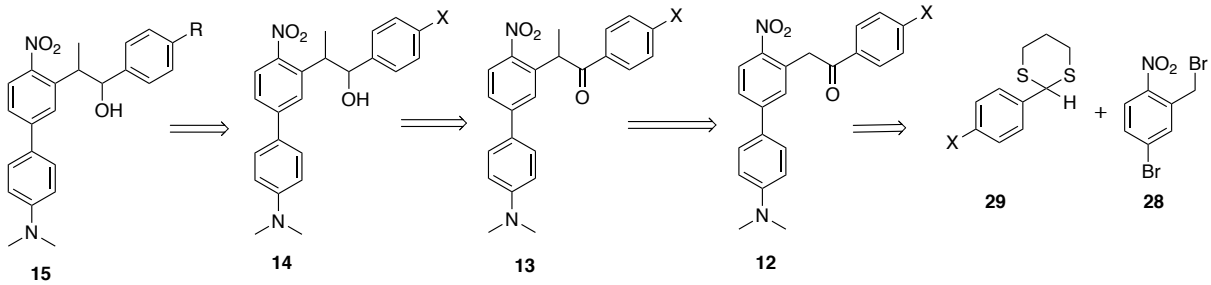

Scheme II.21: Retrosynthesis of compound **14** via umpolung effect of thio-protected carbonyl **29** and nitrobenzene derivative **28**.

The first step of this strategy is the synthesis of thiol-protected aldehyde **29** using 1,3-propandithiol and 4-bromo benzaldehyde **30**. This synthesis was done in an acidic medium using *p*-toluene sulfonic acid (*p*-TsOH). The deprotonation of the cyclic dithiane **29** needs *n*-BuLi, so it is important to avoid the use of any halogenated aldehydes. Therefore, we decide to extend the conjugation of the pro-fluorescent EANBP derivatives by using Sonogashira cross coupling reaction.

Therefore, we decided to synthesis the protected alkyne derivative **31**. This later compound was obtained through a Sonogashira reaction between compound **29** and trimethylsilyl acetylene. In parallel, the synthesis of compound **28** was done in 3 steps; the first step is the nitration of 3-bromo benzaldehyde **32** in a mixture of nitric and sulfuric acid. The following step is the reduction of the aldehyde function into a primary alcohol in the presence of $NaBH_4$ to obtain compound **34**. The final step is the bromination of the alcohol function using PPh_3 and CBr_4 to obtain the target compound **28** (Scheme II.22).

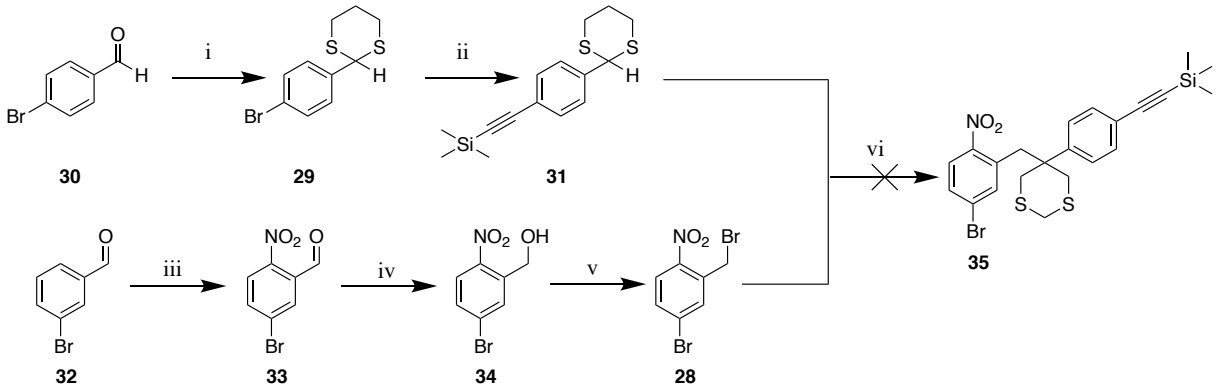

Scheme II.22: Synthesis of precursors **28** and **31** for the umpolung reaction leading to the formation of **35**

(i)1,3-propandithiol, *p*-TsOH, CH_2Cl_2, 50°C, 24h, 78%. (ii) trimethylsilyl acetylene, $Pd(PPh_3)_4$, CuI, Et_3N, THF, 50°C, overnight, 92%. (iii) H_2SO_4, HNO_3, 0°C, 2h, 72%. (iv) $NaBH_4$, THF, room temperature, 2h, 94%. (v) PPh_3, CBr_4, THF, room temperature, 4h, 65%. (vi) *n*-BuLi, THF, -80°C, room temperature, 14h-24h.

At -80°C, compound **31** was reacted with *n*-BuLi in an anhydrous and oxygen-free medium for 30 minutes before adding the electrophile **28** and leaving the reaction overnight. The reaction shows only starting materials with no traces of product **35** characterized by the disappearance of the peak at 5.76 ppm corresponding to the proton of the dithiane **31**.

Seeing that the 3 explored strategies produce lots of synthetic problems in terms of reactivity of reagents and stability of products in the reaction media, an alternative strategy should be proposed. The strategy should provide easy access to products that are stable, and their synthesis should be reproducible in big scales.

As mentioned in the chapter I, *o*-Nitroaryls are divided into two major categories: the *o*-nitrophenethyls and *o*-nitrobenzyls. This chapter focused on the possibility to access exclusively on pro-fluorescent *o*-nitrophenethyl derivatives.

In the following chapter III, we will describe an original strategy based on biphenyl epoxide derivatives, that due to its dissymmetric structure, could give access to both *o*-nitrophenethyl and *o*-nitrobenzyl PPGs family.

CHAPTER III

Towards the Synthesis of O-Nitroaryls Groups: via Epoxidation

1. Strategy

Epoxides were found to be really important chemical compounds that are useful in constructing several complex structures like nucleic acids (Hemminki *et al.,* 1980), sugars (Manzano et al., 2008) and modified amino acids (Babič *et al.,* 2006). Direct transformations of carbonyl groups into other versatile functional groups, such as epoxides, further increase the importance of these groups in synthesis. Several ways to obtain epoxides were demonstrated to be efficient, fast, good yielding and reproducible (Scheme III.1). The conversion of aldehydes into epoxides is usually done by using sulfur ylides enabling the transformation of alkenes to epoxides in presence of alkyl hydroperoxides (*tert*-butyl hydroperoxide ^{t}BuOOH as an example) and catalyzed by Vanadium (V), Molybdenum (VI) or Titanium (II) and α, β–haloalcohols give epoxides under the action of suitable base (NaOH as an example).

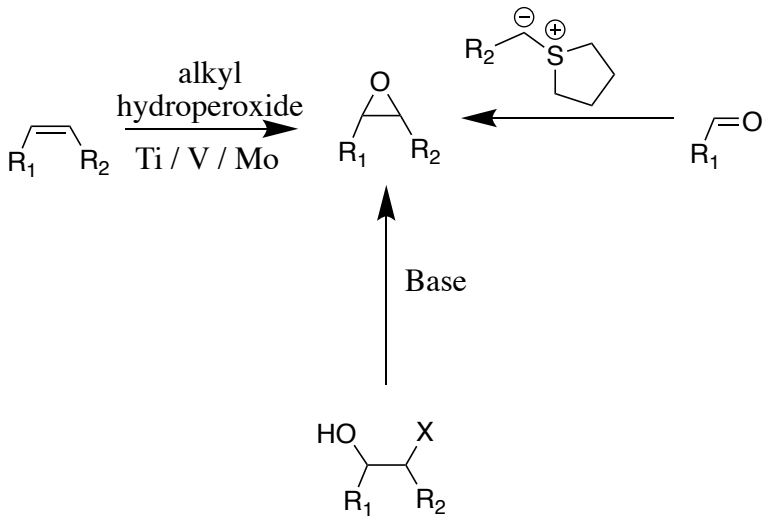

Scheme III.1: The plausible ways to synthesize di-substituted epoxides.

It could be useful to implement the use of di-substituted epoxides to construct pro-fluorescent *o*-nitroaryls PPGs. Interestingly, the construction of a di-substituted yet non-symmetrical epoxide **E** would be advantageous since the opening of this epoxide leads to two separate products with different properties. In our case, the epoxide opening of **E** will lead to the formation of two products: an *o*-nitrophenethyl derivative **A** and an *o*-nitrobenzyl derivative **B** (Scheme III.2). So, by synthesizing this epoxide **E** and after its opening, we can get access to both families of pro-fluorescent PPGs.

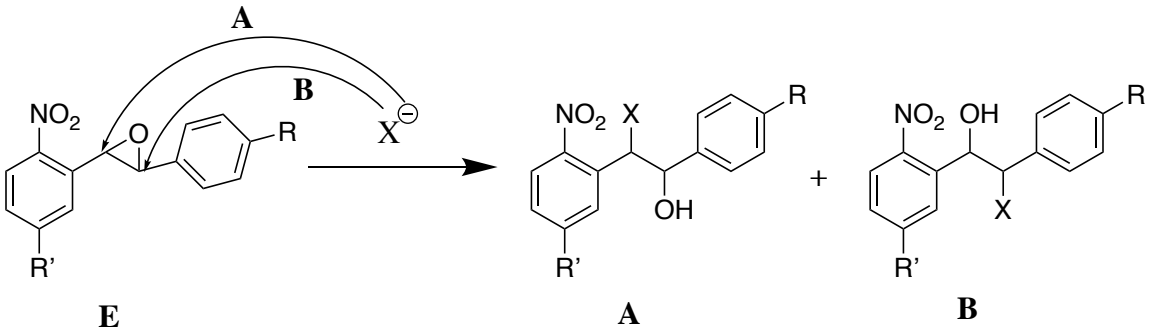

Scheme III.2: Synthesis of *o*-nitrophenethyls **A** and *o*-nitrobenzyls **B** via epoxide opening.

2. Design

2.1. Retrosynthetic Analysis

The design of the target epoxide **36** takes into account the presence of the nitrobiphenyl core and to be able to introduce a halogenoaryl function that serves as a reactive entity to increase the conjugation of the pro-fluorescent *o*-nitro-biphenyl PPGs.

A proposed retrosynthetic analysis for the target epoxide is presented in Scheme III.3.

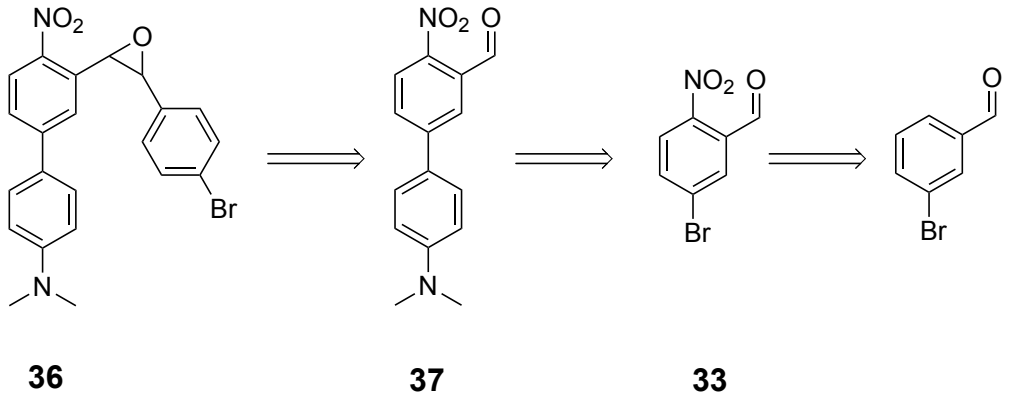

Scheme III.3: Retrosynthetic analysis to obtain the target epoxide **36**.

We chose to synthesize the epoxide via a sulfur ylide nucleophilic addition on benzaldehyde derivatives because this synthetical strategy has been demonstrated to be the shortest and best yielding compared to the strategies that use haloalcohols and olefins to access the epoxide. After constructing the nitrobiphenyl aldehyde **37** we could obtain the target epoxide **36** by reacting the aldehyde with the sulfur ylides **42**.

2.2. Epoxide Synthesis

The synthesis of the epoxide is divided in two parts: I) the synthesis of the nitrobiphenyl aldehyde **37** and II) the synthesis of the sulfur salt **42**.

For the synthesis of aldehyde **37**, the 3-bromobenzaldehyde is nitrated in the presence of a mixture of sulfuric and nitric acid in order to obtain the 5-bromo-2-nitrobenzaldehyde **33** in 72% yield.

To construct the biphenyl core via a Suzuki cross-coupling it was necessary to protect the aldehyde function in order to avoid any competing reaction of the palladium on the *o*-nitro benzaldehyde moiety. The protection of the aldehyde was done in the presence of ethylene glycol in toluene in the presence of a catalytical amount of *p*-toluene sulfonic acid using a Dean-Stark apparatus in order to azeotropically remove water from the reaction medium leading to the formation of dioxolane **39**.

After having protected the aldehyde function, the pallado-catalyzed Suzuki cross-coupling reaction between **39** and 4-(dimethylamino) phenylboronic acid leads to the formation of the nitro biphenyl dioxolane **38** in 85% yield (15% is lost due to the homocoupling of the boronic acid).

After deprotection of the aldehyde in presence of *p*-TsOH the nitrobiphenyl aldehyde **37** was obtained quantitatively (Scheme III.4)

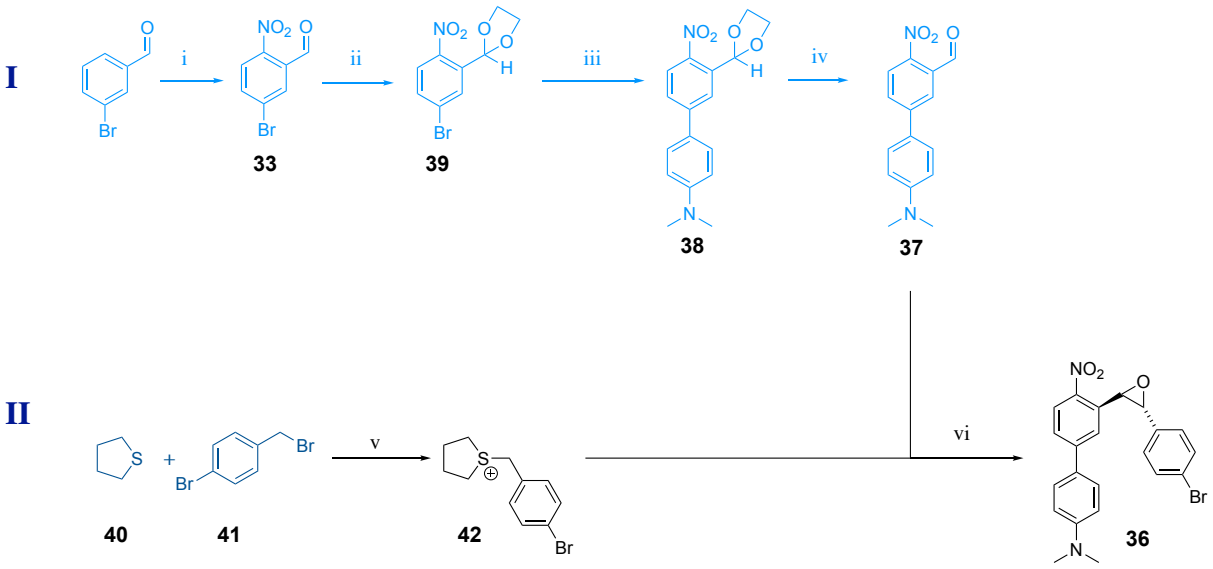

Scheme III.4: Total synthesis of epoxide **36** in two parts I) synthesis of the nitrobiphenyl aldehyde **37** and II) synthesis of the sulfur salts **42**.

(i) H_2SO_4, HNO_3, 0°C, 2h, 72%. (ii) ethylene glycol, *p*-TsOH, toluene, 130°C, 2h, 98%. (iii) 4-(dimethylamino) phenylboronic acid, K_2CO_3, Bu_4NBr, Pd $(OAc)_2$, EtOH/H_2O (2:1), microwave, 160°C, 15 min, 85 %. (iv) *p*-TsOH, H_2O, CH_2Cl_2, CH_3CN, 80°C, 100%. (v) acetone, 14h, 93%. (vi) 1,5,7-triazabicyclodec-5-ene, CH_2Cl_2, 90%.

The tetrahydrothiophenium bromide salt **42** is prepared from tetrahydrothiophene **40** and 4-bromobenzyl bromide **41** in anhydrous acetone, and these salts start to appear progressively and precipitate in the solution.

The synthesis of the epoxide **38** needs a base that is efficient in deprotonating the thiophenium salt **42** and forming the sulfur ylide. We tried hydroxides (KOH and NaOH) as well as carbonates ($CsCO_3$), but using these bases no formation of epoxide product **36** was observed. The use of the azabicyclo-undecene base, led to the formation of the product and interestingly, the use of 1,5,7-triazabicyclodec-5-ene (TBD) as a base led to the formation of the target epoxide **38** in 90% yield with no undesired side reactions.

This epoxide could result in the formation of the two families of PPG of interest (Scheme III.2) upon its opening using nucleophiles like organometallic compounds (organozincates, organocupprates, organolithiums and organoaluminates) or metallic salts (lithium halides, lithium hydroxides…). In our case of interest, opening the epoxide with a methyl anion will lead to the formation of our 2 target compounds (**A** and **B**, Scheme III.2, X=CH_3).

2.3. Epoxide Opening

Several researches about the reactions of epoxides have been done in order to demonstrate the orientation of the epoxide opening (Parker *et al.,* 1959 and Solladié-Cavallo *et al.,* 2005). In the general case of reaction with an unsymmetrically substituted epoxide two products are possible depending on the nature of the medium:

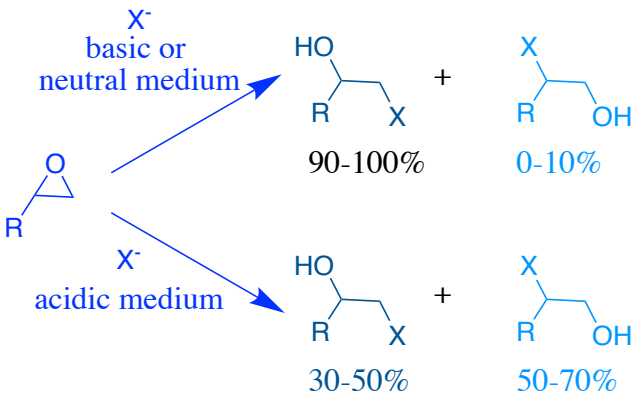

Scheme III.5: Epoxide opening products depending on the pH of the medium.

Examinations of orientational studies on these types of epoxides are divided into reactions carried out under basic or neutral conditions and reactions carried out under acidic conditions. These examination show that, under basic or neutral conditions, the product corresponding to the attack on the least substituted carbon atom is nearly always the major or only isolated product.

This provides strong evidence for an SN_2 attack of a reagent molecule or ion on the epoxide ring carbon atom. In the case of a reaction in acidic medium, the orientation is carried out via an SN_1 type attack by the formation of the more stable carbocation (the carbon holding more substituents) followed by the attack of the nucleophilic reagent or ion.

In our strategy, we decided to use organometallic methylating agents in order to insert the methyl substituent on the two products that we expect to obtain: *o*-nitrophenethyl and *o*-nitrobenzyl groups. We used a wide diversity of methyl organometallic reagents like MeLi, Me_3Al, MeMgBr, $Me_2Cu(CN)Li$ (prepared from MeLi and CuCN) and Me_3ZnLi (prepared from MeLi and $ZnCl_2$), using epoxide activators like $BF_3.OEt_2$, CuI, PPh_3 and $AlCl_3$, and anhydrous solvents like diethyl ether, toluene, and THF. The results of all the experiments done are presented in the Table 4 below.

Methylating agent	Activator	Solvent / temperature	Yield
MeLi (3eq)	-	THF / -78° C	-
MeLi (3eq)	$BF_3.OEt_2$ (3eq)	THF / -78° C	-
MeLi (3eq)	CuI (1,5eq)	Ether -78° C	-
MeLi (5eq)	CuI (3eq)	Ether / 0° C	-
MeLi (2eq) + CuCN (1eq)	$BF_3.OEt_2$ (2eq)	THF / -78° C	-
MeLi (1.2eq)	$AlCl_3$ (2eq)	THF / -78° C	-
Me_3Al (1.2eq)	$AlCl_3$ (1,2eq)	THF / -78° C	-
MeLi (3eq)	$BF_3.OEt_2$ (3eq)	Toluene / -78° C	-
MeLi (3eq)	$BF_3.OEt_2$ (3eq)	Ether / -78° C	-
Me_3Al (1eq)	PPh_3 (5%)	Toluene / 25° C	-
MeMgBr (1.5eq)	CuI (10%)	THF / -30° C	-
$ZnCl_2$(1eq) + MeLi (3eq)	-	THF / -85° C	-
$ZnCl_2$(1eq) + MeLi (3eq)	$BF_3.OEt_2$ (3eq)	THF / -85° C	-

Table 4: Epoxide opening using various methylating agents and activators in different solvents.

All the above trials were done in basic medium due to the basic character of all the organometallic compounds used (order of the basicity of these compounds depend on the polarity of the carbon-metal bond and the nature of the metal).

Due to the basicity of these reagents, all the above reactions yielded starting material; the acid-base reaction between the proton at the benzylic position of the *o*-nitrobenzyl moiety and the organometallic reagent occurs faster than the epoxide opening reaction yielding, after hydrolysis, to starting material (Scheme III.6).

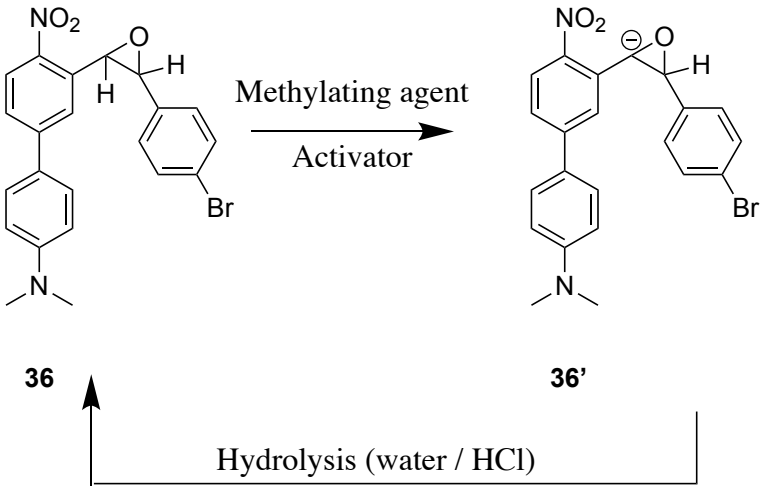

Scheme III.6: Acid-base reaction occurring upon the addition of the organometallic reagent on the epoxide **36**.

The presence of a nitro group gives the epoxide proton at the benzylic position of the *o*-nitrobenzyl moiety, a highly acidic character leading to the formation of **36'** upon the addition of the methylating agent. This latter presents a basic character and thus leads to the formation of the deprotonated compound rather than the expected SN_2 product that leads to the opening of the epoxide and giving the target product.

2.4. Epoxide Reduction

The reduction of epoxides has attracted lot of attention in the synthesis of asymmetric alcohols and several ways to reduce epoxides were applied. Seeing that the opening of epoxides is problematic due to the acid base exchange, we thought about reducing the epoxide to its corresponding alcohols using the common known reducing agents like aluminum hydrides and boron hydrides (Solladié-Cavallo *et al.,* 2002; Florio *et al.,* 2014). The reduction of our non-symmetric epoxide **36** leads to the formation of two corresponding alcohols **43** and **43'** (Scheme III.7).

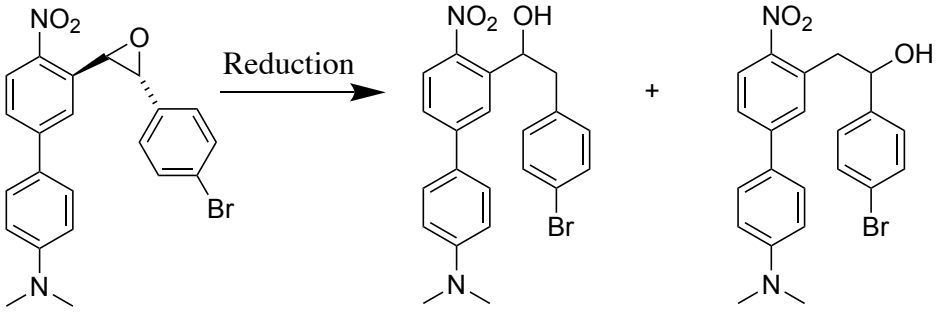

36 **43** 70% **43'** 30%

Scheme III.7: Reduction of epoxide **36** leading to the formation of the 2 alcohols **43** and **43'**.

We used several chemoselective reducing agents like aluminum hydrides ($LiAlH_4$ and DIBAL-H) and boron hydrides like $NaBH_4$, it is important to note that the use of H_2 over Pd/C is not advised since we can risk the reduction of the nitro group to its amino function. The results of all the reactions tried for reducing epoxide **36** are presented in the table 5 below.

Entry	Reducing agent	Activator	Solvent/Temperature	Conversion
1	$LiAlH_4$	-	Ether / 0° C	0%
2	$LiAlH_4$ (2eq)	$AlCl_3$	Ether / 0° C	60%
3	$LiAlH_4$ (5eq)	$AlCl_3$	Ether / 0° C	60%
4	$LiAlH_4$ (5eq)	$AlCl_3$	THF / 0° C	60%
5	$LiAlH_4$ (5eq)	$AlCl_3$	THF / 50° C	60%
6	DIBAL-H (3eq)	-	CH_2Cl_2 / -40° C	0%
7	DIBAL-H (3eq)	$AlCl_3$	CH_2Cl_2 / -40° C	0%
8	$NaBH_4$	-	THF / 0° C	0%

Table 5: Epoxide reduction using various aluminum and boron hydrides with activators in different solvents.

The use of lithium aluminum hydride ($LiAlH_4$) as reducing agent in diethyl ether didn't show any result without an activator (Entry 1), whereas upon adding an activator like aluminum trichloride ($AlCl_3$) we observed a 60% conversion of starting material (Entry 2), unfortunately, this conversion was not affected by the increase of equivalents of $LiAlH_4$ (Entry 3).

We decided to change the solvent to anhydrous THF due to the low solubility of the epoxide in ether at 0°C and keeping the same number of equivalents of $LiAlH_4$ we observed no change in the conversion even upon heating the solution to 50°C (Entries 4 and 5).

Another aluminum hydride alternative is diisobutylaluminum hydride (DIBAL-H) in anhydrous dichloromethane, unfortunately, this reducing agent shows no conversion of the starting material with or without activator (Entries 6 and 7). The final trial was using sodium borohydride ($NaBH_4$) in anhydrous THF, this reducing agent shows no reaction with our epoxide and thus yielding only starting material **36** (Entry 8). Only the reactions with $LiAlH_4$ tend to convert partially (60%) the starting material **36** and we observed the formation of **43** and **43'**in approximately 70% to 30% respectively (in reference to the NMR spectrum of the crude product). The starting material and the obtained products **43** and **43'** show similar polarity and thus it was impossible to purify these compounds neither over column nor using HPLC and thus we couldn't obtain a pure compound to proceed further.

2.5. Epoxide Alkylation

Due to the problem of purification of the reduced epoxide products, we suggested a new reaction that takes advantage of the acidity of the proton in alpha to nitro (discussed in section 2.3). Since in the presence of methylating agents we only observed acid-base reaction, we decided to take advantage of this undesirable reaction to alkylate the epoxide and then reducing it to its corresponding alcohols (Scheme III.8).

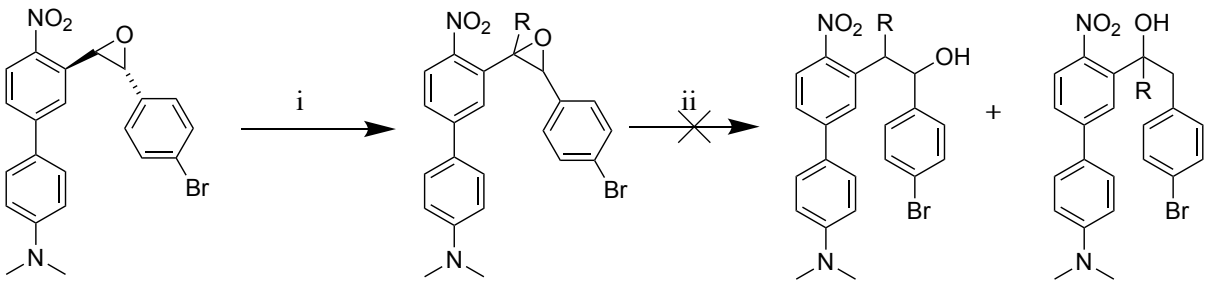

36 **44** **43'** **45'**

Scheme III.8: the alkylation of the epoxide **36** followed by the reduction of the corresponding product **44** into the alcohols **45** and **45'**.

(i) MeLi, RX, THF, -80°C→room temperature. (ii) $LiAlH_4$, THF, $AlCl_3$, 0°C.

We chose MeLi as the base since it has the most basic character among the other organometallic species, and we decided not only to methylate the epoxide using MeI but also to add a propargyl substituent using propargyl bromide which could serve in rendering the final molecule soluble by introducing PEG chains via click chemistry. The reactions that were done and their results are presented in Table 6.

Base	R-X	Solvent / Temperature	Conversion
MeLi	Me-I (1,5eq)	THF / -80° C	30%
MeLi	Me-I (5eq)	THF / -80° C	30%
MeLi	Propargyl-Br (5eq)	THF / -80° C	0%
MeLi	(TMS-propargyl)-Br (5eq)	THF / -80° C	70%

Table 6: Alkylation of epoxide **36** with methyl or propargyl using MeLi (1.2 eq) as base to obtain **44**.

Using MeLi as a base we were able to deprotonate the epoxide **36** and alkylate it using iodomethane but the conversion was not total even when we increased the equivalents of MeI from 1.5 to 5, the conversion remained at 30% unchanged. The obtained fraction with 30% of product couldn't be purified due to the close polarity of the product **44** and starting epoxide **36**. The use of propargyl bromide led to the formation of the product of attack of propargylate over the propargyl bromide and not on the epoxide so we used the protected propargyl (TMS-propargyl-Br). Interestingly this reaction, in anhydrous THF and 1.2 eq of MeLi, led to a 70% conversion of the starting material **36** and the formation of product **44** (R = propargyl) that was isolated as pure compound. The reduction of **44** using $LiAlH_4$ in presence of $AlCl_3$ as activator in anhydrous THF led only to starting material with no traces of the corresponding alcohols **45** and **45'** (R = propargyl).

The opening of the epoxide before or after alkylation seems to be problematic which could be explained by the steric hindrance of the epoxide making it inaccessible by anions and due to the electronic densities around the epoxide is makes it more difficult to activate and thus less reactive towards organometallic reagents and hydrides.

All in all, the synthesis of the epoxide was an interesting alternative to access conjugated EANBP analogs. The production of the epoxide is high yielding and reproducible, but we faced lots of problems during the epoxide opening and reduction.

The presence of a nitro group near the epoxide moiety led to an acid-base reaction between the proton at the benzylic position and the organometallic compound used for the opening of the epoxide. Also, during the reduction, and due to close polarities of the product and the starting material, we were not able to isolate the target compound.

The synthesized epoxide has a conjugated system in its architecture which could induce a fluorescence signal in solution. Interestingly, this epoxide has a reactive bromoaryl function that could be used to increase the conjugation and obtain a higher fluorescence emission wavelengths. If this is the case, this epoxide could be an interesting candidate as a fluorescent dye for imaging studies in biological systems (via the synthesis of a soluble version). In the following section, we decided to evaluate the fluorescence quantum yield of the obtained epoxide as well as its two-photon absorption cross section and compare them to the starting aldehyde.

2.6. Determination of the Two-Photon Absorption (2-PA) Cross-Section δ_a

The experimental determination of the 2-PA cross section (δ_a) of a molecule, which represents its efficiency in absorbing photons in two-photonic excitation, is possible using different techniques (Twarowski and Kliger, 1977). The two most commonly used experimental methods for the determination of two-photon absorption cross sections are the Z-Scan method (Sheik-Bahae *et al.,* 1990) and the two-photon excitation-induced fluorescence method (Xu and Webb, 1996). In our case, we decided to check the efficiency of our epoxide **36** in absorbing two-photons which can make this compound a remarkable candidate for imaging. We were interested in determining its absorption cross-section section in 2-PE (δ_a) by the measurement of fluorescence intensity induced by two-photon excitation.

2.6.1. Determination of δ_a using the method of fluorescence

The direct measurement of the two-photon absorption cross section (δ_a) is difficult to obtain, therefore, it is more common to obtain this value indirectly through a reference compound by measuring its two-photon fluorescence (δ_f) cross section according to equation (3):

$$\delta_f = \delta_a \,.\, \phi_f \qquad (3)$$

Therefore, in order to obtain the value of δ_a, we have to be able, first, to experimentally determine the fluorescence quantum yield (ϕ_f) of our epoxide **36**. The method used in order to be able to measure the fluorescence quantum yield of a compound through a known reference is discussed in the section below.

2.6.1.1. Determination of the Fluorescence Quantum Yield ϕ_f

The quantum fluorescence yield (ϕ_f) is defined as the ratio of the number of photons emitted to the number of photons absorbed by the sample. Normally, a quantum yield of fluorescence for an unknown compound is determined using a reference compound whose quantum yield is well known.

It is necessary to obtain the values of the fluorescence intensities of our studied compound ($I^{epoxide}$) and of the compound taken as a reference (I^{ref}), these values have to be obtained using the same absorbance for both the compound and the reference.

We selected the Quinin Sulfate in solution in sulfuric acid as a reference with a quantum yield of fluorescence ($\phi_f = 0.54$) as determined by direct method (Heller *et al.,* 1974).

In the measurements of the spectra, the concentrations of the compound to be studied and the compound taken as reference are chosen so that the absorbance of the two solutions are identical for the selected excitation wavelength.

Equation (4) can be simplified by deleting the ratio of the respective absorbances. Since the sample solvent of our epoxide (Toluene) is not the same as the reference (water), a corrective factor of their respective refractive indices must be introduced in the calculation of quantum yield (Durham *et al.,* 1982).

$$\phi_f^{epoxide} = \phi_f^{ref} \left(\frac{A^{ref}}{A^{epoxide}}\right) \left(\frac{I^{epoxide}}{I^{ref}}\right) \left(\frac{n_D^{epoxide}}{n_D^{ref}}\right)^2 \qquad (4)$$

$\phi_f^{epoxide}$: Quantum yield of fluorescence of epoxide to be determined

ϕ_f^{ref} : Quantum yield of fluorescence of reference Quinin Sulfate

$A^{ref,epoxide}$: Absorbance of the reference and the epoxide respectively

$I^{epoxide,ref}$: Emission intensity of the epoxide and the reference respectively

$n_D^{epoxide,ref}$: Refractive index of the solvent used for the epoxide and the reference respectively

Simply, by replacing the terms in equation (4) by their corresponding values, we obtained a quantum yield of fluorescence $\phi_f^{epoxide}$ = 0.18 for our epoxide **36**. In the same manner, we calculated the $\phi_f^{aldehyde}$ and we found a value of 0.18. These values were calculated and validated from 3 separate trials. The interest of calculating this term for the aldehyde **37** is to calculate the efficiency of this compound in 2-PA and compare it with that of the epoxide.

2.6.1.2. Determination of the Two-Photon Absorption Cross-Section δ_a

The two-photon absorption cross-section (δ_a) of the epoxide **36** has been determined by comparing its fluorescence intensity by two-photon excitation with that of Rhodamine B, whose two-photon absorption spectra and fluorescence quantum yield are precisely known (Xu *et al.,* 1995). In practice, a femtosecond pulse Ti: Sapphire laser was used to irradiate the solutions containing the reference Rhodamine B (Rho B) in ethanol and our epoxide **36** in toluene.
We irradiated by scanning the wavelength (λ) between 700 and 900 nm and noting the values of the resulting two-photon fluorescence intensities.
Similar to the experimental determination of the quantum fluorescence yield, the 2-PA cross section can be calculated according to equation (5):

$$\delta_a^{epoxide} = \delta_a^{RhoB} \left(\frac{A^{RhoB}}{A^{epoxide}}\right)\left(\frac{I^{epoxide}}{I^{RhoB}}\right)\left(\frac{\phi_f^{RhoB}}{\phi_f^{epoxide}}\right)\left(\frac{n_D^{RhoB}}{n_D^{epoxide}}\right) \qquad (5)$$

δ_a^{RhoB} : Two-photon absorption cross-section of the Rhodamine B

$\delta_a^{epoxide}$: Two-photon absorption cross-section of the epoxide

$\phi_f^{epoxide}$: Quantum yield of fluorescence of epoxide calculated

ϕ_f^{RhoB} : Quantum yield of fluorescence of reference Rhodamine B

$A^{RhoB,epoxide}$: Absorbance of the reference and the epoxide respectively

$I^{epoxide,RhoB}$: Emission intensity of the epoxide and Rho B respectively

$n_D^{epoxide,RhoB}$: Refractive index of the solvent used for the epoxide (toluene) and Rho B (ethanol) respectively

Both the reference, Rhodamine B, and the compound of interest, epoxide **36** and aldehyde **37**, were irradiated by the laser and the intensities of fluorescence (I) obtained were replaced by their values in equation (5) and we were able to construct the two-photon absorption spectra of both the aldehyde and the epoxide (Scheme II.9).

Interestingly, the fluorescence quadratic-intensity dependence correlates linearly with the power of the laser which indicates clearly the process of two-photon absorption.

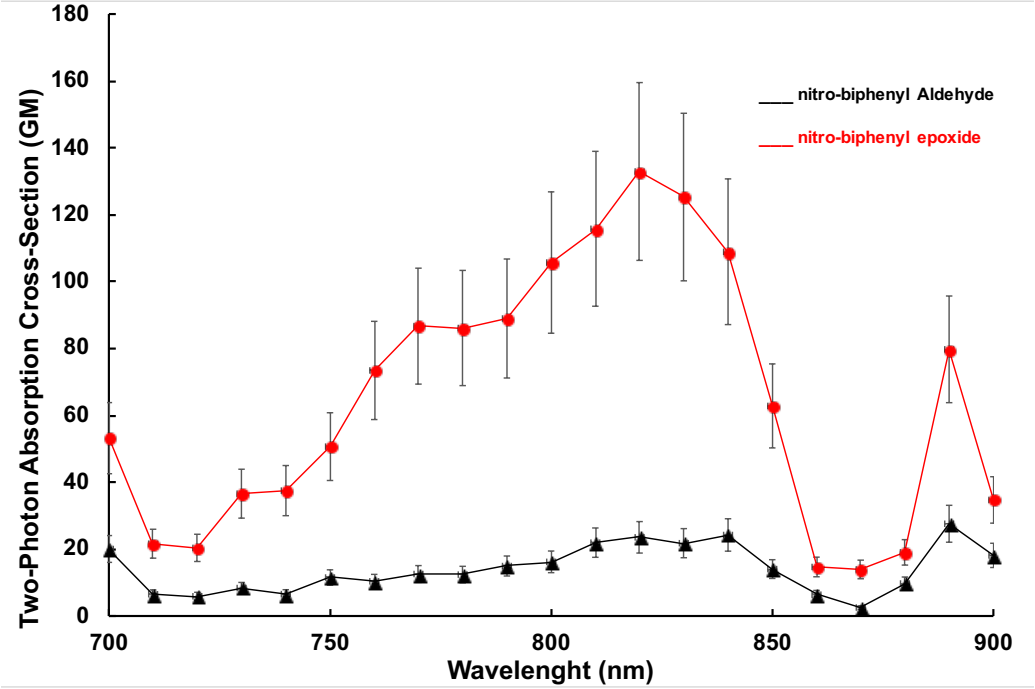

Scheme II.9: Two-photon absorption spectra of epoxide **36** (red) and aldehyde **37** (black).

In reference to the spectra, it is evident that the epoxide is more efficient in 2-PA than the corresponding aldehyde in toluene. Even though they both show the same quantum yield of fluorescence $\phi_f^{aldehyde} = \phi_f^{epoxide} = 0.18$, the epoxide tends to produce more intense emission under the action of laser irradiations. The epoxide possesses a two-photon absorption cross-section (δ_a) values up to 140 GM whereas the aldehyde shows a max of 20 GM in the wavelength range of 700-830 nm.

Using this mentioned method, same experiments were done on the two compounds but in dichloromethane, a non-polar and non-aromatic solvent, but we observed no fluorescence signal using two-photon excitations for both compounds no matter the wavelength used.

Even though the epoxide is not a Photoremovable Protecting Group and cannot be used for biological activities for the release of biological molecules, yet it can act as an interesting fluorophore for imaging and we can at all times modify the structure by increasing the conjugation and/or solubility.

To conclude, even though the synthetic strategy for epoxide seemed promising as an access to both *o*-nitroaryl groups of interest, but, due to several mechanistic, reactivity, structural and functional reasons this strategy had lots of limitations. Staying in the same synthetic route, we decided to take advantage of the aldehyde **37** in order to synthesize one group of the *o*-nitroaryl family, the *o*-nitrobenzyl Photoremovable Protecting Group.

CHAPTER IV

Towards the Synthesis of *O*-Nitrobenzyl Group: A Pro-Fluorescent Photoremovable Protecting Group

1. Strategy

After all the trails on the epoxide opening, reduction and alkylation, we decided to change the strategy again but this time staying in the same synthetic route. The synthesis of the epoxide was done through the reaction of an aldehyde **37** function with a sulfur ylide, since the aldehyde is easily synthesized in good yielding multiple steps, we decided to use this aldehyde and react it with organometallic compounds in order to generate the alcohol **47**. Theoretically, this strategy would give access to a photoremovable group in just one additional step. The retrosynthetic analysis is described in Scheme IV.1.

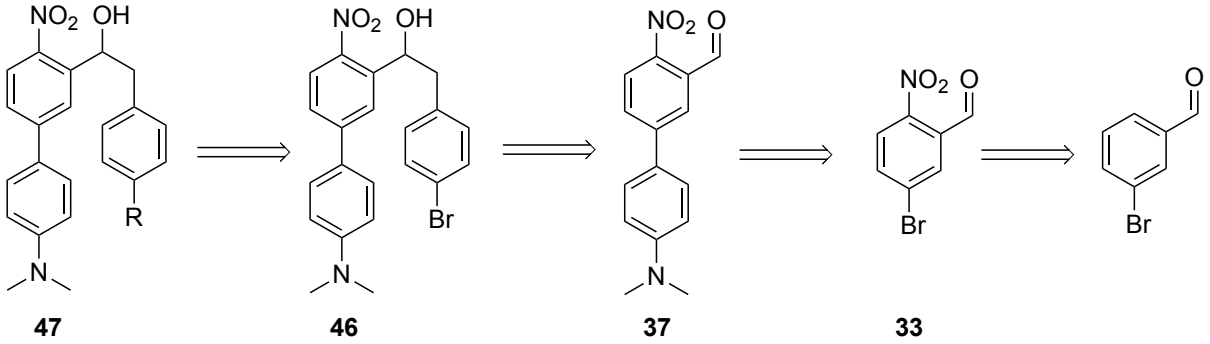

Scheme IV.1: Retrosynthetic analysis for the synthesis of conjugated photoremovable protecting group **47**.

Using the aldehyde **37** we can access the alcohol **46** that could undergo further cross coupling reactions in order to increase the conjugation and obtain compound **47**. This strategy gives direct access to only one group of the *o*-nitroaryl family; the *o*-nitrobenzyl photoremovable protecting group. Even though it doesn't grant access to the *o*-nitrophenethyl group, yet it is chemically accessible and synthetically possible.

2. Synthesis of *o*-nitrobenzyl Photoremovable Protecting Group

2.1. Synthesis of the bromo derivative of *o*-nitrobenzyl PPG

The synthesis of compound **46** is presented in the Scheme IV.2. The first part (I) is the same procedure that has already been used for the epoxide synthesis and led to the production of the aldehyde **37**, the second part (II) is the generation of the organometallic compound that will be used for the nucleophile attack on the electrophilic aldehyde function of compound **37**.

The generation of the organometallic compound is a challenging reaction due to the low stability of the formed compounds in solutions and the risk of intramolecular reaction.

The synthesis of the organometallic derivative of bromobenzyl bromide **41** was done using zinc powder activated with lithium chloride (LiCl), 1,2-dibromoethane (DBE) and trimethylsilylchloride (TMSCl) under microwave heating in freshly distilled anhydrous THF at 70°C for 1h. We were able to generate a solution of bromobenzyl zinc bromide **48** that was titrated iodometrically in order to know its corresponding concentration in THF. The freshly synthesized reagent **48** was added to the solution of aldehyde **37** at -78°C for a duration of 14h leading to the formation of the *o*-nitrobenzyl biphenyl Photoremovable Protecting Group **46** in 80% yield. We observed the presence of the intramolecular reaction product **48'** that is produced upon the undesired reaction between the organozinc compound **48** and the starting 4-bromobenzylbromide **41**.

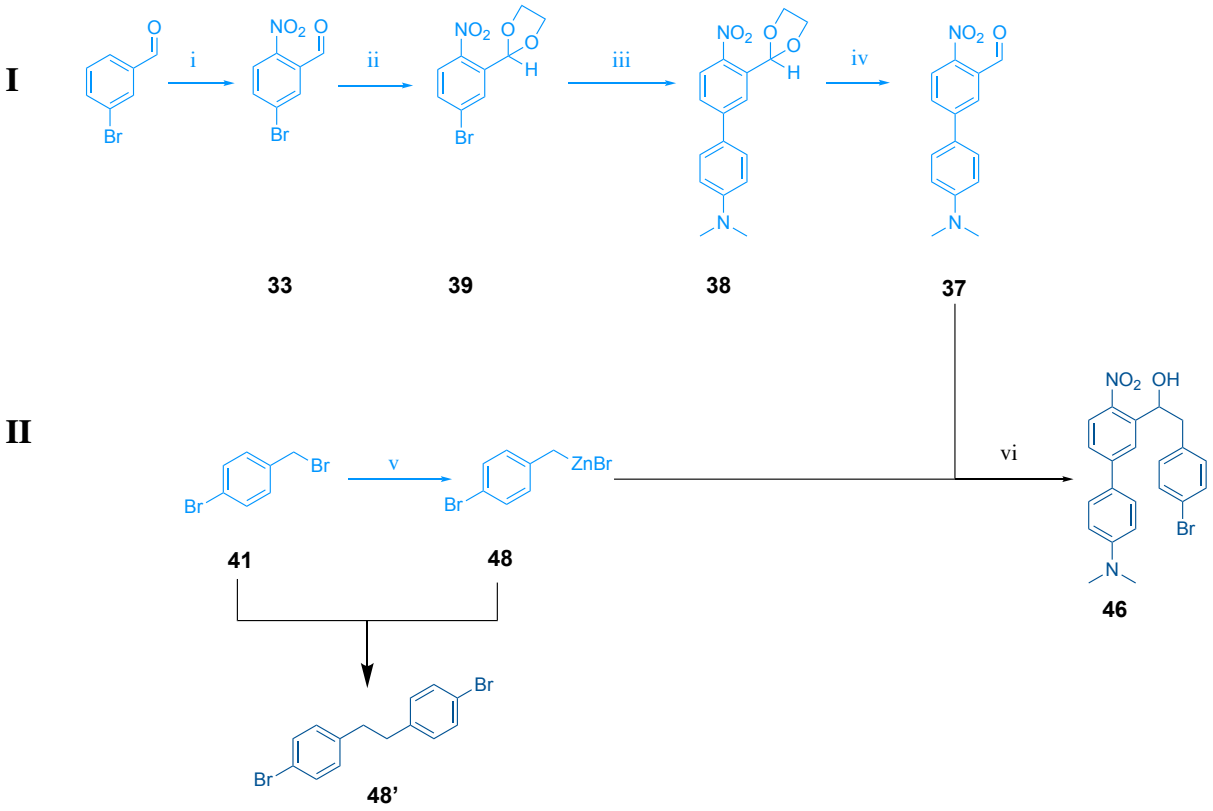

Scheme VI.2: Total synthesis of *o*-nitrobenzyl PPG **46** in two parts I) synthesis of the *o*-nitrobiphenyl aldehyde **37** and II) synthesis of the bromobenzyl zinc bromide **48**.

(i) H_2SO_4, HNO_3, 0°C, 2h, 72%. (ii) ethylene glycol, *p*-TsOH, toluene, 130°C, 2h, 98%. (iii) 4-(dimethylamino) phenylboronic acid, K_2CO_3, Bu_4NBr, Pd $(OAc)_2$, EtOH/H_2O (2:1), microwave, 160°C, 15 min, 85 %. (iv) *p*-TsOH, H_2O, CH_2Cl_2, CH_3CN, 80°C, 100%. (v) Zn, LiCl, 1,2-dibromoethane, trimethylsilyl chloride, 85°C, 5 min, 4-bromobenzylbromide **41**, anhydrous THF, microwave, 70°C, 1h. (vi) anhydrous THF, -78°C, overnight, 80%.

In order to study the behaviour of this newly synthesized Photoremovable Protecting Group **46** and its photochemical and photophysical properties, we attached an organic acid that acts as a chromophore in order to follow the photocleavage and quantify the cleavage efficiency by HPLC.

For this reason, we have coupled 3,4-dimethoxyphenyl acetic acid (MPAA) to our PPG in order to obtain the caged compound **49** (Scheme IV.3).

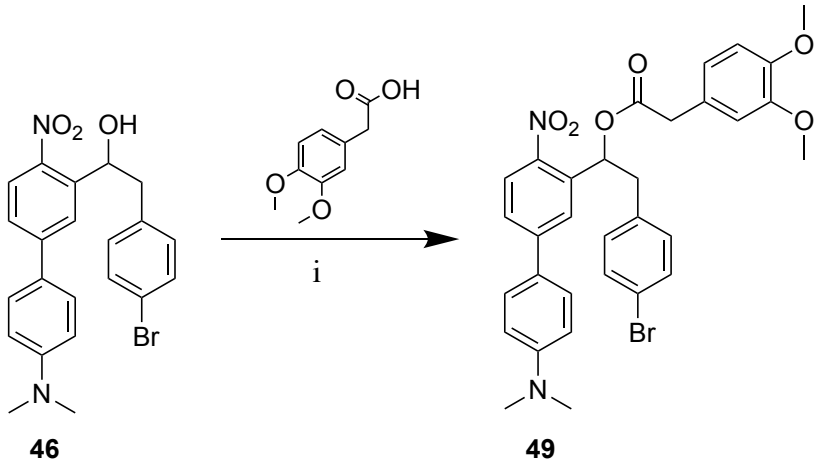

46 **49**

Scheme IV.3: Synthesis of the *o*-nitrobenzyl "caged" acid **49**.

(i) DIC, DMAP, CH_2Cl_2, 0°C, 3h, 68%.

The coupling reaction was done using MPAA with N,N'-diisopropyl carbodiimide (DIC) with catalytic amount of dimethylaminopyridin (DMAP) in dichloromethane in order to get access to the ester **49** in 68 % yield. Previous trials for the same coupling were done in the lab using DCC as coupling agent, but in our case, we replaced this latter with DIC since it is more soluble in dichloromethane (the reaction solvent) and the corresponding urea salts, produced at the end of the reaction, could be removed by simple crystallization in cold acetonitrile.

2.1.1.Study of the Photolysis by one-photon Excitation

The photolysis of the *o*-nitrobenzyl series occurs according to the mechanism described in Scheme I.14. Upon irradiation of a sample of **49** with known concentration, a photolysis by-product **49'** is released (Scheme IV.4). The nitrosoketone product **49'** is present in equilibrium with its tautomeric nitroso-enol form **49''**, the ratio of these products depends on the concentration of the solution and/or the conjugation of the product after cleavage i.e. by increasing the conjugation of the system, the nitroso-enol becomes the favored form.

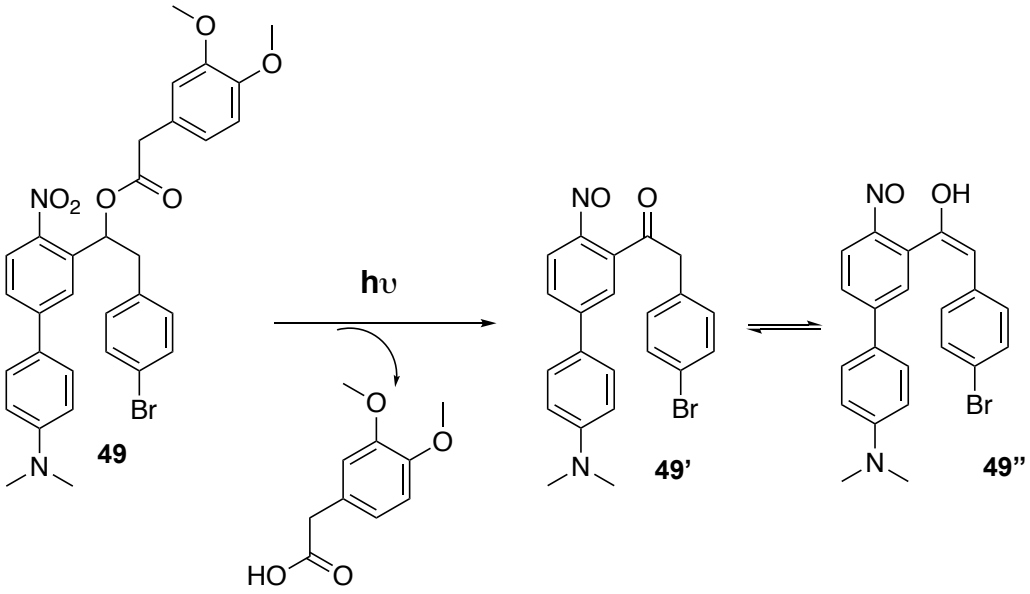

Scheme IV.4: Photolysis of **49** by irradiation at 405 nm leading to the release of MPAA.

2.1.1.1. Absorption / Emission Profiles

A solution of **49** with a concentration of 135 µM in a mixture of acetonitrile / PBS (1/1 v/v) was irradiated at 405 nm with the help of an LED lamp. For every irradiation time, few µL of the solution were injected in HPLC in order to follow the progress of the photolytical reaction by observing the decrease of the peak of the starting material and the appearance of the by-product's peak. Also, upon each irradiation, the UV/Vis profile was recorded (Scheme IV.5).

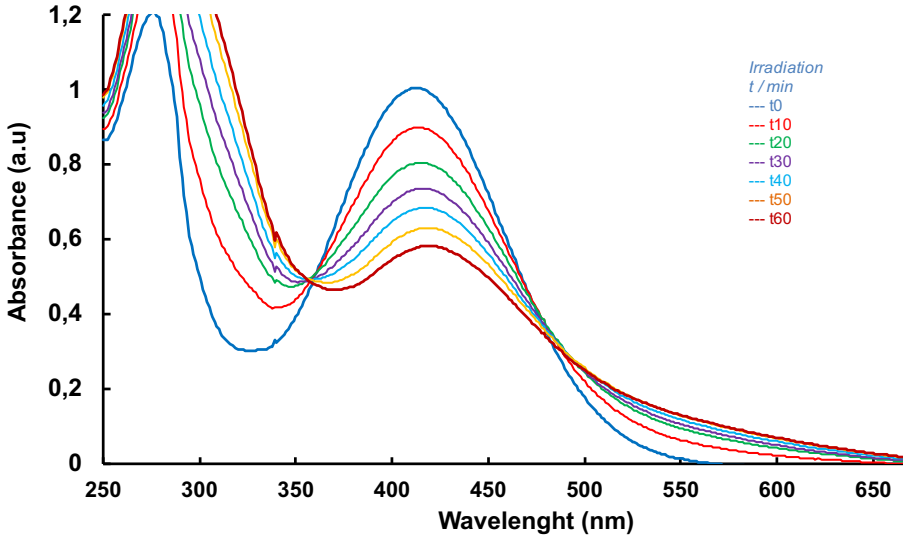

Scheme IV.5: Variation of UV absorbance after irradiation at 405 nm of 135 µM solution (Acetonitrile/PBS 1:1 in vol.) of **49**.

By referring to the UV spectrum, compound **49** shows an absorbance maximum at λ_{max} = 413 nm characteristic of the nitro-biphenyl core with an ε = 7750 $M^{-1}.cm^{-1}$. Two isosbestic points are observed for this compound at 360 nm and 485 nm respectively, indicating a clean photochemical process leading to stable photoproducts. As we irradiate the sample we observe a decrease in the absorbance values that indicates the decrease of the concentration of the starting compound **49**, and by HPLC peak integrations we observed that after 60 minutes of irradiation, 75% of the chromophore MPAA was released and only 25% of **49** was remaining.

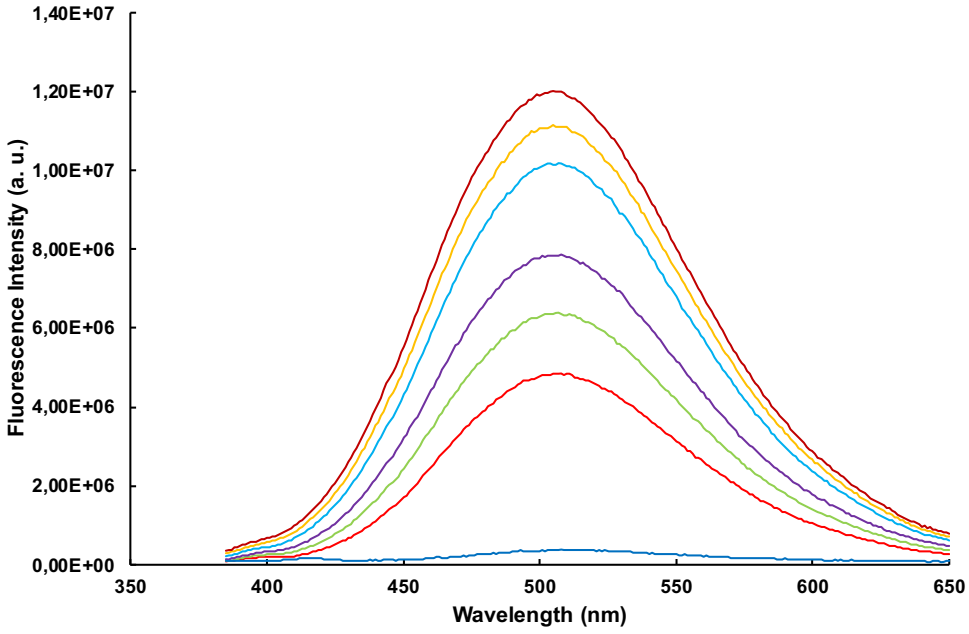

Scheme IV.6: Variation of fluorescence emission after irradiation at 405 nm of 135 µM solution (Acetonitrile/PBS 1:1 in vol.) of **49**.

Interestingly, as we irradiate our sample, we observe a significant increase in the fluorescence intensity and the emission of the compound is centered at λ_{em} = 504 nm (Scheme IV.6). The starting compound **49** shows a weak fluorescence at t = 0 in acetonitrile/PBS 1/1 and after full cleavage, we observed a ratio of I_{full} / I_0 = 40 times increase in the fluorescence intensity.

2.1.1.2. Titration of the release of MPAA

In order to quantify the actual amount of the MPAA released over time, it is necessary to perform an HPLC analysis through the measurement of the peak area formed over time, in order to draw a standard calibration curve (Scheme IV.7).

This standard curve was obtained by injecting successively in HPLC 100 µL of five different concentrations (25, 50, 100, 125 and 150 µM), and each point designates the concentration injected with the corresponding area (expressed in µV.sec).

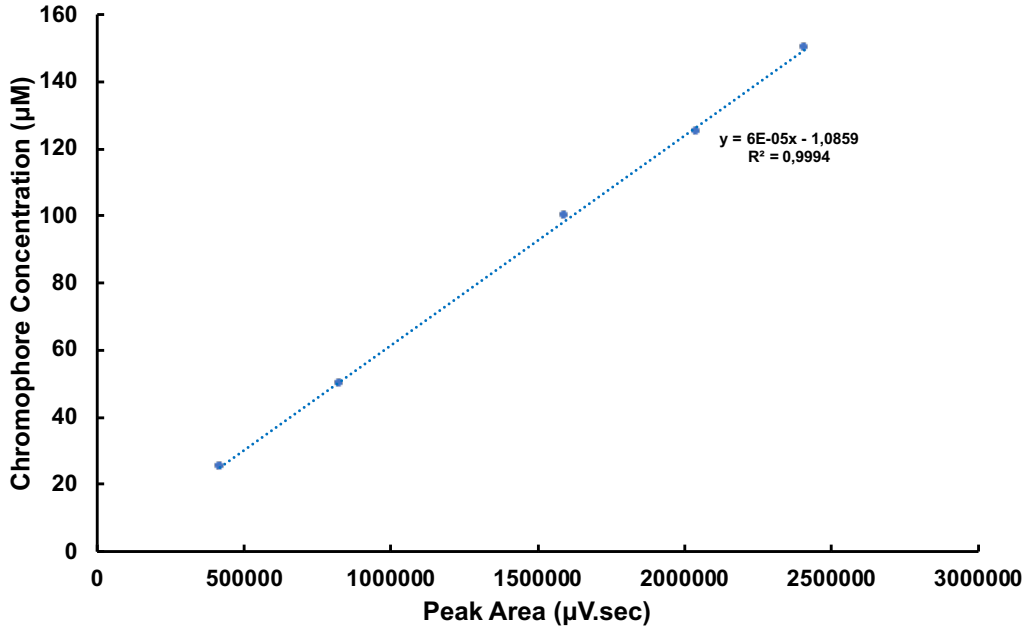

Scheme IV.7: Calibration curve of different concentrations of MPAA (25µM – 150µM). Each concentration was injected three times in HPLC and the average value of the area was taken.

After obtaining five points, the equation expressing the concentration of MPAA (y) in function of the peak area (x) was determined:

$$y = 6 \times 10^{-5}x - 1.0859 \qquad (6)$$

It is possible, by the help of the equation (6), to determine the percentage released at any time of photolysis. For example, after HPLC injection of a batch containing a constant volume (µL) of 135 µM solution of **49** being irradiated for 60 min, the area obtained by integration of the peak corresponds to x = 1 630 000 µV.sec, which gives according to the equation (6) y = 96 µM or 75% of MPAA released after 60 min of photolysis corresponding to 95% of the expected value (75% x 135 µM = 101 µM).

All the quantifications of the amount of MPAA release, will be calculated in the same manner, for all upcoming results.

2.2. Synthesis of the conjugated derivatives of *o*-nitrobenzyl PPG

The aim of this work is to synthesize a Photoremovable Protecting Group that could release a fluorescent by-product of photocleavage, the bromo derivative **49** gave promising results, and in order to achieve better shift in emission wavelength, a more intense fluorescence and a better ratio of increase (I_{full} / I_0), we suggest increasing the conjugation of the caging group that could induce a more intense red-shifted fluorescent signal after photolysis.

In order to increase the conjugation of our newly-developed *o*-nitrobenzyl PPG, we suggested a series of pallado-catalyzed Suzuki couplings on **49** with various *p*-substituted phenylboronic acids (*p*-NMe_2, *p*-NO_2, *p*-OMe). The suggested synthesis is presented in Scheme IV.8.

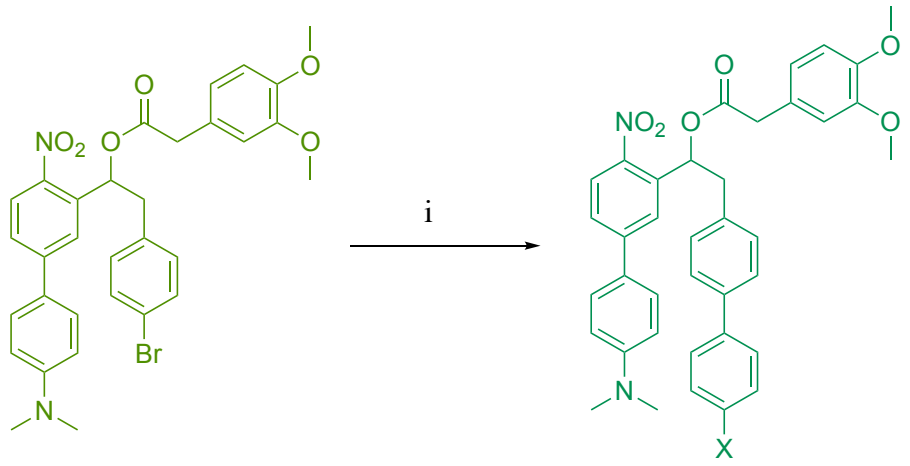

49

50a X = NMe_2
50b X = NO_2
50c X = OMe

Scheme IV.8: Synthesis of the conjugated derivatives of *o*-nitrobenzyl Photoremovable Protecting Group **50a-c**.

(i) K_2CO_3, Ethanol/water/toluene (2/1/7), $Pd(PPh_3)_4$, microwave, 80°C, 45 min for **50a** dimethylaminophenyl boronic acid, 55% , for **50b** 4-nitrophenyl boronic acid, 58%, for **50c** 4-methoxyphenyl boronic acid, 46%.

The bromoaryl derivative **49** was used to increase the conjugation of this system with electron donating (NMe_2 and OMe) or electron withdrawing (NO_2) groups using Suzuki-Miyaura cross-coupling reaction, under microwave heating at 80°C in presence of potassium carbonate as a base, leading to the formation of compound **50a-c** in 46-58 % yields.

2.2.1.Study of the photolysis reaction

Similarly to the bromo derivative **49**, compounds **50a-c** were irradiated using LED lamp at 405 nm and their photochemical and photophysical properties were evaluated. The construction of these derivative by increasing the conjugation aims to red-shift the wavelength of emission and to obtain an enhanced fluorescent intensity. Also, this conjugation increase will help the equilibrium described in Scheme IV.4 to shifts towards the formation of the nitroso-enol form were the 2 biphenyl units are linked by a double bond. After irradiation for a certain amount to time, the released chromophore (MPAA) was quantified and the properties of the released by-product **50'a-c** were well determined (Scheme IV.9).

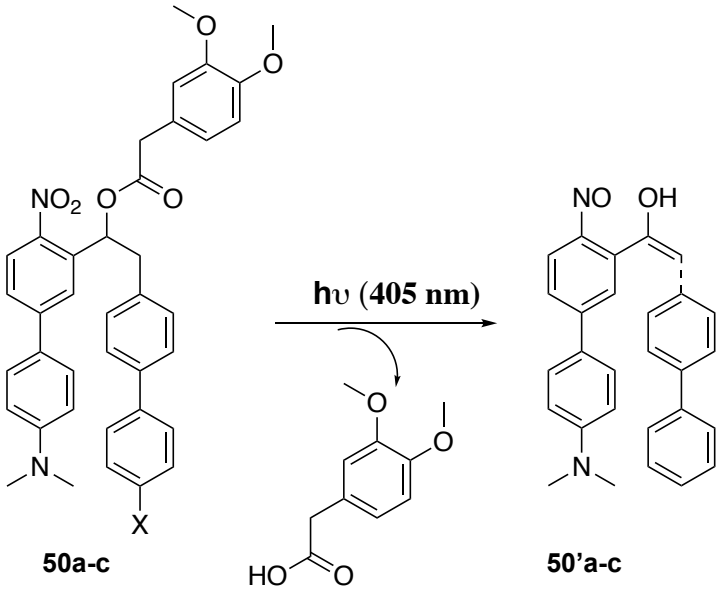

Scheme IV.9: Photolysis reaction of derivatives **50a-c** by the irradiation at 405 nm.

2.2.1.1. Absorption / Emission Profiles

By referring to the UV spectrum, compound **50a** shows an absorbance maximum at λ_{max} = 413 nm characteristic of the nitro-biphenyl core. Two isosbestic points are observed for this compound at 387 nm and 480 nm respectively, indicating a clean photochemical process as well (Scheme IV.10). As we irradiate the sample we observe a decrease in the absorbance values that indicates the decrease of the concentration of the starting compound **50a**, and by HPLC peak integrations we observed that after 37 minutes of irradiation, 55% of the chromophore MPAA was released and 45% of **49** was left.

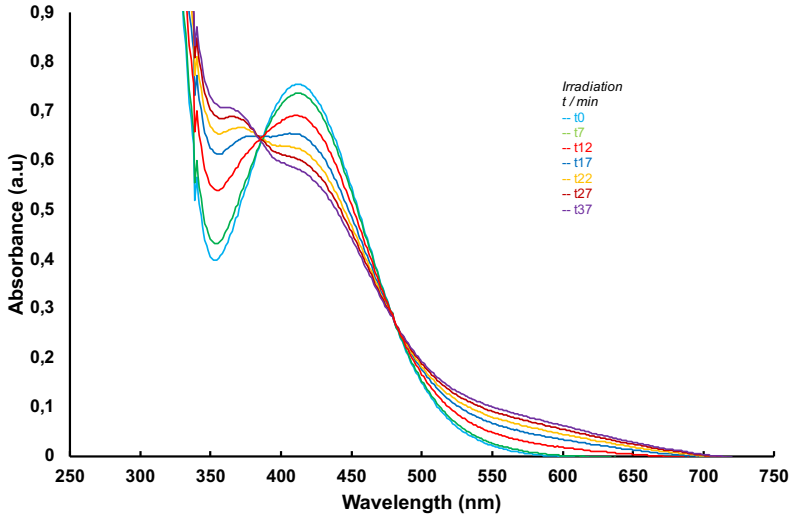

Scheme IV.10: Variation of UV absorbance after irradiation at 405 nm of 100 µM solution (Acetonitrile/PBS 1:1 in vol.) of **50a**.

As we irradiate our sample, we observe a significant increase in the fluorescence intensity and the emission of the compound is centered at λ_{em} = 489 nm (Scheme IV.11). The starting compound **50a** shows a weak fluorescence at t = 0 in acetonitrile/PBS 1/1 and after full cleavage, we observed a ratio of $I_{full} / I_0 = 32$ times increase in the fluorescence intensity. We expected a red-shifted emission and an improved ratio of increase for **50a** compared to **49** since we are increasing the conjugation with an electron donating group (NMe_2). Evidently, the amino group tends to get protonated in the solution of analysis to form the corresponding cation and thus becoming an electron poor group that tends to withdraw electrons from the system thus acting as an electron-attracting group and leading to a blue shifted emission instead.

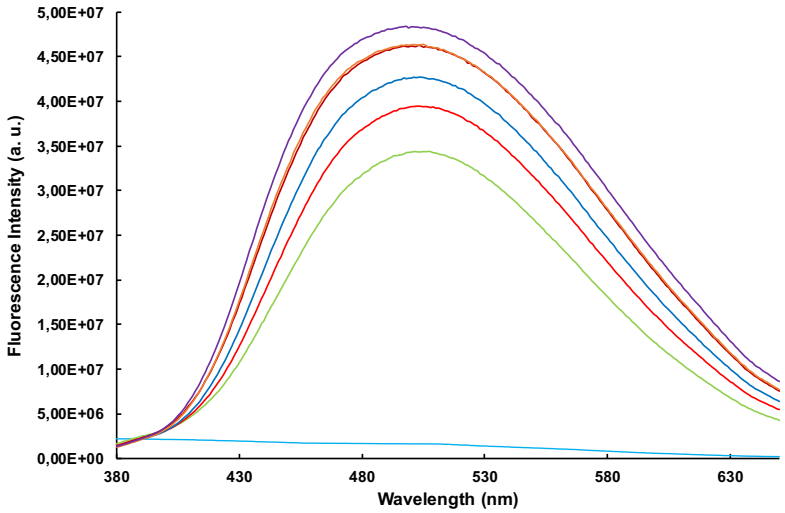

Scheme IV.11: Variation of fluorescence emission after irradiation at 405 nm of 100 µM solution (Acetonitrile/PBS 1:1 in vol.) of **50a**.

By referring to the UV spectrum, compound **50b** shows an absorbance maximum at λ_{max} = 413 nm characteristic of the nitro-biphenyl core. No isosbestic points are observed for this compound which indicates a complex photolysis pathway (Scheme IV.12). As we irradiate the sample we observe a decrease in the absorbance values that indicates the decrease of the concentration of the starting compound **50b**, and by HPLC peak integrations we observed that after 40 minutes of irradiation, 53% of the chromophore MPAA was released and 47% of **50b** was left.

Compound **50b** showed during irradiation a more complex fluorescent behavior presumably due to the photodegradation of the photolytical by-product leading first to an increase followed by a decrease of the fluorescence intensity (Scheme IV.13). This compound shows an emission at λ_{em} = 480 nm which is blue-shifted compared to the bromo and dimethyl methoxy derivatives **49** and **50a** respectively, this due to the strong electron-attracting character of the nitro group. We were not able to evaluate the ratio of increase I_{full} / I_0 due to the photobleaching of the fluorophore formed after irradiation of **50b**.

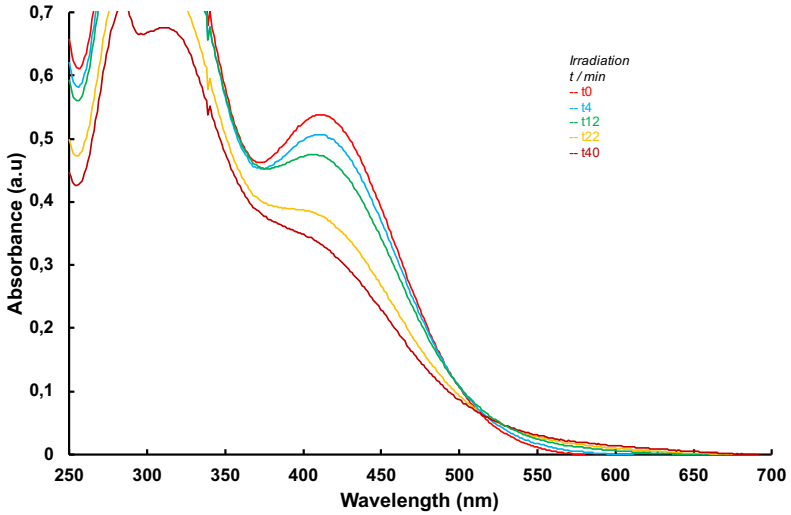

Scheme IV.12: Variation of UV absorbance after irradiation at 405 nm of 75 µM solution (Acetonitrile/PBS 1:1 in vol.) of **50b**.

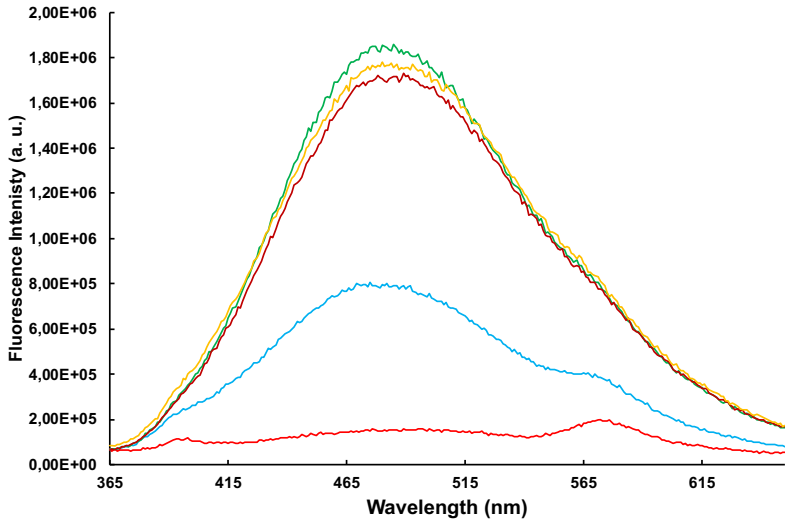

Scheme IV.13: Variation of fluorescence emission after irradiation at 405 nm of 75 µM solution (Acetonitrile/PBS 1:1 in vol.) of **50b**.

The UV profile of the photolysis of compound **50c** shows an absorbance maximum at λ_{max} = 413 nm with two isosbestic points are observed for this compound at 370 nm. and 495 nm respectively, indicating a clean photochemical process as well (Scheme IV.14). As we irradiate the sample we observe a decrease in the absorbance values that indicates the decrease of the concentration of the starting compound **50b**, and by HPLC peak integrations we observed that after 25 minutes of irradiation, 59% of the chromophore MPAA was released and 41% of **50c** was left.

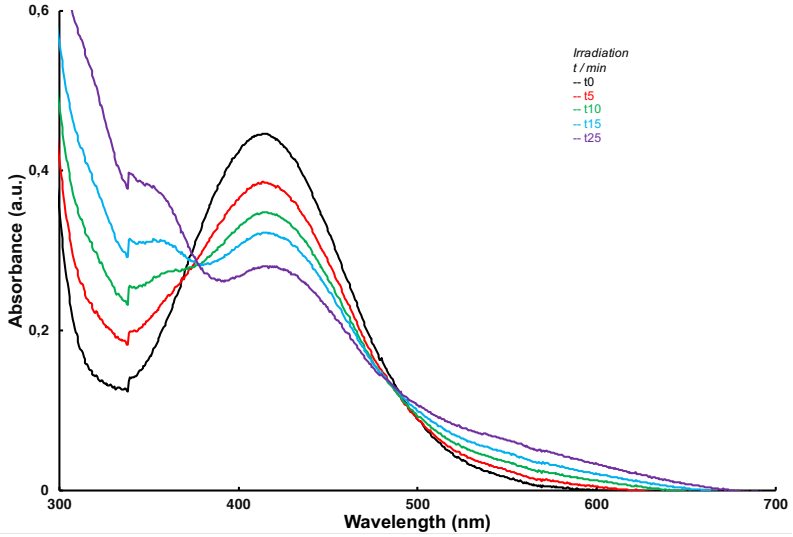

Scheme IV.14: Variation of UV absorbance after irradiation at 405 nm of 55 µM solution (Acetonitrile/PBS 1:1 in vol.) of **50c**.

As we irradiate our sample, we observe a significant increase in the fluorescence intensity and the emission of the compound is centered at λ_{em} = 526 nm (Scheme IV.15). The starting compound **50a** shows a weak fluorescence at t = 0 in acetonitrile/PBS 1/1 and after full cleavage, we observed a ratio of I_{full} / I_0 = 208 times increase in the fluorescence intensity. As expected, a red-shifted emission was observed due to the electron-donating property of the OMe group and an improved ratio of increase for **50c** compared to **49**, **50a** and **50b** due to the increase in conjugation with an electron donating group (OMe).

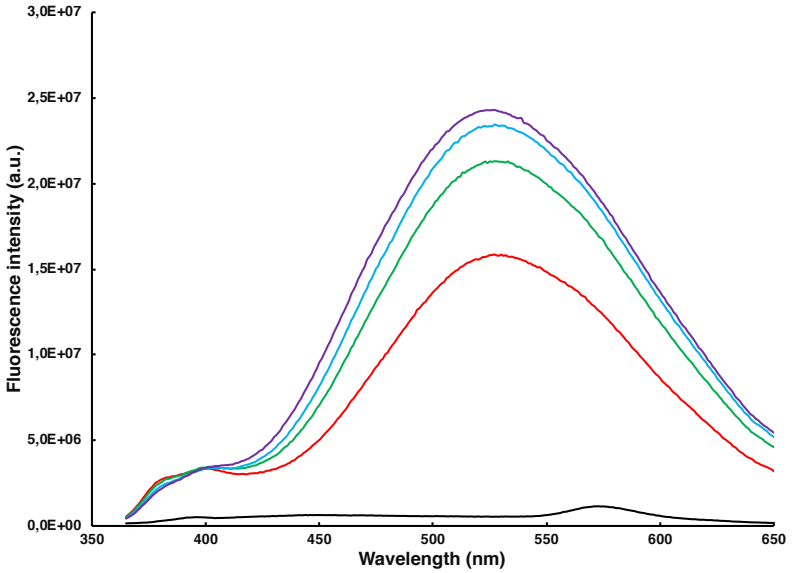

Scheme IV.15: Variation of fluorescence emission after irradiation at 405 nm of 55 µM solution (Acetonitrile/PBS 1:1 in vol.) of **50c**.

2.2.1.2. Dosing the release of MPAA

By the help of the equation (6), we were able to determine the percentage of MPAA released at any time of photolysis for every compound **50a-c**. For example, after HPLC injection of a constant volume (µL) of 100 µM solution of **50a** being irradiated for 37 min, the area obtained by integration of the peak corresponds to x = 870 600 µV.sec, which gives according to the equation (6) y = 51 µM or 55% of MPAA released after 37 min of photolysis corresponding to 93% of the expected value (55% x 100 µM = 55 µM).

For compound **50b**, a sample of 75 µM irradiated for 40 min, was injected in HPLC and a peak area of x = 568 100 µV.sec, which gives according to the equation (6) y = 33 µM or 55% of MPAA released after 40 min of photolysis corresponding to 83% of the expected value (53% x 75 µM = 40 µM).

Finally, for compound **50c**, a sample of 55 µM being irradiated for 25 min showed an area (by integration of the peak) corresponding to x = 543 100 µV.sec, which gives according to the equation (6) y = 31 µM or 59% of MPAA released after 25 min of photolysis corresponding to 97% of the expected value (59% x 55 µM = 32 µM).

To sum up, the bromoaryl derivative **49** was used in order to increase the conjugation of this new *o*-nitrobenzyl Photoremovable Protecting Group system with electron donating or electron withdrawing groups using Suzuki-Miyaura cross-coupling reaction leading to the formation of compound **50a-c**. These 4 newly-developed *o*-nitrobenzyl PPG derivatives **49** and **50a-c** show interesting photochemical and photophysical properties. The extension of conjugation on these derivatives led to monitoring the emission properties of these compounds. MPAA coupling was chosen in this study to easily quantify the uncaging efficacy by HPLC analysis.

All compound showed a similar absorbance peak at 413 nm characteristic of the amino-nitro-biphenyl system. Interestingly, each compound shows a very weak fluorescence (in the blue-green region) before irradiation, which increases upon the liberation of the acid by irradiation. Table 7 sums up the totality of the photochemical and photophysical properties of compounds **49** and **50a-c**.

Compound[a]	λ_{em} (nm)	$I_0 \times 10^8$	Average % of photocleavage[b]	Average** $I_{full} \times 10^8$	I_{full}/I_0
49	504	0.5254	95	21.006	40
50a	489	4.4211	93	143.233	32
50b	480	0.3409	83	-[c]	-[c]
50c	526	1.0296	97	214.721	208

Table 7: Variation of fluorescence intensity ratio and emission wavelength of derivatives **49** and **50a-c**.
[a]100 µM solutions (PBS/acetonitrile 1/1 v/v)/ [b]Calculated from 3 separate irradiation times/ [c]Due to photo-bleaching, it was difficult to calculate I_{full} for **50b**.

2.2.2. Hydrolytical stability

In order to study the hydrolytic stability of these PPGs in solution, we explored their stability by HPLC in acetonitrile/phosphate buffer (pH = 7.4) mixture (1/1, v/v) at room temperature. No hydrolysis was observed after 24 h for **49** and **50a-c**. In addition to that, we dissolved the compound in a mixture of acetonitrile/acid (1/1 v/v) and varying the acids with various pH; citric acid/sodium citrate (pH = 3.2) and acetic acid/sodium acetate (pH = 4.4), similarly, we didn't observe neither hydrolysis of the ester bond nor any product degradation after 24h.

2.3. Characterization of the nitroso photo-product

The postulated mechanism for the photo-induced liberation of a nitrosoketone derivative should be able to achieve a keto-enol tautomerism to generate a conjugated α-nitrosohydroxystilbene derivative stabilized by intramolecular hydrogen bond between the nitrogen of the nitroso group and the H of the enol group (Scheme IV.16).

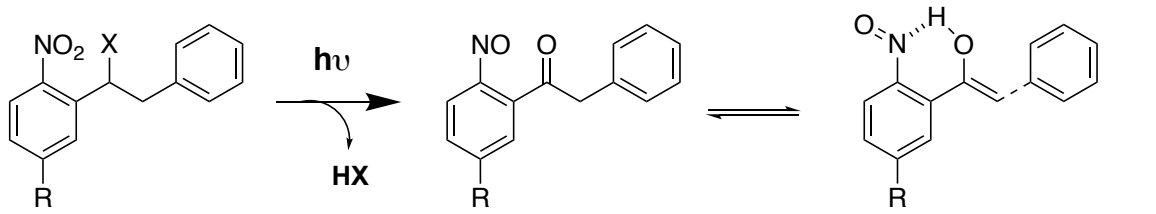

***o*-nitrobenzyl** **nitrosoketone** **α−nitrosohydroxystilbene**

Scheme IV.16: Mechanism of photolysis of *o*-nitrobenzyl derivative.

In order to validate the formation of these photo-products, we proceeded with FT-IR, ^{1}H NMR and UV/HPLC analysis in order to characterize the photo-product released after the irradiation of each newly developed *o*-nitrobenzyl PPG.

2.3.1.FT-IR Analysis

A 267 µM solution of compound **50c** was prepared in acetonitrile and its corresponding IR spectrum was recorded before and after irradiation and the results are presented in Scheme IV.17 and Scheme IV.18.

The IR spectra of this product before and after irradiation show main differences in the 1300-1500 cm^{-1} region. The band at 1465 cm^{-1} which can be attributed to the 19a vibration of NO_2 group (according to Wilson *et al.,* 1934) is decreasing while a band is appearing at 1446 cm^{-1} attributed to the 19b vibration of NO group (Richner *et al.,* 2011) and at 1372 cm^{-1} attributed to an enol form (Dutta *et al.,* 2014). In addition to these characteristic bands, a weak absorption was detected at 3175 cm^{-1} could also indicate an enol O-H bond vibration, the weakness of this band is explained due to the formation of the hydrogen bond between the enolic proton and the nitrogen of the nitroso group.

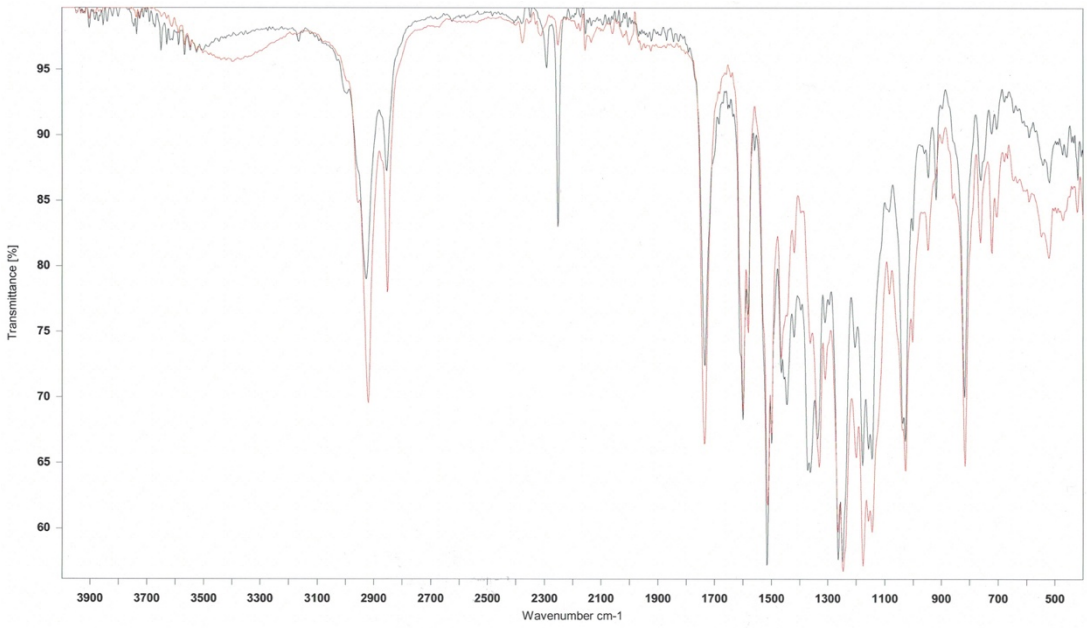

Scheme IV.17: Full Infrared spectrum of the non-irradiated (red) and irradiated 40 minutes (black) samples of **50c** with concentration of 267 µM.

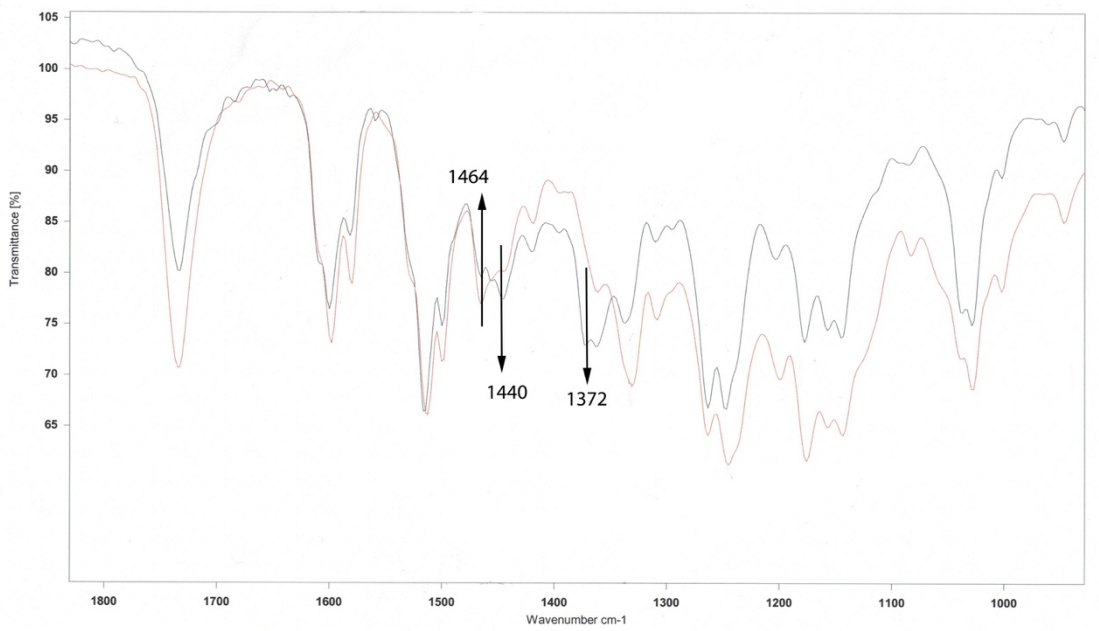

Scheme IV.18: Infrared spectrum of the non-irradiated (red) and irradiated 40 minutes (black) samples of **50c** with concentration of 267 µM (zone 900 - 1850 cm^{-1}).

2.3.2. ^{1}H NMR Analysis

To confirm the keto-enol tautomerism, a ^{1}H-NMR study was undertaken using compound **49** in deuterated acetonitrile CD_3CN at respectively 267µM and 405 µM. The 267µM solution was irradiated for 90 minutes and showed 85% cleavage, and the 405 µM solution was irradiated 150 minutes and showed 80% cleavage (calculated by HPLC peak integration).

The NMR spectra nicely showed the release of the MPAA together with 3 major sub-products based on the ^{1}H dimethyl-amino signals (3.00-3.05 ppm). More interestingly, in a concentration dependent manner, 3 new NMR signals together with 2 new signals were detected respectively between 4-5.2 ppm and 9.5-10 ppm (Scheme IV.19). The singlet at 4.1 ppm is in good agreement with the CH_2 of the nitroso-keto sub-product. And the two singlets at 4.87 ppm and 5.19 ppm together with the two singlets at 9.69 ppm and 9.97 ppm are also in good agreement with the ^{1}H expected signals for respectively the Alkene =C**H** and the O**H** signals of the 2 stereoisomers (cis and trans) of the enols sub-products (Scheme IV.20 and Scheme IV.21).

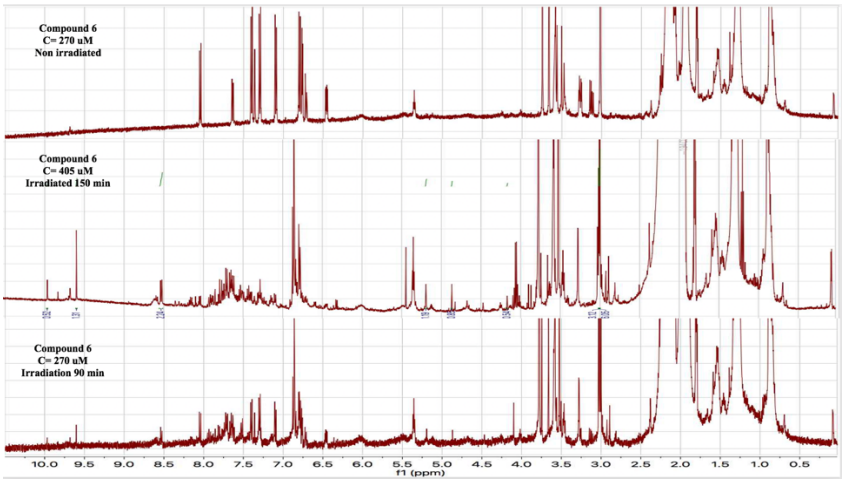

Scheme IV.19: Full ^{1}H-NMR spectra overlap of the non-irradiated (top), irradiated 405 µM solution of **49** (middle) and irradiated 267 µM solution of **49** (bottom).

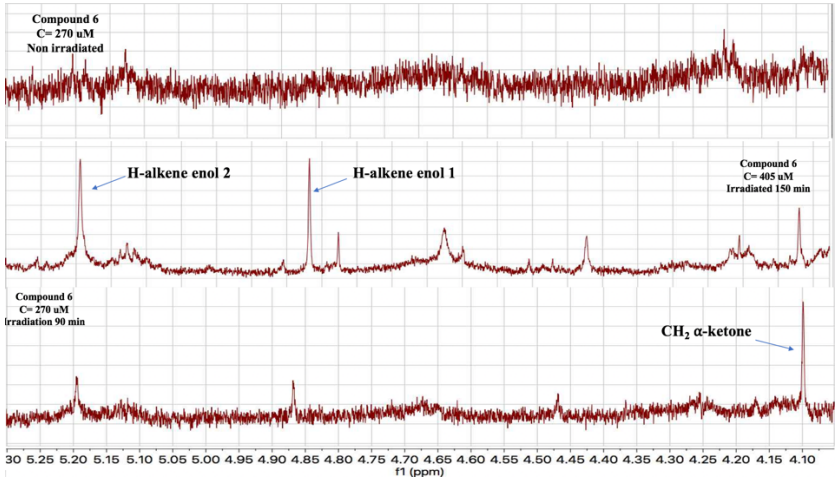

Scheme IV.20: ^{1}H-NMR spectra overlap of the non-irradiated (top), irradiated 405 µM solution of **49** (middle) and irradiated 267 µM solution of **49** (bottom) zone 4.0-5.3 ppm.

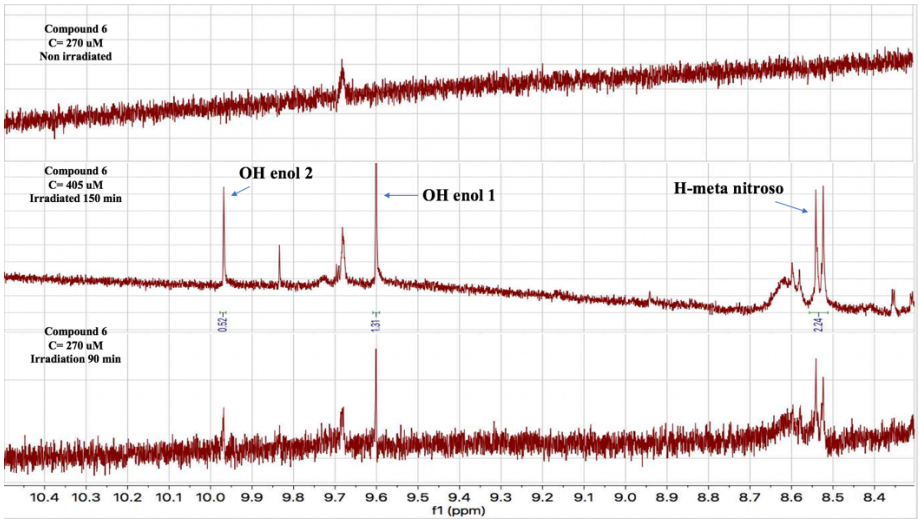

Scheme IV.21: ^{1}H-NMR spectra overlap of the non-irradiated (top), irradiated 405 µM solution of **49** (middle) and irradiated 267 µM solution of **49** (bottom) zone 8.5-10.5 ppm.

2.3.3. HPLC and UV profiles

As mentioned, a constant volume (µL) of a solution of each compound in PBS/acetonitrile (1/1 v/v) was injected in HPLC before irradiation and after each irradiation time in order to evaluate the photolysis and to quantify the liberated acid. A sample of 100 µM of **49**, injected before irradiation, shows a retention time t_R = 24.77 min (Scheme IV.22-left) and after irradiating this sample for 60 minutes we observed only 30% of the remaining starting compound and a new peak appeared at t_R = 23.53 min (Scheme IV.22-right).

It is most probable that this latter corresponds to the nitroso by-product since it shows a red-shifted absorbance around 430 nm explained by the formation of the conjugated form **49''** (Scheme IV.22).

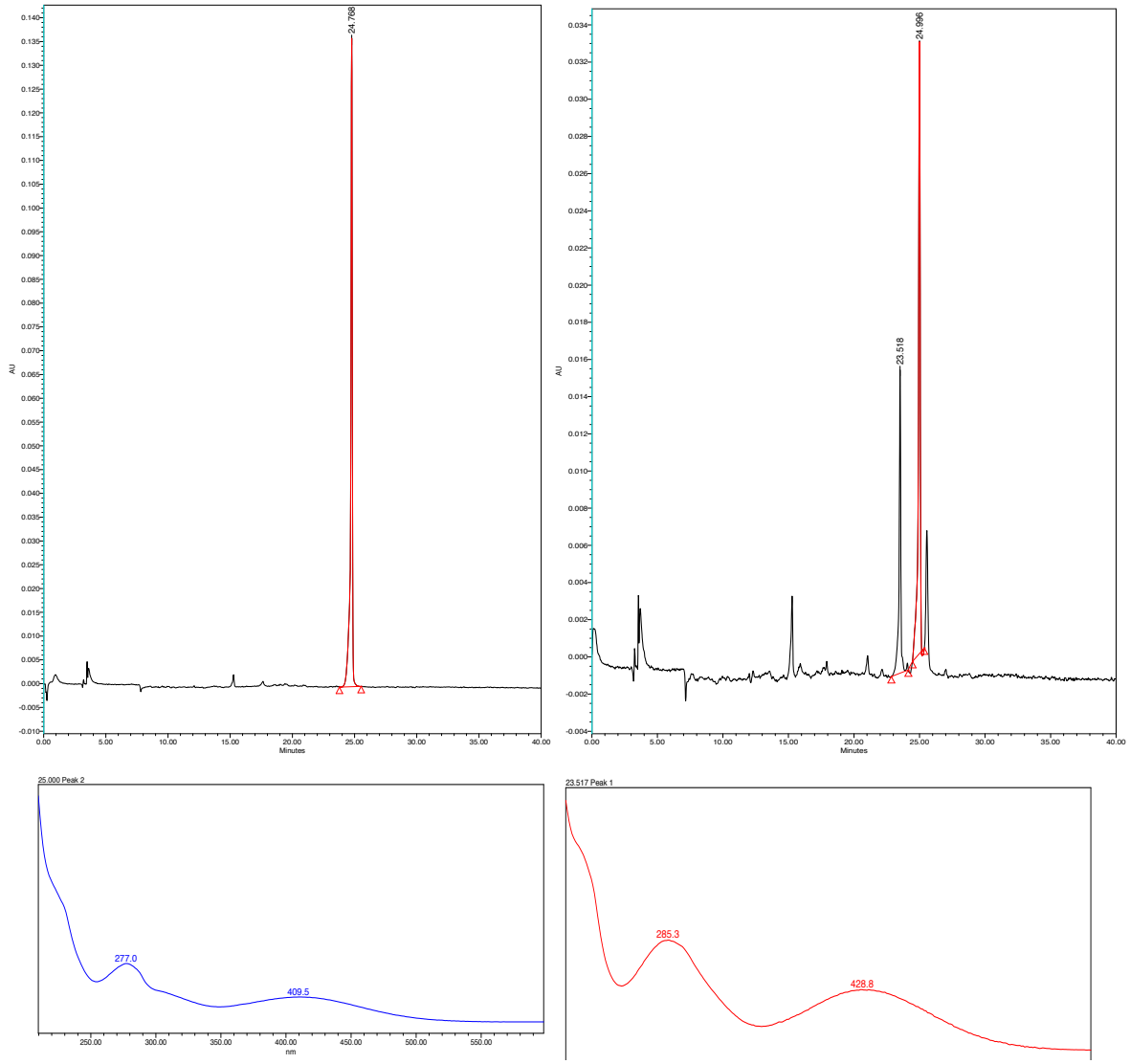

Scheme IV.22: HPLC profiles of the non-irradiated (top left) and irradiated (top right) sample of **49** 100 µM and their corresponding UV profiles: non-irradiated (bottom blue) and irradiated (bottom red).

After these analyses, we were able to characterize the nitroso photo-product released after the photocleavage of the *o*-nitrobenzyl series of PPG recently developed. The nitrosoketone by-product tend to be transformed into nitroso-enol, its tautomeric form, that is stabilized by the extended conjugation of the system due to the formation of a double bond between the two cores of the molecule.

Interestingly, this conjugation is the reason behind the fluorescence of the photo-products of each compound, and their emission intensity varies with the length of the conjugation and the electronic nature of the substituent donor and/or acceptor.

3. Fluorescent uncaging report in cells

After the successful synthesis of the conjugated *o*-nitrobenzyl Photoremovable Protecting Group derivatives, and after evaluating the photophysical and photochemical properties of each compound of this family of PPGs, we were interested in studying the behaviour of this series in cellular medium. What stays the most important requirement for application in *vivo* when it comes to photoremovable protecting groups, is the ability to follow the uncaging event in cells, one, and the most efficient way to achieve that is fluorescence. Since the newly developed series of compounds show interesting emission properties, we decided to verify the reproducibility of these properties on cells.

3.1. Synthesis of a soluble *o*-nitrobenzyl derivative

After evaluating the photolysis reaction of each compound and after determining their respective photophysical and photochemical properties, we have chosen compound **50c** as the best candidate to test on cells. This compound has shown the highest increase in the fluorescence intensity after photocleavage (I_{full} / I_0 = 208) in addition to a red-shifted emission wavelength (λ_{em} = 526 nm). In order to use this compound on cells, we should first, proceed with the synthesis of a soluble version of this derivative, one way is by attaching polyethylene glycol chain (PEG) that induces solubility in water.

We have decided to synthesize a pegylated carboxylic acid that replaces MPAA and enhances the solubility of the final molecule. The total synthesis of the pegylated version of methoxy *o*-nitrobenzyl derivative **55** is described in Scheme IV.23.

Using the commercial Octaethylene Glycol Monomethyl Ether **51**, we were able to obtain the pegyl-tert-butyl ester **52** in 87% yield. The tert-butyl group was removed by the action of TFA (trifluoroacetic acid) in dichloromethane in order to obtain the PEG-COOH **53** quantitatively.

In the same coupling manner with MPAA, this PEG-COOH was coupled to the bromo derivative **46** using DMAP and DIC in order to obtain the bromo pegylated version **54**.

The final compound **55** was obtained after a Suzuki coupling of **54** with 4-methoxyphenyl boronic acid in 30% yield.

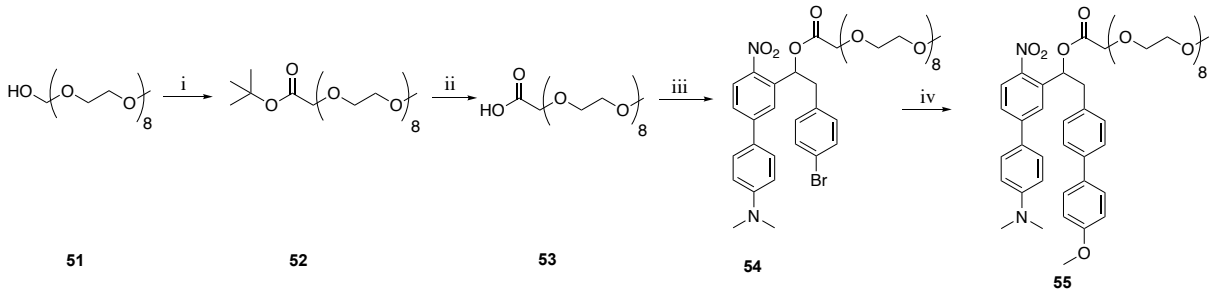

Scheme IV.23: Synthesis of **55**: a PEGylated version of the *o*-nitrobiphenyl methoxy derivative.

(i) NaH, tert-butyl bromoacetate, THF, 0°C, 2h, 87%. (ii) CF_3COOH/dichloromethane, 3h, room temperature, 100%. (iii) **46**, DMAP, diisopropylcarbodiimide, dichloromethane, 0°C, 48%. (vi) 4-methoxyphenyl boronic acid, K_2CO_3, Ethanol/Toluene/Water, $Pd(PPh_3)_4$, 80°C, 45 min, 30%.

3.2. Uncaging on cells

A 40 µM solution of **55** was prepared in a mixture of PBS/acetonitrile (8/2 v/v), the compound was diluted in the cell culture medium to obtain a concentration of 1 µM on cells (<0.5% of acetonitrile).

Two separate batches of cells were prepared for these experiments:

1- HeLa cells were incubated with compound **55** for 35 minutes with no irradiation in order to evaluate the stability of the compound in cellular medium; to ensure that the fluorescent signal is not due to the hydrolysis of the compound whereas it is due to the accumulation of the side-product of photolysis. Interestingly, HeLa cells incubated 35 min with a 1 µM solution showed only weak fluorescence intensity (Entry F, Scheme IV.24).

2- HeLa cells were incubated 5 min with a 1 µM solution of **55** and these cells were irradiated with 365 nm light from an SPE microscope for 5-minute intervals. A confocal image was taken each 5 min for 20 min of continuous irradiation (the experiment was stopped after 20 min due to phototoxicity of the UV irradiation). A clear increase in the detected fluorescence intensity was observed upon irradiation due to the accumulation of the conjugated side-product (Entries A-E, Scheme IV.24).

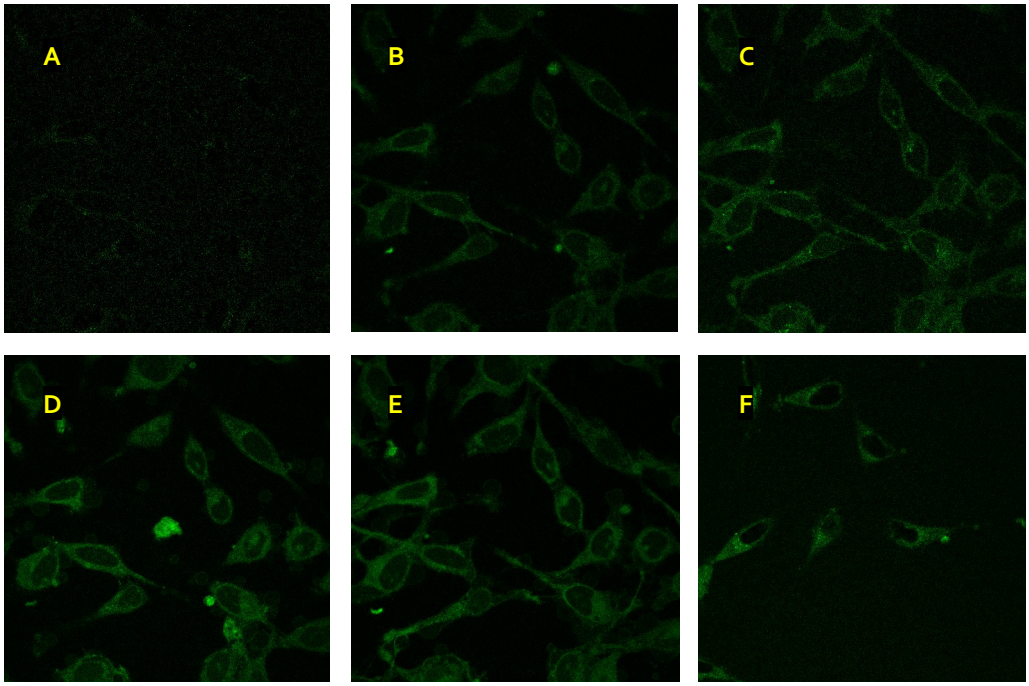

Scheme IV.24: Evaluation of fluorescence intensity on HeLa cells **(A)** incubated for 5 minutes with no irradiation **(B)** 10 minutes total incubation time irradiated for 5 minutes **(C)** 15 minutes total incubation time irradiated for 5 minutes **(D)** 15 minutes total incubation time irradiated for 5 minutes **(E)** 20 minutes total incubation time irradiated for 5 minutes **(F)** incubated for 30 minutes no irradiation.

A quantitative analysis of the fluorescence intensity was performed on 5 cells. It shows a linear increase in the fluorescence intensity for the first 15 minutes of irradiation and reaching a plateau starting from the 20th minutes of irradiation (Scheme IV.25).

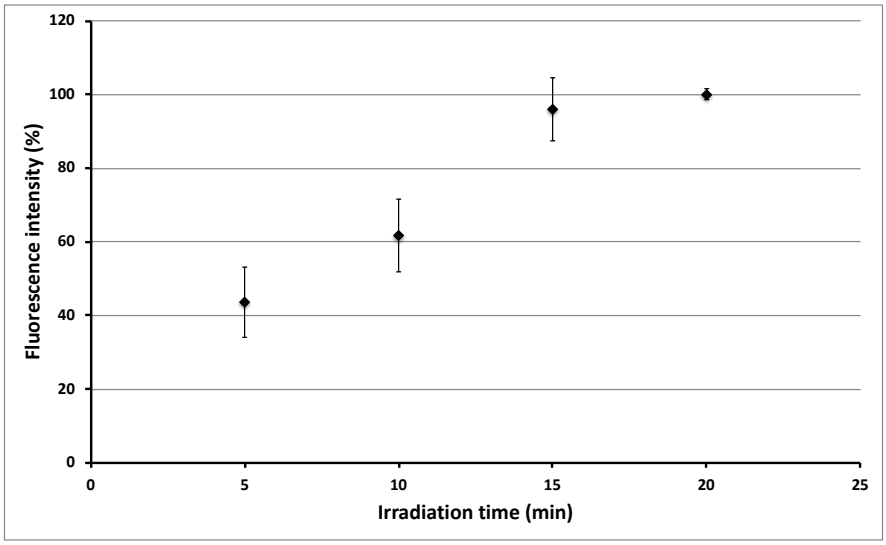

Scheme IV.25: Fluorescence increase in function of irradiation time observed on HeLa cells treated with 1 µM of compound **55**.

These tests showed clearly that our compound releases a fluorescent by-product after photolysis and the use of this family of photoremovable protecting groups could help in monitoring the uncaging event in cells.

This work has introduced the **very first example** of ***o*-nitrobenzyl** PPG releasing a **fluorescent by-product** that helps in monitoring the uncaging event on cells "optically" via fluorescence. The development of these new conjugated *o*-nitrobenzyl derivatives demonstrated the fact that the generation of a fluorescent signal of a by-product from a non-fluorescent compound is the important solution for monitoring biological events through fluorescence; being one of the most important reporters of uncaging.

Throughout this work, we described new *o*-nitrobenzyl (*o*-NB) based photocleavable protecting groups with the capability of optical reporting as an important tool for the quantification of bioactive molecules photodelivery. The *o*-nitrobenzyl derivatives have been known to be very interesting PPGs. However, the need for bioactive evaluation after photoirradiation have increased, and we were able to modify the *o*-nitrobenzyl derivatives to release the fluorescent side product after photoirradiation by conjugating stilbene derivatives. This approach is very effective to monitor the real-time biological events.

These groups present, beside their baggage of advantages, one limitation: their low sensitivity to light. This limitation is translated in long irradiation times that is not well received in biological applications. What is interesting for these applications is to obtain a very rapid concentration jump of the bioactive molecule, in our case, the *o*-NB derivatives show irradiation times to the order of minutes. In the coming chapter, we will present the design and synthesis of a new, more light-sensitive, *o*-nitrobenzyl PPG efficient using two-photon excitation.

CHAPTER V

Towards the Synthesis of Thiophene-based *O*-Nitrobenzyl Group: A Pro-Fluorescent Photoremovable Protecting Group

1. State of Art

Throughout the previous chapter we have detailed the design of the first example of two-photon sensitive photoremovable protecting group of the *o*-nitrobenzyl family releasing a fluorescent by-product of photocleavage. The only drawback for this group is the long irradiation times that limits the use of this group in biological application since the interest of biologists is to observe a rapid concentration jump of the biological effector, so the irradiation times cannot go up to the order of minutes. That's why we tried to combine the two-photon performance of the previously developed PPG with the fluorescence characteristic of the by-product into a new more sensitive to light PPG in the *o*-nitrobenzyl series. In this chapter, we will detail the design and synthesis of a new family of *o*-nitrobenzyl photoremovable protecting group with a fluorescent reporter of uncaging.

What was interesting for us was the PPG recently developed by Ellis-Davies and his group, that was discussed in section 3.2 as a new generation of caged calcium based on an *o*-nitrobenzyl moiety for the release of Calcium as second messenger (Agarwal *et al.,* 2016). This *o*-nitrobenzyl PPG showed extremely interesting photophysical and photochemical properties. Since the synthetical method described previously (organozinc chemistry) is able to generate pro-fluorescent PPGs as discussed in the previous chapter, it could be applied to any *o*-NB group. Therefore, we were interested in applying the same strategy on the PPG developed by Ellis-Davies. This type of PPG presented two main advantages:

1- The *o*-nitrobenzyl series have been widely used over the whole history of photoremovable protecting groups for the release of molecules using one-photon. There have been several interests in modifying the structure of this series in order to render it more efficient for two-photon excitation for absorbing wavelength in the near infra-red region (Agarwal *et al.,* 2016 and Jakkampudi *et al.,* 2016). These two research groups have demonstrated the efficiency of this series in the release of calcium ions by two-photon excitation and they developed photoremovable protecting groups that presented interesting two-photon uncaging cross-sections (Scheme V.1).

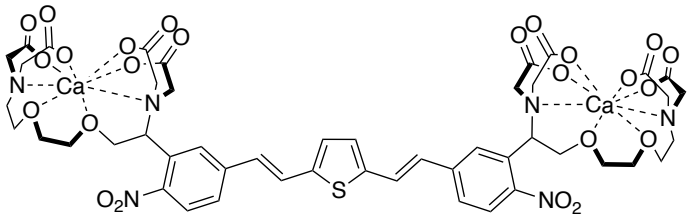

Agarwal et al., 2016

δ_u = **80 GM at 775 nm in DMSO**

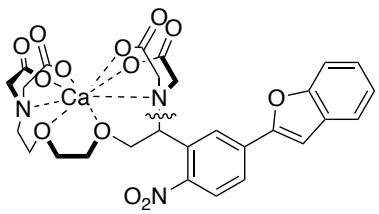

Jakkampudi et al., 2016

δ_u = **21 GM at 740 nm in DMSO**

Scheme V.1: Structures of new generation *o*-nitrobenzyl based photoremovable protecting groups presenting interesting two-photon efficiency in DMSO. The irradiation at 740 and 775 nm is able to release free calcium ions by breaking the breaking the complexation between the chelate and the calcium ion.

2- The mechanism of photocleavage of *o*-nitrobenzyl proceeds through one mechanistic pathway presented in section 1.3.6.1 releasing a nitrosocarbonyl by-product. This means that the photocleavage of *o*-nitrobenzyl series proceeds by a clean photolytical reaction through a unique photochemical mechanism passing by an *aci*-nitro intermediate.

2. Design and Synthetic Strategy

The aim of the synthesis was to develop a two-photon sensitive photoremovable protecting group based on the *o*-nitrobenzyl core. The structure of this new PPG was inspired from that developed by Ellis-Davies's group (Agarwal *et al.,* 2016) since it shows values of uncaging cross-sections in two-photon excitation more promising than those of the PPG developed by Jakkampudi's group (Jakkampudi *et al.,* 2016). Using this chromophore and the strategy developed and presented in Chapter IV, we should be able to develop a PPG that is photosensitive, two-photon efficient and releases a fluorescent by-product.

This molecule presents as well, two reactive sites for extending the conjugation to release a fluorescent by-product and also the gives the possibility to attach two times the same biological effector. An important property that should be taken into account, is the solubility since the majority of PPG are tested and used in non-physiological solvents like DMSO and acetonitrile. This latter property could be addressed by incorporating solubilizing groups into the structure like sugars and PolyEthylene Glycol (PEG) groups.

2.1. Retrosynthetic Analysis

Taking in consideration all the requirements for the development of an efficient pro-fluorescent PPG, we proposed to synthesize a new *o*-NB based PPG represented in Scheme V.2 under the name **BNPET-BB 57** that stands for 2,5-**B**is (**N**itro**P**henyl**E**thynyl)**T**hiophene-**B**romo**B**enzyl.

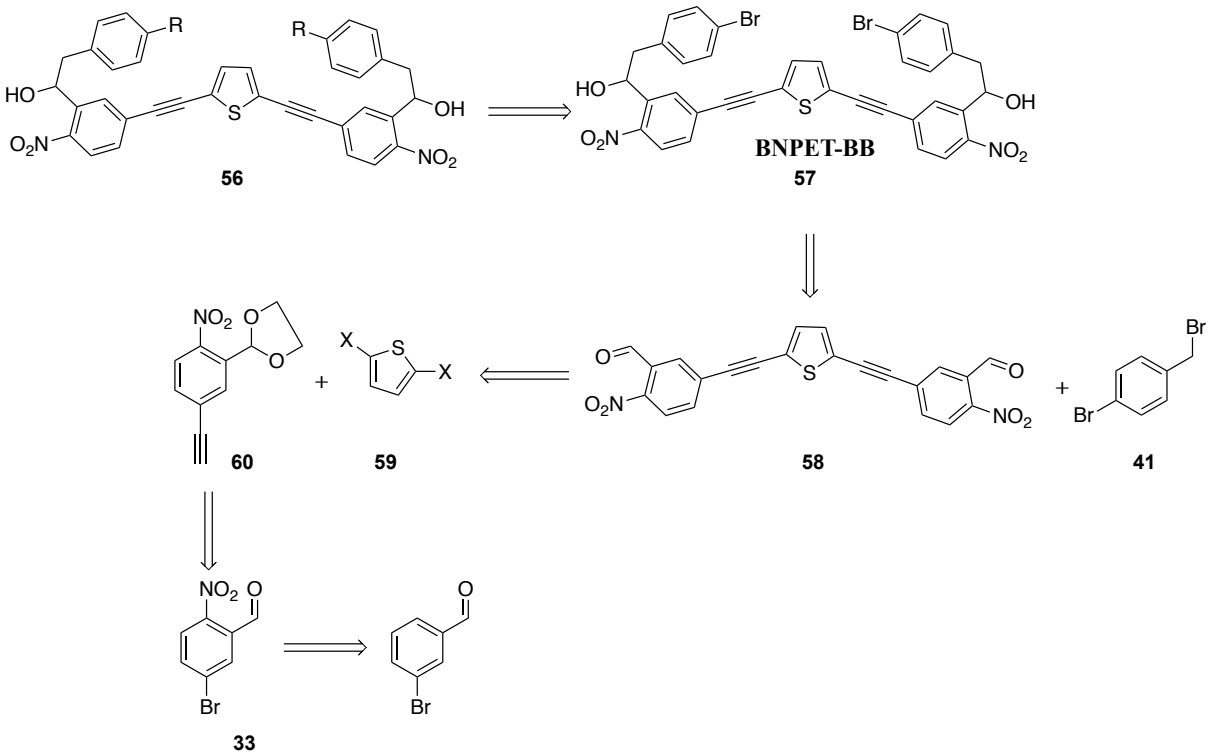

Scheme V.2: Retrosynthetic scheme for the synthesis of the *o*-nitrobenzyl photoremovable protecting group with a thiophene core, BNPET-BB

2.2. Design

The design of the newly developed PPG shows a lot of strong points of interest in terms of structure or properties:

a) Heterocyclic core:

In the design of a two-photon efficient chromophores the presence of electron donor and electron acceptors is necessary for the electronic distribution and the presence of a non-carbon atom in the core of the chromophoric structure can lead to important modulation of the optical and chemical properties.

Several chromophores have been designed containing pyrole, furan and thiophene cores. These compounds have been found to possess excellent properties in non-linear optics (Beverina *et al.,* 2005; Cheng *et al.,* 1991; Mignani *et al.,* 1990).
During the last 8 years, several research groups have introduced the thiophene core inside fluorophores for two-photon imaging in biological applications (Andrade *et al.,* 2010; Yao *et al.,* 2012).

b) Coplanarity:

One of the important factors that affects the performance of a molecule in two-photon excitation is the geometry that affects directly the delocalization of the electrons throughout the whole structure. In order to increase the efficiency and to enhance its performance of our newly developed PPG in two-photon excitation by enhancing the value of the two-photon absorption cross section (δ_a), we decided to replace the double bonds of the structure developed by Ellis-Davies's group (Agarwal *et al.,* 2016) by triple bonds that render the structure more rigid and decrease the steric hindrance generated from the double bonds and also preserves the coplanarity of the molecule due to the enhanced electron delocalization. In the lab, Dr Sylvestre GUG (unpublished results) has demonstrated the effect of the nature of the bond inside the conjugated system on the efficiency of the molecule in two-photon excitation.
Double bonds in a delocalized π-system are suspected to undergo photo-isomerization under the action of light; during irradiations a part of the absorbed energy is devoted for the isomerization rather than for the photolysis reaction. This was demonstrated in the lab with the liberation of glutamate from 4 different *o*-nitrophenethyl groups where the insertion of double bonds in the structure led to enormous decrease in the yield of liberation (Scheme V.3).

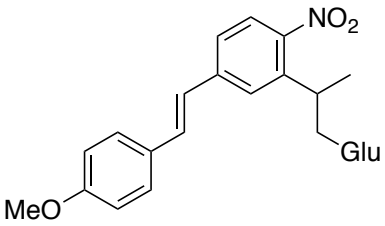

PMNS-Glu
R_{lib} = 48 %

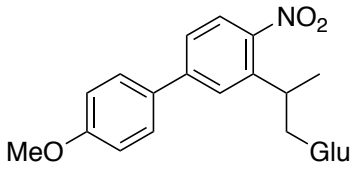

PMNB-Glu
R_{lib} = 90 %

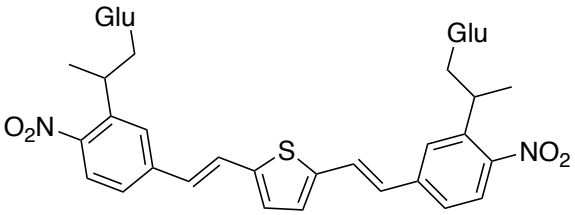

BNSPT-Glu
R_{lib} = 5 %

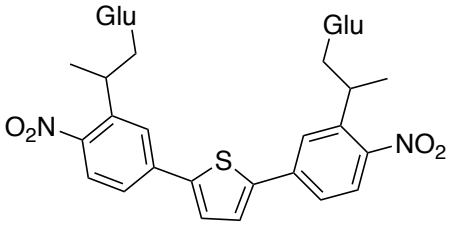

BNPT-Glu
R_{lib} = 100 %

Scheme V.3: Comparison of the yield of liberation of 4 different groups of the *o*-nitrophenethyl series. It is evident that the presence of the double bonds inside the π-system consumes a big part of the absorbed energy to undergo photo-isomerization rather than a photolysis reaction.

c) The PolyEthylene Glycol (PEG) chains:

After the results obtained with the photoremovable group developed in the previous chapter, we decided to incorporate PEG chains into the structure of the BNPET through metallo-catalyzed reaction with the benzyl bromide of BNPET (Scheme V.2) in order to enhance the solubility of our compound. Since our compound contains two sites of attachment, we can attach two PEG chains and enhance more and more the solubility.

2.3. Synthesis of pro-fluorescent BNPET-BB derivative

The multi-step synthesis of the BNPET-BB **57** starts with the nitration of the commercial 3-bromobenzaldehyde through an electrophilic aromatic substitution to obtain compound **33**. The second step is the protection of the aldehyde function, using ethylene glycol in the presence of *p*-TsOH as acid catalyst by the help of a Dean-Stark apparatus, that serves for trapping water molecules released during the reaction and preventing them from returning to the mixture and hydrolyzing the dioxolane protection group of the formed 5-bromo-2-nitro-dioxolane **39**. Compound **61** was obtained through a Sonogashira coupling between **39** and timethylsilyacetylene in the presence of a palladium catalyst (Sonogashira *et al.,* 1975).

The protection step is necessary before the coupling reaction in order to prevent that nucleophilic attack of the cupprate species obtained during the transmetallation step on the highly electrophilic aldehyde function; it has been reported that without this step the yields of this coupling reaction drops to 30%. The free alkyne **60** is obtained in 94% yield by the removal of the silyl group in basic medium using potassium carbonate (Scheme V.4).

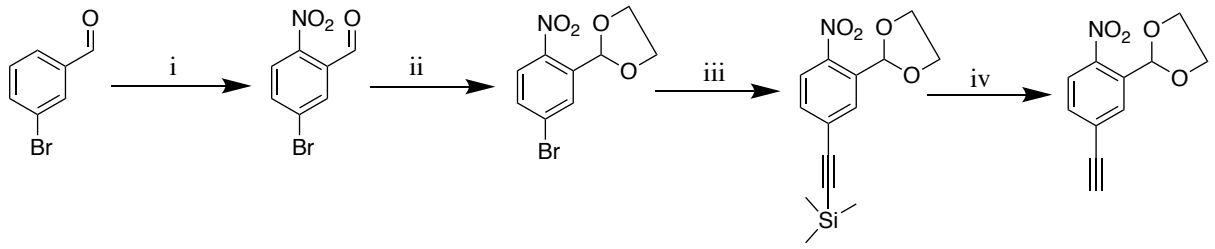

Scheme V.4: Synthesis of the free alkyne **60**.

(i) HNO_3, H_2SO_4, 1h30, RT, 85%. (ii) Ethylene glycol, *p*-TsOH, anhydrous toluene, 1h30, 120°C, 99%. (iii) trimethylsilylacetylene, DIPEA, CuI, $Pd(PPh_3)_2Cl_2$, THF, RT, 16h, 94%. (iv) K_2CO_3, CH_3OH, RT, 30 min, 94 %.

The following step is another Sonogashira coupling between the free alkyne **60** and dihalothiophene **59** and this step was previously optimized in the lab by Dr Bastien Goegan. The coupling was tested first using the 2,5-dibromothiophene **59** (X=Br) and by using catalysts like $Pd(PPh_3)_4$, $Pd(OAc)_2$ or $Pd(PPh_3)_2Cl_2$ and CuI in co-catalytical amount (4 mol %) and by varying the reaction time, the solvent used, the type of base and also the method of heating (heating plate or microwave reactor) the reaction never yielded more than 20% of the target compound **62** but rather yielded the product of homocoupling of the alkyne **62'** (Scheme V.5).

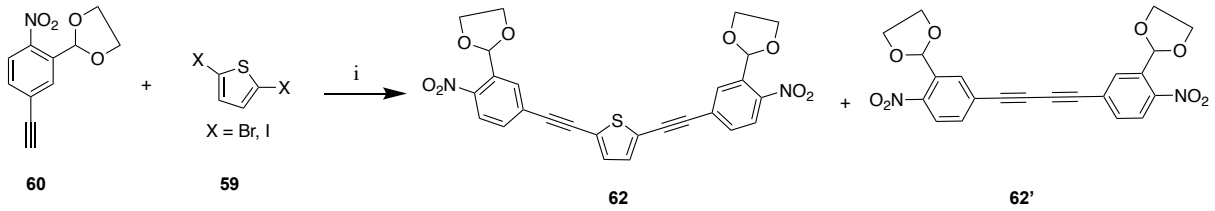

Scheme V.5: The double Sonogashira coupling between the free alkyne **60** and the 2,5-dihalothiophene **59** to obtain the bis-coupled compound **62**.

This metal catalyzed coupling reaction demonstrated showed that the use of copper (I) as co-catalyst in the presence of palladium accelerates the coupling reactions and makes it possible to do the reaction at room temperature rather than at high temperature (classic conditions) (Sonogashira *et al.,* 1975).

The presence of CuI in the mixture with base promotes the formation of copper acetylene that causes the production of the homocoupling product after the oxidation of Pd(0) to Pd(II) by an oxidant. The homocoupling side product also known as the Glaser homocoupling product (Siemsen *et al.,* 2000; 2002) is formed after the palladium being oxidized from Pd(0) to Pd(II) with two acetylene ligands leading to the reductive elimination of the Glaser product **62'** (Scheme V.6).

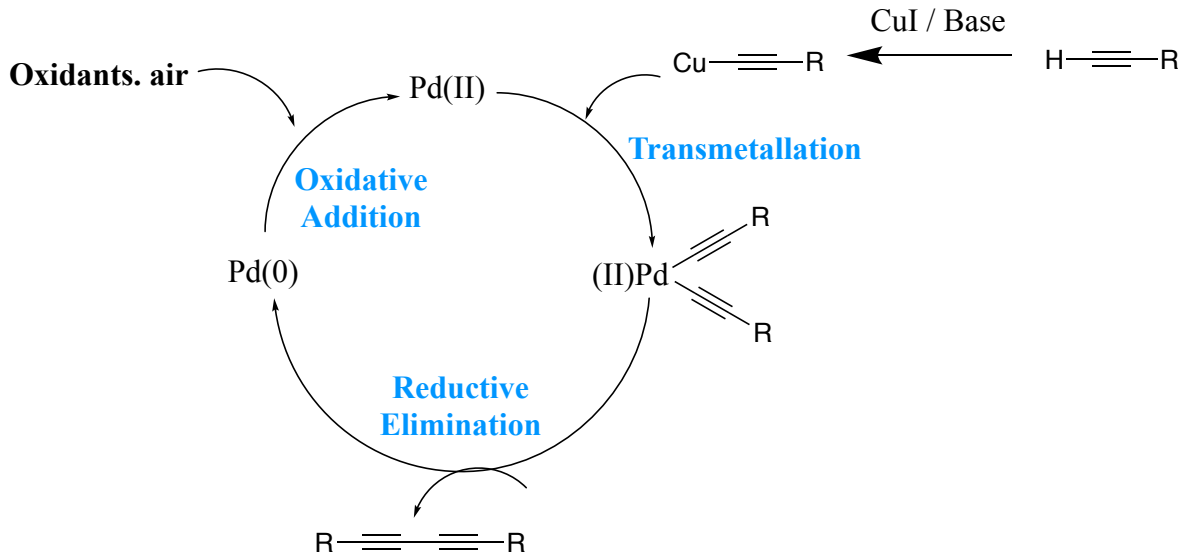

Scheme V.6: Catalytical cycle demonstrating the proposed mechanism for the formation of the Glaser homocoupling product upon the oxidation of Pd(0) into Pd(II).

The major problem of this reaction is the oxidation of palladium that is induced by the presence of an oxidant which is probably air in our case and which is kinetically faster to occur. In order to prevent the oxidation problem, we decided to proceed by degazing of the reaction medium before adding the palladium and this was done by following a "freeze-thaw-pump cycles" procedure in order to remove any traces of air from the solution (solvents and reagents). Another limitation for this reaction is the 2,5-dihalothiophene **59** used; the use of 2,5-dibromothiophene could be also one reason for the formation of the homocoupling product due to the oxidant properties of such a reagent. That's why one solution was the use of 2,5-diiodothiophene to perform this double coupling of Sonogashira because the Iodo analog shows higher reactivity compared to that of the Bromo analog.

After several trials to optimize this reaction and the formation of the target product **62** in high yields and with the lowest yield of Glaser homocoupling, the optimum condition was the use of Palladium bis (triphenylphosphine) dichloride $Pd(PPh_3)Cl_2$ (10 mol %) with triethylamine as the base and copper iodide as co-catalyst (4 mol%) at 50°C for 4h with classical heating method.

These conditions led in our case to the formation of the target product **62** with 88% yield along with only 12% of the Glaser homocoupled product **62'** (Scheme V.5).

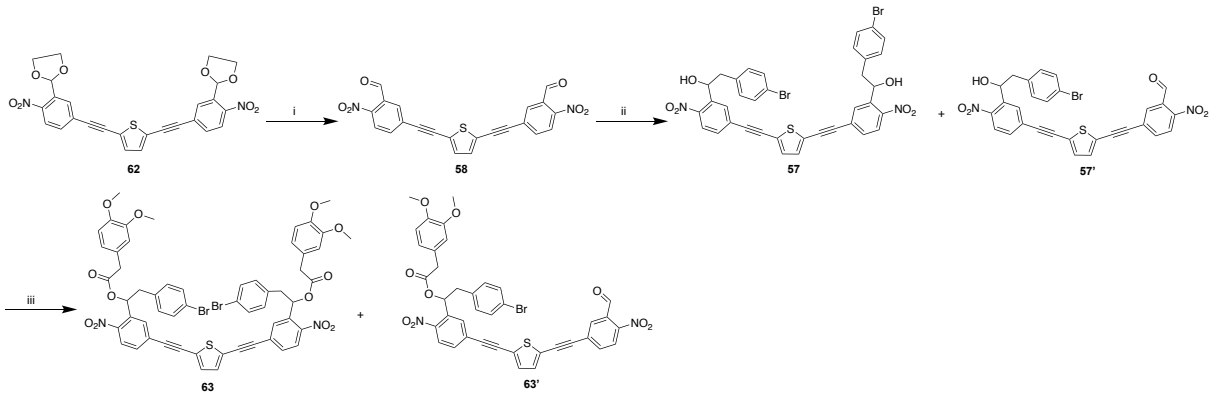

Scheme V.7: Synthetic scheme for the formation of the new photoremovable group BNPET-BB caged acid **63**.

(i) *p*TsOH, H_2O/ACN/DCM, 80 °C, 6 h, 99 %. (ii) **a)** LiCl, Zinc, THF, trimethylsilylchloride, 80°C, 5 min, 1,2- dibromoethane, 80°C, 5 min, Bromobenzyl bromide, 70°C, 1h **b)** 0°C to room temperature, THF, overnight. (iii) 3,4-dimethoxyphenyl acetic acid, DIC, DMAP, DCM, 0°C to room temperature, overnight, 80%.

The formed dioxolane **62** is deprotected in presence of *p*-TsOH in order to form the BNPET bisaldehyde **58** in quantitative yield. Similarly to the procedure described in the previous chapter, a freshly prepared batch of bromobenzyl zinc bromide was added to the bisaldehyde **58** in order to form the target product **57**. This reaction was optimized in order to obtain the highest yield of compound **57**, since we observed the formation of the monosubstituted product **57'** along with the target disubstituted compound. The use of bromobenzyl zinc bromide in huge excess (10 eq) gave the best conversion; 80% of **57** and 20% of **57'**. Both compounds were inseparable by silica gel purification at this step, so the mixture was used as it is for the coupling reaction with the MPAA chromophoric acid. Using the same coupling conditions, DIC and DMAP, and using the same acid chromophore MPAA, we were able to isolate the target ester **63** in 80% after HPLC purification.

2.4. Study of the Photolysis by One-Photon

We have described in the previous chapter (IV) the photolysis of the *o*-nitrobenzyl series, and we were able to demonstrate the mechanism described in Scheme I.14. this mechanism that proceeds by releasing a nitrosoketone product that is present in equilibrium with its tautomeric nitroso-enol form.

And we have validated the formation of the nitroso-enol form where it favors the conjugation of the system by the creation of a double bond between the two extremities of the molecule. In the case of the new BNPET PPG **63**, we could observe the formation of the nitroso-enol form on both sides **63''** with the release of 2 equivalents of MPAA (Scheme V.8).

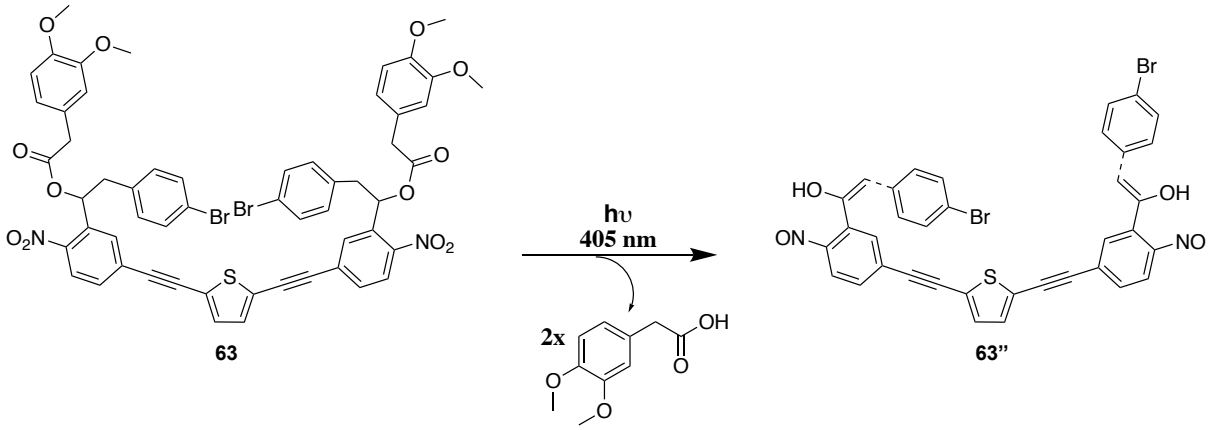

Scheme V.8: Photolysis of **63** upon irradiation at 405 nm and the release of the MPAA chromophore along with the nitroso-enol **63''**.

2.4.1. Absorption / Emission Profiles

A solution of **63** at a concentration of 50 µM in a mixture of acetonitrile / PBS (3/7 v/v) was irradiated at 405 nm with the help of an LED lamp. For every irradiation time, few µL of the solution were injected in HPLC in order to follow the progress of the photolytical reaction by following the decrease of the peak of the starting material and the appearance of the by-product's peak. The starting material presents 2 absorption bands at 280 nm and 387 nm respectively with a molar extinction coefficient of $\varepsilon = 27000\ M^{-1}.cm^{-1}$. Upon each irradiation, the UV/Vis profile was recorded (Scheme IV.9).

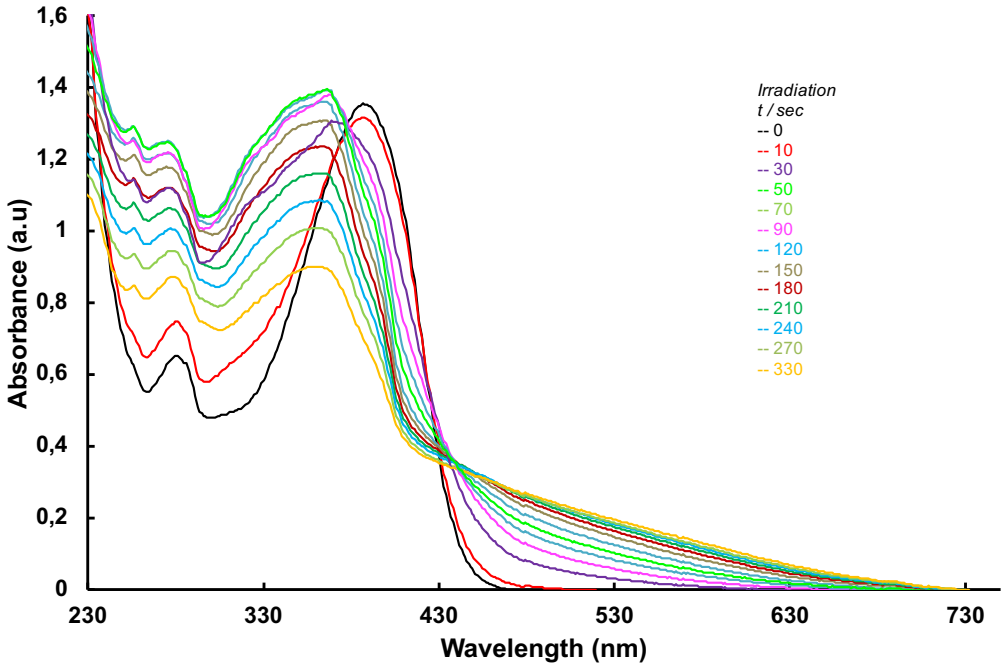

Scheme V.9: Variation of UV absorbance after irradiation at 405 nm of 50 µM solution (Acetonitrile/PBS 3:7 in vol.) of **63**.

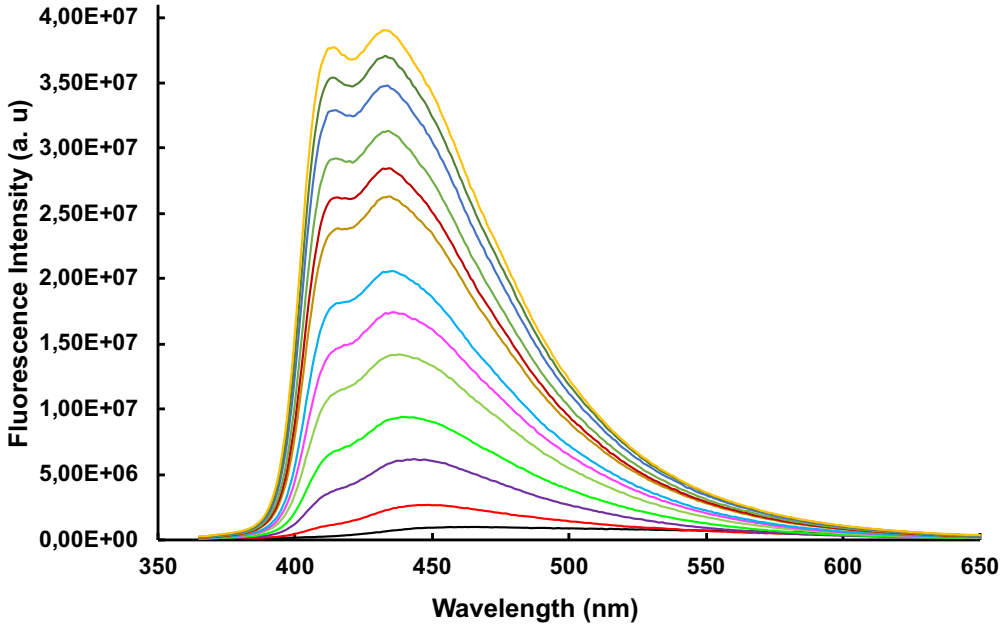

Scheme V.10: Variation of fluorescence emission after irradiation at 405 nm of 50 µM solution (Acetonitrile/PBS 3:7 in vol.) of **63**.

Interestingly, this PPG shows a complete loss of starting material after only 30 seconds of irradiation (black and red) and an appearance of a new compound (purple) most probable to be the mono released compound with an absorption maximum at 375 nm. This latter disappears completely after 50 seconds and a new absorbance appears with a maximum of absorption at 365 nm (green).

Starting from 70 seconds, this absorption starts to decrease progressively, and a very broad band appears after 330 seconds (5.5 minutes) with a possible absorption maximum around 400 nm and extends till 730 nm (orange). On HPLC, after 30 seconds we observed the complete disappearance of the starting material peak and the appearance of a new peak. The MPAA HPLC assay showed that after 30 seconds of irradiation, 100% of released MPAA was detected, that refers to the cleavage on one side of the BNPET PPG. Upon further irradiation, we observed the gradual disappearance of the second peak and a gradual appearance of a third peak accompanied by the increase of the peak of MPAA that reflects the release of more chromophore in the solution.

Before irradiation, compound **63** shows a very weak fluorescence but, interestingly, as we irradiate our sample, we observe a significant increase in the fluorescence intensity with 2 emission bands of the compound at λ_{em} = 435 nm and λ_{em} = 415 nm (Scheme V.10). We weren't able to evaluate the fluorescence intensity at full cleavage (I_{full}) since the compound **63** tend to partially cleave (one side cleavage) at first releasing one fluorescent by-product and upon further irradiation we observe the cleavage on the second side leading to the release of another fluorescent by-product in a mixture of PBS/acetonitrile.

In order to be able to correlate the fluorescent uncaging report with the control by light of a biological event (for example with the release of a neurotransmitter), we decided to synthesize a water-soluble version. Therefore, a PEGylated version of the BNPET PPG was designed. We decided to graft PEG chains on this PPG using metallo-catalyzed coupling of a pegylated aryl directly on molecule **63**.
As a result, we have decided to increase the conjugation of **63** and its solubility via the addition of PEG_8 by a Suzuki coupling.

3. Towards the synthesis of the PEGylated derivative of BNPET

3.1. Suzuki Cross-Coupling Reaction via Synthesis of Boronic Derivatives

We realized first the synthesis of the PEGylated aryl derivative. The first step consists of a tosylation of the starting product, Octaethylene glycol monomethyl ether **51** using *p*-Tosyl chloride under basic conditions to obtain the tosylated PEG_8 product **64** with a yield of 93%. This latter was reacted with 4-bromophenol to form the product **65** with a yield of 88% after purification (Scheme V.11).

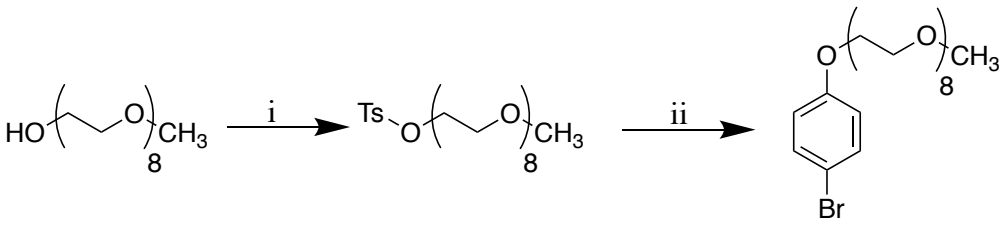

51 **64** **65**

Scheme V.11: Synthesis of PEG_8 bromo aryl **65** from PEG_8-OH.

(i) *p*-TsCl, NaOH, THF, 0°C, overnight, 93%. (ii) 4-bromophenol, K_2CO_3, DMF, 80°C, 24h, 88%.

The third step is the formation of the boronic derivative for the Suzuki coupling, we proposed two separate synthetic routes in order to access this derivative. The first proposed route is using *n*-BuLi and Trimethylborate (Route A, Scheme V.12). This reaction yielded no target product **66** and no conversion of the starting product into the desired product was observed. We therefore chose to perform this reaction catalytically using a palladium complex $PdCl_2(dppf)_2$ and Bis(pinacolato) diborane (Route B, Scheme V.12). The target product **67** was obtained once and this reaction was unreproducible due to the poor reactivity of the bromo derivative **65**, so we switched to the iodo derivative (4-iodophenol) that is suspected to have better reactivity towards palladium complexes.

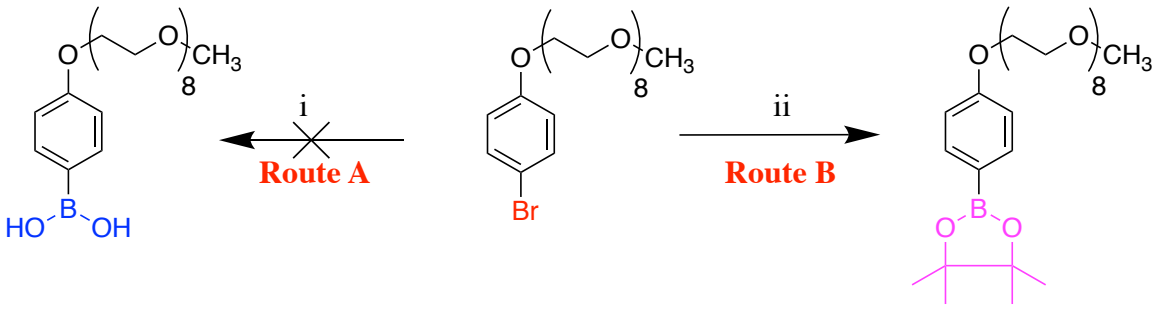

66 **65** **67**

Scheme V.12: Two proposed synthetic routes for the synthesis of the boronic derivative of **65**.
Route A using *n*-BuLi and trimethyl borate and **Route B** catalytically using palladium complex.

(i) *n*-BuLi, $B(OCH_3)_2$, THF, -78°C, 14h, HCl (ii) $PdCl_2(dppf)_2$, Bis(pinacolato) diborane, CH_3COOK, DMSO, 90°C, 14h.

Due to the unavailability of the commercial PEG_8-OH **51** in the lab, we managed to synthesize the PEG_7-OH **70** derivative which has the same solubility properties as its PEG_8 analog. Starting from this PEG_7-OH derivative **70**, and after its tosylation into **71**, we were able to isolate the PEG_7-iodophenyl **72** in 65% yield. The catalytical reaction between this latter and the $Pd(dppf)_2$ complex led to the formation of the target PEG_7-phenyl boronic ester **73** but in a partial conversion.

Due to the presence of some starting iodo derivative **72** in the crude, we proceeded to the purification in order to isolate a pure boronic derivative, in order to prevent the Suzuki between the leftover of **72** and the formed **73** (Scheme V.13). Since the formed PEG_7 derivative **73** is too polar, the purification was performed in presence of 5% MeOH, this latter led to the trans-esterification of the boronic derivative **73** giving $B(OCH_3)_2$ as a non-reactive species.

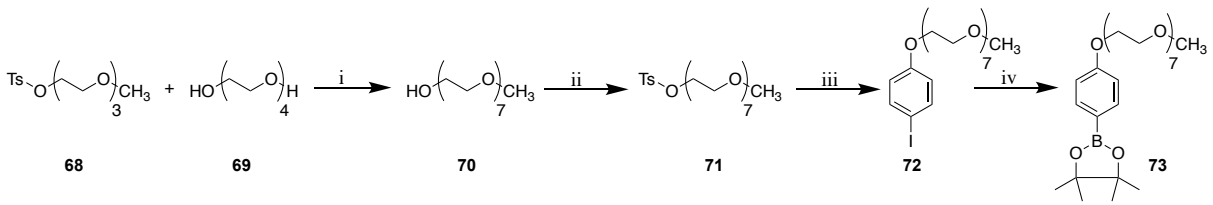

Scheme V.13: Synthesis of PEG_7 phenylboronic ester **73** from PEG-iodo aryl **72.**

(i) K_2CO_3, DMF, 80°C, 24h, 60%. (ii) *p*-TsCl, NaOH, THF, 0°C, overnight, 88%. (iii) 4-iodophenol, K_2CO_3, DMF, 80°C, 24h, 65%. (iv) $PdCl_2(dppf)_2$, Bis(pinacolato) diborane, CH_3COOK, DMSO, 90°C, 14h, 65%.

We decided to switch to a less polar i.e. shorter PEG chains in order to be able to purify the boronic ester by a methanol-free silical gel purification.

In order to achieve that, we decided to work with PEG_4-OH **74** that was tosylated to form PEG_4-OTs **75**. This latter was reacted with 4-iodophenol to form **76** in 68% yield and via the catalytical pathway we were able to obtain PEG-4 phenylboronic ester **77** after purification in 63% yield (Scheme V.14).

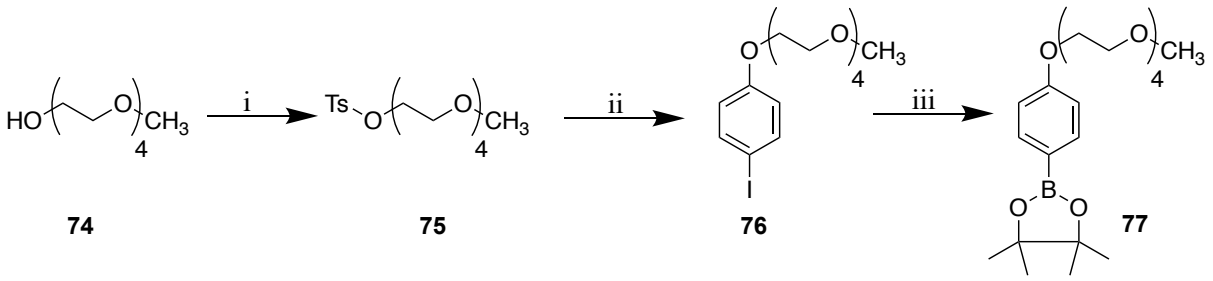

Scheme V.14: Synthesis of PEG_4 phenylboronic ester **77** from PEG_4-iodo aryl **76.**

(i) *p*-TsCl, NaOH, THF, 0°C, overnight, 82%. (ii) 4-iodophenol, K_2CO_3, DMF, 80°C, 24h, 63%. (iii) $PdCl_2(dppf)_2$, Bis(pinacolato) diborane, CH_3COOK, DMSO, 90°C, 14h, 63%.

After having obtained the PEGylated boronic ester, we proceeded to the Suzuki cross-coupling of this latter with our BNPET-BB compound **63** using palladium catalyst (Scheme V.15).

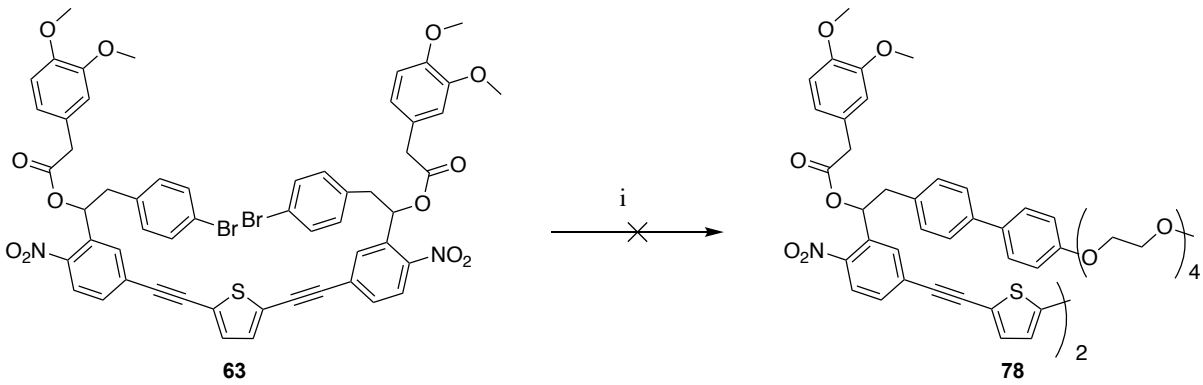

Scheme V.15: Synthesis of PEGylated BNPET-BB **78** via a Suzuki cross-coupling using PEG_4-phenylboronic ester **77.**

(i) **77**, $Pd(PPh_3)_4$, K_2CO_3, Toluene/Ethanol/water (7/2/1 v/v/v), microwave, 80°C, 45 min.

The reaction was done using a palladium (0) complex in a mixture of toluene, ethanol and water under microwave heating at 80°C for 45 minutes. Unfortunately, we were not able to see the formation of the pegylated product **78**, the reaction yielded only starting material **63**.

Another alternative for the synthesis of the pegylated version of the pro-fluorescent BNPET PPG is the use of a Sonogashira cross-coupling using Pegylated phenyl acetylene derivatives. This strategy was explored and detailed in the following section.

3.2. Sonogashira Cross-Coupling Reaction via Synthesis of Acetylene Derivatives

Using PEGylated phenyl acetylene derivatives is advantageous since it doesn't just increase the solubility of the target product but should also dramatically increase the conjugation of the system by the introduction of a triple bond. And also, acetylene derivatives are known to be stable, so this eliminates the risk of degradation during purification like in the case of PEGylated boronic esters.

We realized the synthesis of the PEGylated phenyl acetylene derivative **81** using the already prepared PEG_7-OTs **71**. The first step for the preparation of **71** consists of an acetylation of the 4-iodophenol using trimethylsilyl acetylene and $PdCl_2(PPh_3)_2$ with CuI catalysts in order to obtain the protected alkyne **80** in 88%.

This latter was reacted with PEG_7-OTs **71** in presence of K_2CO_3 to obtain in one step the deprotection of the alkyne and the tosylation of the phenyl to form the free PEGylated phenyl acetylene **81** with a yield of 73% after purification (Scheme V.16).

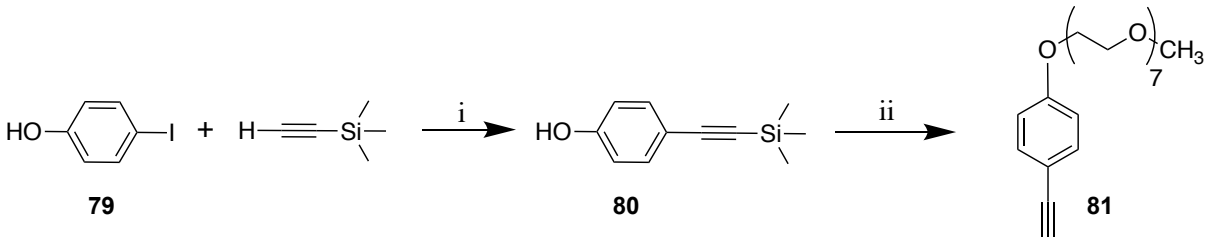

Scheme V.16: Synthesis of PEG_7 phenylacetylene **81** from 4-iodo phenol **79.**

(i) $PdCl_2(PPh_3)_2$, CuI, Et_3N, THF, 80°C, 3h, 88%. (ii) K_2CO_3, DMF, 80°C, 14h, 73%.

After having obtained the free alkyne **81**, we tried a Sonogashira coupling reaction with the previously obtained BNPET-BB **63** in order to get access to a water soluble version of this BNPET derivative (**82**, Scheme V.17).

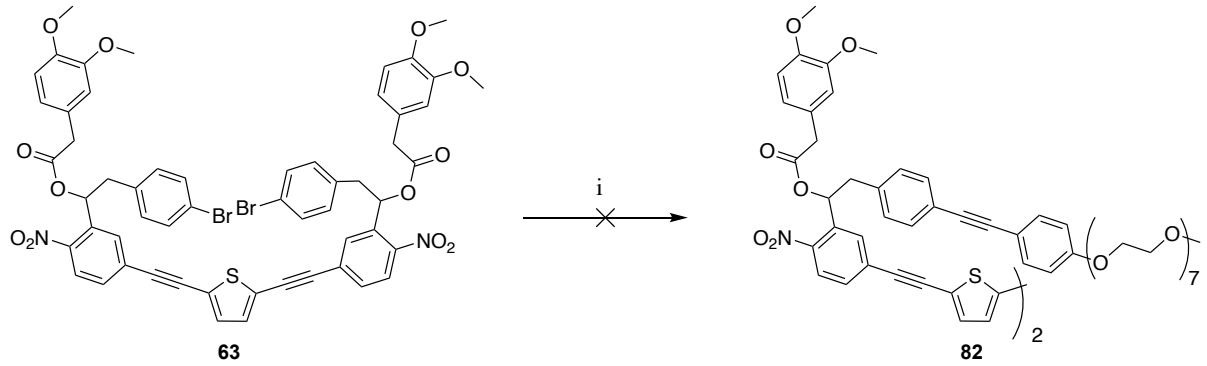

Scheme V.17: Synthesis of PEGylated BNPET-BB **82** via a Sonogashira cross-coupling using PEG_7-phenylacetylene **81.**

(i) **81**, [Pd], CuI, Et_3N, THF, 80°C, 45 min.

This reaction was tried twice changing the palladium catalyst and the order of addition of reagents. Trial 1 was done using Pd(II) catalyst $PdCl_2(PPh_3)_2$ in presence of CuI as co-catalyst in THF and triethylamine base, under heating at 80°C and following the reaction by HPLC. After 5h of heating no product appeared only starting material and the homocoupling of the acetylene derivative **81** were observed.

Trial 2 was done using Pd(0) catalyst $Pd(PPh_3)_4$ and adding copper iodide at the end to prevent the formation of the homocoupling of the acetylene derivative. The reaction was heated at 80°C and followed by HPLC and after 7h we observed a degradation of the BNPET derivative originating from the degradation of its thiophene core.

These results could be explained by the steric hindrance of the BNPET-BB derivative as well as the weak reactivity of the bromo aryl toward metal-catalyzed cross-coupling (Suzuki or Sonogashira).

One solution would be to prepare the iodo derivative of BNPET-BB that, evidently, is more reactive than its bromo analog towards Sonogashira or Suzuki crosss-coupling reactions. This could be done by preparing the iodobenzyl zinc iodide and reacting this latter with the BNPET-dialdehyde **58** in order to obtain the iodo analog of **57**. This is one solution to overcome this synthetic problem, and as soon as the target compound is obtained it will be tested for the release of neurotransmitters and following the uncaging event by fluorescence.

4. Photo-Physical Properties of BNPET Derivative

After the synthesis of this photoremovable protecting group with the heteroatom core **63**, we were interested in investigating the photo-physical properties of this compound. The core of this molecule (nitrophenyl ethynyl) being new, we are interested in determining its photo-physical and photo-chemical properties of this molecule in order to evaluate its efficiency in two-photon excitation. Similarly to the epoxide, to determine the two-photon uncaging cross-section (δ_u), it is necessary to determine the two-photon absorption cross-section (δ_a) using the equation (2) of chapter I:

$$\delta_u = \delta_a \phi_u \qquad (2)$$

The characterization that were done on this chromophore BNPET represented in SchemeV.18 and the experimental procedures of the synthesis of this chromophore were adopted by Jung's group (Jung *et al.,* 2000).

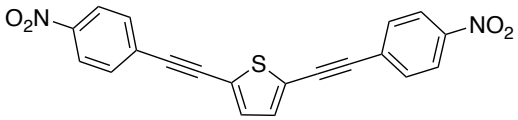

BNPET

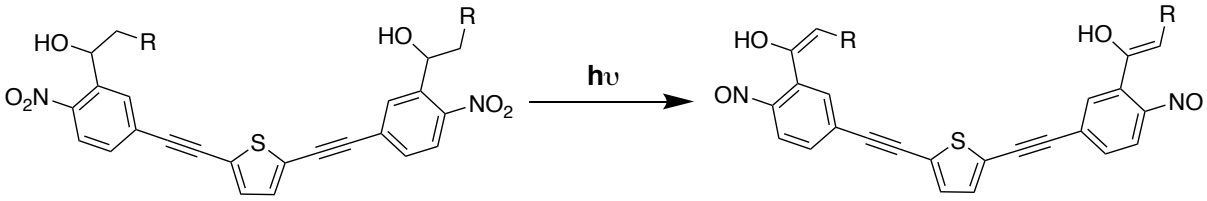

BNPET-BB
63

Photolysis by-product

Scheme V.18: Structure of BNPET chromophore and the photochemical mechanism of cleavage of BNPET-BB and the release of the α-nitrosohydroxystilbene by-product.

4.1. Determination of the Two-Photon Absorption Cross-Section (δ_a) of BNPET

We used here the same method applied to determine the 2-PA cross-section of the epoxide in order to determine the photophysical characteristics of BNPET chromophore.

In order to determine the fluorescence quantum yield of BNPET (ϕ_f) we selected Harmalol as a solution in a mixture of ethanol-sulfuric acid as a reference with a quantum yield of fluorescence ($\phi_f = 0.48$) as determined by direct method (Pardo *et al.,* 1988).

In the measurements of the spectra, the concentrations of the compound to be studied and the compound taken as reference are chosen so that the absorbances of the two solutions are identical for the selected excitation wavelength. Since the sample solvent of our BNPET chromophore (CH_2Cl_2) is not the same as the reference (EtOH, H_2SO_4), a corrective factor of their respective refractive indices must be introduced in the calculation of quantum yield described by equation (4) in Chapter III. Simply, by replacing the terms in equation (4) by their corresponding values, we obtained a quantum yield of fluorescence $\phi_f^{BNPET} = 0.16$ for our BNPET.

In order to determine the 2-PA cross-section (δ_a) of the BNPET, we used the same method applied to the epoxide in Chapter III using Rhodamine B as a reference and varying the wavelength between 700 and 900 nm.

Both the reference, Rhodamine B, and the compound of interest, BNPET, were irradiated by the laser and the intensities of fluorescence (I) obtained were replaced by their values in equation (5) and we were able to construct the two-photon absorption spectra of both the BNPET (Scheme V.19). interestingly, the fluorescence quadratic-intensity dependence correlates linearly with the power of the laser which indicates clearly the process of two-photon absorption.

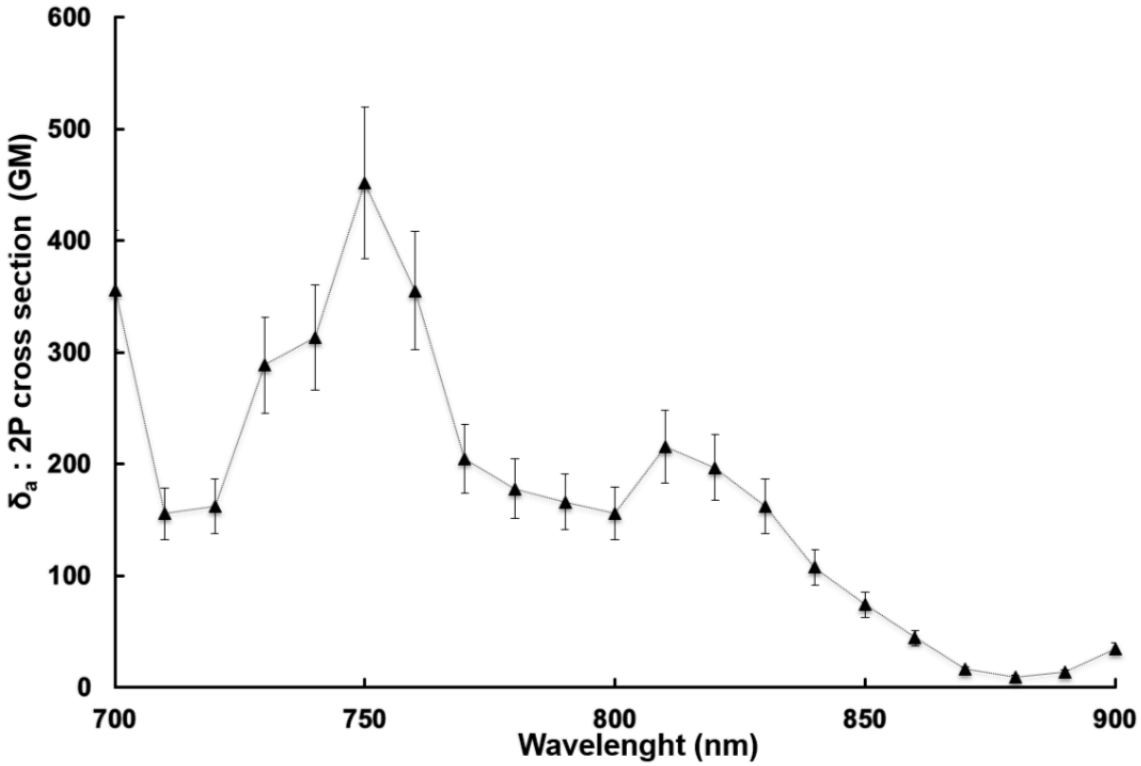

Scheme V.19: Two-photon absorption spectra of BNPET chromophore.

In reference to the spectra, it is evident that the BNPET is efficient in 2-PA, it possesses two-photon absorption cross-section (δ_a) values up to 150 GM in the wavelength range of 700-830 nm. This wavelength range is very interesting for *in vivo* applications since these wavelengths fall in the near-infrared region, this zone where the biological chromophores tend to weakly absorb light irradiations.

This BNPET chromophore has several characteristics that makes it a very useful PPG for biological applications: (1) We succeeded to synthesize a conjugated analog of BNPET and this latter showed interesting fluorescence reporting properties after uncaging. This photoremovable protecting group shows interestingly (2) short irradiation times and (3) high efficiency in two-photon absorption.

However, to be able to correlate the fluorescent uncaging report with the control by light of a biological event (for example with the release of a neurotransmitter) we still have to be able to generate a more soluble version of this new photoremovable protection group with uncaging fluorescent properties.

CHAPTER VI

Use of *o*-Nitroaryl PPGs for Light-Controlled Cell Adhesion

1. State of Art

This project was done in collaboration with the Group of Doctor Christophe Tribet from the Ecole Normale Supérieure (ENS): Biophysical Chemistry Department-Paris. This group works on a functionalized copolymer that permits the control of the adhesive property of cellular surfaces. This copolymer is constituted mainly of a poly-L-Lysine (PLL) chain grafted with a poly-ethylene glycol (PEG) chain (Dalier *et al*., 2016).

The principle behind the method of PLL coating, is that the polycationic polylysine molecules adsorb strongly to various solid surfaces, leaving cationic sites which combine with the anionic sites on cell surfaces. The cell adhesion is interpreted simply as the interaction between the polyanionic cell surfaces and the polycationic layer of adsorbed polylysine. The attachment of cells to the polylysine-treated surfaces can be exploited for a variety of experimental manipulations.

In this project, we aim to introduce to this copolymer a photocleavable bond by the insertion of modified, previously synthesized, photoremovable protecting groups **PPG** (*o*-nitrobenzyls and *o*-nitrophenethyls) that will help the light-control and quantification of cell adhesion (Scheme VI.1).

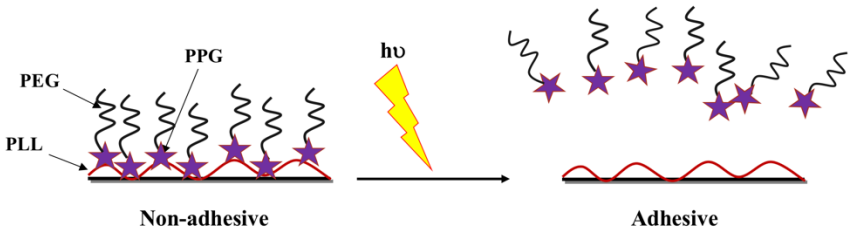

Scheme VI.1: Use of photoremovable protecting groups in order to control cell adhesion by light.

Cell adhesion is involved in stimulating signals that regulate cell differentiation, cell cycle, cell migration, and cell survival. Cell adhesion is also essential in cell communication and regulation and showed of fundamental importance in the development and maintenance of tissues. Changes in cell adhesion can be the defining event in a wide range of diseases including cancer (Khalili *et al.,* 2015).

In order to achieve the best architecture for the copolymer system used for light-controlled cell adhesion, the cleavage of the bond should occur at a wavelength>350 nm to avoid cellular damage. The best candidate for this purpose is the *o*-nitrobiphenyl PPG that was recently developed in the lab. For this purpose, we need to modify the structure of the PPG in order to introduce functions that can be used to graft the polymer chain and the PLL chain.

2. Design and Synthesis

2.1. Synthesis of *o*-nitrophenethyl (*o*-NPP) caged copolymer

The first proposed photoremovable group is the *o*-nitrophenethyl with the *o*-nitrobiphenyl core bearing a triple bond and an alcohol function. The proposed architecture of this compound is presented in Scheme VI.2.

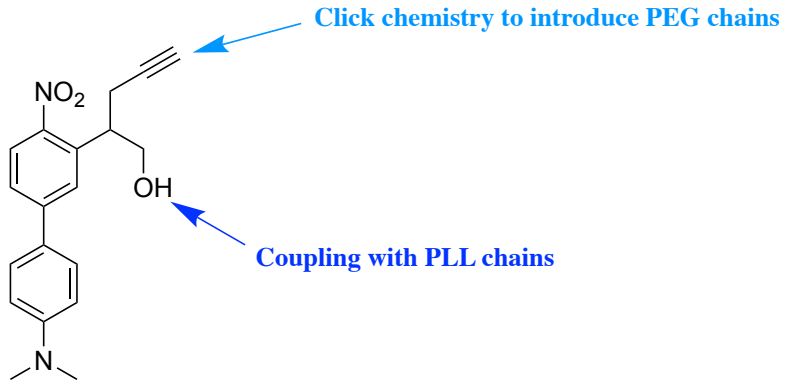

Scheme VI.2: Proposed architecture for the *o*-nitrophenethyl caged PLL.

This compound is synthesized in 6 steps starting with a vicarious nucleophilic substitution of 4-nitrobromobenzene **1** with *tert*-butyl chloroacetate to obtain compound 2 in 55% yield. The following step is the acid-catalyzed trans-esterification of **2** in MeOH in order to obtain the methyl ester **83** in quantitative yield. The alkylation of **83** using trimethylsilylpropargyl bromide was done in anhydrous acetonitrile and using DBU as base led to the formation of **84** in 72% yield. In order to obtain the free alcohol function, the methyl ester was reduced using DIBAL-H to obtain compound **85** in 73% yield (Scheme VI.3).

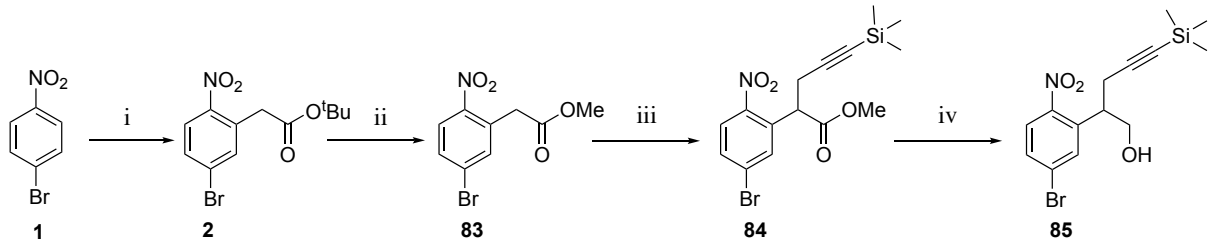

Scheme VI.3: 1st part of the synthesis of the target cage compound starting from 4-nitrobromo benzene.

(i) tert-butyl chloroacetate, DMF, 0°C, room temperature, 14h, 55%. (ii) MeOH, H_2SO_4, 65°C, 4h, 100%. (iii) trimethylsilylpropargyl bromide, DBU, acetonitrile, 24h, 72%. (iv) DIBAL-H, THF, 0°C, 4h, 73%.

After obtaining compound **85**, we proceeded with the Suzuki coupling in order to construct the biphenyl core; this reaction was done in presence of $Pd(PPh_3)_4$ catalyst in a mixture of Toluene/Ethanol/Water to obtain the nitrobiphenyl **86** in 55% yield. The free alkyne **87** was obtained in quantitative yield after deprotection of the TMS protecting group using TBAF in THF for 1h.

After obtaining the free alkyne **86**, we were able to attach the PEG_{52}-NH_2 chain using CuAAC in presence of Copper in a mixture of anhydrous DMF/*tert*-butanol/water in order to obtain the target compound **88** in 90% yield (Scheme VI.4).

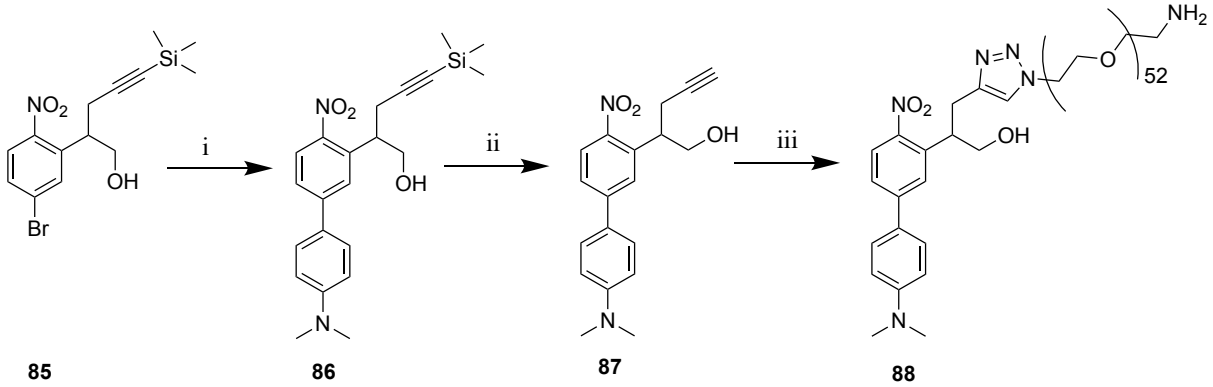

Scheme VI.4: 2nd part of the synthesis of the target cage compound starting from compound **85**

(i) 4-(dimethylamino) phenylboronic, K_2CO_3, Toluene/EtOH/Water (7/2/1 v/v/v), $Pd(PPh_3)_4$, microwave, 80°C, 45 min, 55%. (ii) Tetrabutylamonium fluoride (TBAF), THF, room temperature, 1h, 100%. (iii) N_3-CH_2-PEG_{52}-CH_2-NH_2, DMF/^{t}BuOH/H_2O (1/15/1 v/v/v), Ascorbic acid, L-Proline, $CuSO_4.5H_2O$, 65°C, 48h, 90%.

2.1.1. Evaluation of surface adhesive properties via surface fluorescence loss

In order to evaluate the control of cell adhesion by light, one proposed method is using loss of fluorescence on the surface. In other words, a fluorescent dye is statistically coupled to our PPG, this dye will help quantify the release of the PPG from the surface by the loss of fluorescence rising from the departure of the PPG-dye core from the surface after photocleavage.

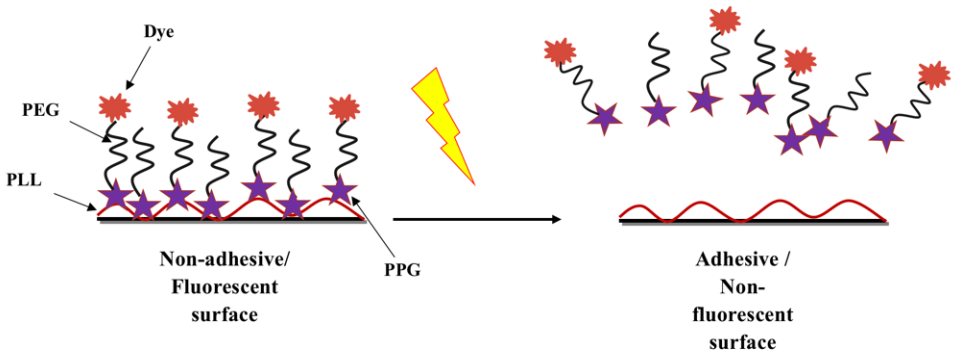

Scheme VI.5: Evaluation of surface adhesive properties by surface fluorescence loss.

In order to apply this method, a cyanine dye (Cy_3-NHS ester) was statistically coupled to our PPG-PEG compound **88** using diisopropylethylamine (D^iPEA) as base in anhydrous DMF in order to obtain the compound **89**. This latter was reacted with acetic acid in presence of D^iPEA as base and PyBoP as coupling reagent. This caping step is crucial in order to protect the amino function that may undergo, in presence of a base, intramolecular cyclisation after the coupling with trisphosgene. After obtaining the N-caped compound **90**, PLL was coupled to our compound using D^iPEA and trisphosgene in anhydrous THF to obtain the final compound **91** (Scheme VI.6). It is important to note that the PLL coupling was done in a manner to achieve 30% of surface modification.

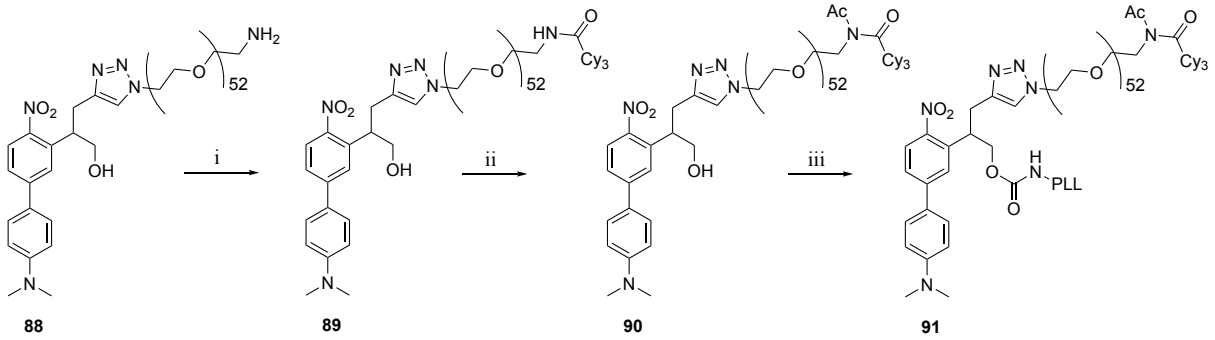

Scheme VI.6: Synthesis of Cage-PEG-PLL coupled with a dye for the evaluation of the adhesive properties by surface fluorescence loss.

(i) D^iPEA, Cy_3-NHS ester, anhydrous DMF, 0°C, room temperature, 3h, 95%. (ii) PyBoP, acetic acid, D^iPEA, anhydrous DMF, 0°C, room temperature, 3h, 100%. (iii) D^iPEA, trisphosgene, Poly-L-Lysine, anhydrous THF, 0°C, room temperature, 2h.

The compound was attached to a surface and this surface was irradiated at 405 nm and the emission intensity was recorded before and after photocleavage. We noticed an important loss of the surface fluorescence but unfortunately, the cyanine dye tends to photobleach upon irradiation at the mentioned wavelength. Therefore, we were not able to quantify the release of PLL copolymer by light using fluorescence imaging.

2.1.2. Evaluation of surface adhesive properties via surface mass loss

An alternative method for the evaluation of surface adhesive properties is via the measurement of surface mass loss using a Quartz Crystal Microbalance with Dissipation monitoring (QCM-D). This method studies the polymer behavior on surfaces via the measurement of the mass lost on surface that will help evaluate the percentage of cleavage by light. Upon irradiation of the surface, the PPG-PEG is cleaved from the surface releasing the PLL chains; the evaluation of this mass loss after photocleavage is a mean to evaluate the amount of PEG-PPG released after irradiation (Scheme VI.7).

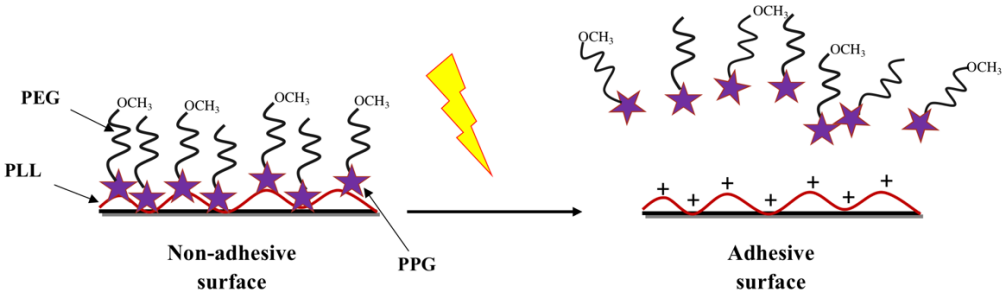

Scheme VI.7: Evaluation of surface adhesive properties by surface mass loss.

In order to apply this method, an alternative PEG chain was used: PEG_{32}-OCH_3, this latter was clicked to the free alkyne **87** to obtain compound **92** after 72h. Poly-L-Lysine chains were coupled to compound 92 using trisphosgene in basic medium to obtain the target compound **93** after dialysis in water (Scheme VI.8).

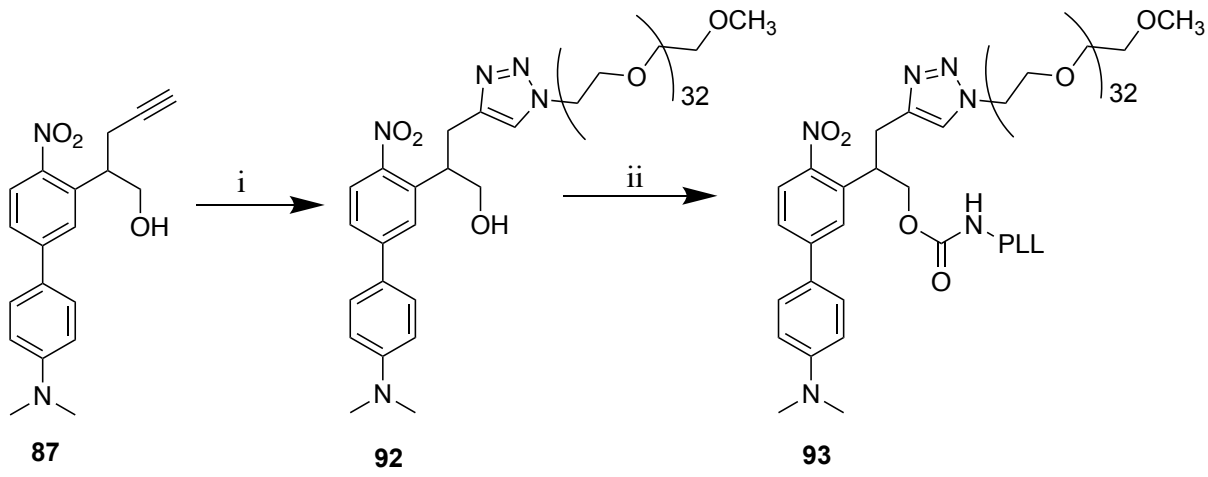

Scheme VI.8: Synthesis of Cage-PEG-PLL with OCH_3 terminal for the evaluation of the adhesive properties by surface zeta potential.

(i) N_3-CH_2-PEG_{32}-CH_2-OCH_3, DMF/^{t}BuOH/H_2O (1/15/1 v/v/v), Ascorbic acid, L-Proline, $CuSO_4.5H_2O$, 65°C, 72h, 95%. (ii) D^{i}PEA, trisphosgene, Poly-L-Lysine, anhydrous THF, 0°C, room temperature, 2h.

This *o*-nitrophenethyl-PEG system was irradiated on surface and the mass loss was recorded using the QCM-D technique. We observed only a 5% mass loss; this could be explained by the fact that *o*-NPP PPGs tend to have lower photolytical efficiency when in water solution. The photochemistry of this class of photoresponsive molecules (i.e. orthonitrophenethyl derivatives) is strongly dependent on solvent and basicity (Walbert *et al.,* 2001). One could speculate that the hydrophobic environment near the EANBP caging group in the polymer could potentially lead to a new major photochemical pathway and a photorearrangement producing a hydroxy-nitroso product. (Scheme I.20). Yet, 5% of mass loss could not mainly mean that no cleavage occurred, it could mean that this family of photoremovable group cleave weakly in water in presence of polymeric chains. That's why we switched to the *o*-nitrobenzyl PPG that we discovered in previous chapters that they tend to cleave in a quantitative manner.

2.2. Synthesis of *o*-nitrobenzyl (*o*-NB) caged copolymer

Due to the problems of cleavage and light sensitivity in water faced with the *o*-NPP, we decided to switch to the other series of the *o*-nitroaryls; *o*-nitrobenzyl (*o*-NB) that we know, from previous results (Chapter IV) that the cleavage is almost quantitative.

We suggested a similar PPG-copolymer architecture to that described for *o*-NPP in the previous section with a free alkyne for click chemistry with the PEG chain and the alcohol function for the coupling with PLL (Scheme VI.9).

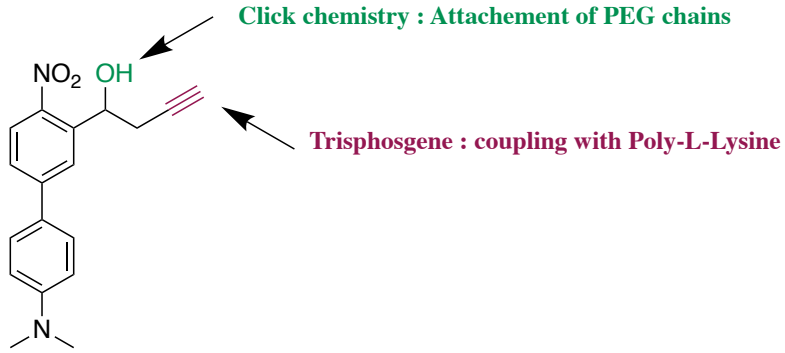

Scheme VI.9: Proposed architecture for the *o*-NB caged-PLL

The synthesis of this compound requires the reaction between an aldehyde function (electrophilic center) and propargylzinc bromide (nucleophile). Form the previously synthesized biphenyl aldehyde **37**, we initiated the synthesis of the target compound using freshly prepared propargylzinc bromide. Using propargyl bromide with activated zinc on **37** led to the formation of the target compound **95** in 94% yield (Scheme VI.10).

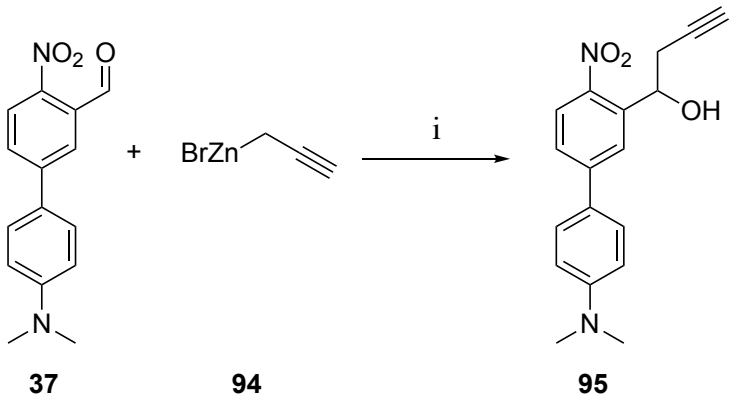

37 **94** **95**

Scheme VI.10: Synthesis of *o*-NB photoremovable group for caging PLL.

(i) THF, -78°C, 2h, room temperature, 14h, 94%.

2.2.1. Evaluation of adhesive properties via after cleavage on-surface click reactions

The purpose behind this method is to be able to apply post irradiation surface modification using reactive chain terminals. In other words, the terminal chain function will be used in order to modify the surface fluorescence after the release of the PPG-PEG entity. In our case, we used a PEG-azide terminal function in order to attach a fluorophore, on the surface, after irradiation via click chemistry (Scheme VI.11).

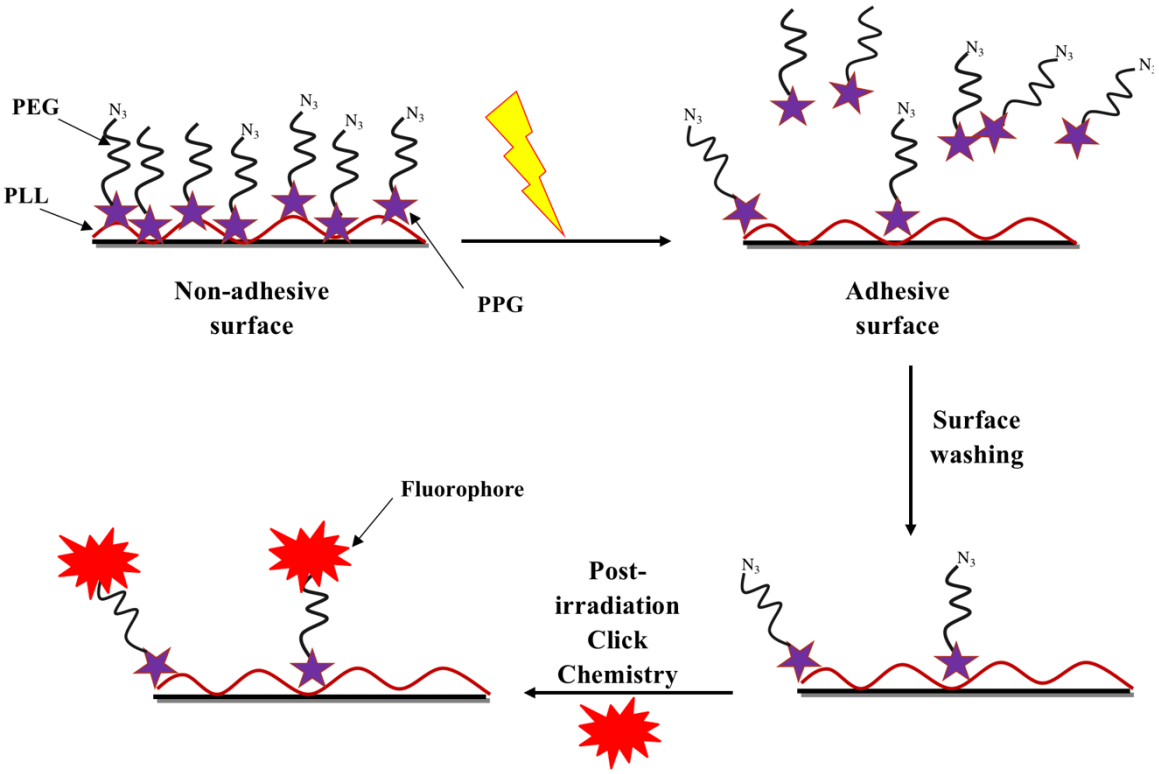

Scheme VI.11: Evaluation of surface adhesive properties by post-irradiation surface modification by attaching a fluorophore on the surface via click chemistry.

The aim of this strategy is to evaluate the fluorescence of the surface after cleavage via the attachment of a fluorophore. The post-cleavage fluorescence intensity will help in quantifying the release of the PLL. This depends on the free azide functions left on the surface after cleavage.

After the synthesis of the target PPG **95**, the PEG chain was attached to the compound via a click reaction in a mixture of solvents in order to obtain the PPG-PEG system **96** in 92% yield. This latter was coupled to a HOOC-PEG_7-CH_2-N_3 chain to obtain compound **97**. The synthesis of this product needs to be optimized and sent to our collaborator for post irradiation surface modification (Scheme VI.12).

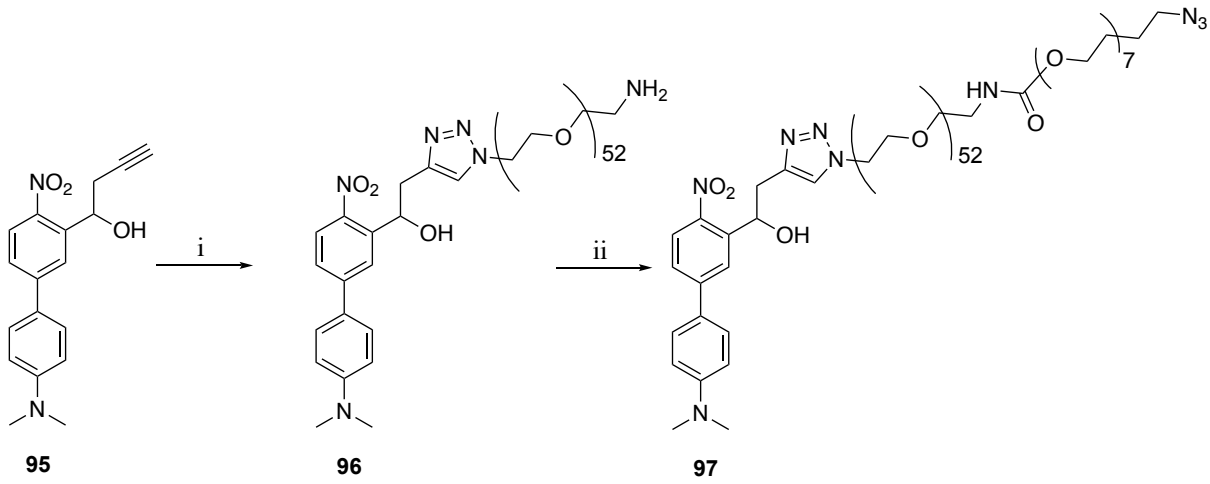

95 **96** **97**

Scheme VI.12: Synthesis of Cage-PEG-azide for post cleavage surface modification using click chemistry with a fluorophore.

(i) N_3-CH_2-PEG_{52}-CH_2-NH_2, DMF/^{t}BuOH/H_2O (1/15/1 v/v/v), Ascorbic acid, L-Proline, $CuSO_4.5H_2O$, 65°C, 72h, 92%. (ii) PyBoP, HOOC-PEG_7-CH_2-N_3, D^{i}PEA, anhydrous DMF, 0°C, room temperature, 3h, 100%.

2.2.2. Evaluation of surface adhesive properties on *o*-NB containing PLL polymers

The final trial in this project is the evaluation of the surface adhesive properties by measuring the surface mass loss before and after cleavage in order to quantify the release of PLL. Similarly to the method described in section 2.1.2 with *o*-NPP, we synthesized the PPG-PEG-PLL system using *o*-NB compound **95**.

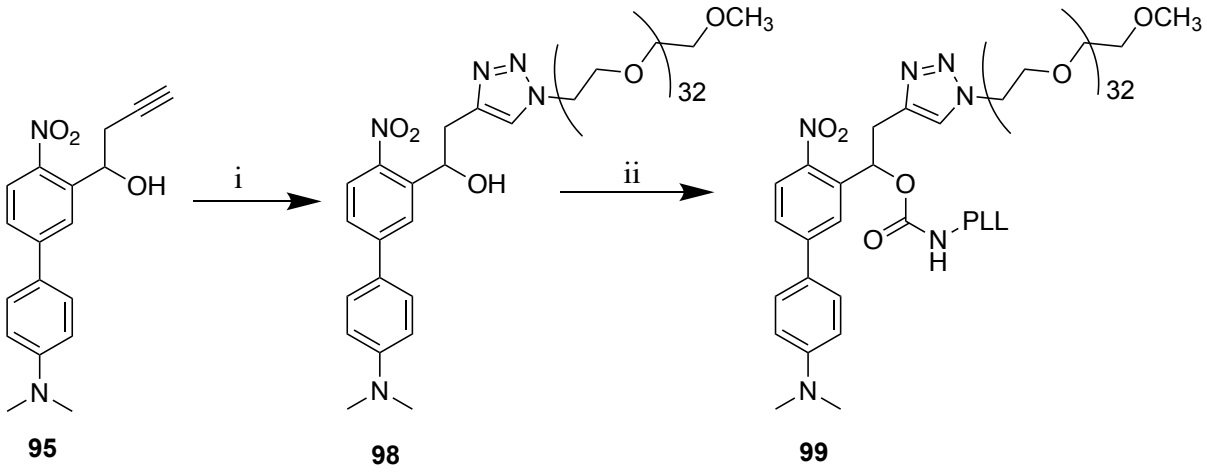

Scheme VI.13: Synthesis of *o*-NB Cage-PEG-PLL with OCH_3 terminal for the evaluation of the adhesive properties by surface mass loss.

(i) N_3-CH_2-PEG_{32}-CH_2-OCH_3, DMF/^{t}BuOH/H_2O (1/15/1 v/v/v), Ascorbic acid, L-Proline, $CuSO_4.5H_2O$, 65°C, 72h, 95%. (ii) D^{i}PEA, trisphosgene, Poly-L-Lysine, anhydrous THF, 0°C, room temperature, 2h.

Compound **98** was obtained after a CuAAC reaction between **95** and N_3-CH_2-PEG_{32}-CH_2-OCH_3. This latter was coupled to Poly-L-Lysine in the presence of trisphosgene and D^{i}PEA to obtain compound **99**.

2.2.2.1. UV/Visible Profiles of Irradiation

Three solutions of compound **99** with similar concentration of 0.5 mg/mL was prepared in a mixture of PBS/acetonitrile (1/1 v/v, Scheme VI.14), Ethanol/PBS (1/1 v/v, Scheme VI.15) and pure PBS (Scheme VI.16). These solutions were irradiated at 405 nm for the shown times and their corresponding UV absorbances were recorded at each irradiation time. The UV/Visible profiles show clean photochemical reactions in the used solvents with well-defined isosbestic points.

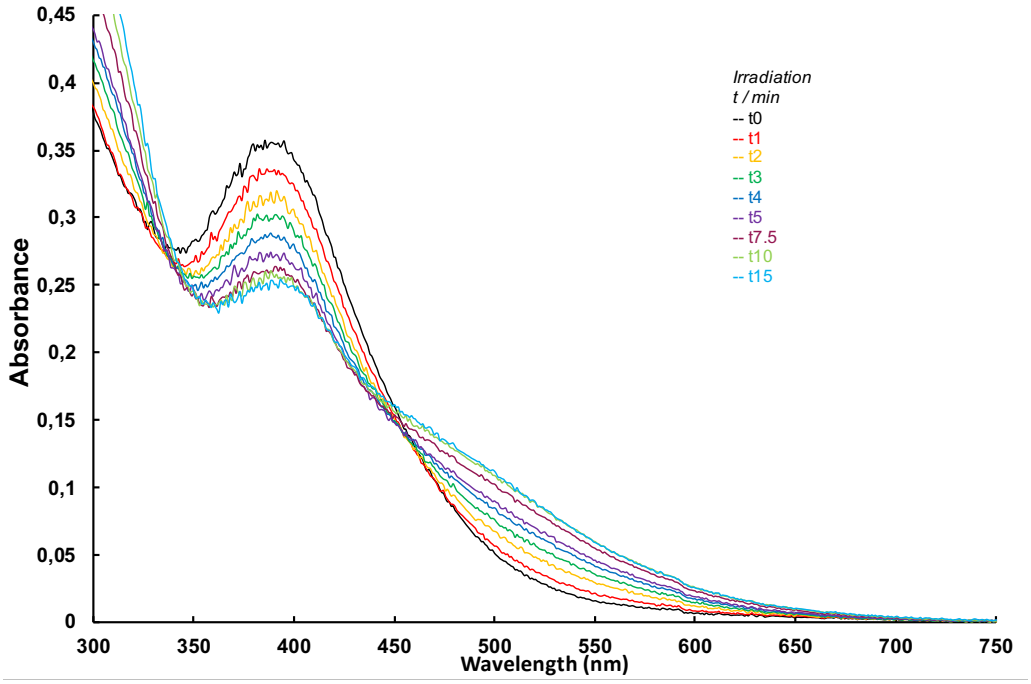

Scheme VI.14: UV/Visible profile upon irradiation of a solution of **99** (0.5 mg/mL) in Acetonitrile/PBS (1/1 v/v) at 405 nm.

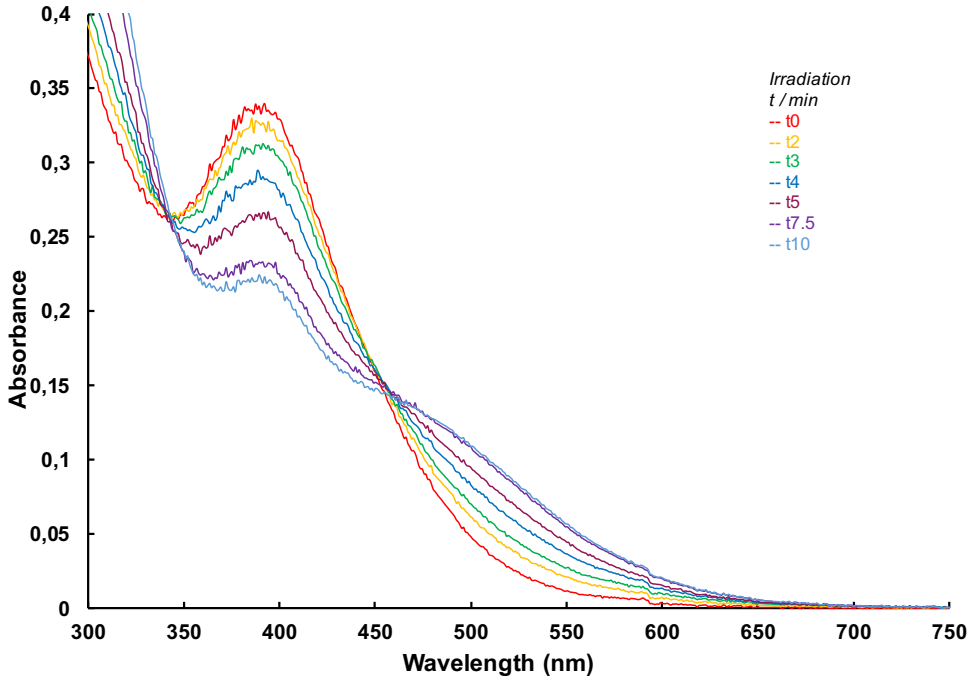

Scheme VI.15: UV/Visible profile upon irradiation of a solution of **99** (0.5 mg/mL) in Ethanol/PBS (1/1 v/v) at 405 nm.

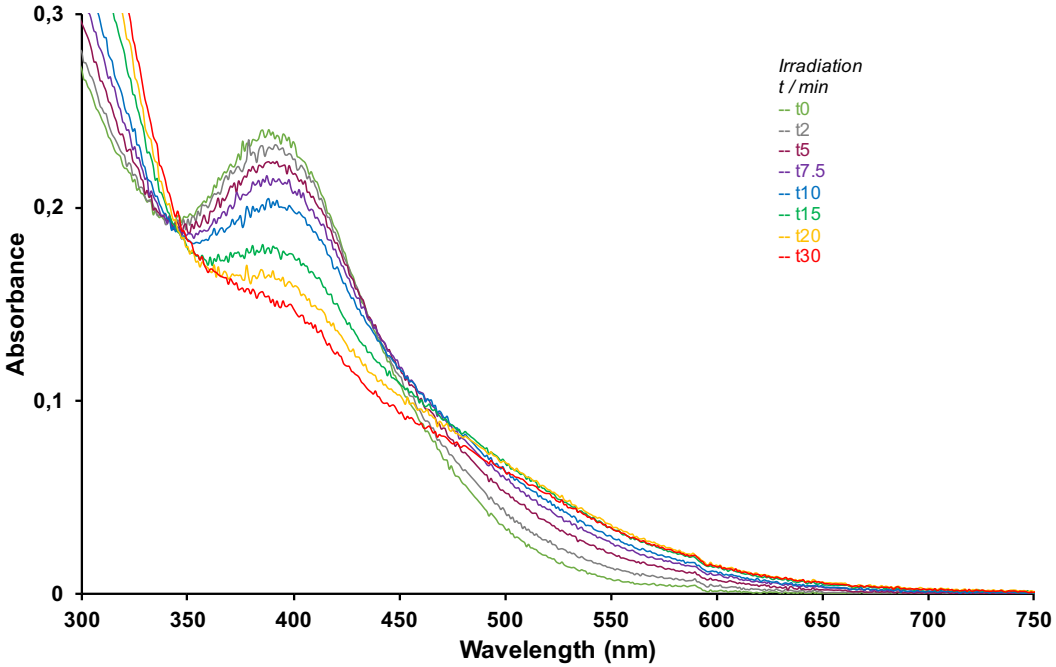

Scheme VI.16: UV/Visible profile upon irradiation of a solution of **99** (0.5 mg/mL) in 100% PBS at 405 nm.

The main aim of this project was to develop a new PPG-PEG-PLL system for the light-controlled evaluation of the adhesive properties of a surface. We were able to optimize the synthesis of caged poly-L-Lysine using two series of *o*-nitroaryls: the *o*-nitrophenethyls and *o*-nitrobenzyls.

Using different physical properties like fluorescence and surface mass loss, we aimed to evaluate the surface adhesive properties before and after cleavage. The synthetic part was done in the lab and the final pure compounds were sent to our collaborators for the irradiation experiments and the surface adhesive properties.

CHAPTER VII

Conclusions and Perspectives

1. Conclusions

There is a great need for photoremovable protecting groups able to generate an easy way to quantify their side-products, in particular to be able to monitor in real time the light induced concentration jump of a given biological effector. One of the ways to monitor the release of a biomolecule is via fluorescence as an "optical reporter" of the uncaging event. So, the aim of this thesis work was to design photoremovable protecting groups that are able to release a fluorescent by-product of uncaging. In order to achieve this goal, we suggested several strategies in order to construct our target compound that was inspired by the structure of EANBP PPG previously developed in the lab (Scheme VII.1). Both strategies; the vicarious nucleophilic substitution and the deprotonation of an alkyl benzene followed by an addition to a carbonyl function, showed lots of reactivity and reproducibility problems.

An alternative method was developed using biphenyl benzyl epoxide opening in order to get access to both *o*-nitroaryls families: *o*-nitrophenethyls and *o*-nitrobenzyls. The multi-step synthesis of the epoxide was successful, and the yields of every individual step was promising. The epoxide opening didn't work due to the acidity of the proton in the benzylic position to the nitro benzyl moiety and the basicity of the organometallic compound used. As an alternative, we proposed a reduction/alkylation of the epoxide in order to get access to our pro-fluorescent PPGs. However, the low yield of conversion and the close polarity of the starting epoxide and the target product could not lead to an efficient synthetical pathway to get access to pro-fluorescent PPGs. Despite these synthetic, reactivity and polarity problems, the synthesized epoxide showed interesting fluorescence properties in toluene compared to the starting aldehyde. This fluorescence; that could be tuned by increasing the conjugation of the epoxide; could act as an optical reporter for cell biology imaging studies or as a fluorescent probe.

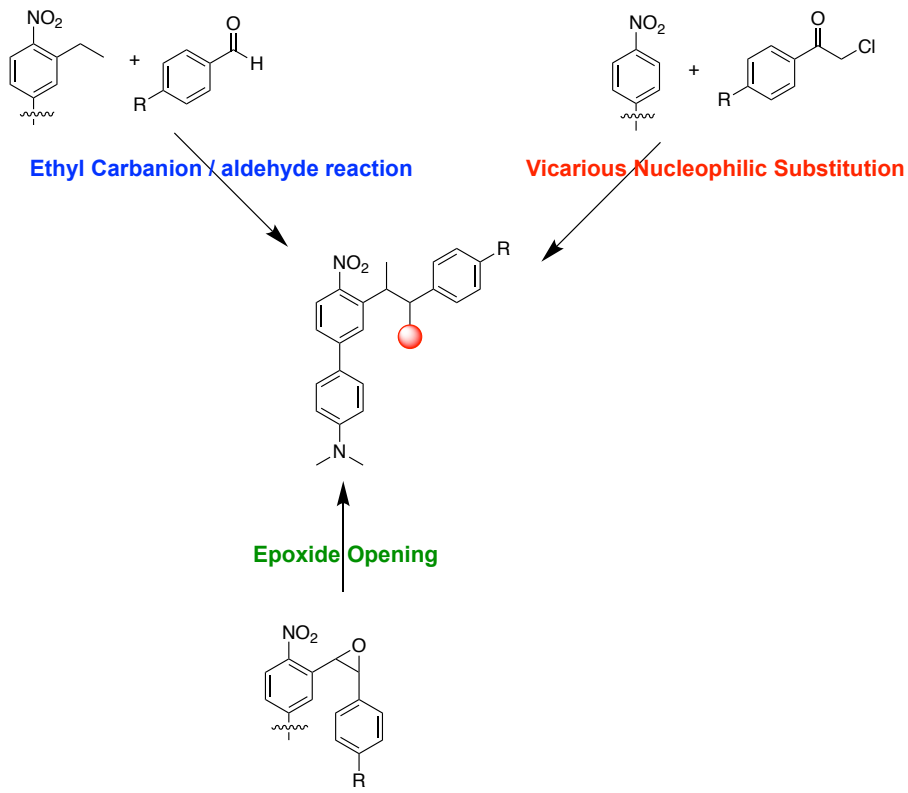

Scheme VII.1: The proposed strategies to access *o*-nitrophenethyl photoremovable protecting groups.

In order to solve all these problems, and to achieve the synthesis of the target compounds, we decided to use the aldehyde isolated during the total synthesis of the epoxide. Although this method doesn't give access to both families of *o*-nitroaryls PPGs, yet it is a way to synthesize *o*-nitrobenzyl PPGs that can be chemically modified to get access to a pro-fluorescent photoremovable protecting groups. This leads us to synthesize a new class of *o*-nitrobenzyl photoremovable groups able to generate a fluorescent side-product. These compounds were designed in order to produce after the photoreaction a nitrosoketone by-product able to achieve a keto–enol tautomerism leading to a conjugated α-hydroxystilbene product.

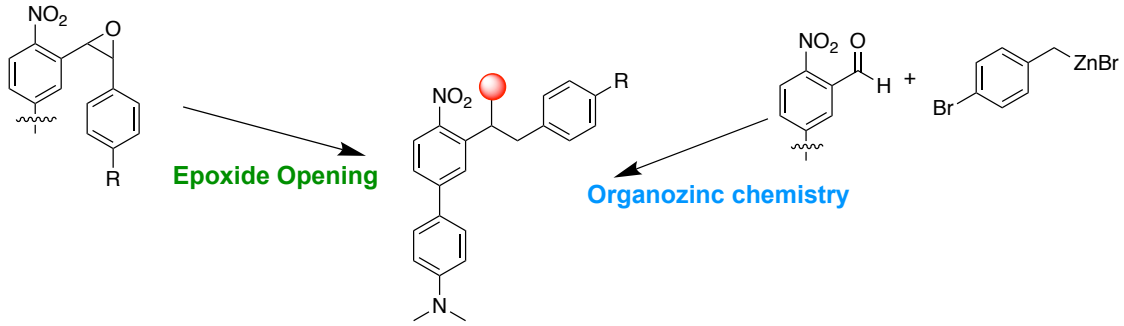

Scheme VII.2: The proposed strategies to access *o*-nitrobenzyl photoremovable protecting groups.

A 1,2- addition of bromoaryl organozinc halides to dimethylamino-nitrobiphenyl carbaldehyde followed by Miyaura–Suzuki cross coupling reactions was used in order to synthesize biphenyl

substituted *o*-nitrobenzyl (*o*-NB) photoremovable groups. Interestingly each synthesized *o*-NB PPG shows a very weak fluorescence signal before irradiation. To be able to quantify the photorelease of carboxylic acid functions a chromophoric 3,4-dimethoxyphenylacetic acid (MPAA) was coupled to our *o*-NB PPGs. Except for the *p*-nitrobiphenyl derivative, an almost quantitative (≥93%) release of MPAA was measured by HPLC after complete photo-conversion for each photolytic precursor of MPAA. More interestingly, all these compounds showed an interesting fluorescence signal increase induced by the photolytic reaction. In particular, the *p*-methoxy biphenyl derivative showed 200 times increase in the green (λ = 526 nm) emission intensity after full photocleavage.

Therefore, a water-soluble version of this compound has been successfully synthesized and used for in vitro cell imaging and real time monitoring of the uncaging event. These experiments showed an increase in the fluorescence of the cells upon each irradiation time due to the accumulation of the by-product inside the cytoplasm. We were able to synthesize and report the first *o*-nitrobenzyl photoremovable protecting group that is capable of releasing a fluorescent by-product that serves as an optical reporter of the uncaging event. The only disadvantage of these newly developed PPGs is the long irradiation times needed to accomplish full cleavage, these irradiation times (in the order of minutes) is no compatible with the release of biological effectors. Therefore, we aimed to develop a new, thiophene-based, PPG system that was previously tested in the lab (non-fluorescent version) and was found to be highly sensitive to light.

The architecture of the new system is based on 2 nitrophenyl ethylene moieties linked by a thiophene core. This PPG has shown an interesting sensitivity to light translated by short irradiation times (order of seconds). This property led us to use the same synthetic strategy applied to the newly developed *o*-NB on this thiophene-based PPG. By reacting the bis-nitrophenyl aldehyde with bromobenzyl zinc bromide, we succeeded to obtain di-substituted *o*-NB compound that was later coupled to MPAA. This latter showed interesting fluorescent properties; as we irradiated the compound we observed a significant increase of the fluorescent intensity due to the formation of a conjugated system.

This compound is expected to show interesting results for the release of biological effectors, that's why we tried to synthesize a soluble version by attaching PEG chains via Suzuki or sonogashira couplings. Unfortunately, both cross-coupling reactions didn't work which could be due to the steric hindrance of the PPG.

2. Perspectives

Our future studies will focus on the use of more efficient visible light sensitive photoremovable groups in the *o*-NB series (BNPET) in order to follow the uncaging events simultaneously by fluorescence analysis and with a physiological event (for example induced by the photorelease of a neurotransmitter).

The solubility of the BNPET PPG needs to be enhanced in order to use it in biological applications. This could be achieved by adding solubilizing groups like PEG chains or sugar derivatives. The coupling of the PEG chains should be optimized, for example, by replacing the bromobenzyl zinc bromide by iodobenzyl zinc iodide since iodo derivatives are known to be more reactive towards metal cross-coupling reactions compared to the bromo derivatives.

Once the soluble version of the BNPET PPG is obtained, the molecule will be tested in biological media mainly on neurons. The BNPET will be used to cage neurotransmitters (excitatory: glutamate and inhibitory: GABA), and its activity will be tested, and the uncaging event will be followed by biological response and by fluorescent signal (Scheme VII.3).

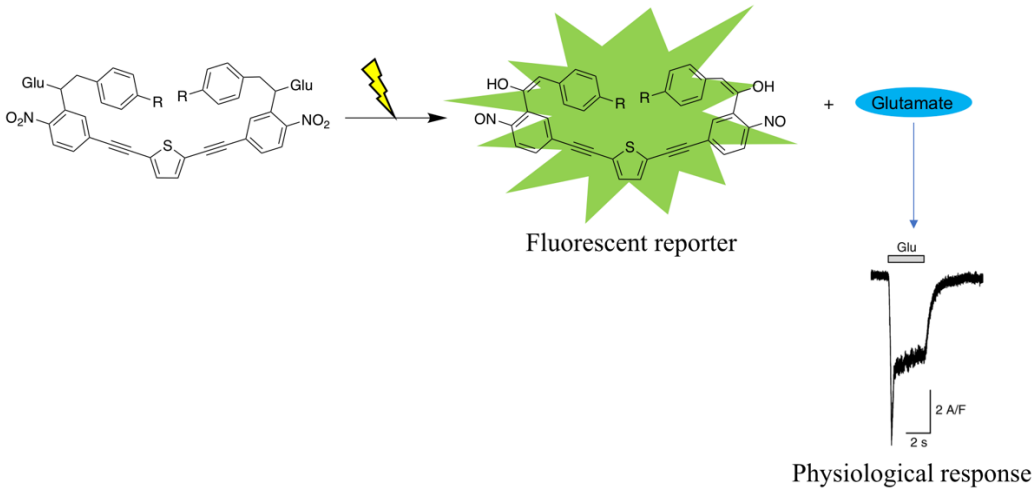

Scheme VII.3: Photorelease of glutamates from a pro-fluorescent BNPET photoremovable group.

CHAPTER VIII

Experimental Part
and
Bibliographic References

1. Experimental Part

1.1. Materials and Methods

NMR Spectroscopy.

The NMR spectra of proton (^{1}H) and carbon-13 (^{13}C) of all compounds were realized on NMR spectrometers 400 et 500 MHz Brucker® in the Faculty of Pharmacy. The chemical shifts (δ) are indicated in ppm with respect to an internal reference corresponding to the references of deuterated solvents ($CDCl_3$: 7.26 ppm, CD_3OD: 3.31 ppm, CD_3CN: 1.94 ppm, $(CD_3)_2CO$: 2.05 ppm in ^{1}H-NMR and $CDCl_3$: 77.16 ppm, CD_3OD: 49.00 ppm, CD_3CN: 1.31 et 118.26 ppm, $(CD_3)_2CO$: 29.84 et 206.26 ppm in ^{13}C-NMR). The attributions are given in the following manner: chemical shift followed in bracket: Multiplicity of the signal (s, d, t, q, m, dd, et dq corresponding respectively to singlet, doublet, triplet, quadruplet, multiplet, double doublet and double quadruplet), Coupling constant in Hz, and Number of protons.

Mass Spectrometry.

The LCMS analysis were realized using an Agilent 1200 SL/QTof 6520 spectrometer coupled to a Hypersil Gold C18 column with 1.9 µm particles size and 1x30 mm dimensions and the ESI mass spectra were realized using an Agilent 1200 SL spectrometer MicroTOF (Bruker®) equipped with an electrospray source.

UV-Visible absorption and emission spectroscopy.

UV-visible absorption spectra were measured using a double beam spectrophotometer UVIKON XS. The fluorescence emission spectra were obtained using a spectrofluorometer fluoroMax from Horiba-Jobin Yvon. Fluorescence quantum yields were measured by the relative method, using quinine sulfate as reference. The absorbance of the samples and the reference were chosen so that they were in the 0.1-0.15 range and nearly identical at the same excitation wavelength. Emission quantum yields were then calculated according to the method described by Crosby and Demas, taking into account the differences between the refractive indices of the sample and reference solutions.

Micro-wave.

The pallado-catalysed reactions were done using an Anton Paar Monowave 300.

Chromatography.

Thin Layer Chromatography (TLC) were realized using plates covered with silica gel 60 F254 Merck. Column chromatography were done on silica gel 60 (230-400 mesh, 0,040-0,063 mm) Merck.

High Performance Liquid Chromatography (HPLC).

HPLC analysis were realized over a series of high performance chromatography Waters® (Waters 600 double body pumps with diode detector Dionex UVD340V or Waters 1525 pump with Waters 2996 detector) equipped with Phenomenex C18 PolarRP 4-micron (4.6, 250 mm) analytical columns, Thermo Betabasic 5-micron (4.6, 250 mm) analytical columns, Agilent Zorbax SB-C18 5-microns (4.6, 250 mm) columns or Kromasil 100-5C18 (4.6, 250 mm) columns. The analysis were done using a gradient starting from 100% mQ H2O acidified with 0.01% of TFA and reaching 100% of acetonitrile in 30 min. HPLC purifications were realized over a series of high performance chromatography Waters® (Waters 600 double body pumps with diode detector Dionex UVD340V equipped with a semi-preparative Phenomenex C18 PolarRP 10-micron (10, 250 mm) column, Thermo Betabasic 5-micron (10, 250 mm) column, ou Kromasil 100-5C18 (10, 250 mm) column. These purifications were done using an isocratic solvent elution.

Solvents et reagents.

The reagents and anhydrous solvents used for the synthesis were ordered at Sigma-Aldrich, Alfa Aesar, TCI EUROPE or Acros Organics. All commercial reagents were used for the synthesis without any further purification. The tetrahydrofuran used in the reactions was freshly distilled using sodium metal and benzophenone.

Irradiation procedure.

The same irradiation procedure was followed for the irradiations of **49**,**50a-c** and **55**: A 2 mL solution of **49** (135 µM), **50a** (100 µM), **50b** (75 µM), **50c** (60 µM) and **55** (40 µM) in 10 mM pH 7.4 phosphate buffer/acetonitrile (1:1 v:v) was exposed to a LUMOS 43 LED source (Atlas Photonics Inc.) at 405 nm (Typical optical output: 200 mW/cm^2). The reaction was monitored by UV and aliquots of samples (100 µL) were analyzed by HPLC to determine the percentage of released (3,4-dimethoxyphenyl) acetic acid (MPAA) using a calibration curve.

UV-Visible monitoring of photolysis.

The irradiations were monitored by UV spectroscopy by measuring the absorbance at each irradiation time using a using a double beam spectrophotometer UVIKON XS with acetonitrile as a blank between 250 and 750 nm.

FTIR study of the photolysis.

A sample of compound 7b was prepared in acetonitrile (C = 267 µM). The solution was irradiated using the LUMOS 43 LED source (Atlas Photonics Inc.) at 405 nm (Typical optical output: 200 mW/cm^2) for 40 minutes. The infrared spectra of the starting material and the photolysis products were recorded on a brucker FT-IR ALPHA.

NMR protocol for the study of the photolytical reaction.

Two samples of compound **49** were prepared in deuterated acetonitrile (CD_3CN) with respective concentrations of 267 µM and 405 µM. The samples were irradiated at 405 nm for 90 minutes and 150 minutes respectively and their respective NMR spectra were recorded immediately. The acquisitions for the NMR spectra were recorded on a 500 MHz Bruker Avance II and ^1H NMR spectra were recorded at 500 and 130 MHz. This spectrometer is equipped with a dual cryoprobe $^1H/^{13}C$ (5 mm cryoprobe double resonance probe fixed frequency DCH $^{13}C/^1H/D$ z-grad).

Fluorescence on cells.

Studies on cell culture were performed on HeLa cells. HeLa cells were cultured in DMEM complete culture medium containing phenol red at 37°C with 5% CO_2. They were seeded and maintained in 25 mL Falcon culture flask or multi well LabTek (Lab-Tek® II) culture flasks. The imaging experiments were performed in IBIDI 60 µ-Dish. Confocal images were obtained on a Leica DMI4000B TSP SPE microscope. Photolysis was performed on the same microscope stand with using a Leica EL6000 light source with a DAPI filter cube (ex. 340- 380 nm, dicroïc 400 nm, em. LP 425 nm) in epifluorescence mode.

1.2. Synthesis

For any additional information on the synthesis of the molecules mentioned in this dissertation and all the analysis data and characterization of the compounds, please contact the author:

Elie Abou Nakad : elieabounakad@hotmail.com

Alexandre Specht : specht@unistra.fr

2. Bibliographic References

- Abe, M., Chitose, Y., Jakkampudi, S., Thuy, P. T. T., Lin, Q., Van, B. T., Yamada, A., Oyama, R., Sasaki, M., Katan, C., *Synthesis*, **2017**, 49, 3337.
- Adam, W., *Tetrahedron Lett.*, **1995**, *36*, 3669.
- Agarwal, H. K., Janicek, R., Chi, S-H., Perry, J. W., Niggli, E., Ellis-Davies, G. C. R., *J. Am. Chem.* Soc., **2016**, 138, 3687.
- Albini, A., Fagnoni, M., Wiley: Weinheim, Germany, **2010**; Chapter 13, p 417.
- Albota, M., Beljonne, D., Brødas, J.-L., Ehrlich, J. E., Fu, J.-Y., Heikal, A. A., Hess, S. E., Kogej, T., Levin, M. D., Marder, S. R., McCord-Maughon, D., Perry, J. W., Röckel, H., Rumi, M., Subramaniam, G., Webb, W. W., Wu, X.-L., Xu, C., *Science*, **1998**, 281, 1653.
- Alexakis, A., Vrancken, E., Mangeney, P., *Synlett*, **1998**, 10, 1165.
- Amit, B., Ben-Efraim, D. A., Patchornik, A., *J. Am. Chem. Soc.,* **1976**, 98, 843.
- Andrade, C. D., Yanez, C. O., Rodriguez, L., Belfield, K. D., *J. Org. Chem.,* **2010**, 75, 3975–3982.
- Andrejevic, V., Bjelakovid, M., Mihailovie, M. M., Mihailovtf, M. L., *Helv. Chim. Acta.,* **1985**, 68, 2030.
- Anømian, R., Morel, Y., Baldeck, P. L., Paci, B., Kretsch, K., Nunzi, J.-M., Andraud, C., *J. Mater. Chem.,* **2003**, 13, 2157.
- Auernheimer, J., Dahmen, C., Hersel, U., Bausch, A., Kessler, H., *J. Am. Chem. Soc.*, **2005**, 127, 16107.
- Aujard, I., Benbrahim, C., Gouget, M., Ruel, O., Baudin, J.-B., Neveu, P., Jullien, L., *Chem. Eur. J.,* **2006**, 12, 6865.
- Babič, A., Sova, M., Gobec, S., Pečar, S., *Tetrahedron Lett.,* **2006**, 47, 1733.
- Baldwin, J. E., McConnaughie, A. W., Moloney, M. G., Pratt, A. J., Shim, S. B., *Tetrahedron,* **1990**, 46, 6879.
- Barltrop, J. A., Plant, P. J., Schofield, P. J., *Chem. Soc. Chem. Commun.,* **1966**, 22, 822.
- Barltrop, J. A., Schofield, P., *Tetrahedron Lett.,* **1962**, 16, 697.
- Bartoli, G., Bosco, M., Dalpozzo, R., *Tetrahedron Lett.,* **1985**, 26, 115.
- Barton, D. H. R., Chow, Y. L., Cox, A., Kirby, G. W., *J. Chem. Soc.,* **1965**, 3571.
- Barton, D. H. R., Chow, Y. L., Cox, A., Kirby, G. W., *Tetrahedron Lett.,* **1962**, 23, 1055.
- Becker, A., Hessenius, C., Licha, K., Ebert, B., Sukowski, U., Semmler,W., Wiedenmann, B., Grotzinger, C., *Nat. Biotechnol.*, **2001**, 19, 327.
- Becker, Y., Unger, E., Fichte, M. A. H., Gacek, D. A., Dreuw, A., Wachtveitl, J., Walla, P. J., Heckel, A., *Chem. Sci.,* **2018**, 9, 2797.

- Belfield, K. D., Bondar, M. V., Liu, Y., Przhonska, O. V., *J. Phys. Org. Chem.,* **2003**, 16, 69.
- Belfield, K. D., Schafer, K. J., *Chem. Mater.* **2002**, 14, 3656.
- Belfield, K. D., *Spectrum,* **2001**, Spring, 1.
- Berhal, F., Tardy, S., Pérard-Viret, J., Royer, J., *Eur. J. Org. Chem.,* **2009**, 3, 437.
- Beverina, L., Fu, J., Leclercq, A., Zojer, E., Pacher, P., Barlow, S., Van Stryland, E. W., Hagan, D. J., Brédas, J-L., Marder, S. R., *J. Am. Chem. Soc.,* **2005**, 127, 7282–7283.
- Bochet, C. G., Blanc, A., Photolabile Protecting Groups in Organic Synthesis. *In Handbook of Synthetic Photochemistry.*
- Bochet, C. G., *J. Chem. Soc., Perkin Trans. 1*, **2002**, 2, 125.
- Brieke, C., Rohrbach, F., Gottschalk, A., Mayer, G., Heckel, A., *Angew. Chem., Int. Ed.,* **2012**, 51, 8446.
- Bühler, S., I. Lagoja, H. Giegrich, K-L. Stengele, W. Pfleiderer, *Helvetica Chimica Acta.,* **2004**, 87, 620.
- Bui, A. T., Grichine, A., Duperray, A., Lidon, P., Riobé, F., Andraud, C., Maury, O., *J. Am. Chem. Soc.,* **2017**, 139, 7693.
- Cabrera, R., Filevich, O., Garcìa-Acosta, B., Athilingam, J., K. Bender, J., Poskanzer, K. E., Etchenique, R., *ACS Chem. Neurosci.,* **2017**, 8, 1036.
- Callaway, E. M., Yuste, R., *Current Opinion in Neurobiology*, **2002**, 12, 587.
- Canepari, M., Nelson, L., Papageorgiou, G., Corrie, J. E. T., Ogden, D., *J. Neurosci. Methods*, **2001**, 112, 29.
- Casey, K. G., Quitevis, E. L., *J. Phys. Chem.,* **1988**, 92, 6590.
- Chaudhuri, A., Venkatesh, Y., Behara, K. K., Singh, N. D. P., *Org. Lett.,* **2017**, 19, 1598.
- Cheng, L. T., Tam, W., Stevenson, S. H., Meredith, G. R., Rikken, G., Marder, S. R., *J. Phys. Chem.,* **1991**, 95, 10631.
- Chinchilla, R., Nájera, C., *Chem. Rev*., **2007**, 107, 874.
- Cho, B. R., Son, K. H., Lee, S. H., Song, Y.-S., Lee, Y.-K., Jeon, S.-J., Choi, J. H., Lee, H., Cho, M., *J. Am. Chem. Soc.,* **2001**, 123, 10039.
- Ciamician, G., Silber, P., *Chem. Ber.* **1901**, 34, 2040.
- Ciesienski, K. L., Franz, K. J., *Angew. Chem., Int. Ed.,* **2011**, 50, 814.
- Corey, E. J., Seebach, D., *Angew. Chem. Int. Ed.,* **1965**, 4, 1075.
- Corey, E. J., Seebach, D., *Angew. Chem.,* **1965**, 77, 1134.
- Corredor, C. C., Belfield, K. D., Bondar, M. V., Przhonska, O. V., Hernandez, F. E., Kachkovsky, O. D., *J. Photochem. Photobiol.,* A **2006**, 184, 177.
- Coutant, E. P., Janin, Y. L., *Synthesis*, **2015**, 47, 511.
- Crespy, D., Landfester, K., Schubert, U. S., Schiller, A., *Chem. Commun.,* **2010**, 46, 6651.

- Croix, C. M. S., Leelavanichkul, K., Watkins, S. C., *Adv. Drug Delivery Rev.,* **2006**, 58, 834.
- Cumpston, B. H., Ananthavel, S. P., Barlow, S., Dyer, D. L., Ehrlich, J. E., Erskine, L. L., Heikal, A. A., Kuebler, S. M., Lee, I. Y. S., McCord-Maughon, D., Qin, J. Q., Rockel, H., Rumi, M., Wu, X. L., Marder, S. R., Perry, J. W., *Nature,* **1999**, 398, 51.
- Curley, K., Lawrence, D. S., *Pharmacol. Ther.* **1999**, 82, 347.
- Dakin, K., Li, W. H., *Nat. Methods*, **2006**, 3, 959.
- Dalier, F., Eghiaian, F., Scheuring, S., Marie, E., Tribet, C., *Biomacromolecules,* **2016**, 17, 1727.
- Das, A. T., Tenenbaum, L., Berkhout, B., *Curr. Gene. Ther.,* **2016**, 16, 156- 167.
- Davies, S. G., Wollowltz, S., *Tetrahedron Lett.,* **1980**, 71, 4175.
- Davis, M. J., Kragor, C. H., Reddie, K. G., Wilson, H. C., Dore, Y. T. M., *J. Org. Chem.,* **2009**, 74, 1721.
- Deiters, A., *Curr. Opin. Chem. Biol.*, **2009**, 13, 678.
- Denk, W., Piston, D. W., Webb, W. W., Two-Photon Molecular Excitation in Laser-Scanning Microscopy. *In Handbook of Biological Confocal Microscopy*; J. B. Pawley, Ed.; *Plenum Press: New York,* **1995**.
- Donato, L., Mourot, A., Davenport, C. M., Herbivo, C., Warther, D., Léonard, J., Bolze, F., Nicoud, J.-F., Kramer, R. H., Goeldner, M., Specht, A., *Angew. Chem. Int. Ed.,* **2012**, 51, 1840.
- Dorman, G., Prestwich, G. D., *Trends Biotechnol.*, **2000**, 18, 64.
- Dougherty, T. J., *Adv. Photochem.* **1992**, 17, 275.
- Durham, B., Caspar, J. V., Nagle, J. K., Meyer, T. J., *J. Am. Chem. Soc.,* **1982**, 104, 4803.
- Dutta, P., Saikia, M., Jyoti Das, R., Borah, R., *J. Chem. Sci.,* **2014**, 126, 1629.
- Dvornikov, A. S., Bouas-Laurent, H., Desvergne, J. P., Rentzepis, P. M., *J. Mater. Chem.,* **1999**, 9, 1081.
- Eliel, E. L., Delmonte, D. W., *J. Am. Chem. Soc.,* **1956**, 78, 3226.
- Eliel, E. L., Delmonte, D. W., *J. Am. Chem. Soc.*, **1958**, 80, 1744.
- Ellis-Davies, G. C. R., *Chem. Rev.*, **2008**, 108, 1603.
- Ellis-Davies, G. C. R., Kaplan, J. H., *Proc. Natl. Acad. Sci.,* USA, 91, **1994**, 187
- Ellis-Davies, G. C. R., Matzusaki, M., Paukert, M., Kasai, H., Bergles, D. E., *J. Neurosci.,* **2007**, 27, 6601.
- Ellis-Davies, G. C. R., *Nat. Methods,* **2007**, 4, 619.
- Esengil, H., Chang, V., Mich, J. K., Chen, J. K., *Nat. Chem. Biol.* **2007**, 3, 154.
- Falvey, D. E., Sundararajan, C., *Photochem. Photobiol. Sci.,* **2004**, 3, 831.
- Fehrentz, T., Schonberger, M., Trauner, D., *Angew. Chem., Int. Ed.*, **2011**, 50, 12156.

- Fichte, M. A. H., Weyel, X. M. M., Junek, S., Schäfer, F., Herbivo, C., Goeldner, M., Specht, A., Wachtveitl, J., Heckel, A., *Angew. Chem., Int. Ed.,* **2016**, 55, 8948.
- Florio, S., Perna, F. M., Salomone, A., Vitale, P., Reduction of Epoxides in *Comprehensive Organic Synthesis II*, **2014**, 8, 1086.
- Fournier, L., Aujard, I., Le Saux, T., Maurin, S., Beaupierre, S., Baudin, J-B., Jullien, L., *Chem. Eur. J.,* **2013**, 19, 17494.
- Fukaminato, T. J., *Photochem. Photobiol.,* **2011**, 12, 177.
- Furuta, T., Iwamura, M., *Methods Enzymol.,* **1998**, 291, 50.
- Furuta, T., Wang, S. S.-H., Dantzker, J. L., Dore, T. M., Bybee, W. J., Callaway, E. M., Denk, W., Tsien, R. Y., *Proc. Natl. Acad. Sci.* USA **1999**, 96, 1193.
- Gagey, N., Neveu, P., Benbrahim, C., Goetz, B., Aujard, I., Baudin, J.-B., Jullien, L., *J. Am. Chem. Soc.,* **2007**, 129, 9986.
- Gautier, A., Gauron, C., Volovitch, M., Bensimon, D., Jullien, L., Vriz, S., *Nat. Chem. Biol.,* **2014**, 10, 533.
- Gilbert, D., Funk, K., Dekowski, B., Lechler, R., Keller, S., Moehrlen, F., Frings, S., Hagen, V., *Chem. Bio. Chem.,* **2007**, 8, 89.
- Giovannardi, S., Lando, L., Peres, A., *News Physiol. Sci.*, **1998**, 13, 251.
- Givens, R. S., Matuszewski, B., *J. Am. Chem. Soc.,* **1984**, 106, 6860.
- Givens, R. S., Rubina, M., Wirz, J., *Photochem. Photobiol. Sci.*, **2012**, 11, 472.
- Goegan, B., Terzi, F., Bolze, F., Cambridge, S., Specht, A., *ChemBioChem.,* **2018**, 19, 1341.
- Goeldner, M., Givens, R. S., *Dynamic Studies in Biology;* Wiley- VCH: Weinheim, Germany, **2006**.
- Göppert-Mayer, M., *Ann. Phys.*, **1931**, 9, 273.
- Gorostiza, P., Isacoff, E., *Mol. Biosyst.*, **2007**, 3, 686.
- Gossen, M., Bujard, H., *Proc. Natl. Acad. Sci.*, USA **1992**, 89, 5547 – 5551
- Gossen, M., Freundlieb, S., Bender, G., Müller, G., Hillen, W., Bujard, H., *Science*, **1995**, 268, 1766 – 1769.
- Gug, S., Bolze, F., Specht, A., Bourgogne, C., Goeldner, M., Nicoud, J-F., *Angew. Chem.,* **2008**, 120, 9667.
- He, G. S., Tan, L.-S., Zheng, Q., Prasad, P. N., *Chem. Rev.*, **2008**, 108, 1245 – 1330.
- Heller, C. A., Henry, R. A., McLaughlin, B. A., Bliss, D. E., *J. Chem. Eng. Data.,* **1974**, 19, 214.
- Hemminki, K., Paasivirta, J., Kurkirinne, T., Virkki, L., *Chem.-Biol. Interactions,* **1980**, 30, 259.
- Herbivo, C., Omran, Z., Revol, J., Javot, H., Specht, A., *ChemBioChem.,* **2013**, 14, 2277.

- Herrmann, A., *Angew. Chem., Int. Ed.,* **2007**, 46, 5836.
- Herrmann, A., *Photochem. Photobiol. Sci.*, **2012**, 11, 446.
- Hikage, S., Nishiyama, Y., Sasaki, Y., Tanimoto, H., Morimoto, T., Kakiuchi, K., *ACS Omega*, **2017**, 2, 2300
- Hirohashi, S., Kanai, Y., *Cancer Sci.,* **2003**, 94, 575.
- Hoffmann, N., *Chem. Rev.*, **2008**, 108, 1052.
- Huang, S., Ingber, D. E., *Nat. Cell Biol.,* **1999**, 1, E131.
- Huynh, C., Derguini-Boumechal, F., Linstrumelle, G., *Tetrahedron Lett.,* **1979**, 17, 1503.
- Imogaï, H. Larchevêque, M., *Tetrahedron: Asymmetry,* **1997**, 8, 965.
- Jenei, A., Kirsch, A. K., Subramaniam, V., Arndt-Jovin, D. J., Jovin, T. M., *Biophys. J.*, **1999**, 76, 1092.
- Jung, T. S., Kim, J. H., Jang, E. K., Kim, D. H., Shim, Y.-B., Park, B., Shin, S. C., *J. Organomet. Chem.,* **2000**, 599, 232.
- Juzenas, P., Juzeniene, A., Kaalhus, O., Iani, V., Moan, J., *Photochem. Photobiol. Sci. Off. J. Eur. Photochem. Assoc. Eur. Soc. Photobiol.,* **2002**, 1, 745.
- Kalbag, S.M., Roeseke, R.W., *J. Am. Chem. Soc.,* **1975**, 97, 440.
- Katz, J. S., Burdick, J. A., *Macromol. Biosci.,* **2010**, 10, 339.
- Kauffman, J. F., Turner, J. M., Alabugin, I. V., Breiner, B., Kovalenko, S. V., Badaeva, E. A., Masunov, A., Tretiak, S., *J. Phys. Chem.,* **2006**, 110, 241.
- Kawata, S., Sun, H. B., *J. Photopolym. Sci. Technol.*, **2002**, 15, 471.
- Kawata, S., Sun, H. B., Tanaka, T., Takada, K., *Nature,* **2001**, 412, 697.
- Kerry, C. J., Ramsey, R. L., Sansom, M. S. P., Usherwood, P. N. R., *Biophys. J.,* **1988**, 53, 39.
- Khalili, A. A., Ahmad, M. R., *Int. J. Mol. Sci.,* **2015**, 16, 18149.
- Kielar, F., Congreve, A., Law, G. L., New, E. J., Parker, D., Wong, K. L., Castreno, P., de Mendoza, J., *Chem. Comm.,* **2008**, 21, 2435.
- Kienzle, F., *Helvetica Chimica Acta.,* **1978**, 61, 449.
- Kim, H. C., Kreiling, S., Greiner, A., Hampp, N., *Chem. Phys. Lett.,* **2003**, 372, 899.
- Kim, H. M., Cho, B. R., *Chem. Commun.*, **2009**, 153 – 164.
- Kim, H. M., Kim, B. R., Hong, J. H., Park, J. S., Lee, K. J., Cho, B. R., *Angew. Chem., Int. Ed.*, **2007**, 46, 7445.
- Klàn, P., Solomek, T., Bochet, C. G., Blanc, A., Givens, R., Rubina, M., Popik, V., Kostikov, A., Wirz, J., *Chem. Rev.,* **2013**, 113, 119.
- König, K. J., *Microsc.* (Oxford, U.K.) **2000**, 200, 83.

- Kosower, N. S., Kosower, E. M., Newton, G. L., Ranney, H. M., *Proc. Natl. Acad. Sci.,* U. S. A. **1979**, 76, 3382.
- Kramer, R. H., Chambers, J. J., Trauner, D., *Nature Chem. Biol.,* **2005**, 1, 360.
- Kramer, R. H., Mourot, A., Adesnik, H., *Nat. Neurosci.,* **2013**, 16, 816.
- Krauss, U., Drepper, T., Jaeger, K.-E., *Chem. Eur. J.,* **2011**, 17, 2552.
- Kubin, R. F., Fletcher, A. N., *J. Luminescence,* **1982**, 27, 455.
La Regina, G., Bai, R., Coluccia, A., Famiglini, V., Pelliccia, S., Passacantilli, S., Mazzoccoli, C., Ruggieri, V., Verrico, A., Miele, A., Monti, L., Nalli, M., Alfonsi, R., Di Marcotullio, L., Gulino, A., Ricci, B., Soriani, A., Santoni, A., Caraglia, M., Porto, S., Da Pozzo, E., Martini, C., Brancale, A., Marinelli, L., Novellino, E., Vultaggio, S., Varasi, M., Mercurio, C., Bigogno, C., Dondio, G., Hamel, E., Lavia, P., Silvestri, R., *J. Med. Chem.,* **2015**, 58, 5789.
- Lakowicz, J. R., Two-Photon and Non-Linear Induced Fluorescence; *Plenum Press: New York,* **1991**.
- Lawrence, D. S., *Curr. Opin. Chem. Biol.*, **2005**, 9, 570.
- Lee, H.-M., Larson, D. R., Lawrence, D. S., *ACS Chem. Biol.*, **2009**, 4, 409.
- Lee, J. C., Bae, Y. H., Chang, S-K., *Bull. Korean Chem. Soc.,* **2003**, 24, 408.
- Lerch, M. M., Hansen, M. J., Van Dam, G. M., Szymanski, W., Feringa, B. L., *Angew. Chem., Int. Ed.,* **2016**, 55, 10978.
- Li, J., Joeng, S., Esser, L., Harran, P. G., *Angew. Chem. Int. Ed.,* **2001**, 40, 4765.
- Li, W.-H., Zheng, G., *Photochem. Photobiol. Sci.*, **2012**, 11, 460.
- Lin, C. -C., Anseth, K. S., *Pharm. Res.* **2009**, 26, 631.
- Lin, Q., Bao, C., Cheng, S., Yang, Y., Ji, W., Zhu, L., *J. Am. Chem. Soc.*, **2012**, 134, 5052.
- Lin, Q., Yang, L., Wang, Z., Hua, Y., Zhang, D., Bao, B., Bao, C., Gong, X., Zhu, L., *Angew. Chem., Int. Ed.,* **2018**, 57, 3722.
- Lincker, F., Masson, P., Didier, P., Guidoni, L., Bigot, J.-Y., Nicoud, J.-F., *J. Nonlinear Opt. Phys. Mater.,* **2005**, 14, 319.
- Lovell, J. F., Liu, T. W. B., Chen, J., Zheng, G., *Chem. Rev.,* **2010**, 110, 2839.
- Lu, Y., Suzuki, T., Zhang, W., Moore, J. S., Mariñas, B. J., *Chemistry of Materials,* **2007**, 19, 3194.
- Maciejewski A., Steer, R.P., *Chem. Rev.,* **1993** 93, 67−98.
- Maier, W., Corrie, J. E. T., Papageorgiou, G., Laube, B., Grewer, C., *J. Neurosci. Methods,* **2005**, 142, 1.
- Makosza, M., *Chem. Soc. Rev.,* **2010**, 39, 2855.
- Makosza, M., Winiarski, J., *Acc. Chem. Res.,* **1987**, 20, 282.
- Manzano, V. E., Uhrig, M. L., Varela, O., *J. Org. Chem.*, **2008**, 73, 7224.

- Marshall, J. M., Andersen, M. W., *J. Org. Chem.*, **1992**, 57, 5851.
- Matsuzaki, M., Ellis-Davies, G. C. R., Nemoto, T., Miyashita, Y., Iino, M., Kasai, H., *Nat Neurosci.* **2001**, 11, 1086.
- Mayer, G., Heckel, A., *Angew. Chem., Int. Ed.,* **2006**, 45, 4900.
- Meldrum, B. S., *J. Nutr.,* **2000**, 130, 1007.
- Mews, A., Jachiet, D., Normant, J. F., *Tetrahedron*, **1986**, 42, 5601.
- Mignani, G., Leising, F., Meyrueix, R., Samson, H., *Tetrahedron Lett.,* **1990**, 31, 4743.
- Milbradt, A. G., Loweneck, M., Krupka, S. S., Reif, M., Sinner, E. K., Moroder, L., Renner, C., *Biopolymers*, **2005**, 77, 304.
- Miyaura, N., Suzuki, A., *Chem. Rev.,* **1995**, 95.
- Mongin, O., Porrès, L., Charlot, M., Katan, C., Blanchard-Desce, M., *Chem. Eur. J.*, **2007**, 13, 1481 – 1498.
- Montoya, L. A., Shen, X., McDermott, J. J., Kevil, C. G., Pluth, M. D., *Chem. Sci.,* **2015**, 6, 294.
- Nadler, A., Yushchenko, A. D. A., Müller, R., Stein, F., Feng, S., Muller, C., Carta, M., Schultz, C., *Nat. Commun.,* **2015**, 6, 1.
- Nakanishi, J., Kikuchi, Y., Inoue, S., Yamaguchi, K., Takarada, T., Maeda, M., *J. Am. Chem. Soc.,* **2007**, 129, 6694.
- Oguni, N., Miyagi, Y., Itoh, K., *Tetrahedron Lett.,* **1998**, 39, 9023.
- Okano, T., Yamada, M., Okuhara, M., Sakai, H., Sakurai, Y., *Biomaterials,* **1995**, 16, 297.
- Okegawa, T., Pong, R. C., Li, Y., Hsieh, J. T., *Acta Biochim. Pol.,* **2004**, 51, 445.
- Olson, J. P., Kwon, H. B., Takasaki, K. T., Chiu, C. Q., Higley, M. J., Sabatini, B. L., Ellis-Davies, G. C. R., *J. Am. Chem. Soc.,* **2013**, 135, 5954.
- Ooi, T., Morikawa, J., Ichikawa, H., Maruoka, K., *Tetrahedron Lett*., **1999**, 40, 5881.
- Palma-Cerda, F., Auger, C., Crawford, D. J., Hodgson, A. C., Reynolds, S. J., Cowell, J. K., Swift, K. A., Cais, O., Vyklicky, L., Corrie, J. E., Ogden, D., *Neuropharmacology*, **2012**, 63, 624.
- Pan, J., Zhang, M., Zhang, S., *Org. Biomol. Chem.,* **2012**, 10, 1060.
- Papageorgiou, G., Ogden, D. C., Barth, A., Corrie, J. E. T., *J. Am. Chem. Soc.,* **1999**, 121, 6503.
- Pardo, A., Reyman, D., Martin, D., Poyato, J. M. L., Camacho, J. J., Hidalgo, J., Sanchez, M., *J. Lumin.,* **1988**, 42, 163.
- Parker, R. E., Isaacs, N. S., *Chem. Rev.,* **1959**, 59, 737.
- Patchornik, A., Amit, B., Woodward, R. B., *J. Am. Chem. Soc.,* **1970**, 92, 6333.
- Patchornik, A., Amit, B., Woodward, R. B., *J. Am. Chem. Soc.,* **1970**, 64, 5042.

- Paul, A., Mengji, R., Chandy, O. A., Nandi, S., Bera, M., Jana, A., Anoop, A., Pradeep Singh, N. D., *Org. Biomol. Chem.,* **2017**, 15, 8544.
- Pawlicki, M., Collins, H. A., Denning, R. G., Anderson, H. L., *Angew. Chem., Int. Ed.,* **2009**, 48, 3244.
- Pelliccioli, A. P., Wirz, J., *Photochem. Photobiol. Sci.,* **2002**, 1, 441.
- Petersen, S., Alonso, J. M., Specht, A., Duodu, P., Goeldner, M., del Campo, A., *Angew. Chem., Int. Ed.,* **2008**, 47, 3192.
- Peterson, J. A., Wijesooriya, C., Gehrmann, E. J., Mahoney, K. M., Goswami, P. P., Albright, T. R., Syed, A., Dutton, A. S., Smith, E. A., Winter, A. H., *J. Am. Chem. Soc.*, **2018**, 140, 7343.
- Phillips, D. J., Graham, A. E., *Synlett*, **2010**, 5, 769.
- Piant, S., Bolze, F., Specht, A., *Opt. Mater. Express,* **2016**, 6, 1679.
- Pond, S. J. K., Tsutsumi, O., Rumi, M., Kwon, O., Zojer, E., Bredas, J. L., Marder, S. R., Perry, J. W., *J. Am. Chem. Soc.,* **2004**, 126, 9291.
- Priestman, M. A., Lawrence, D. S., *Biochim. Biophys. Acta*., **2010**, 1804, 547.
- Puliti, D., Warther, D., Orange, C., Specht, A., Goeldner, M., *Bioorg. Med. Chem.,* **2011**, 19, 1023.
- R. M. Szeimies, Calzavara-Pinton, P., Karrer, S., Ortel, B., Landthaler, M. J., *Photochem. Photobiol.,* **1996**, 36, 213.
- Rea, A. C., Vandenberg, L. N., Ball, R. E., Snouffer, A. A., Hudson, A. G., Zhu, Y., McLain, D. E., Johnston, L. L., Lauderdale, J. D., Levin, M., Dore, T. M., *Chem. Biol.,* **2013**, 20, 1536.
- Richers, M. T., Amatrudo, J. M., Olson, J. P., Ellis-Davies, G. C. R., *Angew. Chem., Int. Ed.,* **2017**, 56, 193–197.
- Richner, G., Van Bokhoven, J. A., Neuhold, Y.-M., Makosch, M., Hungerbuhler, K., *Phys. Chem. Chem. Phys.,* **2011**, 13, 12463.
- Ridley, A., Peckham, M., Clark, P., *cell motility: from molecules to organisms,* Wiley **2004**, Chicester, UK.
- Riggsbee, C. W., Deiters, A., *Trends Biotechnol.,* **2010**, 28, 468.
- Rock, R. S., Chan, S. I., *J. Org. Chem.,* **1996**, 61, 1526.
- Rock, R. S., Hansen, K. C., Larsen, R. W., Chan, S. I., *Chem. Phys.,* **2004**, 307, 201.
- Rodriguez, J. G., Esquivias, J., Lafuente, A., Rubio, L., *Tetrahedron,* **2006**, 62, 3112.
- Roy, R. K., Gowd, E. B., Ramakrishnan, S., *Macromolecules*, **2012**, 45, 3063.
- Rubart, M., *Circ. Res.* **2004**, 95, 1154.
- Rubinstein, M., Amit, B., Patchornik, A., *Tet. Let*., **1975**, 17, 1445.
- Rumi, M., Barlow, S., Wang, J., Perry, J. W., Marder, S. R., *Adv. Polym. Sci.,* **2008**, 213, 1 – 95.

- Russell, A. G., Ragoussi, M.-E., Ramalho, R., Wharton, C. W., Carteau, D., Bassani, D. M., Snaith, J. S., *J. Org. Chem.,* **2010**, 75, 4648.
- S. Loudwig, Specht, A., Goeldner, M., *Actual. Chim.,* **2002**, 1, 7.
- Sankaranarayanan, J., Muthukrishnan, S., Gudmundsdottir, A. D., *Adv. Phys. Org. Chem.*, **2009**, 43, 39.
- Schade, B., Hagen, V., Schmidt, R., Herbrich, R., Krause, E., Eckardt, T., Bendig, J., *J. Org. Chem.*, **1999**, 64, 9109.
- Schatzschneider, U., *Eur. J. Inorg. Chem.*, **2010**, 10, 1451.
- Schutt, M., Krupka, S. S., Milbradt, A. G., Deindl, S., Sinner, E. K., Oesterhelt, D., Renner, C., Moroder, L., *Chem. Biol.*, **2003**, 10, 487.
- Seebach, D., Corey, E. J., *J. Org. Chem.,* **1975**, 40, 231.
- Sheehan, J. C., Umezawa, K., *J. Org. Chem.,* **1973**, 38, 3771.
- Sheehan, J. C., Wilson, R. M., *J. Am. Chem. Soc.,* **1964**, 86, 5277.
- Sheehan, J. C., Wilson, R. M., Oxford, A. W., *J. Am. Chem. Soc.*, **1971**, 93, 7222.
- Sheik-Bahae, M., Said, A. A., Wei, T.-H., Hagan, D. J., Van Stryland, E. W., *IEEE J. Quantum Electron.,* **1990,** 26, 760.
- Shembekar, V. R., Chen, Y., Carpenter, B. K., Hess, G. P., *Biochemistry*, **2005**, 44, 7107.
- Shigeri, Y., Tatsu, Y., Yumoto, N., *Pharmacol. Ther.,* **2001**, 91, 85.
- Siamaki, A. R., Khder, A. E. R. S., Abdelsayed, V., El-Shall, M. S., Gupton, B. F., *J. Catal.,* **2011**, 279, 1.
- Siemsen, P., Livingston, R. C., Diederich, F., *Angew. Chem. Int. Ed*., **2000**, 39, 2632.
- Sjulson, L., Miesenböck, G., *Chem. Rev.* **2008**, 108, 1588.
- Smirnova, J., Wöll, D., Pfleiderer, W., Steiner, U., *Helvetica Chimica Acta.,* **2005**, 88, 891.
- Smith, J. G., *Synthesis*, **1984**, 8, 629.
- Snider, B.B., Busuyeck, M.V., *Tet.,* **2001**, 57, 3301.
- Solladié-Cavallo, A., Lupattelli, P., Bonini, C., *J. Org. Chem.,* **2005**, 70, 1605.
- Solladié-Cavallo, A., Lupattelli, P., Marsol, C., Isarno, T., Bonini, C., Caruso, L., Maiorella, A., *Eur. J. Org. Chem.,* **2002**, 8, 1439.
- Solladié-Cavallo, A., Roje, M., Giraud-Roux, M., Chen, Y., Berova, N., Sunjic, V., *Chirality*, **2004**, 16, 196.
- Sonogashira, K., Tohda, Y., Hagihara, N., *Tetrahedron Lett.*, **1975**, 16, 4467.
- Specht, A., Bolze, F., Omran, Z., Nicoud, J.-F., Goeldner, M., *HFSP J.*, **2009**, 3, 255.
- Specht, A., Thomann, J. S., Alarcon, K., Wittayanan, W., Ogden, D., Furuta, T., Kurakawa, Y., Goeldner, M., *ChemBioChem*., **2006**, 7, 1690.
- Speckmeier, E., Klimkait, M., Zeitler, K., *J. Org. Chem.*, **2018**, 83, 3738.

- Steer, R. P., Ramamurthy, V., *Acc. Chem. Res.,* **1988**, 21, 380−386.
- Strehmel, B., Strehmel, V., *Adv. Photochem.*, **2007**, 29, 111.
- Stutz, A., Pitsch, S., *Synlett.,* **1999**, SI, 930.
- Tang, X., Dmochowski, I. J., *Mol. Biosyst.*, **2007**, 3, 100.
- Terenziani, F., Katan, C., Badaeva, E., Tretiak, S., Blanchard-Desce, M., *Adv. Mater.*, **2008**, 20, 4641.
- Tsien, R. W., Lipscombe, D., Madison, D. V., Bley, K. R., Fox, A. P., *TrendsNeurosci.,* **1988**, 10, 431.
- Turner, A. D., Pizzo, S. V., Rozakis, G., Porter, N. A., *J. Am. Chem. Soc*. **1988**, 110, 244 – 250.
- Twarowski, A. J., Kliger, D. S., *Chem. Phys.,* **1977**, 20, 259.
- Uchiyama, M., Kameda, M., Mishima, O., Yokoyama, N., Koike, M., Kondo, Y., Sakamoto, T., *J. Am. Chem. Soc.,* **1998**, 120, 4934-4946.
- Urdabayev, N. K., Popik, V. V., *J. Am. Chem. Soc.,* **2004**, 126, 4058.
- Urlinger, S., Baron, U., Thellmann, M., Hasan, M. T., Bujard, H., Hillen, W., *Proc. Natl. Acad. Sci.*, USA **2000**, 97, 7963 – 7968.
- Volman, D. H., Hammond, G. S., Neckers, D. C., Wiley-VCH: Weinheim, Germany, **1992**; Vol. 17, 275.
- Walbert, S., Pfleiderer, W., Steiner, U. E., *Helvetica Chimica Acta.,* **2001**, 84, 1601.
- Wang, J-X., Jiaa, X., Menga, T., Xina, L., *Synthesis*, **2005**, 17, 2838.
- Wang, X., Chen, X., Yang, Y., *Nat. Methods.* **2012**, 9, 266.
- Warther, D., Gug, S., Specht, A., Bolze, F., Nicoud, J. -F., Mourot, A., Goeldner, M., *Bioorg. Med. Chem.,* **2010**, 18, 7753.
- Weissleder, R., *Nat. Biotechnol.,* **2001**, 19, 316.
- Xiangming, M., Xiaoyun, C., Yao, F., Qingxiang, G., *Progr. Chem.*, **2008**, 20, 2034.
- Xu, C., Denk, W., Guild, J., Webb, W. W., *Opt. Lett.,* **1995**, 20, 2372.
- Xu, C., Webb, W. W., *J. Opt. Soc. Am. B,* **1996**, 13, 481.
- Xu, C., Zipfel, W., Shear, J. B., Williams, R. M., Webb, W. W., *Proc. Natl. Acad. Sci.,* U.S.A **1996**, 93, 10763.
- Yang, W. J., Kim, D. Y., Kim, C. H., Jeong, M.-Y., Lee, S. K., Jeon, S.-J., Cho, B. R., *Org. Lett.,* **2004**, 6, 1389.
- Yao, S., Belfield, K. D., *Eur. J. Org. Chem.,* **2012**, 3199–3217.
- Yeo, W. S., Hodneland, C. D., Mrksich, M., *ChemBioChem,* **2001**, 2, 590.
- Yu, H., Li, J., Wu, D., Qiu, Z., Zhang, Y., *Chem. Soc. Rev.*, **2010**, 39, 464.
- Zehavi, U., Amit, B., Patchornik, A., *J. Org. Chem.,* **1972**, 37, 2281.

- Zehavi, U., Patchornik, A., *J. Org. Chem.,* **1972**, 37, 2285.
- Zoumi, A., Yeh, A., Tromberg, B., *J. Proc. Natl. Acad. Sci.,* U.S.A **2002**, 99, 11014.

Publications

Organic & Biomolecular Chemistry

PAPER

Cite this: *Org. Biomol. Chem.*, 2018, **16**, 6115

o-Nitrobenzyl photoremovable groups with fluorescence uncaging reporting properties†

E. Abou Nakad, F. Bolze and A. Specht *

Received 6th June 2018,
Accepted 2nd August 2018

DOI: 10.1039/c8ob01330f

rsc.li/obc

o-Nitrobenzyl (*o*-NB) derivatives are the most widely applied photoremovable groups for the study of dynamic biological processes. By introducing different substituents to the benzylic position we were able to generate a fluorescence signal upon irradiation. This signal originates from the formation of a nitroso-ketone by-product able to achieve a keto–enol tautomerism leading to pi-conjugated α-hydroxystilbene derivatives. These *o*-NB caging groups can be used to directly monitor the uncaging event by the release of a detectable fluorescent side-product.

Introduction

Biological processes are very complex phenomena ruled by a series of precise spatio-temporal events. To reveal the intimate mechanism of these phenomena, cellular activity needs to be precisely controlled and tuned with the help of orthogonal tools. During the last decade, light has become one of the major orthogonal triggers[1–4] which was initially developed for neuroscience[1–6] and is used today in many fields of biology, such as genetics or embryology.[1–4,7] Chemical photo-triggers provide the capability to rapidly cause the initiation of a wide range of dynamic biological processes. This strategy uses light irradiation to induce a photolytic reaction, leading to the release of chemically or biologically active compounds. During the last two decades, the challenge has been to overcome the dilemma that only high energy light can induce photochemical reactions. One strategy to lower the phototoxicity within the domain of the one-photon excitation process is to tailor the caging groups with extended π-conjugation and introduce heteroatoms and functional groups in the ring system so that a larger dipole change can be generated when being excited.[1–4,8,9]

Therefore, blue light sensitive photoremovable groups have been reported in coumarin,[10–12] cinnamate,[13–18] orthonitrophenethyl[19–24] and orthonitrobenzyl[25–27] series. *o*-Nitrobenzyl (*o*-NB) derivatives have been the most widely applied photoremovable protecting groups (PPGs) for the study of dynamic biological processes.[1–4,8,9] However, this type of PPG and the uncaging secondary product exhibit similar weak brightness leading to light induced triggering of the studied responses without the possibility of quantification of the biological effector delivery.

It would be very advantageous to monitor the uncaging event, for example by the emergence of a fluorescence signal (*e.g.* optical reporting). Except for cinnamate[13–18] type and thiochromone-type[28–31] photoremovable groups, the development of optical reporters of uncaging has only attracted little attention.[32,33] Interestingly, these two PPGs have been designed to release a fluorophore as a side product.[13–18,28–31] In this work, we propose a new caging group designed to allow direct monitoring of the uncaging event by the release of an easily detectable fluorescent side product in the *o*-NB series by using 1-(2-nitrophenyl)-2-phenylethan-1-ol PPGs.

Results and discussion

Design

Based on the photolytic release mechanism of the *o*-NB PPG leading to the formation of a nitrosoketone derivative,[9] we decided to introduce benzyl substituents at the benzylic position of this class of PPGs. This new class of PPGs should lead to the formation of a nitrosoketone derivative able to achieve a keto–enol tautomerism to generate a conjugated α-hydroxystilbene derivative.

We postulate that this conjugated compound could lead to a fluorescent chromophore (Scheme 1).

To achieve our goal, we selected a blue light sensitive chromophore in the *o*-NB series. The *N*,*N*-dimethyl-4′-nitro-[1,1′-biphenyl]-4-amine core was selected since this chromophore showed long wavelength absorption (around 400 nm) induced by the introduction of electron-donating groups to promote internal charge transfer (ICT) and good two-photon

Laboratoire de Conception et Application de Molécules Bioactives, Equipe de Chimie et Neurobiologie Moléculaire, Université de Strasbourg, CNRS, CAMB UMR 7199, F-67000 Strasbourg, France. E-mail: specht@unistra.fr; Fax: (+33)368854306

†Electronic supplementary information (ESI) available. See DOI: 10.1039/c8ob01330f

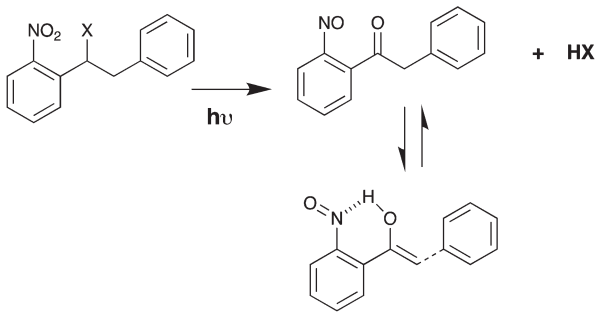

Scheme 1 Proposed photolytic reaction for aryl substituted (1-(2-nitrophenyl)ethyl) derivatives.

absorption cross-sections induced by a push–pull donor–acceptor biphenyl system.

Synthesis

Substituted *o*-NB derivatives based on the *N*,*N*-dimethyl-4′-nitro-[1,1′-biphenyl]-4-amine core were synthesized following the sequence of reactions shown in Scheme 2. Commercially available 3-bromobenzaldehyde **1** was nitrated at the *ortho* position using a mixture of concentrated nitric and sulfuric acids leading to 5-bromo-2-nitrobenzaldehyde **2** with 70% yield. The aldehyde function of the latter was protected, using ethylene glycol, leading quantitatively to the dioxolane **3**. The biphenyl derivative **4** was obtained in 75% yield after a Suzuki–Miyaura cross-coupling reaction[34] between the dioxolane **3** and 4-(dimethylamino)phenylboronic acid followed by the deprotection of the dioxolane to obtain compound **4**. The 2-(4-bromophenyl)-1-(4′-(dimethylamino)-4-nitro-[1,1′-biphenyl]-3-yl)ethan-1-ol key intermediate **5** was obtained in 85% yield by the reaction of freshly prepared 4-bromobenzyl zinc bromide[35] with aldehyde **4**. However, intermediate **5** could not be separated from 1,2-bis (4-bromophenyl)ethane obtained by homocoupling as a side product in this step. 3,4-Dimethoxyphenylacetic acid (MPAA) was then grafted to this first *o*-NB substituted PPG **5** using *N*,*N*′-diisopropyl carbodiimide (DIC) with a catalytic amount of *N*,*N*′-dimethylaminopyridine (DMAP) in order to get access to the pure ester **6** in 68% yield. Of note is that MPAA coupling was chosen in this study instead of a biologically relevant acid (*e.g.* glutamate, GABA, *etc*) to easily quantify the uncaging efficacy by HPLC analysis. Finally, the bromoaryl derivative **6** was used in order to increase the conjugation of this system with electron donating or electron withdrawing groups using a Suzuki–Miyaura cross-coupling reaction leading to the formation of compounds **7a–c** in 46–58% yield.

Photophysical and photochemical characterization

The photophysical properties of compounds **6** and **7a–c** (100 μM) were studied in a 1/1 (v/v) mixture of phosphate buffer (pH 7.4, 0.1 mM) in acetonitrile. All compounds showed a similar absorbance peak at 413 nm with an absorption coefficient of 7750 M^{-1} cm^{-1} due to the 4,4′-amino-nitro-biphenyl system. Interestingly each compound shows a very weak fluorescence (in the blue-green region, Φ < 0.2%) before irradiation. The photoinduced liberation of MPAA from **6** and **7a–c** was monitored by UV-visible spectroscopy and HPLC.

Photolysis was carried out by irradiation of samples (between 60 and 135 μM) at 405 nm (using a LUMOS 43 LED source from Atlas Photonics Inc.) in an acetonitrile/phosphate buffer (pH 7.4, 0.1 mM) mixture (1/1, v/v). The isosbestic points at 360 nm and 485 nm for **6** (see the ESI†), at 387 nm and 480 nm for **7a** (see the ESI†) and at 370 and 495 nm for **7b** (Fig. 1A) indicate that a clean photochemical reaction occurred leading to stable photoproducts. However, the absence of isosbestic points for **7c** (Fig. S25†) indicates a much complex photochemical behavior for this compound. An almost quantitative (≥95%) release of MPAA was measured by HPLC for the photo-conversion of **6** and **7a–c**. The hydrolytic stability was

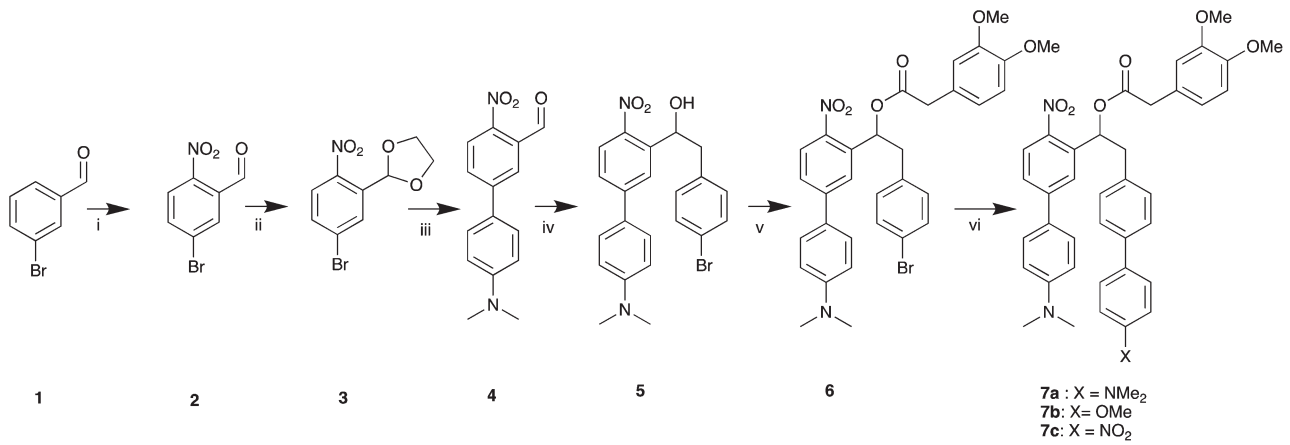

Scheme 2 Synthesis of substituted 4′-nitro-[1,1′-biphenyl]-4-amine *o*-NB at the benzylic position. (i) HNO_3/H_2SO_4, 0 °C, 3 h, 70%, (ii) ethylene glycol, toluene, 165 °C, 4 h, 100%, (iii) 4-(dimethylamino)phenyl boronic acid, K_2CO_3, Bu_4NBr, $Pd(OAc)_2$, ethanol/water, 160 °C, 15 min, *p*-TsOH, acetonitrile/water/dichloromethane, 80 °C, 3 h, 88%, (iv) bromobenzylzinc bromide, THF, −78 °C, overnight, 80%, (v) 2-(3,4-dimethoxyphenyl)acetic acid, DMAP, diisopropylcarbodiimide, dichloromethane, 0 °C, 3 h, 68% and (vi) K_2CO_3, ethanol/water/toluene, $Pd(PPh_3)_4$, 80 °C, 45 min for **7a** dimethylamino phenyl boronic acid, 55%, for **7b** 4-methoxy phenyl boronic acid, 46%, for **7c** 4-nitro phenyl boronic acid, 58%.

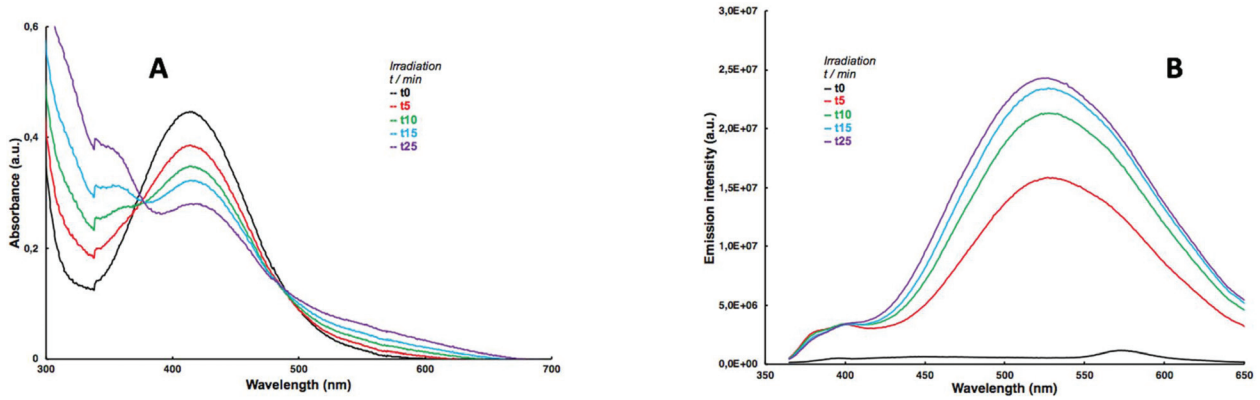

Fig. 1 Variation of UV absorbance (A) and fluorescence emission (B) after irradiation at 405 nm of a 55 μM solution (acetonitrile/PBS 1 : 1 in v/v) of **7b**.

also explored by HPLC in an acetonitrile/phosphate buffer (pH 7.4, 0.1 mM) mixture (1/1, v/v) at room temperature. No hydrolysis was observed after 24 h for **6** and **7a–c**. The postulated mechanism for the photo-induced liberation of a nitrosoketone derivative (adapted from the literature) should be able to achieve a keto–enol tautomerism to generate a conjugated α-hydroxystilbene derivative stabilized by an intramolecular hydrogen bond between the nitrogen from the nitroso group and the H of the enol group.

In order to characterize the formation of the nitroso photoproducts (see Scheme 1) an FT-IR study was undertaken using compound **7b** in acetonitrile. The IR spectra of this product before and after irradiation (Fig. S28 and S29†) show the main differences in the 1300–1500 cm^{-1} region. The band at 1465 cm^{-1} which can be attributed to the 19a vibration of the NO_2 group (according to the Wilson notation[36]) is decreasing while a band is appearing at 1446 cm^{-1} (attributed to the 19b vibration of the NO group[37]) and at 1372 cm^{-1} (which could be attributed to an enol form signature).[38]

A weak absorption can be detected at 3175 cm^{-1} which could also indicate an enol O–H bond vibration.

To confirm the keto–enol tautomerism, a ^{1}H-NMR study was undertaken using compound **6** in deuterated acetonitrile (CD_3CN) at 267 and 405 μM, respectively. After 85% and 80% cleavage respectively, the NMR spectra nicely showed the release of the MPAA (see the ESI†) together with 3 major sub-products based on the ^{1}H dimethyl-amino signals. More interestingly, in a concentration dependent manner, 3 new NMR signals together with 2 new signals were detected respectively between 4–5.2 ppm and 9.5–10 ppm (Fig. S31 and S32†). The singlet at 4.1 ppm is in good agreement with the CH_2 of the nitroso-keto sub-product. And the two singlets at 4.87 ppm and 5.19 ppm together with the two singlets at 9.69 ppm and 9.97 ppm are also in good agreement with the ^{1}H expected signals for the alkene =CH and the OH signals of the enol sub-products (*cis* and *trans*), respectively.

After having confirmed the occurrence of a keto–enol tautomerism in the uncaging sub-product, we assumed that the elongated conjugated system of the α-hydroxystilbene should induce a strong enhancement of the UV-vis absorption and emission properties. In order to study the photo-induced changes in fluorescence, emission spectra were recorded for the irradiated samples (100 μM, 405 nm) in an acetonitrile/phosphate buffer (pH 7.4, 0.1 mM) mixture (1/1, v/v). For all four compounds, the fluorescence emission is very weak before photocleavage (with a maximum at 504, 489, 575 and 480 nm for **6**, **7a**, **7b** and **7c** respectively). After complete photoconversion, compounds **6** and **7a** showed a moderate increase in their emission intensity (×40 and ×32 for **6** and **7a** respectively). In contrast, for **7b** an intense red shifted (526 nm) emission was observed with more than 200 times increase in the fluorescence intensity (Fig. 1B). Of note is that this emission band seems to indicate that the increase of the conjugation length of the system and substitution with strong electron donating groups are able to generate a red-shifted emission band upon photocleavage. Finally, compound **7c** showed during irradiation a more complex fluorescence behavior presumably due to the photodegradation of the photolytic by-product leading first to an increase followed by a decrease in the fluorescence intensity (Table S4†).

All photochemical and photophysical properties of compounds **6** and **7a–c** are summarized in Table 1.

Table 1 Variation of the fluorescence intensity ratio and emission wavelength of derivatives **6** and **7a–c**

Compound[a]	λ_{em} (nm)	$I_0 \times 10^8$	Average % of photocleavage[b]	Average[b] $I_{full} \times 10^8$	I_{full}/I_0
6	504	0.5254	95	21.006	40
7a	489	4.4211	93	143.233	32
7b	526	1.0296	97	214.721	208
7c	480	0.3409	83	—[c]	—[c]

[a] 100 μM solutions. [b] Average of 3 separate irradiation times. [c] Not calculated due to the high bleaching of the sub-product.

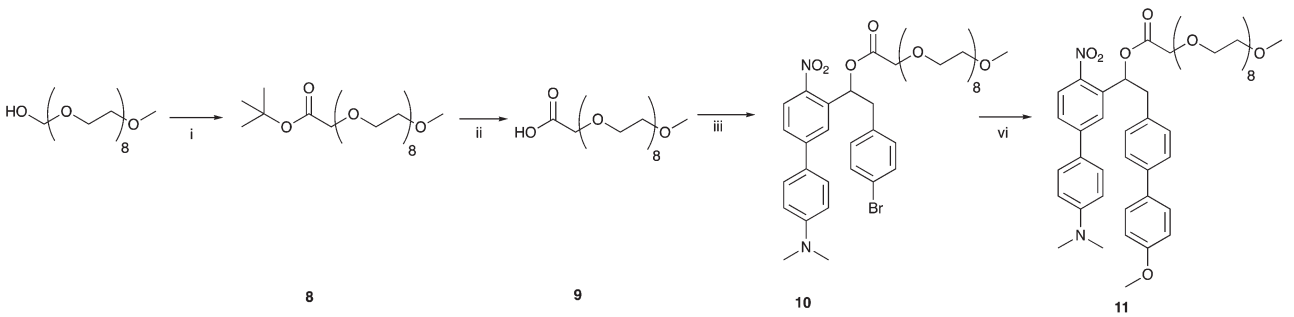

Scheme 3 Synthesis of **11**: a PEGylated version of the *o*-nitrobiphenyl methoxy derivative. (i) NaH, *tert*-butylbromoacetate, THF, 0 °C, 2 h, 87%; (ii) CF_3COOH/dichloromethane, 3 h, room temperature, 100%; (iii) **5**, DMAP, diisopropylcarbodiimide, dichloromethane, 0 °C, 48%; (vi) 4-methoxyphenyl boronic acid, K_2CO_3, ethanol/toluene/water, $Pd(PPh_3)_4$, 80 °C, 45 min, 30%.

Biological evaluation of the uncaging fluorescence reporting property on HeLa cells

Since compound **7b** showed the highest photoinduced fluorescence linear increase and the most red-shifted fluorescence emission upon irradiation, we decided to use this compound to evaluate the possibility to monitor the uncaging events by fluorescence recording on cell culture. For this reason, we synthesized compound **11**, a PEGylated version of the *o*-nitrobiphenyl methoxy derivative **7b**. The product was synthesized (Scheme 3) in 4 steps starting from an octaethylene glycol monomethyl ether which was reacted with *tert*-butyl-bromoacetate to form **8** which was then deprotected to afford compound **9**. This was reacted with **5** followed by a Suzuki coupling to give **11** in 30% yield.

HeLa cells were incubated for 5 min with a 1 μM solution of **11**. The cells were irradiated with 365 nm light from an EL6000 lamp (see the ESI†) of a Leica SPE microscope. A confocal image was obtained each 5 min for 15 min of continuous irradiation (the experiment was stopped after 15 min due to the phototoxicity of the UV irradiation). A clear increase in the detected fluorescence intensity was observed upon irradiation (see Fig. S33†). Of note is that the HeLa cells incubated for 35 min with a 1 μM solution of **11** showed only weak fluorescence intensity. A quantitative analysis of the fluorescence intensity was performed on 5 cells showing a linear increase in the fluorescence intensity for the first 15 min and reaching a plateau (Fig. 2). Therefore, we could follow the uncaging event of this new type of *o*-nitrobenzyl PPG by the increase of fluorescence signal on cells.

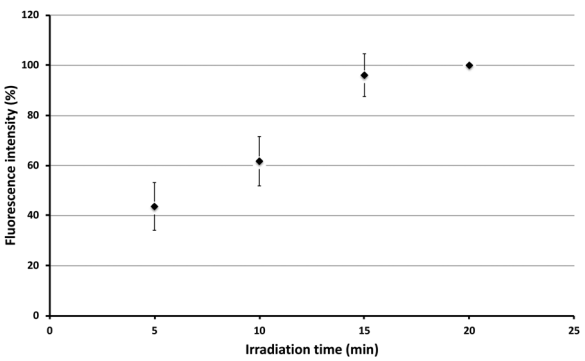

Fig. 2 Fluorescence increase as a function of irradiation time observed for HeLa cells treated with 1 μM of **11**.

Conclusions

There is a great need for photoremovable groups able to generate an easy way to quantify their side-products, in particular to be able to monitor in real time the light induced concentration jump of a given biological effector. This leads us to synthesize a new class of *o*-nitrobenzyl photoremovable groups able to generate a fluorescent side-product. These compounds were designed in order to produce after the photoreaction a nitrosoketone by-product able to achieve a keto–enol tautomerism leading to a conjugated α-hydroxystilbene product. A 1,2-addition of bromoaryl organozinc halides to 4′-(dimethylamino)-4-nitro-[1,1′-biphenyl]-3-carbaldehyde followed by Miyaura–Suzuki cross coupling reactions was used in order to synthesize biphenyl substituted (1-(2-nitrophenyl)ethyl) photoremovable groups. Interestingly each synthesized *o*-NB PPG shows a very weak fluorescence signal before irradiation. To be able to quantify the photorelease of carboxylic acid functions a chromophoric 3,4-dimethoxyphenylacetic acid was coupled to our *o*-NB PPGs. Except for the *p*-nitrobiphenyl derivative **7c**, an almost quantitative (≥93%) release of MPAA was measured by HPLC after complete photo-conversion for each photolytic precursor of MPAA. More interestingly, all these compounds showed an interesting fluorescence signal increase induced by the photolytic reaction. In particular, the *p*-methoxy biphenyl derivative **7b** showed a 200 times increase in the green (526 nm) emission intensity after full photocleavage. Therefore, a water-soluble version of this compound has been successfully used for *in vitro* cell imaging and real time monitoring of the uncaging event. Our future studies will focus on the use of this strategy for the development of more efficient visible light sensitive photoremovable groups in the *o*-NB series[8] in order to follow the uncaging events simultaneously by fluorescence analysis and with a physiological event (for example induced by the photorelease of a neurotransmitter).

Experimental

Nitro-3-bromo-benzaldehyde (2)

3-Bromobenzaldehyde (16.21 mmol, 0.35 mL) was dissolved in 15 mL of 98% H_2SO_4. To this mixture, HNO_3 (52 mmol, 3.6 mL) was added dropwise under vigorous stirring at 0 °C for 1 h and then at room temperature for 2 h. The mixture was poured into ice water and extracted with ethyl acetate, the combined organic phases were dehydrated with $MgSO_4$ and the crude product was purified over a SiO_2 column using heptane/ethyl acetate (9/1) as the eluent. The target compound **2** was isolated as pale-yellow crystals (2.6 g, 70%, R_f = 0.31).

^{1}H NMR (400 MHz, $CDCl_3$): δ = 10.41 (s, 1 H), 8.06 (s, 1H), 8.03 (d, ^3J(H,H) = 8.6 Hz, 1H), 7.88 (dd, ^3J(H,H) = 8.6 Hz, ^4J(H,H) = 2.2 Hz, 1H) ppm.

^{13}C NMR (100 MHz, $CDCl_3$): δ = 186.9, 148.2, 136.6, 132.8, 132.7, 129.7, 126.3 ppm.

MS(ESI): $[M + H]^+$ ($C_7H_5BrNO_3^+$) m/z calcd: 229.93, m/z found: 229.82.

2-(5-Bromo-2-nitrophenyl)-1,3-dioxolane (3)

In 50 mL of anhydrous toluene, **2** (655 mg, 2.84 mmol) was dissolved and ethylene glycol (0.2 mL, 3.41 mmol) was added to a mixture with *p*-toluene sulfonic acid (55 mg, 0.284 mmol). The mixture was heated under reflux using a Dean–Stark apparatus. After 4 h the reaction was complete (monitored by TLC) and the solvent was evaporated. The mixture was extracted 3 times with dichloromethane and washed with water affording the target compound **3** as a light brown solid (780 mg, 100%, R_f = 0.52 AcOEt/heptane 1/9 in vol.).

^{1}H NMR (400 MHz, $CDCl_3$): δ = 7.94 (s, 1H), 7.81 (d, ^3J(H,H) = 9 Hz, 1H), 7.63 (d, ^3J(H,H) = 9 Hz, ^4J(H,H) = 2.2 Hz, 1H), 6.48 (s, 1H), 4.05 (m, 4H) ppm.

^{13}C NMR (100 MHz, $CDCl_3$): δ = 147.5, 135.3, 132.7, 130.9, 127.9, 126.1, 99.1, 65.4 ppm.

MS(ESI): $[M + H]^+$ ($C_9H_8BrNO_4^+$) m/z calcd: 273.96, m/z found: 273.84.

3′-(1,3-Dioxolan-2-yl)-*N*,*N*-dimethyl-4′-nitro-[1,1′-biphenyl]-4-amine

In a microwave vial, 365 mg of **3** (1.33 mmol) with 264 mg of 4-(dimethyl amino)phenyl boronic acid (1.6 mmol), potassium carbonate (3.6 mmol) and tetrabutylammonium bromide (1.33 mmol) were dissolved in 13 mL of ethanol and 6.5 mL of water (2/1 v/v). The mixture was degassed 2 times (freeze–thaw cycles) and then $Pd(OAc)_2$ (30 mg, 0.133 mmol) was added and the mixture was degassed 1 more time before heating under microwave radiation at 160 °C for 15 minutes. The solvent was evaporated, and the residue was extracted with water and ethyl acetate and dried over $MgSO_4$. The solvent was evaporated under vacuum and the biphenyl acetal product was isolated as a reddish-brown solid (418 mg, 85%, R_f = 0.46 AcOEt/heptane 1/9 in vol.). The yield obtained is estimated since the side product (15% homocoupling of boronic acid from ^{1}H NMR integration) has the same R_f as the target product, so in this step the product was used without further purification.

^{1}H NMR (400 MHz, $CDCl_3$): δ = 8.01 (d, ^3J(H,H) = 7.6 Hz, 1H), 7.97 (s, 1H), 7.63 (d, ^3J(H,H) = 9.6 Hz, ^4J(H,H) = 2.2 Hz, 1H), 7.56 (d, ^3J(H,H) = 8.4 Hz, 2H), 6.79 (d, ^3J(H,H) = 9.6 Hz, 2H), 6.60 (s, 1H), 4.07 (m, 4H), 3.03 (s, 6H) ppm.

MS(ESI): $[M + H]^+$ ($C_{17}H_{19}N_2O_4^+$) m/z calcd: 315.13, m/z found: 315.05.

4′-(Dimethylamino)-4-nitro-[1,1′-biphenyl]-3-carbaldehyde (4)

A solution of *p*-toluenesulfonic acid (2.61 g, 13.75 mmol) in acetonitrile (20 mL) and water (7 mL) was added to a solution of biphenyl aldehyde (432 mg, 1.375 mmol) in dichloromethane (8 mL). The mixture was then stirred at 80 °C under reflux for 3 h (monitored by TLC). After cooling to room temperature, the solvent was evaporated, and the residue was extracted with dichloromethane and washed with water. The crude product was purified over a column to afford the target product **4** as a bright red solid (297 mg, 88%, R_f = 0.3 AcOEt/heptane 15/85 in vol.).

^{1}H NMR (400 MHz, $CDCl_3$): δ = 10.53 (s, 1H), 8.17 (d, ^3J(H,H) = 8 Hz, 1H), 8.07 (s, 1H), 7.86 (d,^3J(H,H) = 7.2 Hz, ^4J(H,H) = 2.2 Hz, 1H), 7.6 (d, ^3J(H,H) = 8 Hz, 2H), 6.79 (d, ^3J(H,H) = 9.2 Hz, 2H), 3.03 (s, 6H) ppm.

^{13}C NMR (100 MHz, $CDCl_3$): δ = 189.1, 151.2, 147.3, 146.3, 132.5, 129.3, 128.1, 125.9, 125.5, 124.5, 124.3, 112.4, 40.2 ppm.

MS(ESI): $[M + H]^+$ ($C_{15}H_{15}N_2O_3^+$) m/z calcd: 271.01, m/z found: 270.99.

4-Bromobenzyl zinc bromide: preparation

LiCl (170 mg, 4 mmol) was added to a microwave reaction vial and dried with a flame for a few minutes in open air. This vial was allowed to cool down in a desiccator under vacuum. Air was used to back pressurize the desiccator and Zn powder (265 mg, 4 mmol) was added. The vial was heated again on a flame for a few minutes in open air and allowed to cool down in a desiccator under vacuum, and argon was added to back pressurize the desiccator. A stirring bar was added, the vial was sealed, and 3 mL of anhydrous THF was injected *via* the septum followed by 1,2-dibromoethane (10 μL, 0.1 mmol). The mixture was heated in a microwave oven at 85 °C for 5 minutes. TMSCl (2.5 μL, 0.02 mmol) was added to the suspension and once again it was heated at 85 °C for 5 minutes. 4-Bromobenzyl bromide (500 mg, 2 mmol) was then added as a solution in 2 mL THF and the vial was heated for 1 h at 70 °C. Iodometric titration indicated that the obtained solution of 4-bromobenzyl zinc bromide had a concentration of 0.4 M.

2-(4-Bromophenyl)-1-(4′-(dimethylamino)-4-nitro-[1,1′-biphenyl]-3-yl)ethan-1-ol (5)

In 10 mL of anhydrous THF, **4** (130 mg, 0.48 mmol) was dissolved. At −78 °C, a solution of 4-bromobenzyl zinc bromide (3.6 mL, 1.44 mmol) was added dropwise and the mixture was stirred for 1 h at −78 °C and allowed to warm up to room temperature and stirred overnight. The reaction was quenched with 10% HCl and extracted with water and ethyl acetate and the crude compound was purified on a column with heptane/

AcOEt 85/15 in vol. as the eluent to afford **5** as orange-red paste (210 mg, 80%, R_f = 0.32 AcOEt/heptane 15/85 in vol.).

^{1}H NMR (400 MHz, $CDCl_3$): δ = 8.08 (d, ^3J(H,H) = 8 Hz, 1H), 8.01 (s, 1H), 7.59 (d, ^3J(H,H) = 9.6 Hz, ^4J(H,H) = 2.2 Hz, 1H), 7.55 (d, ^3J(H,H) = 9.6 Hz, 2H), 7.48 (d, ^3J(H,H) = 9.6 Hz, 2H), 7.23 (d, ^3J(H,H) = 9.6 Hz, 2H), 6.79 (d, ^3J(H,H) = 9.6 Hz, 2H), 5.59 (d, ^3J(H,H) = 10 Hz, 1H), 3.26 (d, ^3J(H,H) = 12.4 Hz, 1H), 3.03 (s, 6H), 2.8–2.86 (dd, ^2J(H,H) = 23, ^3J(H,H) = 13.6, 1H) ppm.

HRMS(ESI): $[M + H]^+$ ($C_{22}H_{22}N_2O_3^+$) *m*/*z* calcd: 441.0703, *m*/*z* found: 441.0177.

2-(4-Bromophenyl)-1-(4′-(dimethylamino)-4-nitro-[1,1′-biphenyl]-3-yl)ethyl-2-(3,4-dimethoxyphenyl)acetate (6)

In 25 mL anhydrous dichloromethane, compound **5** (450 mg, 1.02 mmol) was dissolved and 2-(3,4-dimethoxyphenyl)acetic acid (300 mg, 1.53 mmol) was added along with 4-dimethyl aminopyridine (DMAP) (7 mg, 0.051 mmol) under argon. At 0 °C, *N*,*N*′-diisopropyl carbodiimide (DIC) (0.24 mL, 1.53 mmol) was added dropwise and the reaction was stirred for 1 h at 0 °C, and then for 2 h at room temperature. The reaction was monitored by HPLC. The mixture was filtered on a glass-frit funnel and the filtrate was extracted with dichloromethane and water. To remove diisopropyl urea salts, the product is dissolved in cold acetonitrile. The crude product was purified over a column with silica gel using 20/80 AcOEt/heptane in vol. as the eluent to afford **6** as orange powder (430 mg, 68%, R_f = 0.38 AcOEt/heptane 20/80 in vol.).

^{1}H NMR (400 MHz, $CDCl_3$): δ = 8.1 (d, ^3J(H,H) = 8 Hz, 1H), 7.55 (d, ^3J(H,H) = 9.6 Hz, ^4J(H,H) = 2.2 Hz, 1H), 7.41 (d, ^3J(H,H) = 9.6 Hz, 2H), 7.38 (s, 1H), 7.23 (d, ^3J(H,H) = 9.6 Hz, 2H), 7.18 (d, ^3J(H,H) = 9.6 Hz, 2H), 6.79 (d, ^3J(H,H) = 9.6 Hz, 2H), 6.65–6.75 (m, 3H), 6.57 (d, ^3J(H,H) = 10 Hz, 1H), 3.85 (s, 3H), 3.75 (s, 3H), 3.52 (s, 2H), 3.32 (d, ^3J(H,H) = 12.4 Hz, 1H), 3.16 (s, 6H), 2.9–3.01 (dd, ^2J(H,H) = 23 Hz, ^3J(H,H) = 13.6 Hz, 1H) ppm.

HMMS(ESI): $[M + H]^+$ ($C_{32}H_{32}N_2O_6Br^+$) *m*/*z* calcd: 619.1443, *m*/*z* found: 619.1436.

1-(4′-(Dimethylamino)-4-nitro-[1,1′-biphenyl]-3-yl)-2-(4′-methoxy-[1,1′-biphenyl]-4-yl)ethyl-2-(3,4-dimethoxyphenyl) acetate (7b)

In a microwave vial, 52 mg of **6** (0.084 mmol) with 15 mg of 4-methoxyphenyl boronic acid (0.1 mmol) and potassium carbonate (30 mg, 0.21 mmol) were dissolved in 2 mL of ethanol, 1 mL of water and 7 mL of toluene (2/1/7 in vol.). The mixture was degassed 2 times (freeze–thaw cycles) and then $Pd(PPh_3)_4$ (5 mg, 4.2×10^{-3} mmol) was added and the mixture was degassed 1 more time before heating under microwave radiation at 80 °C for 45 minutes. The solvents were evaporated, and the residue was extracted with ethyl acetate, washed with water and dried over $MgSO_4$. The solvent was evaporated under vacuum and the crude product was purified over a column with silica gel using 40/60 AcOEt/heptane as the eluent to afford product **7b** as reddish paste (25 mg, 46%, R_f = 0.32 AcOEt/heptane 40/60 in vol.).

The same procedure was followed for the synthesis of **7a** (4-(dimethyl amino)phenyl boronic acid) with a yield of 55% and **7c** (4-nitrophenyl boronic acid) with a yield of 58%.

^{1}H NMR (400 MHz, $CDCl_3$): δ = 8.08 (d, ^3J(H,H) = 8.4 Hz, 1H), 7.54 (d, ^3J(H,H) = 8.8 Hz, 2H), 7.52 (d, ^3J(H,H) = 7.6 Hz, 1H), 7.45 (d, ^3J(H,H) = 8.4 Hz, 2H), 7.31 (s, 1H), 7.19–7.24 (m, 4H), 6.98 (d, ^3J(H,H) = 9.8 Hz, 2H), 6.67–6.72 (m, 5H), 6.63 (d, ^3J(H,H) = 8.4 Hz, 1H), 3.86 (s, 3H), 3.77 (s, 3H), 3.70 (s, 3H), 3.52 (s, 2H), 3.39 (d, ^3J(H,H) = 14 Hz, 1H), 3.05–3.11 (dd, ^2J(H,H) = 22.8 Hz, ^3J(H,H) = 15.2 Hz, 1H), 3.02 (s, 6H) ppm.

HRMS(ESI): $[M + H]^+$ ($C_{39}H_{39}N_2O_7^+$) *m*/*z* calcd: 647.2757, *m*/*z* found: 647.2767.

1-(4′-(Dimethylamino)-4-nitro-[1,1′-biphenyl]-3-yl)-2-(4′-(dimethylamino)-[1,1′-biphenyl]-4-yl)ethyl-2-(3,4-dimethoxyphenyl)acetate (7a)

This compound was obtained in 55% yield.

^{1}H NMR (400 MHz, $CDCl_3$): δ = 8.08 (d, ^3J(H,H) = 9.36 Hz, 1H), 7.52 (d, ^3J(H,H) = 9.6 Hz, ^4J(H,H) = 2.2 Hz, 1H), 7.46 (d, ^3J(H,H) = 7.6 Hz, 2H), 7.31 (s, 1H), 7.19–7.22 (m, 4H), 6.82 (d, ^3J(H,H) = 7.6 Hz, 2H), 6.68–6.71 (m, 5H), 6.63 (d, ^3J(H,H) = 8.8 Hz, 1H), 3.77 (s, 3H), 3.71 (s, 3H), 3.53 (s, 2H), 3.38 (d, ^3J(H,H) = 14.4 Hz, 1H), 3.05–3.11 (dd, ^2J(H,H) = 23.6 Hz, ^3J(H,H) = 13.6 Hz, 1H), 3.01 (s, 6H), 3.00 (s, 6H) ppm.

HRMS(ESI): $[M + H]^+$ ($C_{40}H_{42}N_3O_6^+$) *m*/*z* calcd: 660.3073, *m*/*z* found: 660.3047.

1-(4′-(Dimethylamino)-4-nitro-[1,1′-biphenyl]-3-yl)-2-(4′-nitro-[1,1′-biphenyl]-4-yl)ethyl-2-(3,4-dimethoxyphenyl)acetate (7c)

This compound was obtained in 58% yield.

^{1}H NMR (400 MHz, $CDCl_3$): δ = 8.17 (d, ^3J(H,H) = 8.8 Hz, 2H), 7.96 (d, ^3J(H,H) = 9.6 Hz, 1H), 7.6 (d, ^3J(H,H) = 7.6 Hz, ^4J(H,H) = 2.2 Hz, 2H), 7.41 (d, ^3J(H,H) = 8.8 Hz, 1H), 7.38 (d, ^3J(H,H) = 8.8 Hz, 2H), 7.18 (d, ^3J(H,H) = 8 Hz, 2H), 7.13 (s, 1H), 7.09 (d, ^3J(H,H) = 6.8 Hz, 2H), 6.56–6.63 (m, 5H), 6.54 (d, ^3J(H,H) = 8.4 Hz, 1H), 3.67 (s, 3H), 3.58 (s, 3H), 3.43 (s, 2H), 3.28 (d, ^3J(H,H) = 13.2 Hz, 1H), 2.97–3.02 (dd, ^2J(H,H) = 23.6 Hz, ^3J(H,H) = 13.6 Hz, 1H), 2.90 (s, 6H) ppm.

HRMS(ESI): $[M + H]^+$ ($C_{38}H_{36}N_3O_8^+$) *m*/*z* calcd: 662.2502, *m*/*z* found: 662.2502.

tert-Butyl-2-(2-methoxyoctaethoxy)acetate (8)

To a stirred solution of octaethylene glycol monomethyl ether (250 mg, 0.65 mmol) in anhydrous THF (8 mL) was added NaH (40 mg, 1.62 mmol, 60% dispersion in mineral oil) at 0 °C. The solution was stirred for 30 minutes at 0 °C, and *tert*-butyl bromoacetate (0.18 mL, 1.17 mmol) was added dropwise over 2 minutes. The resulting solution was allowed to warm to room temperature and stirred for 2 h. The reaction was quenched with a saturated solution of NH_4Cl, the aqueous phase was washed three times with dichloromethane, the combined organic extracts were dried over $MgSO_4$ and the solvent was evaporated under reduced pressure. The residue was purified by silica gel column chromatography using 100% AcOEt and then 98/2 AcOEt/MeOH (in vol.) as the eluent to afford **8**

(282 mg, 87%, R_f = 0.32 AcOEt/MeOH 98/2 in vol.) as a yellowish oil.

^{1}H NMR (400 MHz, $CDCl_3$): δ = 4.01 (s, 2H), 3.62–3.72 (m, 30H), 3.52–3.56 (m, 2H), 3.37 (s, 3H), 1.46 (s, 9H) ppm.

^{13}C NMR (100 MHz, $CDCl_3$): δ = 168.3, 83.5, 71.6, 70.1, 69.5, 68.1, 56.9, 31.7 ppm.

2-(2-Methoxyoctaethoxy)acetic acid (9)

272 mg of **8** was dissolved in 3 mL of CH_2Cl_2 and 1.5 mL of CF_3COOH (2/1 in vol.) and stirred for 3 h. The solvent was evaporated and the remaining CF_3COOH was co-evaporated 3 times with CH_2Cl_2 to afford **9** in quantitative yield (240 mg, R_f = 0.33 AcOEt/MeOH 98/2 in vol.).

^{1}H NMR (400 MHz, $CDCl_3$): δ = 10.1 (broad s, 1H), 4.17 (s, 2H), 3.62–3.77 (m, 30H), 3.54–3.58 (m, 2H), 3.38 (s, 3H) ppm.

^{13}C NMR (100 MHz, $CDCl_3$): δ = 173.3, 71.6, 70.1, 69.5, 68.1, 67.5, 56.9 ppm.

2-(4-Bromophenyl)-1-(4′-(dimethylamino)-4-nitro-[1,1′-biphenyl]-3-yl)ethyl-2-(2-methoxyoctaethoxy)acetate (10)

In 10 mL anhydrous dichloromethane, compound **5** (210 mg, 0.47 mmol) was dissolved and **9** (306 mg, 0.71 mmol) was added along with *N*,*N*′-dimethylaminopyridine (DMAP) (7 mg, 0.026 mmol) under argon. At 0 °C, *N*,*N*′-diisopropyl carbodiimide (DIC) (0.11 mL, 0.71 mmol) was added dropwise and the reaction was stirred for 1 h at 0 °C, and then for 2 h at room temperature. The reaction was monitored by HPLC. The mixture was filtered on a glass-frit funnel and the filtrate was extracted with dichloromethane and water. To remove diisopropyl urea salts, the product is dissolved in cold acetonitrile. The crude product was purified over a column with silica gel using 100% AcOEt and then 98/2 AcOEt/MeOH in vol. as the eluent to afford **10** (194 mg, 48%, R_f = 0.38 AcOEt/MeOH 98/2 in vol.) as an orange paste.

^{1}H NMR (400 MHz, $CDCl_3$): δ = 8.06 (d, ^3J(H,H) = 9.2 Hz, 1H), 7.54 (s, 1H), 7.38–7.48 (m, 4H), 7.14–7.23 (m, 3H), 6.76 (d, ^3J(H,H) = 7.6 Hz, 2H), 6.63 (d, ^3J(H,H) = 8.8 Hz, 1H), 4.06 (s, 2H), 3.49–3.72 (m, 32H), 3.34 (s, 3H), 3.31 (d, ^2J(H,H) = 18.6 Hz, 1H), 3.02–3.07 (dd, ^2J(H,H) = 21.3 Hz, ^3J(H,H) = 13.6 Hz, 1H), 3.01 (s, 6H) ppm.

MS(ESI): $[M + H]^+$ ($C_{41}H_{58}N_2O_{13}^+$) *m*/*z* calcd: 865.30, *m*/*z* found: 865.43.

1-(4′-(Dimethylamino)-4-nitro-[1,1′-biphenyl]-3-yl)-2-(4′-methoxy-[1,1′-biphenyl]-4-yl)ethyl-2-(2-methoxyoctaethoxy) acetate (11)

In a microwave vial, 115 mg of **10** (0.135 mmol) with 25 mg of 4-methoxyphenyl boronic acid (0.162 mmol) and potassium carbonate (50 mg, 0.34 mmol) were dissolved in 3 mL of ethanol, 1.5 mL of water and 10 mL of toluene (2/1/7 in vol.). The mixture was degassed 2 times (freeze–thaw cycles), then $Pd(PPh_3)_4$ (8 mg, 6.75 × 10^{-3} mmol) was added and the mixture was degassed 1 more time before heating under microwave radiation at 80 °C for 45 minutes. The solvent was evaporated, and the residue was extracted with water and dichloromethane and dried over $MgSO_4$. The solvent was evaporated under vacuum and the residue was purified over a silica gel column to afford the product **11** as reddish paste (36 mg, 30%, R_f = 0.37 AcOEt/MeOH 98/2 in vol.).

^{1}H NMR (400 MHz, $CDCl_3$): δ = 8.09 (d, ^3J(H,H) = 8 Hz, 1H), 7.57 (dd, ^3J(H,H) = 10.4 Hz, ^4J(H,H) = 2.2 Hz, 1H), 7.48–7.53 (m, 5H), 7.40 (d, ^3J(H,H) = 9.6 Hz, 2H), 7.32 (d, ^3J(H,H) = 7.6 Hz, 2H), 6.97 (d, ^3J(H,H) = 7.6 Hz, 2H), 6.72–6.75 (m, 3H), 4.11 (s, 2H), 3.85 (s, 3H), 3.75 (s, 3H), 3.51–3.66 (m, 32H), 3.44 (d, ^3J(H,H) = 14 Hz, 1H), 3.12–3.19 (dd, ^2J(H,H) = 22 Hz, ^3J(H,H) = 12.7 Hz, 1H), 3.01 (s, 6H) ppm.

MS(ESI): $[M + H]^+$ ($C_{48}H_{65}N_2O_{14}^+$) *m*/*z* calcd: 893.44, *m*/*z* found: 893.57.

Conflicts of interest

There are no conflicts to declare.

Acknowledgements

This work was supported by the Université de Strasbourg (IdEx Grant to A. S.), the CNRS and a grant from the Agence Nationale de la Recherche (Contract No. ANR-13-JSJV-0009-01 to A. S.). The authors thank Laura Bom and Maurice Coppe from the faculty of chemistry (University of Strasbourg) for FT-IR and NMR spectra measurements, respectively.

Notes and references

1 C. Brieke, F. Rohrbach, A. Gottschalk, G. Mayer and A. Heckel, *Angew. Chem., Int. Ed.*, 2012, **51**, 8446–8476.
2 A. Gautier, C. Gauron, M. Volovitch, D. Bensimon, L. Jullien and S. Vriz, *Nat. Chem. Biol.*, 2014, **10**, 533–541.
3 S. Piant, F. Bolze and A. Specht, *Opt. Mater. Express*, 2016, **6**, 1679–1691.
4 M. M. Lerch, M. J. Hansen, G. M. van Dam, W. Szymanski and B. L. Feringa, *Angew. Chem., Int. Ed.*, 2016, **55**, 10978–10999.
5 T. Fehrentz, M. Schönberger and D. Trauner, *Angew. Chem.*, 2011, **123**, 12362–12390.
6 R. H. Kramer, A. Mourot and H. Adesnik, *Nat. Neurosci.*, 2013, **16**, 816–823.
7 L. Kowalik and J. K. Chen, *Nat. Chem. Biol.*, 2017, **13**, 587–598; A. Deiters, *ChemBioChem*, 2010, **11**, 47–53; I. A. Shestopalov and J. K. Chen, *Chem. Soc. Rev.*, 2008, **37**, 1294–1307.
8 M. Abe, Y. Chitose, S. Jakkampudi, P. T. T. Thuy, Q. Lin, B. T. Van, A. Yamada, R. Oyama, M. Sasaki and C. Katan, *Synthesis*, 2017, 3337–3346.
9 P. Klán, T. Šolomek, C. G. Bochet, A. Blanc, R. Givens, M. Rubina, V. Popik, A. Kostikov and J. Wirz, *Chem. Rev.*, 2013, **113**, 119–191.
10 A. Gandioso, S. Contreras, I. Melnyk, J. Oliva, S. Nonell, D. Velasco, J. García-Amorós and V. Marchán, *J. Org. Chem.*, 2017, **82**, 5398–5408.

11 L. Fournier, C. Gauron, L. Xu, I. Aujard, T. Le Saux, N. Gagey-Eilstein, S. Maurin, S. Dubruille, J. B. Baudin, D. Bensimon, M. Volovitch, S. Vriz and L. Jullien, *ACS Chem. Biol.*, 2013, **8**, 1528–1536.

12 V. Hagen, B. Dekowski, N. Kotzur, R. Lechler, B. Wiesner, B. Briand and M. Beyermann, *Chemistry*, 2008, **14**, 1621–1627.

13 A. Paul, R. Mengji, O. A. Chandy, S. Nandi, M. Bera, A. Jana, A. Anoop and N. D. P. Singh, *Org. Biomol. Chem.*, 2017, **15**, 8544–8552.

14 N. Gagey, P. Neveu, C. Benbrahim, B. Goetz, I. Aujard, J.-B. Baudin and L. Jullien, *J. Am. Chem. Soc.*, 2007, **129**(32), 9986–9998.

15 N. Gagey, P. Neveu and L. Jullien, *Angew. Chem., Int. Ed.*, 2007, **46**(14), 2467–2469.

16 P. M. Koenigs, B. C. Faust and N. A. Porter, *J. Am. Chem. Soc.*, 1993, **115**(21), 9371–9379.

17 A. D. Turner, S. V. Pizzo, G. Rozakis and N. A. Porter, *J. Am. Chem. Soc.*, 1988, **110**(1), 244–250.

18 A. D. Turner, S. V. Pizzo, G. W. Rozakis and N. A. Porter, *J. Am. Chem. Soc.*, 1987, **109**(4), 1274–1275.

19 M. A. Fichte, X. M. Weyel, S. Junek, F. Schafer, C. Herbivo, M. Goeldner, A. Specht, J. Wachtveitl and A. Heckel, *Angew. Chem., Int. Ed.*, 2016, **55**, 8948–8952.

20 A. Specht, F. Bolze, L. Donato, C. Herbivo, S. Charon, D. Warther, S. Gug, J. F. Nicoud and M. Goeldner, *Photochem. Photobiol. Sci.*, 2012, **11**, 578–586.

21 L. Donato, A. Mourot, C. M. Davenport, C. Herbivo, D. Warther, J. Leonard, F. Bolze, J. F. Nicoud, R. H. Kramer, M. Goeldner and A. Specht, *Angew. Chem., Int. Ed.*, 2012, **51**, 1840–1843.

22 D. Warther, F. Bolze, J. Leonard, S. Gug, A. Specht, D. Puliti, X. H. Sun, P. Kessler, Y. Lutz, J. L. Vonesch, B. Winsor, J. F. Nicoud and M. Goeldner, *J. Am. Chem. Soc.*, 2010, **132**, 2585–2590.

23 S. Gug, S. Charon, A. Specht, K. Alarcon, D. Ogden, B. Zietz, J. Leonard, S. Haacke, F. Bolze, J. F. Nicoud and M. Goeldner, *ChemBioChem*, 2008, **9**, 1303–1307.

24 S. Gug, F. Bolze, A. Specht, C. Bourgogne, M. Goeldner and J. F. Nicoud, *Angew. Chem., Int. Ed.*, 2008, **47**, 9525–9529.

25 H. K. Agarwal, R. Janicek, S.-H. Chi, J. W. Perry, E. Niggli and G. C. R. Ellis-Davies, *J. Am. Chem. Soc.*, 2016, **138**(11), 3687–3693.

26 S. Jakkampudi, M. Abe, N. Komori, R. Takagi, K. Furukawa, C. Katan, W. Sawada, N. Takahashi and H. Kasai, *ACS Omega*, 2016, **1**(2), 193–201.

27 I. Aujard, C. Benbrahim, M. Gouget, O. Ruel, J.-B. Baudin, P. Neveu and L. Jullien, *Chem. – Eur. J.*, 2006, **12**, 6865–6879.

28 S. Hikage, Y. Nishiyama, Y. Sasaki, H. Tanimoto, T. Morimoto and K. Kakiuchi, *ACS Omega*, 2017, **2**, 2300–2307.

29 Y. Zhang, H. Zhang, C. Ma, J. Li, Y. Nishiyama, H. Tanimoto, T. Morimoto and K. Kakiuchi, *Tetrahedron Lett.*, 2016, **57**, 5179–5184.

30 Y. Zhang, H. Tanimoto, Y. Nishiyama, T. Morimoto and K. Kakiuchi, *Synlett*, 2012, (3), 367–370.

31 S. Kitani, K. Sugawara, K. Tsutsumi, T. Morimoto and K. Kakiuchi, *Chem. Commun.*, 2008, (18), 2103–2105.

32 P. T. Wong, S. Tang, J. Cannon, J. Mukherjee, D. Isham, K. Gam, M. Payne, S. A. Yanik, J. R. Baker and S. K. Choi, *ChemBioChem*, 2017, **18**, 126–135.

33 R. Labruère, A. Alouane, T. Le Saux, I. Aujard, P. Pelupessy, A. Gautier, S. Dubruille, F. Schmidt and L. Jullien, *Angew. Chem., Int. Ed.*, 2012, **51**, 9344–9347.

34 N. Miyaura and A. Suzuki, *Chem. Rev.*, 1995, **95**(7), 2457–2483.

35 E. Coutant and Y.-L. Janin, *Synthesis*, 2015, 511–516.

36 E. Wilson, *Phys. Rev.*, 1934, **45**, 706–714.

37 G. Richner, J. A. van Bokhoven, Y.-M. Neuhold, M. Makosch and K. Hungerbuhler, *Phys. Chem. Chem. Phys.*, 2011, **13**, 12463–12471.

38 P. Dutta, M. Saikia, R. Jyoti Das and R. Borah, *J. Chem. Sci.*, 2014, **126**(6), 1629–1634.

Université de Strasbourg

ABOU NAKAD Elie

Synthèse de groupements protecteurs photolabile pro-fluorescents sensibles à l'excitation bi-photonique

Résumé

Les groupes protecteurs photolabile (GPP) ont été largement utilisés en synthèse organique et pour des applications biologiques. Parmi la grande diversité de ces groupes, les groupement *o*-nitrobenzyl sont les plus utilisés. En particulier, ils ont été abondement employés dans la préparation de nombreux précurseurs photolabiles d'effecteurs biologiques. Ce qui permet d'utiliser une réaction photochimique afin de transformer un composé biologiquement inerte en composé actif avec formation d'un sous-produit de photolyse. Afin de pouvoir quantifier le saut de concentration de l'effecteur biologique en particulier sur des cellules, nous avons développé des nouveaux GPP dérivés d'*o*-nitrobenzyle, qui libère un sous-produit de photolyse présentant des propriétés de fluorescence. Ainsi en nous basant sur le mécanisme de photolyse de dérivés *o*-nitrobenzyl sensible à l'excitation bi-photonique, nous avons pu concevoir un GPP non-fluorescent qui libère un fluorophore après photoclivage. Les propriétés de fluorescence du sous-produit de photolyse ont également été optimisées. Enfin à l'aide de ces PPG pro-fluorescent nous avons pu valider que la réaction photolytique peut être suivie par microscopie de fluorescence sur des cellules en culture.

Mots-clés : Groupements protecteur photolabiles, absorption bi-photonique, fluorescence, uncaging

Abstract

Photoremovable Protecting Groups (PPG) have been widely used in organic synthesis and in various biological applications. Among the wide diversity of these groups, *o*-nitrobenzyl groups are the mostly used chromophores. In particular, they have been extensively used for the design of caged compounds. Those latter type of compounds are able to release a biological effector together with an uncaging side-product leading to the spatiotemporal control of various biological processes. In order to acutely monitor the uncaging event for example in cells, we developed new PPGs, based on *o*-nitrobenzyl derivatives, able to release a fluorescent side product. Based on the photolytical mechanism of two-photon sensitive *o*-nitrobenzyl PPGs, we were able to design new non-fluorescent PPGs able to release fluorophores as side products. We were also able to tune the fluorescent properties of the photo-released by product using molecular engineering. Finally, those pro-fluorescent PPGs have been used in order to follow the uncaging events by fluorescent microscopy on cell cultures.

Keywords: Photoremovable Protecting Groups, two-photon absorption, fluorescence, uncaging.